UNIVERSITY OF SOUTHAMPTON

Faculty of Medicine, Health and Biological Sciences

School of Biological Sciences

Maternal Diet and Programming of Embryo and Fetal Development in the Mouse.

Volume 1 of 1

By

Rose Panton

Thesis submitted for the degree of Doctor of Philosophy

September 2008

UNIVERSITY OF SOUTHAMPTON
ABSTRACT
FACULTY OF MEDICINE, HEALTH AND BIOLOGICAL SCIENCES

Doctor of Philosophy

MATERNAL DIET AND PROGRAMMING OF EMBRYO AND FETAL
DEVELOPMENT IN THE MOUSE

By Rose Diana Panton

Plasticity is a prominent feature of early development, and is necessary to allow the fetus *in utero* to adapt to the continual variation in nutrient and oxygen supply it receives from the mother. In contrast to adaptations made in adult life, those made during fetal life tend to become permanent and irreversible (i.e. programmed). This is due to the existence of sensitive periods which are brief windows of growth and development in early life during which there is an increased susceptibility to programming influences (Barker, 1999). Under-nutrition (or other adverse influences) occurring during fetal life or immediately after birth may thus induce developmental plasticity.

  This study examined the impact of a relatively mild dietary protein restriction in the mouse during pregnancy on the subsequent development of the fetus. The responses of the fetus to the maternal dietary challenge were studied close to the end of gestation (at day 17) using three broadly different approaches. Fetal hepatic tissue was examined for a response to the maternal dietary challenge in terms of global gene expression with the use of Affymetrix micro-arrays. The protein expression profiles of two related proteins were also studied in response to dietary manipulations in fetal liver tissue. Finally, blastocyst stage embryo-transfers were performed in an attempt to elucidate the relative contributions of the early embryo experience versus the ongoing maternal environment to the subsequent fetal growth. Overall, the approaches used suggest that the growth and protein expression of the fetus are altered by maternal dietary manipulation when the challenge is restricted to the pre implantation period of development.

List of Contents

List of Tables

List of Figures

<u>**Appendix I**</u>

Figure A1.3: MAS 5.0 normalized log expression signal data

Figure AI.4: Pearson correlation plot

Acknowledgements

Abbreviations

Abbreviation	Term
ACE	Angiotensin converting enzyme
ADH	Anti-diuretic hormone
AKR1	Aldo-keto reductase family 1
AP-1	Activating protein-1
APOB	Apolipoprotein B
ATCH	Adreno-corticotrophic hormone
BLAST	Basic Local Alignment Search Tool
BP	Base pair
BSA	Bovine serum albumin
CAMK2B	Calcium/calmodulin-dependent protein kinase II beta
cDNA	Complementary deoxyribonucleic acid
cRNA	Complementary ribonucleic acid
CpG island	Cytosine base joined (by phosphodiester bond) to guanine base in a stretch of DNA
CRH	Corticosteroid releasing hormone
DAVID	Database for annotation, visualisation and integrated discovery
DD	Dideoxy
DiH$_2$O	Deionised water
DOHAD	Developmental Origins of Health and Disease
DNMT1	DNA methyltransferase-1
DNA	Deoxyribonucleic acid
dNTP	Deoxynucleoside 5'-triphosphate
DTT	Dithiothreitol
FDR	False discovery rate
FLCN	Folliculin
FMOL	Femtomole ($1x\ 10^{-15}$)
FSH	Follicle stimulating hormone
GAPDH	Glyceraldehyde-3-phosphate dehydrogenase
GCOS	GeneChip operating system
GOTM	Gene ontology tree machine
GR	Glucocorticoid receptor
GRE	Glucocorticoid response element
HDL	High density lipoprotein
hGR	Human glucocorticoid receptor
HPA axis	Hypothalamic-pituitary-adrenal axis
HSP	Heat shock protein
HRE	Hormone response element
11β HSD	11-beta Hydroxysteroid dehydrogenase
ICM	Inner cell mass
IDV	Integrated density value
IGF	Insulin-like growth factor

IGFBP	Insulin-like growth factor binding protein
IGF1R	IGF-type I receptor
IUGR	Intra-uterine growth restriction
IVT	*In vitro* transcription
kDa	Kilodaltons
LDL	Low density lipoprotein
LH	Luteinizing hormone
LOS	Large offspring syndrome
LPD	Low protein diet
MR	Mineralocorticoid receptor
mRNA	Messenger ribonucleic acid
mTOR	Mammalian target of rapamycin
PAGE	Polyacrylamide gel electrophoresis
PAR	Predictive adaptive response
PBS	Phosphate buffered saline
PCR	Polymerase chain reaction
PEPCK	Phosphoenolpyruvate carboxykinase
PMOL	Picomole (1×10^{-12})
PVP	Polyvinylpyrrolidone
PVDF	Polyvinylidene fluoride
RAS	Renin-angiotensin system
RNA	Ribonucleic acid
RPM	Revolutions per minute
RT	Reverse transcription
SAPE	Streptavidin phycoerythrin
SDS	Sodium dodecyl sulphate
Taq	*Thermus aquaticus* (polymerase)
TBE	Tris-borate-EDTA
TE	Trophectoderm
Tween	Polyoxyethylenesorbitan

Chapter 1

General Introduction

1.1 Developmental Origins of Health & Disease

1.1.1 Programming

Plasticity is a prominent feature of early development, and is necessary to allow the fetus *in utero* to adapt to the continual variation in nutrient and oxygen supply it receives from the mother. In contrast to adaptations made in adult life, those made during fetal life tend to become permanent and irreversible (i.e. programmed). This is due to the existence of sensitive periods which are brief windows of growth and development in fetal life and infancy during which there is an increased susceptibility to programming influences (Barker, 1999).

Under-nutrition (or other adverse influences) occurring during fetal life or immediately after birth may thus induce developmental plasticity and have a permanent effect on the body's structure, physiology and metabolism. The specific effects of under-nutrition depend on the period of development during which it occurs because tissues develop in a predetermined sequence from conception to maturity. Different organs and tissues undergo periods of rapid cell division, during which they are more sensitive, at different times; hence under-nutrition at particular points during early development will programme different effects (Barker, 1999).

1.1.2 The Barker hypothesis

The "**Developmental Origins of Health and Disease**" **(DOHAD)** hypothesis proposes that the developing conceptus adapts to a limited supply of maternal nutrients and permanently alters its physiology and metabolism. This response may protect the growth of its key organs for survival, such as the brain and it is such alterations which may in turn increase its risk of developing disease in later life (Barker, 1999). Evidence from geographical studies provided the first indication that susceptibility to coronary heart disease and stroke in adult life might be linked to under nourishment as a baby (Barker, 1999). Human epidemiological studies have used size at birth as a marker of fetal nutrition and related it in groups of men and women to the occurrence of several chronic diseases in later life:

Hertfordshire

The largest set of records in Britain concerning maternity and infant welfare in the early part of the twentieth century was made by health visitors in Hertfordshire who kept details of the birth weight and early health and development of all children born in the county between 1911 and 1945 (Barker, 1999). Around 1986 the recovery of these records meant that it was possible to relate early growth to health in later life. Men born in Hertfordshire between 1911 and 1930 and women born in the county between 1923 and 1930 were traced. By relating the birth and death records of the men and women traced, the study revealed that standardised mortality ratios for both coronary heart disease and stroke in men fell with increasing birth-weight. In addition, stronger and

highly significant trends existed with weight at one year in men (Figures 1.1, 1.2), notably, no corresponding trends existed where deaths from non-cardiovascular causes were examined. In women, it was revealed that, as in men, deaths from coronary heart disease fell with increasing birth weight, but amongst women there was no trend with weight at one year as there was in men (Figures 1.1, 1.2). Thus, in both men and women, low birth-weight reflective of low rates of fetal growth rather than length of gestation was associated with raised death rates from cardiovascular disease in later life (Barker, 1999).
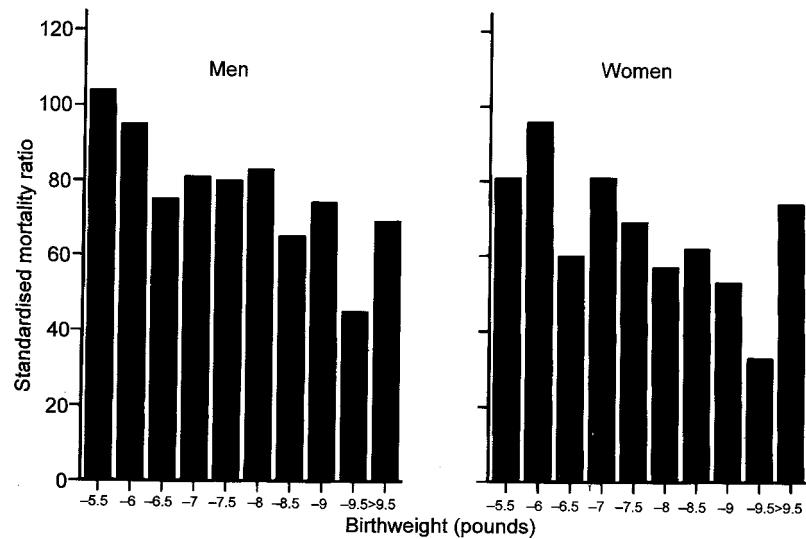
Figure 1.1: **Standardised mortality ratios for coronary heart disease (below the age of 65) according to birth weight for men and women respectively (Barker, 1999).**
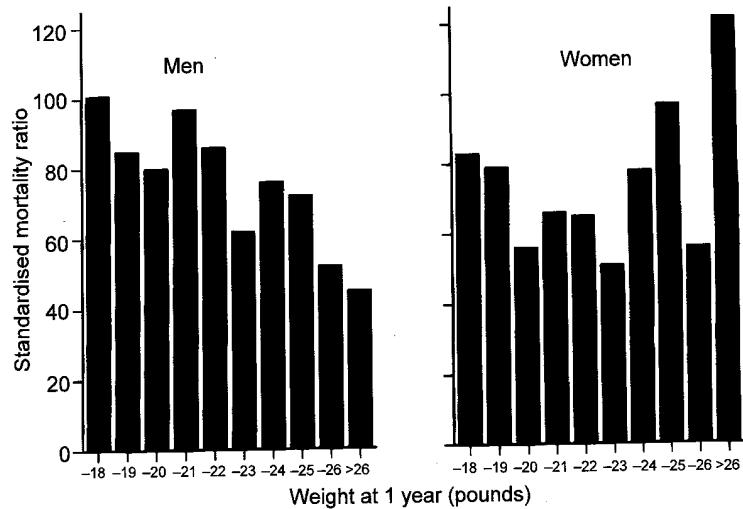
Figure 1.2: **Standardised mortality ratios for coronary heart disease (below the age of 65) according to weight at 1 year for men and women respectively (Barker, 1999).**

In these cohorts from Hertfordshire, the only recorded measure of body size was weight (i.e. birth-weight, weight at one year) so the records provide only a crude summary of newborn and infant physique. Weight measures are more informative when coupled to measures of the body length. This information gives a better idea of the thinness of the infant which is a more representative indicator of early nutrition than weight alone (Barker, 1999). The results from the Hertfordshire study have been confirmed by Barker's group in other cohorts in Preston and Sheffield with more detailed birth size data.

Preston

The aim of this study was to determine whether lower birth weight, used as an indicator of reduced fetal growth and nutrition, is related to the occurrence of "Metabolic Syndrome", also known as Syndrome X. The metabolic syndrome refers to a cluster of

cardiovascular risk factors which include insulin resistance, alterations in glucose and lipid metabolism, increased blood pressure and visceral obesity (Draper and Stewart, 2005).

The Preston cohort included men and women born in Preston, UK, between 1935 and 1943 whose size at birth had been measured in detail. In both men and women, the prevalence of metabolic syndrome fell progressively from those who had the lowest to those who had the highest birth-weights. Amongst 64-year-old men whose birth-weights were 6.5 pounds or less, 22% had metabolic syndrome. Their risk of developing metabolic syndrome was over ten times that of men whose birth-weights were more than 9.5 pounds. In addition to low birth weight, subjects with metabolic syndrome had small head circumference and low ponderal index at birth and low weight at year 1 of age. From the study, it was concluded that type 2 diabetes and hypertension have a common origin in suboptimal development *in utero*, and that metabolic syndrome should be re-named *"the small baby syndrome"* because the prevalence of metabolic syndrome was strongly related to birth-weight (Barker et al., 1993).

1.1.3 Criticism of the Barker hypothesis

The Developmental Origins of Health and Disease model was proposed on the basis of retrospective epidemiological studies of human populations. However, the relative size and importance of such developmental and non-genetic effects has been a matter of dispute. For instance, it is argued that bias in the reporting of results from studies of the

association between birth-weight and subsequent blood pressure may have led to an over-estimation of the strength of the apparent association. Other criticisms of the hypothesis include failure to take sufficient account of the impact of random error and inappropriate and inadequate adjustment for potential confounders (Huxley et al., 2002).

1.1.3.1 The role of birth size

It is argued that birth-weight is of little relevance to blood pressure levels in later life (Huxley et al., 2002). However, the observed relationship between birth size and risk of disease parameters such as raised systolic blood pressure does not simply imply a causal role of being born small but rather it reflects the sensitivity of fetal growth to adverse intrauterine influences. Hence, it is considered that environmental influences during early development act as the causal trigger for disease risk (Gluckman and Hanson, 2004b). Indeed, it is indicated in the Dutch famine of 1944-45 that adverse developmental influences can affect disease risk in the long term in humans without birth-size necessarily being altered (Roseboom et al., 2001). Hence, reduced birth size is not pivotal in predicting disease risk. Gluckman and Hanson point out that the most frequent misunderstanding in this field is the role of birth size, and one which has led to much misinformed criticism of the general paradigm. They highlight that in epidemiological studies where birth size is used it is merely intended to be a crude surrogate measure **reflecting** interactions between fetal environment and fetal genome (Gluckman and Hanson, 2004c). Despite support for the Barker hypothesis from animal studies (see section 1.1.4), in humans it is argued that evidence concerning the effects of maternal diets that influence birth-weight on later blood pressure is limited and often

contradictory (Huxley et al., 2002). Often problems with inconsistent results have arisen

because most studies have used surrogate/indirect or proxy measures of disease risk, such

as systolic blood pressure or fasting insulin/glucose ratios. Indeed, where clinical

cardiovascular or metabolic disease is the measured outcome, the effect of early

environment influences is clearer (Gluckman and Hanson, 2004b) (Figure 1.3).
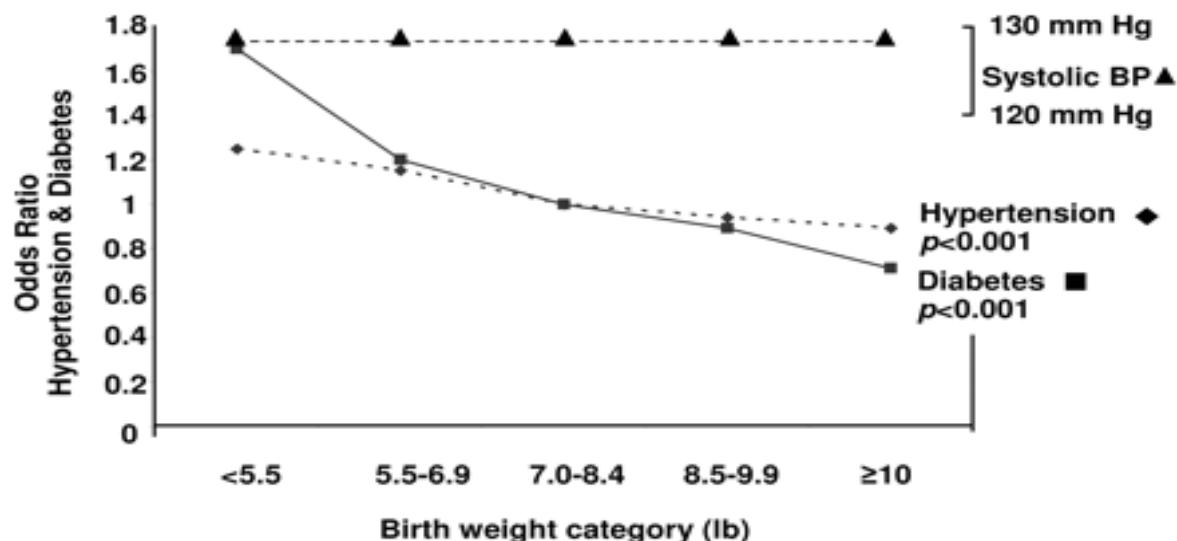
Figure 1.3: **Association in men over 40 years of age between birth size and risk of developing clinically significant hypertension or diabetes mellitus. No relationship exists with systolic blood pressure. The need for studying outcomes rather than surrogate measures of disease is illustrated, (from Gluckman and Hanson, 2004b).**

1.1.4 Support for the Barker hypothesis: Experimental evidence

Numerous rat models support the notion that maternal under-nutrition during pregnancy

alters early growth and development of chronic disease indicators, such as raised systolic

blood pressure, in the adult offspring. Maternal low protein diet models of fetal programming have been extensively used to study the mechanisms that link maternal nutrition with impaired fetal growth and later cardiovascular disease and diabetes (Bertram and Hanson, 2001). For instance, in rats where isocaloric maternal low protein diet was maintained throughout pregnancy but not in offspring, an inverse relationship between maternal protein intake and the systolic blood pressure of the adult offspring was observed. At 9 weeks of age, systolic blood pressure was significantly elevated for all offspring from low protein fed mothers compared with offspring from control fed mothers (Langley and Jackson, 1994).

The effect of fetal exposure to maternal low protein diet was similarly demonstrated by Langley-Evans *et al,* here, hypertension was observed in the weanling offspring of rats exposed to low protein (9% casein) diet during discrete gestational periods in early, mid or late gestation, as well as throughout pregnancy. The effect in early gestation was only significant in male animals. Interestingly, despite the changes in systolic blood pressures evident between the offspring of mothers fed different diets, birth-weights were largely unchanged by the maternal dietary regime (Langley-Evans et al., 1996b). However, in similar studies on rats, offspring birth-weight as well as systolic blood pressure has been altered by the maternal low protein diet, fed throughout pregnancy (Bertram et al., 2001). Similarly, birth-weights of rats exposed to the low protein (9% casein) diet *in utero* were significantly smaller than those of the offspring of rats fed the 18% casein control diet, and the postnatal systolic blood pressures (at 4 weeks or 7 weeks) of male and female rats

exposed to low protein diets *in utero* were significantly higher than those of rats exposed to the control diet *in utero* (Langley-Evans et al., 1996a; Langley-Evans, 1997a). More recently, it has been demonstrated that maternal protein under-nutrition specifically during the period before implantation of the embryo may be critical for the programming of cardiovascular health of the resultant offspring. Male rat pups exposed to low-protein (9% casein) diet for the first 4.25 days of gestation only (with return to control diet for remainder of gestation) had significantly elevated systolic blood pressures at 4 and 11 weeks of age compared with control offspring (Kwong et al., 2000). Similarly, in mice fed low protein diets (9% casein) either throughout pregnancy or 0-3.5 days and then fed a control diet for the remainder of gestation, altered parameters of post-natal health such as persistently raised systolic blood pressure were shown in the offspring from 15 weeks of age, both male and female. This was also shown for offspring of mice exposed to a low protein diet throughout gestation (Watkins et al., 2008).

The protein requirement for pregnant rats is between 9% and 12% by weight (Nelson and Evans, 1953). Hence, the use of the 9% casein low protein diets outlined above represents only a relatively mild dietary manipulation. However, as illustrated in Figure 1.1 for the human, an association with a diseased phenotype is evident even across the normal range of birth-weights (it is not exclusive to the extremes). Even when the maternal dietary regime is not harsh enough to elicit a severely compromised offspring birth-weight, a phenotype in the offspring is still observable. Thus, even a mild maternal dietary restriction may be sufficient to programme a diseased phenotype in the offspring.

It is an important point to note that the diets used by Langley-Evans and subsequent Southampton University-based workers supply extra amounts of the sulphur-containing amino acid methionine, ($CH_3SCH_2CH_2CHNH_2COOH$). Protein in the form of casein, as used in the diets from Langley-Evans et al., provides under half of the cysteine (the other sulphur-containing amino acid) that is required by rats during gestation (Reeves et al., 1993). Thus in order to avoid sulphur deficiency associated with a casein-based diet the extra methionine is added to the diets to compensate, so that rats may produce cysteine by transulfuration of homocysteine (Rees et al., 2000; Langley and Jackson, 1994). As the same methionine supplement (5g/kg) is added to both the low protein and control diets the protein-deficient animals are supplied with an excess of methionine relative to other amino acids, along-side the global casein restriction (Rees et al., 2000). Therefore, it is possible that the critical factor in the nutritional programming of long-term health effects in the fetus is the amino acid balance in the maternal diet rather than total protein content *per se.* Indeed, studies of pregnant rats fed diets devoid of single essential amino acids have revealed that fetal growth is most sensitive to deficiencies of methionine, valine and isoleucine (Niiyama et al., 1973). Similarly, Rees *et al*., (2000) argue that imbalances in specific amino acids associated with maternal low protein diet feeding result in metabolic disturbance which may programme cardiovascular health (Langley-Evans, 2001). Moreover, the balance of specific amino acids may be critical in determining DNA methylation status in the fetus and the specific outcomes of the maternal low protein diet during pregnancy (Rees et al., 2000).

1.1.5 A modified hypothesis

The most recent modification to the Barker hypothesis involves the fetus making

"Predictive Adaptive Responses" in order to prepare its physiology for the level of

nutrient availability in the post natal environment. As opposed to the level of pre-natal

nutrition *per se* influencing disease risk in the offspring, this model highlights the

importance of continuity of the same level of nutrition in both pre- and post-natal

environments. The fetus constantly interprets and responds to changes in the

environment *in utero*. Predictive Adaptive Responses (PARs) are invoked in response to

changes in such environmental stimuli. They confer little immediate survival advantage

but induce future adaptive advantage by establishing a metabolic physiology appropriate

for the predicted postnatal environment (Gluckman and Hanson, 2004a).

Evidence in favour of the concept of PARs comes from the meadow vole (*Microtus*

pennsylvanicus); in this species, the coat at birth is thicker in animals born in the autumn

compared to those born on the spring (Lee and Zucker, 1988). Hence, it is argued that

the fetal vole has predicted the future environment to which it will be exposed after birth

based on maternal signals and, by the processes of developmental plasticity, determined

post-natal coat thickness accordingly while *in utero*. Although this alteration in coat

thickness confers no immediate survival advantage (the temperature to which pups are

exposed *in utero* and in the nest is similar whatever the season), it may reflect an

anticipation of the later environment and hence promotes survival (Gluckman and

Hanson, 2004a).

The appropriateness of the PARs made by the fetus is determined by the predicted and actual postnatal environment. The fetus *in utero* sets a range of homeostatic settings appropriate for postnatal life according to the information about the postnatal environment it receives from its mother. If the nature of the actual postnatal environment matches that which was predicted, the PARs are appropriate and disease risk is low. However, if the actual and predicted post natal environments do not match, risk of disease is increased. For instance, fetal prediction of a nutritionally poor postnatal environment (based upon a compromised environment *in utero*) is associated with a developmental pathway appropriate for a low postnatal nutritional range (Gluckman and Hanson, 2004a). However, if the postnatal environment is plentiful in nutrients, PARs made on the basis of the intra-uterine experience of a deprived environment will be inappropriate and disease risk increased (Gluckman and Hanson, 2004b) (Figure 1.4- see red arrow). There is a considerable potential for such discrepancy between the predicted and actual postnatal environment because of maternal and/or placental disease, and maternal constraint, all of which limit the availability of nutrients to the uterine environment (Gluckman and Hanson, 2004a).
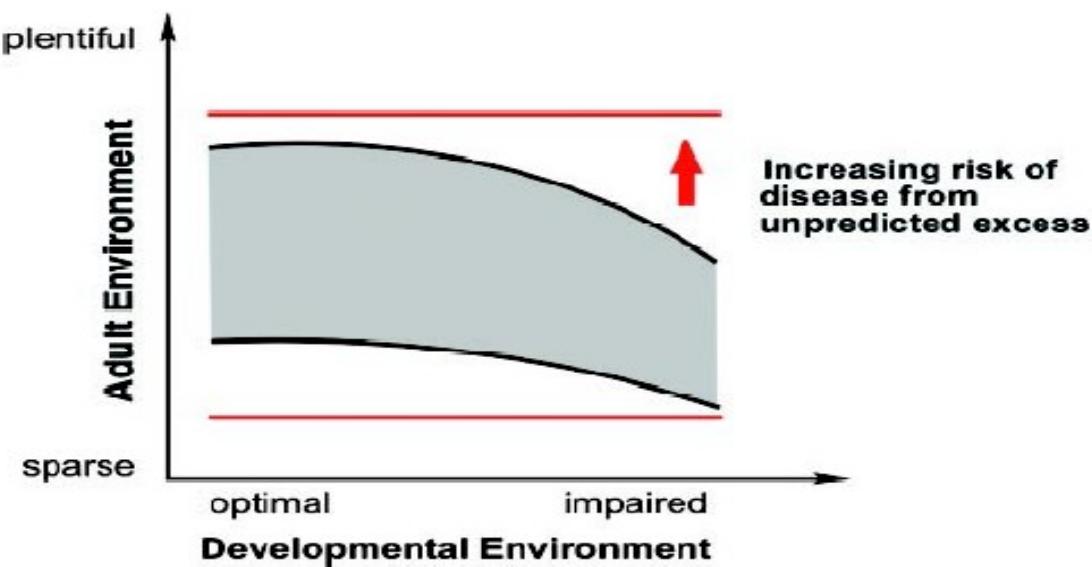
Figure 1.4: PARs model. Appropriate PARs lie within the shaded area; red lines indicate the upper and lower limits of the nutrient range in the postnatal environment (Gluckman and Hanson, 2004b).

This situation of discrepancy between predicted and actual post natal environments, is common in the developing world where fetal growth is often constrained by small maternal size, maternal disease and poor nutrition, and where food availability in the postnatal environment is increasing (Gluckman and Hanson, 2004b). Hence, the PAR model may explain the rapid rise in insulin resistance/metabolic syndrome seen in deprived populations migrating into more prosperous circumstances. For example, the epidemic of type 2 diabetes in the Indian subcontinent may be a consequence of improved nutrition against a background of impaired fetal growth as a result of severe maternal constraint and small maternal size. From this, it is clear that the rate of nutritional transition in a society is critical, due to the prenatal environment changing much more slowly than the postnatal environment. This is because the prenatal

environment is determined by maternal size, body composition and metabolism, features partly laid down when the mother herself was a fetus (Gluckman and Hanson, 2004c)!

Finally, because the upper limit of the postnatal nutrient environment is rising rapidly globally (see upper red line on Figure 1.4), even individuals who had optimal early development may be at risk from disease because of the larger amount of food now available in the postnatal environment in many developed countries; thus, making PARs more likely to fall outside the appropriate range (Gluckman and Hanson, 2004b).

This research project makes use of a mouse model, *Mus musculus* to investigate mechanisms of fetal programming; the findings from which may form the basis upon which to investigate programming mechanisms in the human. Indeed, genes or physiological activities identified as being susceptible to programming in the mouse may become candidates for examination in the human in future research projects. This is because the mouse and the human are both Eutherian (placental) mammals and the growth and development of the embryo is sufficiently similar between the two species for the mouse to provide a useful model of human development. Furthermore, over 90% of the mouse and human genomes can be partitioned into corresponding regions of conserved synteny, reflecting segments in which the gene order in the most recent common ancestor has been conserved in both species (Waterston et al., 2002).

1.2 Murine Reproduction and Embryo Development

1.2.1 Physiology of the uterus

The uterus has two horns and a caudal section (cropus uteri) that is undivided. The uterine horns are suspended from the dorsal body wall by mesometria and extend from the oviducts and unite to form the corpus (Hummel et al., 1966) (Figure 1.5).
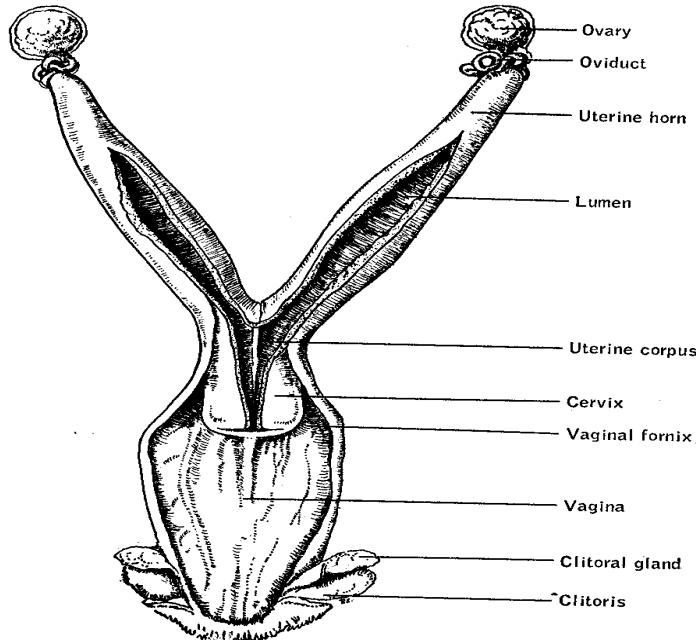
Figure 1.5: Drawing of mouse uterus: uterine horns are the sites of implantation (Hummel et al., 1966).

The uterine mucosa of the horns (endometrium) makes up most of the uterine wall and lies between the epithelia lining the lumen and smooth muscle (myometrium). It is arranged into folds and is well supplied with blood vessels (Hummel et al., 1966).

1.2.2 Oestrus cycle

At maturity, each ovary contains approximately 10^4 oocytes at different stages of

development (Hogan et al., 1994). Female mice reach sexual maturity around 6 weeks of

age, depending on the strain. Sexually mature non-pregnant females maintained under a

constant light-dark cycle tend to ovulate once every 4-5 days, 3-5 hours after the onset of

the dark period, (Hogan et al., 1994). The periodicity of oestrus observed in mature

females is a direct result of cyclic changes in the ovary which are brought about by

alterations in hypothalamic activity and secretion of the gonadotrophins follicle

stimulating hormone (FSH) and luteinizing hormone (LH). The hypothalamus stimulates

FSH secretion by the anterior pituitary gland which promotes ovarian follicle growth.

LH is also secreted by the anterior pituitary and aids in the final development of the

mature follicle. LH also facilitates oestrogen production by theca interna cells of the

FSH-primed follicle (oestrogen acts to suppress further FSH release and promote more

LH secretion). Further LH release results in rupture of the follicle and ovulation of

secondary oocytes into the oviduct (Oestrus). Progesterone released by the ovary during

the follicular growth phase enhances LH release and therefore promotes ovulation. The

development of the corpus luteum is induced by mating and when this does not occur

gonadal hormone levels decrease which allows for the succession of a new cycle

(Bronson et al., 1966). See Figure 1.6.
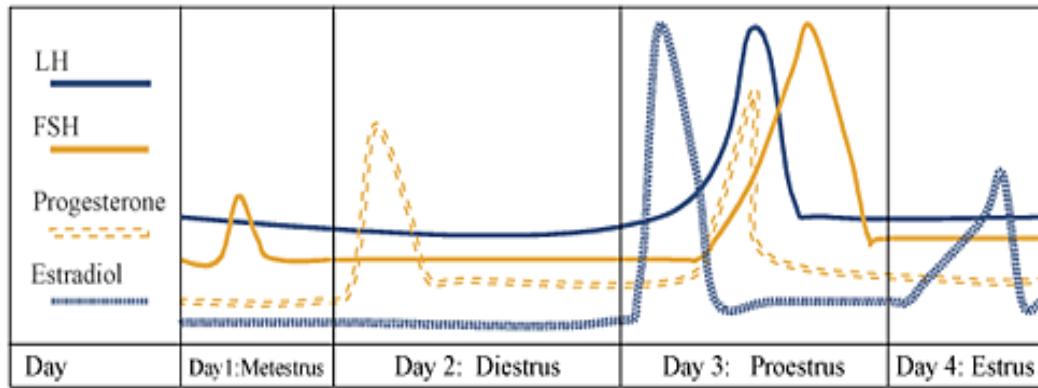
Figure 1.6: **Stages of the oestrus cycle in the rodent (rat) and the sequence of**

endocrine changes involved; taken from

http://pubs.niaaa.nih.gov/publications/arh26-4/images/emanuele3.gif

As outlined in Figure 1.6, there are four stages to the oestrus cycle, namely, Dioestrus,

Proestrus, Oestrus (heat) and Metoestrus. Proestrus and oestrus are anabolic stages

characterised by active growth in the reproductive tract. This part of the cycle culminates

in ovulation. Metoestrus is a catabolic phase and is thus characterised by degenerative

changes in the reproductive tract. The last (or first) stage is dioestrus which is a

quiescent period of slow growth (Bronson et al., 1966).

1.2.3 Mating

Males maintained under the same constant light-dark cycle as female mice will copulate

with females in oestrus (i.e. ovulating females) at around the midpoint of the dark period.

Usually, naturally mated females each contain between 7 and 13 fertilized eggs,

depending on the strain (Hogan et al., 1994); the average litter size is usually between eight and ten.

1.2.4 Fertilisation

Fertilisation of the egg takes place in the ampulla region of the oviduct and involves activation of the ovum by a spermatozoon (sperm cell) and the union of male and female haploid chromosomes (pronuclei) into a single diploid zygote (Rugh R, 1990).

Sperm maturation, by a process known as capacitation, takes place inside the oviduct up to an hour after ejaculation. Once mature, in order to reach the surface of the egg, the sperm must first penetrate the cumulus mass surrounding it and then the zona pellucida membrane. The glycoprotein ZP3 has been identified as the sperm-binding protein in the zona membrane. Sperm binding to ZP3 induces an acrosomal reaction in which hydrolytic enzymes are released from a secretory structure in the sperm head which allow the sperm to penetrate the zona and fertilise the egg. During fertilisation, the sperm head containing a haploid nucleus, the mid-piece and some of the tail all enter into the egg cytoplasm. While the mid-piece of the sperm contributes paternal centrioles and mitochondria to the zygote, the mitochondria are very much diluted out by the oocyte mitochondria (Hogan et al., 1994). The activation by the sperm stimulates the secondary oocyte to complete its second meiotic division by which it develops into a mature haploid ovum. Nuclear membranes form around the maternal and paternal chromosomes forming separate haploid male and female pronuclei that each move towards the centre of the egg

cell. After DNA replication, the pronuclear membranes break down and both sets of chromosomes assemble on a common mitotic spindle; the first cleavage division of the fertilised egg ensues and the diploid embryonic genome is established (Gilbert, 2000; Hogan et al., 1994).

At the time of fertilisation *in vivo,* some studies indicate that the orientation of the future developmental axes is evident upon extrusion of the second polar body from the egg after completion of its second meiotic division. The position of this polar body provides a marker of the animal pole of the zygote and subsequently the animal-vegetal axis of the early embryo is specified. Some studies indicate the embryonic-abembryonic axis develops subsequently perpendicularly to this first axis (Gardner, 1997), although this is disputed. More recently, there have been suggestions that an extrinsic factor, namely the point of sperm entry to the egg, might provide a surface marker for the first cleavage plane of the mouse zygote and thus be involved in spatial patterning of the early mouse embryo (Piotrowska and Zernicka-Goetz, 2001; Plusa et al., 2002) However, this suggestion has been contested due to apparent flaws in the method (Davies and Gardner, 2002).

1.2.5 Embryonic and fetal development

Embryonic development in the mouse begins at fertilisation. The gestational period of development in the mouse is short, usually lasting 19-21 days depending on strain, (Figure 1.7).
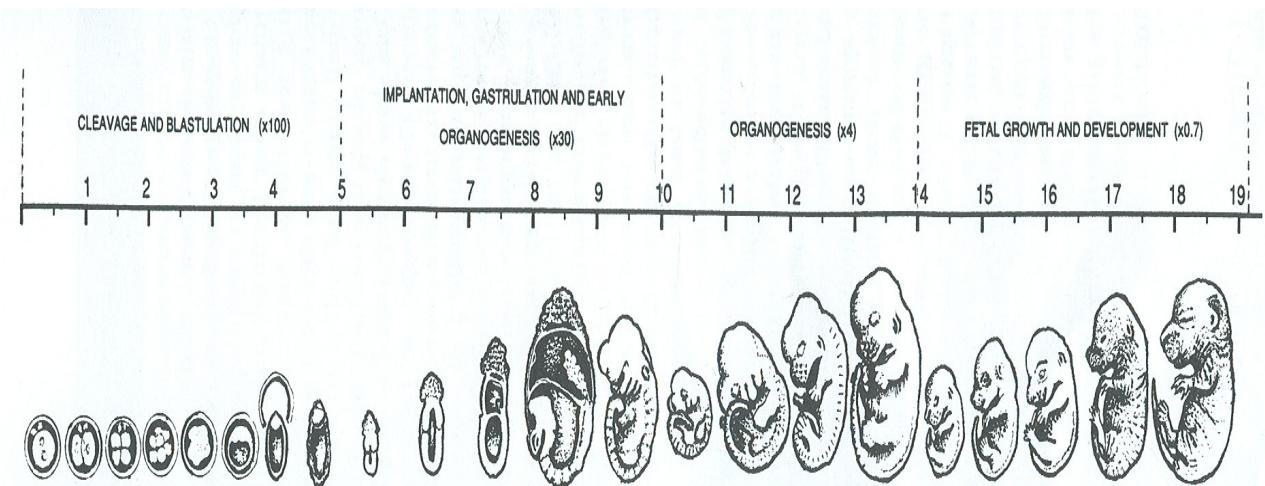
Figure 1.7: Embryonic and fetal development in the mouse: 0-5 days cleavage and blastulation; 5-10 days implantation, gastrulation, and early organogenesis; 10-14 days organogenesis; 14-19 days fetal growth and development (Hogan et al., 1994).

By 24 hours post fertilisation, the mouse embryo is still at the two cell stage and continues to divide slowly over the next couple of days without any increase in mass as it makes its way along the oviduct towards the uterus for implantation into the uterine wall ~4.5 days after fertilisation. Subsequent cleavage divisions generate a 4-cell and then an 8-cell embryo. At the 8-cell stage compaction begins in which the cells of the embryo become differentiated into one of two cell lineages, the differentiated 16-celled embryo is termed a morula; at 3-4 days post fertilisation the 32/64-cell blastocyst is formed (Hogan et al., 1994). See section 1.2.5.1 for further details of the sequence of events taking place during pre-implantation development; sections 1.2.5.2 and 1.2.5.3 summarise developmental events at implantation and beyond.

The relatively slow early development of the mouse embryo enables the uterine tissue time to prepare for receiving the embryo. Whilst in the oviduct shortly before

implantation, the first two differentiated tissue lineages (**trophectoderm** and **primitive endoderm**) are generated in the embryo which form an integral part of the placenta and extra-embryonic yolk sacs required for successful interaction with the mother (Hogan et al., 1994) (Figure 1.8).
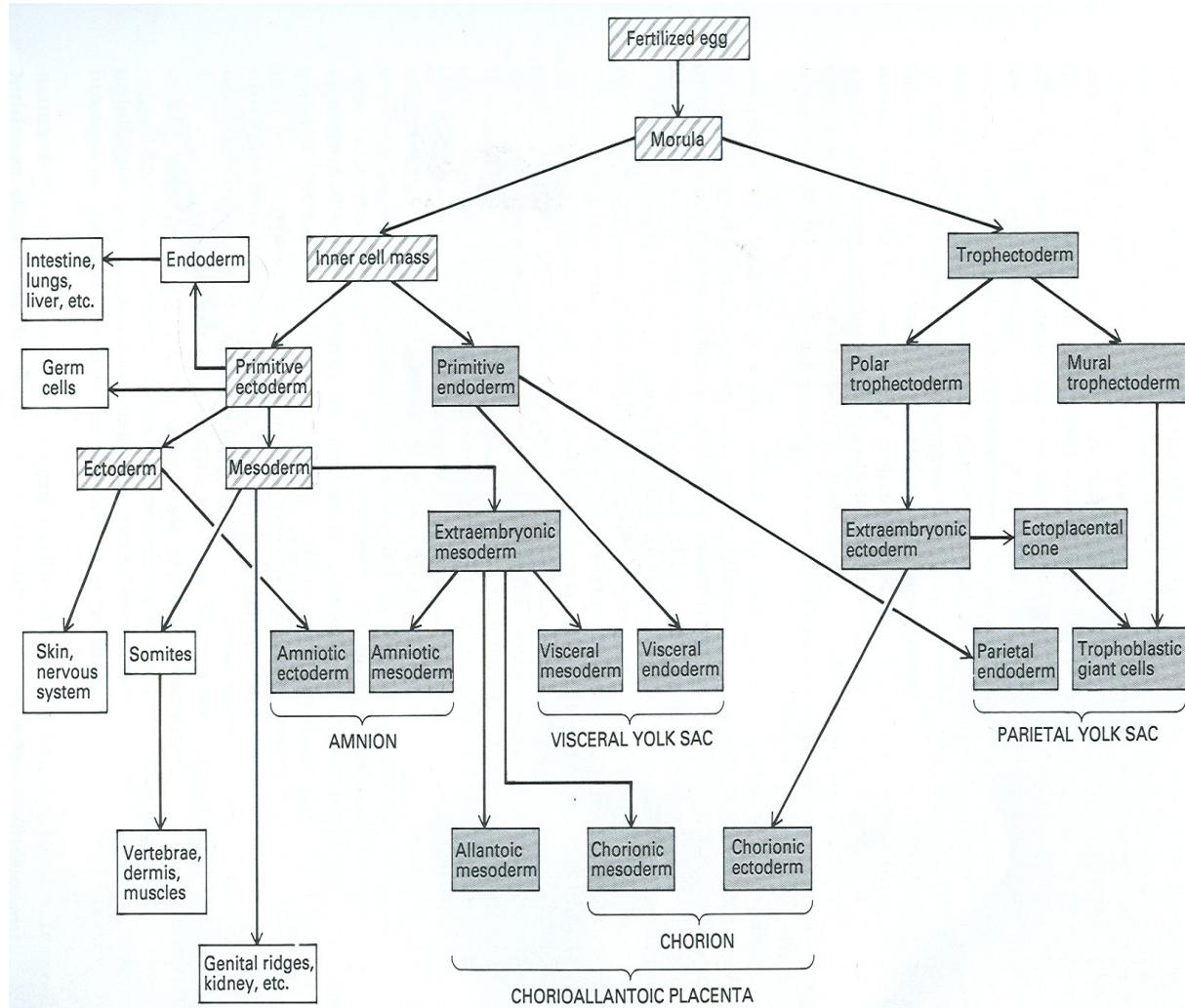
Figure 1.8: Summary of the lineages of tissues constituting the mouse embryo. Hatched boxes = tissues that will give rise to the embryo proper and extraembryonic cells; Shaded boxes = extraembryonic tissues; Open boxes = tissues of the embryo proper (Hogan et al., 1994).

1.2.5.1 Pre-implantation development
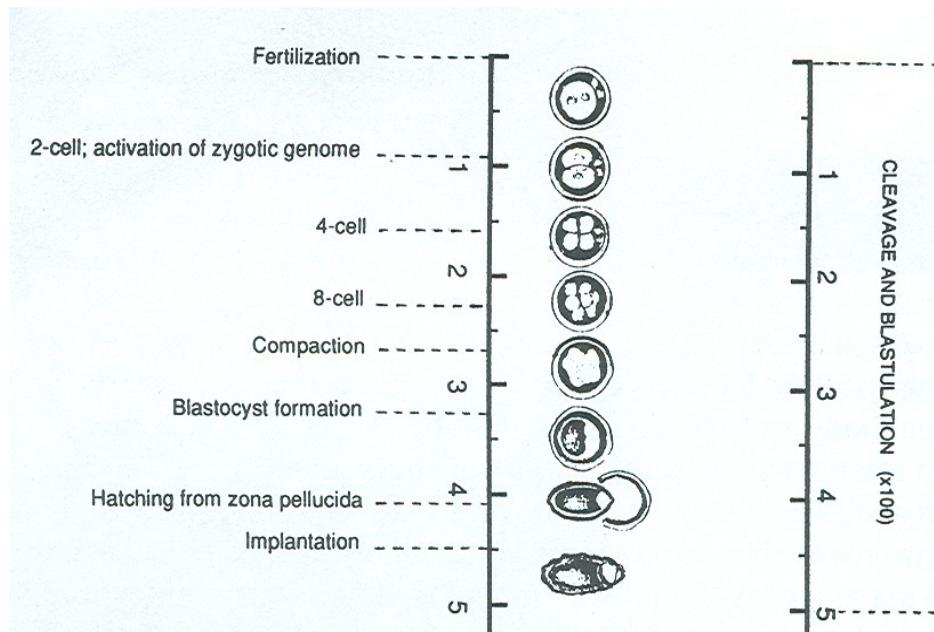
Figure 1.9: **Sequence of events during the pre-implantation period of mouse embryonic development according to days post fertilisation** (Hogan et al., 1994).

Pre-implantation development is illustrated in Figure 1.9. Up until the early 8-cell stage morula, it is believed that the individual cells (blastomeres) of the mouse embryo are each capable of giving rise to a mouse (i.e. they are totipotent). As cleavage divisions continue to the 16 cell stage, however, there is a gradual restriction in the developmental potency of the cells which eventually results in the generation of two distinct cell lineages: trophectoderm (TE) and the inner cell mass (ICM). This process of differentiation begins with compaction of the 8-cell embryo which is characterised by a flattening of blastomeres and increased contacts between them. At this point, blastomeres develop apical and basal membranes and distinct cytoplasmic domains (a process known as polarisation) (Hogan et al., 1994).

After compaction, the cleavage plane of dividing polarised 8-cell blastomeres can generate either polar:polar daughters cells (conservative division) or polar:non-polar daughters (differentiative division). In the 16-cell morula, polar and non-polar cell types occupy outer and inner positions respectively; *in vivo,* cells that end up on the inside of the compacted embryo give rise to the ICM whereas those on the outside surface give rise to TE (Fleming and Johnson, 1988). The cellular differentiation becomes permanent upon the formation of a fully expanded blastocyst (at the 32-cell stage) which consists of a hollow vesicle of TE cells surrounding a fluid-filled cavity (blastocoel) and a group of ICM cells. The TE has the features of a typical epithelium and forms a permeability seal against the outside environment, and transports selected factors into the ICM (Hogan et al., 1994).

The fluid-filled blastocoel cavity is formed by the selective transport of specific ions across the TE into extra-cellular spaces. This produces a concentration gradient which then drives the movement of water into the extra-cellular spaces. Na^+ is one of the main ions involved in the formation of the blastocoel cavity (Manejwala et al., 1989).

The pre-implantation embryo is unique in its capacity to develop in the absence of any direct cellular contact with the reproductive tract before implanting into the uterus. It is free-floating, lacks a blood supply and is moved continuously by the reproductive tract through a changing fluid environment. During this time, it is dependent on the luminal secretions of the oviduct and uterus for its **nutrition**; its cellular activities, such as cell division, gene expression and metabolism, are all influenced by this environment and the factors produced by the cells of the reproductive tract. For normal development and

implantation to occur, there must be effective maternal-embryonic communication, mediated by growth factors e.g. insulin, IGFs. A range of such growth factors are produced by the reproductive tract and pre-implantation embryo, and many of their receptors may be detected on the embryo surface (Hardy and Spanos, 2002) (Figure 1.10). The mammalian reproductive tract is also a good source of exogenous protein and amino acids that the developing embryo can utilise in the biosynthesis of its own proteins (Gardner and Leese, 1990).
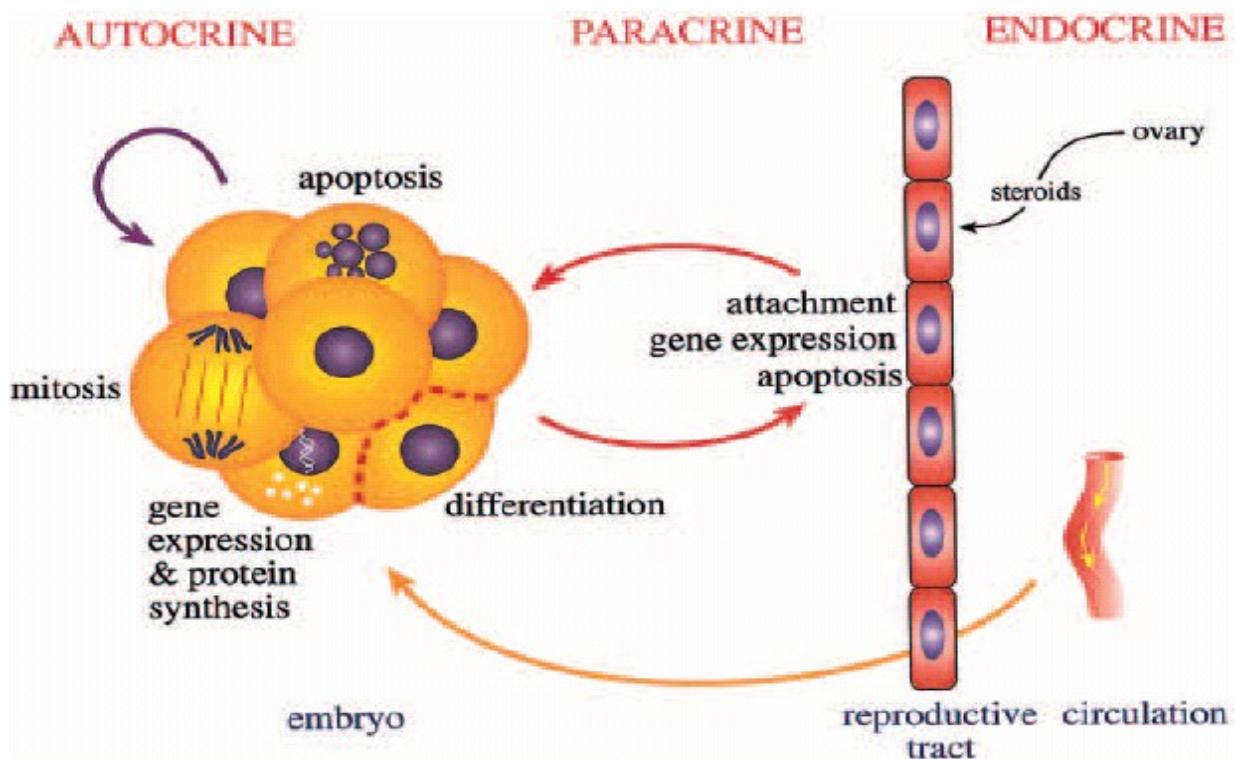
Figure 1.10: Cellular responses of the embryo and maternal reproductive tract to maternally and embryonically derived growth factors (Hardy and Spanos, 2002).

Exogenous growth factors do not however appear to be essential for pre-implantation development as evidenced by mammalian embryos that are able to survive and develop to the blastocyst stage *in vitro* in a simple salt solution supplemented only with the nutrients pyruvate and albumin (Devreker et al., 1998). The nutrient requirements of the mammalian embryo change during pre-implantation development, in particular the preferred energy substrate for metabolism. Glucose, pyruvate and lactate are key nutrients required during the mammalian pre-implantation period. In human embryos *in vitro,* pyruvate uptake was significantly higher in embryos that went on to form blastocysts than by those that failed to develop to the blastocyst stage (Gardner et al., 2001). Likewise pyruvate uptake by fertilised human embryos which arrested at cleavage stages was significantly lower than those which developed to the blastocyst stage (Hardy et al., 1989). This suggests that pyruvate in particular is important for metabolism of the mammalian pre-implantation embryo at the pre-blastocyst stages. Glucose uptake *in vitro* was highest in human blastocysts of the highest morphological 'grade,' whereas pyruvate uptake was similar irrespective of blastocyst grade (Gardner et al., 2001). Therefore, it appears that glucose is the more important nutrient for the metabolism of the mammalian embryo by the blastocyst stage (Gardner et al., 2001; Hardy et al., 1989; Gardner and Leese, 1987; Renard et al., 1980). This is further supported by normal fertilised human embryos in culture, whereby pyruvate uptake exceeds that of glucose in the early developmental stages before glucose becomes the predominant substrate in the blastocyst. Meanwhile, for single human pre-implantation embryos that arrested in culture, values of pyruvate and glucose uptake and lactate production were below that for embryos which developed normally (Gott et al., 1990).

Importantly, the mammalian reproductive tract is regionally specialised to meet the changing metabolic requirements of the embryos as it develops. After ovulation, the human embryo in the oviduct it is exposed to relatively high concentrations of pyruvate and lactate (metabolite of glucose) and a lower concentration of glucose (Gardner et al., 1996). This is appropriate for pre-compact embryos found in this region. While in the uterus, there is a lower concentration of pyruvate and lactate and an increased glucose concentration compared to the oviduct (Gardner et al., 1996), reflecting the altered needs of the embryo at compaction and upon blastocyst formation. This is important particularly as it has been suggested by *in vitro* culture experiments that exposure of the pre-compact mammalian embryo to high levels of glucose may be inhibitory to cleavage development (Conaghan et al., 1993).

1.2.5.2 Implantation

Hatching of the blastocyst from the zona pellucida precedes implantation. At the time of implantation, changes in the surface of the uterine epithelium make it conducive for blastocyst attachment. Blastocyst attachment induces formation of a uterine crypt and stimulates the uterine stroma to form decidual tissue (a spongy mass of cells). This subsequently causes a rapid increase in permeability of local capillaries which causes swelling of the uterine stroma. Stromal cells in the uterine tissue proliferate and increase in size and the epithelium separating blastocyst from the stroma gradually erodes which allows the trophoblast cells to invade the deciduum (Hogan et al., 1994).

At the time of implantation (~ 4.5 days post conception), the blastocyst is made up of

three tissue lineages: **trophectoderm** (TE), **primitive endoderm** (derived from ICM)

and **epiblast** (**primitive ectoderm**- derived from ICM also). At this time, the TE

becomes regionally specialised in terms of morphology and developmental potential

(Figure 1.8); TE cells which overly the ICM directly are known as polar TE, whereas TE

cells surrounding the blastocoel cavity become mural TE. At this point the epiblast is the

smallest population consisting of 20-25 cells only and is situated between the polar

trophectoderm and the primitive endoderm (Hogan et al., 1994) (Figure 1.11).
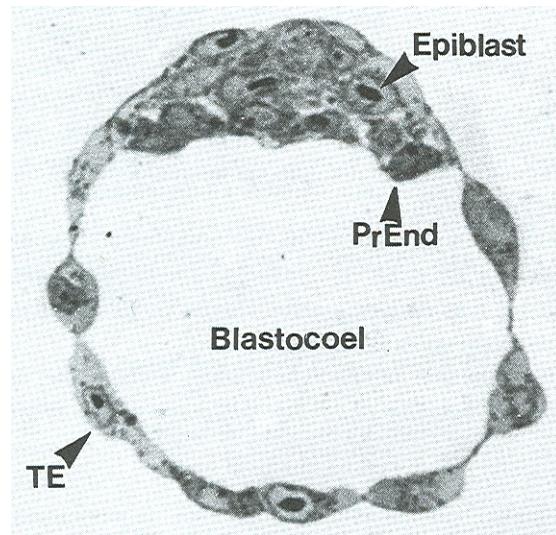
Figure 1.11: Image of a mouse blastocyst ~4.5 days of development (PrEnd =

Primitive endoderm; TE= Trophectoderm) (Hogan et al., 1994).

Differential expression of regulatory transcription factors underlies the lineage

diversification and cell fate as the blastocyst develops. Oct-4 is present in the nuclei of

mouse blastomeres at all cleavage stages but becomes restricted to the ICM and

subsequently the epiblast as development progresses, indicating that Oct-4 is a

pluripotency marker (Palmieri et al., 1994). In contrast, the homeodomain protein Cdx2

is expressed in a reciprocal pattern to Oct-4 and becomes restricted to the TE lineage by

the blastocyst stage (Beck et al., 1995). The importance of Cdx2 for development of

trophoblastic cells derived from the TE lineage is demonstrated by homozygous Cdx-2

knockout embryos failing to implant (Chawengsaksophak et al., 1997).

1.2.5.3 Post-implantation development

Once the blastocyst has implanted into the uterus, there is a major increase in the rate of

embryonic growth. This is especially evident in the small group of pluripotent (epiblast)

cells from which the fetus will develop. 5-10 days post fertilisation, as a result of

gastrulation, the three primary germ layers- ectoderm, mesoderm and definitive

endoderm, differentiate. At this stage the basic body plan and organ primordial of the

future mouse are established. Between 10-14 days organogenesis is completed and

thereafter until term the fetus grows rapidly building upon the basic body axes (Hogan et

al., 1994).

1.3 The Liver

1.3.1 Liver development

Hepatic tissue develops from endoderm in the embryo that extends out from the foregut (Gilbert, 2000). At 16 days post conception the upper part of the peritoneum in the mouse is largely occupied by the liver. The liver is arranged into definitive lobes by this time and histological analyses of hepatic tissue indicate there is a considerable amount of haemopoietic activity at this stage (Kaufman, 1992). In adult mammals the haemopoietic system of stem cells resides in the bone marrow of the larger bones of the skeleton however in the embryo it is to be found at various other sites. Initially, it is in the yolk sac, later it is in the liver, spleen and lymph nodes due to cell migration from the original sites (Slack, 2006).

Many tissues and organs e.g. the brain, gut and kidneys are not imperative for intrauterine life. However, the placenta, yolk sac, fetal liver (all sites of haemopoiesis), and cardiovascular system are central to survival through the embryonic period (Cross and Rossant, 2001). The fetal liver is one of the main sites of fetal gluconeogensis. Under normal physiological conditions there is minimal net gluconeogenesis undertaken by the fetus. However, during adverse conditions such as maternal under-nutrition, glucose production in the fetus is stepped up. In the fetal liver, gluconeogenesis occurs by glycogenolysis from glycogen stores. It may also occur by gluconeogensis from lactate and amino acids. The ability of the fetus to produced glucose in this way increases

towards term, as hepatic glycogen content rises and the activities of the gluconeogenic

enzymes increase (Fowden, 2001).

Nutrients that are taken up by fetal tissues are used primarily for tissue growth or

oxidation, see Figure 1.12 (Fowden, 2001).
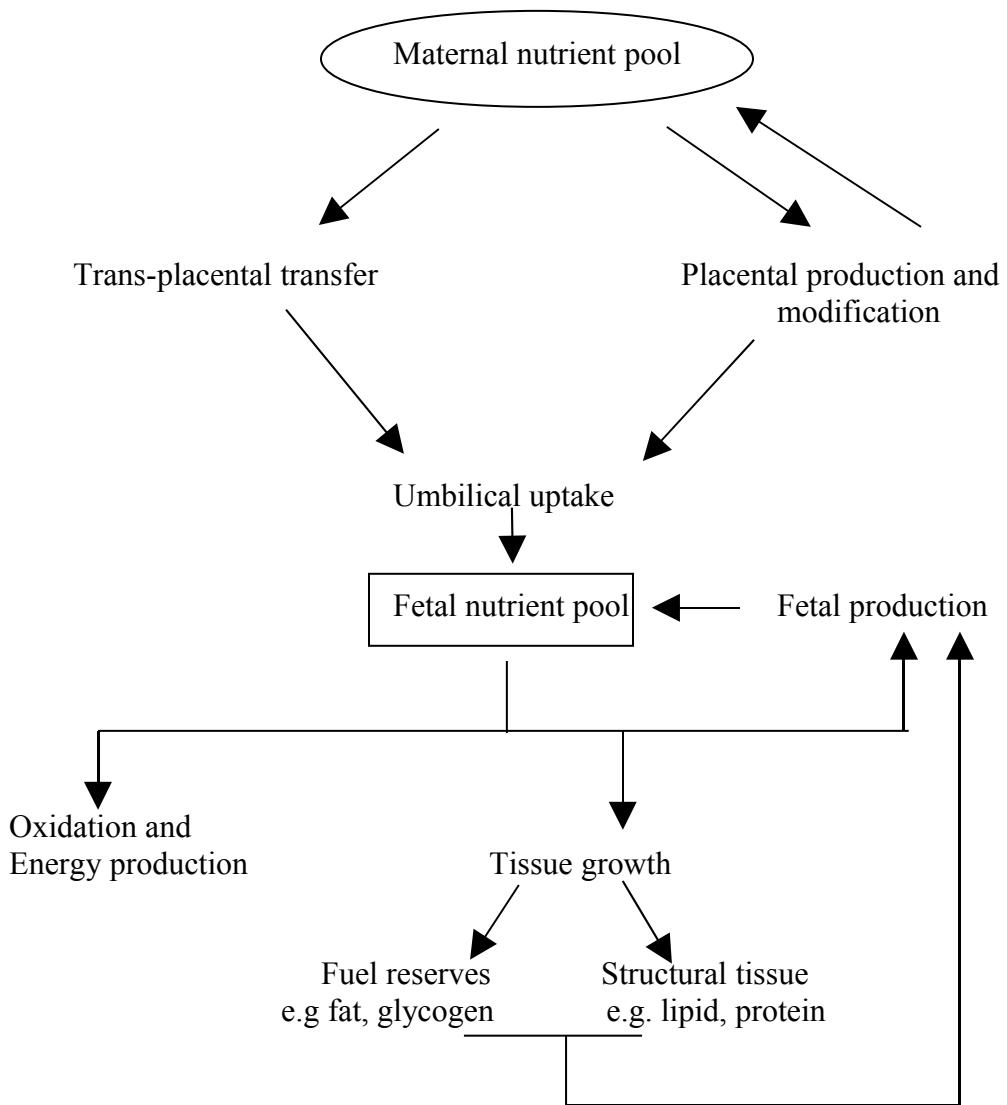
Figure 1.12: Nutrient fluxes between maternal, placental and fetal tissues during

late gestation (Fowden, 2001).

1.3.2 Liver function

The liver is an accessory gland of the mammalian digestive system although it performs a diverse range of functions pivotal to homeostasis. In terms of its role in digestion, the liver produces bile which contains salts that act as detergents to help in the digestion and adsorption of fats (Campbell et al., 1999). Another related function is regulation of blood sugar levels. The hepatic portal vein takes blood, carrying digestion products such as sugars and amino acids, from the intestine directly to the liver. Under the influence of insulin, much of the glucose present is taken up into hepatocytes. Here, glucose is converted into glycogen granules for energy storage and subsequent release into the circulation as required (after conversion back into glucose). Glycogen breakdown and sugar, fat and amino acid metabolism are all under strict hormonal control (Randall et al., 2002).

1.3.3 Diet and hepatic programming

It has been demonstrated that a low protein diet during pregnancy and lactation in rats has an effect on hepatocyte proliferation, liver growth and morphology in the resulting offspring (Burns et al., 1997; El Khattabi et al., 2003). In offspring of rat dams fed a low-protein diet during pregnancy decreased activities of hepatic glucokinase and glutamine synthase, which regulate glucose uptake, have been reported. Plus, an increase in the activity of catabolic enzymes in the liver such as PEPCK, important in regulating gluconeogenesis was observed in these offspring (Desai et al., 1997a; Desai et al., 1997b;

Burns et al., 1997). These authors suggest that rat pups exposed to early maternal malnutrition have their metabolic control point shifted in the direction of poor nutrition so that the liver develops to favour production rather than utilisation of glucose; as the activity of anabolic glucose-utilising enzymes in the liver were decreased while the activity of catabolic glucose-producing enzymes increased.

In studies that have mapped metabolic function within the liver in rats, a diminished perivenous uptake of glucose in the livers of offspring exposed to a low protein diet throughout gestation and lactation has been reported (Burns et al., 1997). Thus, it has been suggested that fetal programming may partly operate through altered glucokinase expression in the perivenous region. Interestingly, patients with type 2 diabetes display decreased activity of hepatic glucokinase also (Caro et al., 1995).

1.4 Mechanisms of Intrauterine Programming

As intrauterine growth retardation can be related to specific postnatal outcomes and hormones regulate fetal growth and the development of fetal tissues, it is likely that hormones will have pivotal role in intrauterine programming. Hormones such as insulin, insulin-like growth factors (IGFs), thyroid hormones and the glucocorticoids act as nutritional and maturational signals *in utero* and adapt fetal development to intrauterine conditions which prevail in order to maximise the chances of survival *in utero* and at

birth. However such adaptations may have long-term consequences as previously mentioned (Fowden and Forhead, 2004).

Hormones present in fetal circulation may be secreted by the fetal endocrine glands, or they may be derived from uteroplacental tissues, by transplacental diffusion (lipophilic hormones) or finally they may come from circulating precursors by metabolism in fetal or placental tissues (Fowden and Forhead, 2004). The concentration of hormones in fetal circulation is affected by nutritional signals; nutritional challenges that reduce fetal nutrient availability will usually decrease the concentration of anabolic hormones (such as insulin, IGF-I and thyroxine - T_4) and increase catabolic hormone concentrations (e.g. cortisol, and growth hormone) (Figure 1.13). Fetal insulin for instance is a growth-promoting hormone, which acts as a signal of nutrient plenty.
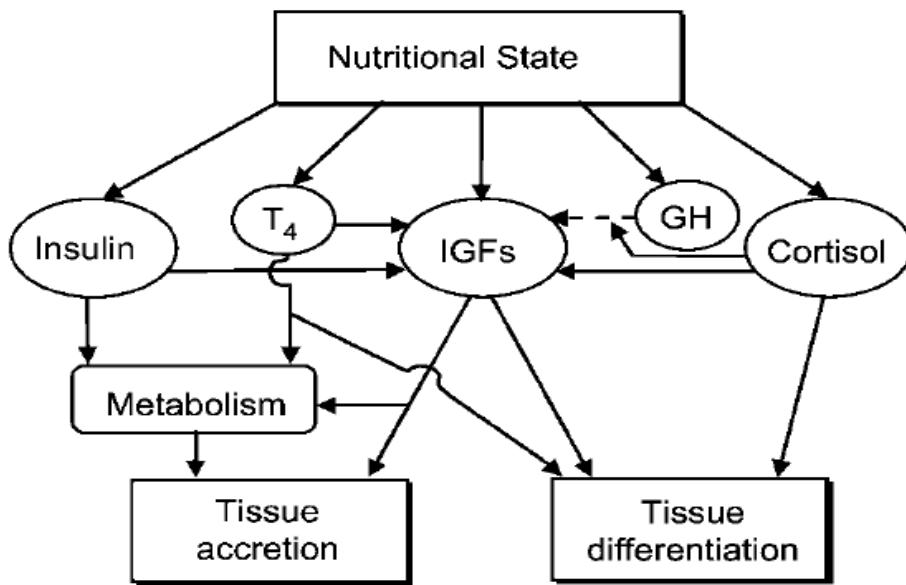
Figure 1.13: Relationship between nutritional state of the fetus, hormone concentrations, metabolism and tissue growth and differentiation (from Fowden and Forhead, 2004).

Of the hormones known to control fetal development, glucocorticoids are most likely to cause tissue programming *in utero.* In the long term, prenatal glucocorticoid exposure can permanently reset endocrine systems (such as the Hypothalamic Pituitary Adrenal – HPA-axis) which may in turn contribute to the pathogenesis of adult metabolic dysfunctions e.g. insulin resistance, dyslipidemia, glucose intolerance, hyperglycaemia (Fowden and Forhead, 2004; Fowden et al., 2005). Patients with circulating cortisol excess, Cushing's syndrome, display many features associated with metabolic syndrome (Draper and Stewart, 2005) which may indicate a role for glucocorticoids in the mechanisms involved in programming of features of metabolic syndrome in offspring from mothers fed protein restricted diets for all or part of pregnancy. Glucocorticoids (cortisol/corticosterone) are steroid hormones synthesised in the *zona fasciculata* region (mid zone) of the adrenal cortex (Funder, 1996). They are released into the blood stream in response to adreno-corticotrophic hormone (ACTH) secretion from the anterior pituitary gland, in turn stimulated by corticosteroid-releasing hormone (CRH) release from the hypothalamus. Hypothalamic CRH is secreted in response to hippocampal signals or pituitary/adrenal feedback messages. Hence, glucocorticoid release is under the control of the Hypothalamic-Pituitary-Adrenal stress axis. The majority of circulating glucocorticoid is bound by corticosteroid-binding-globulin leaving only 10% free to enter cells and interact with glucocorticoid receptors (Bertram and Hanson, 2002). Being lipohilic substances, steroids are able to diffuse readily across cell membranes (Bamberger et al., 1996).

1.4.1 Glucocorticoids and development

Glucocorticoids affect both fetal and adult tissues and have a variety of key physiological roles including the regulation of salt and water homeostasis, blood pressure, immunological responses and metabolism (Bertram and Hanson, 2002). Glucocorticoids also have a key role in mediating anti-inflammatory effects, as evidenced by the therapeutic use of inhaled glucocorticoids in the treatment of asthma (Barnes and Adcock, 1998).

1.4.1.1 Fetal organ maturation

Glucocorticoids exert their maximal effect on mammalian fetal organs, specifically the heart, liver and lung, immediately prior to birth (Thompson et al., 2004). Perinatally, glucocorticoids promote maturational changes to fetal organ systems critical for immediate post-natal survival. For example, glucocorticoids are able to induce catabolic enzymes in the developing fetal liver such as PEPCK, which are key to survival in early post-natal life; glycogen accumulates in the liver and gluconeogenesis is stimulated by glucocorticoids in order to meet glucose demands until feeding begins. The structural and functional maturation of the developing lungs is also regulated perinatally by glucocorticoids which enable them to cope when air enters the alveoli with the first breath (Liggins, 1994). Severe abnormalities are evident in offspring of targeted glucorticoid receptor (GR) gene disruptions; GR-/- mice die within a few hours of birth due to respiratory failure, and newborn liver has a reduced capacity to activate genes for

key gluconeogenesis enzymes, further supporting the role for glucocorticoids in stimulating maturational events perinatally (Cole et al., 1995).

Liggins and Howe (Liggins and Howie, 1972) first provided an important indication that glucocorticoids might serve a vital function in mediating the successful transition of the term fetus to extra-uterine existence which led to the widespread use of prenatal glucocorticoid therapy to prevent life threatening complications of pre-term birth. Indeed, the clinical administration of the synthetic, poorly-metabolised glucocorticoid, dexamethasone, to women in pre-term labour is widely used as a means to promote fetal lung maturation and hence reduce the chances of respiratory distress syndrome occurring (Langley-Evans, 2001). However, fetal exposure to synthetic glucocorticoids *in utero* has been linked to longer term health risks.

1.4.1.2 Fetal growth

During normal mammalian fetal development, circulating glucocorticoid concentrations are considerably lower in the fetal compartment in comparison to the maternal system. In many species there is a natural surge in fetal plasma glucocorticoid concentration in late gestation associated with the maturation of the fetal adrenal (Arishima et al., 1977). As the rate of fetal growth naturally decreases towards term, this has been linked to increased fetal plasma cortisol occurring at this time. This is supported by the observation that fetal adrenalectomy results in increased body weight in the final week of gestation (Bertram and Hanson, 2002).

High levels of maternal glucocorticoid therapy during pregnancy has confirmed the growth-retarding influence of glucocorticoid exposure on the developing fetus in both primates and rodents alike; effects include intra-uterine growth restriction, as evidenced by reduced birth weight of the fetuses of treated mothers, and disproportionate fetal organ growth (Reinisch et al., 1978; Novy and Walsh, 1983). This effect has been further documented by Ikegami *et al* who found that multiple fetal glucocorticoid exposure during the final third of gestation to preterm lambs improved post-natal lung function, but had a detrimental effect on birth weight and postnatal growth (Ikegami et al., 1997).

In contrast to insulin and the thyroid hormones, glucocorticoids affect the expression of both the *Igf* genes (Fowden, Li and Forhead, 1998). In many species, both *Igf1* and *Igf2* are expressed in fetal tissues from the earliest stage of pre-implantation development to the final stage of tissue maturation just prior to birth (Watson et al., 1994; Fowden, Li and Forhead, 1998). In rodents and humans, during mid to late gestation the *Igf2* gene is widespread in fetal tissues and is expressed more abundantly than *Igf1* (Hill, 1990; Delhanty and Han, 1993). However, after birth in rodents there is a fall in IGF-II (protein) expression such that by weaning its expression has disappeared from most tissues (Lee, Lintar and Efstratiadis, 1990). In contrast, tissue expression and plasma levels of the IGF-I protein are low *in utero* compared to post-natal levels (Singh, Rall and Styne, 1991). Such findings have given rise to the concept that that IGF-II is the IGF protein primarily responsible for fetal growth (Gluckman, 1995; Jones and Clemmons, 1995).

In mice, deletion of either the *Igf1* or *Igf2* gene or the *Igf1r* (receptor) gene leads to retardations in fetal growth, shown by reduction in fetus weights in late gestation (Efstratiadis, 1998) whereas over-expression of IGF-II leads to fetal overgrowth (Eggenschwiler et al., 1997).

Both *Igf* genes have a specific role to play in fetal growth but their expression and specific actions are different (Fowden, 2003). Whilst *Igf1* gene expression is low in the fetus, it appears to have a more prominent role than IGF-II in modulating cell proliferation in relation to the nutritional climate *in utero* (Fowden, 2003). Alternatively, the *Igf2* gene is highly expressed *in utero* and has a key role in nutrient transfer across the placenta and placental growth. Whilst it is relatively unresponsive to nutritional stimuli it does respond to changes in the fetal glucorticoid concentration in specific fetal tissues (Fowden, 2003).

1.4.1.3 Fetal cardiovascular control

Glucocorticoids increase blood pressure in fetal and adult animals. Activation of the fetal Renin-Angiotensin System (RAS) may be one mechanism by which cortisol induces hypertension *in utero* (Forhead et al., 2000; Langley-Evans, 1997c) (Figure 1.14). The pre-partum cortisol surge mentioned earlier coincides with an increase in fetal blood pressure and is associated with a number of maturational changes in the activity of the fetal RAS in several species. In fetal sheep, the rise in blood pressure caused by an intravenous infusion of cortisol has been associated with increased vascular sensitivity to exogenous angiotensin II (Tangalakis et al., 1992) as well as increased circulating

concentrations of angiotensin II, renin and angiotensinogen (Forhead et al., 2000).

Glucocorticoid exposure *in utero* may act to induce organisational changes in the activity

of the RAS which persist after birth into adult life and programme hypertension (Forhead

et al., 2000). Indeed, it appears that components of RAS may be permanently influenced

by the intra-uterine environment as indicated by the hypertension seen in adult offspring

of rats fed low protein diet during pregnancy which was accompanied by increased

plasma and pulmonary ACE concentrations (Langley and Jackson, 1994; Langley-Evans

and Jackson, 1995).
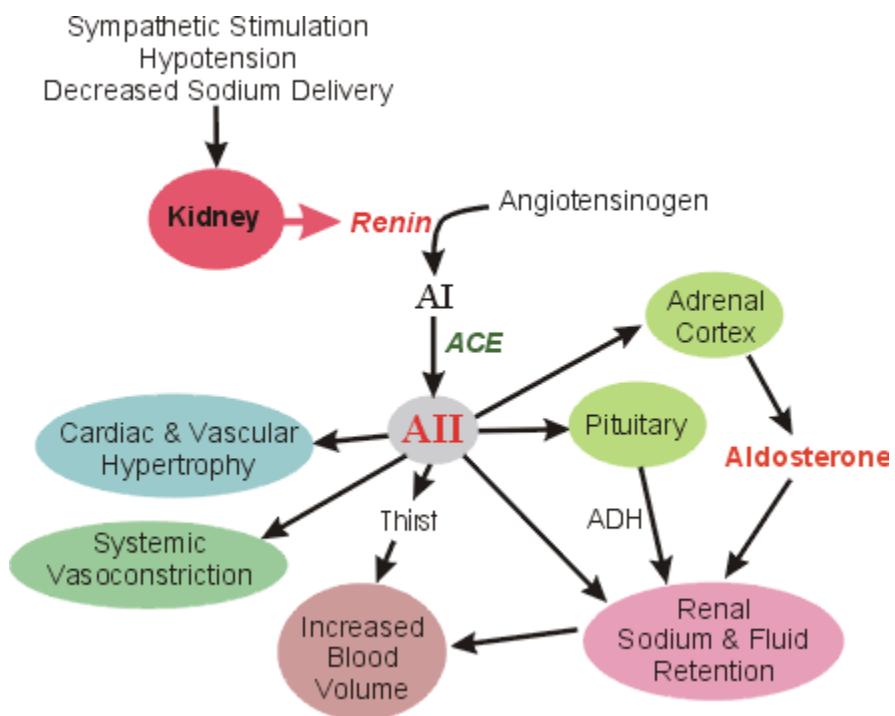
**Figure 1.14: The Renin-Angiotensin System (RAS) plays an important role in the
regulation of the physiological responses of the cardiovascular system. The
hormone Angiotensin II (AII) is the primary effector molecule of this system. AII is
formed by enzymatic cleavage of the circulating precursor Angiotensinogen to**

Angiotensin I (AI) by the protease Renin with subsequent conversion of AI to AII by Angiotensin Converting Enzyme (ACE) as blood passes through the lungs. AII has several important functions which culminate in raised arterial blood pressure.
Schematic taken from: http://www.cvphysiology.com/

In view of the deleterious consequences described of both absence and excess glucocorticoid during fetal life, maintaining fetal exposure to glucocorticoids at appropriate levels is critical for normal embryonic development. Clearly, the tight control of glucocorticoid action within fetal tissues by its receptor (GR) and by enzymic glucocorticoid metabolism is likely to play an imperative role in prenatal development.

1.4.2 Glucocorticoid receptor (GR) structure

The GR is an intracellular steroid hormone receptor belonging to the super-family of nuclear hormone receptors (Mangelsdorf et al., 1995; Funder, 1996). These receptors are capable of interacting with target gene promoters upon cognate ligand binding, so they are also referred to as ligand-dependent transcription factors (Mangelsdorf et al., 1995).

Two phenotypically distinct isoforms of GR have been identified in humans: GRα, (the predominant physiological isoform) and GRβ (Hollenberg et al., 1985) of molecular weight 94 kDa and 90 kDa, respectively (Oakley et al., 1996). In the rodent, GR cDNAs that have been identified are homologues of the GRα isoform (Danielsen et al., 1986).

Each GR isoform in the human is encoded by nine exons, of which the first eight are identical and the ninth heterologous. Exon 1 encodes the 5' un-translated sequence, the amino terminal sequence is found in exon 2, DNA binding domains are encoded by exons 3 and 4, and the cortisol-binding domain is formed from 5-9 exons (Encio and Detera-Wadleigh, 1991) (Figure 1.15).
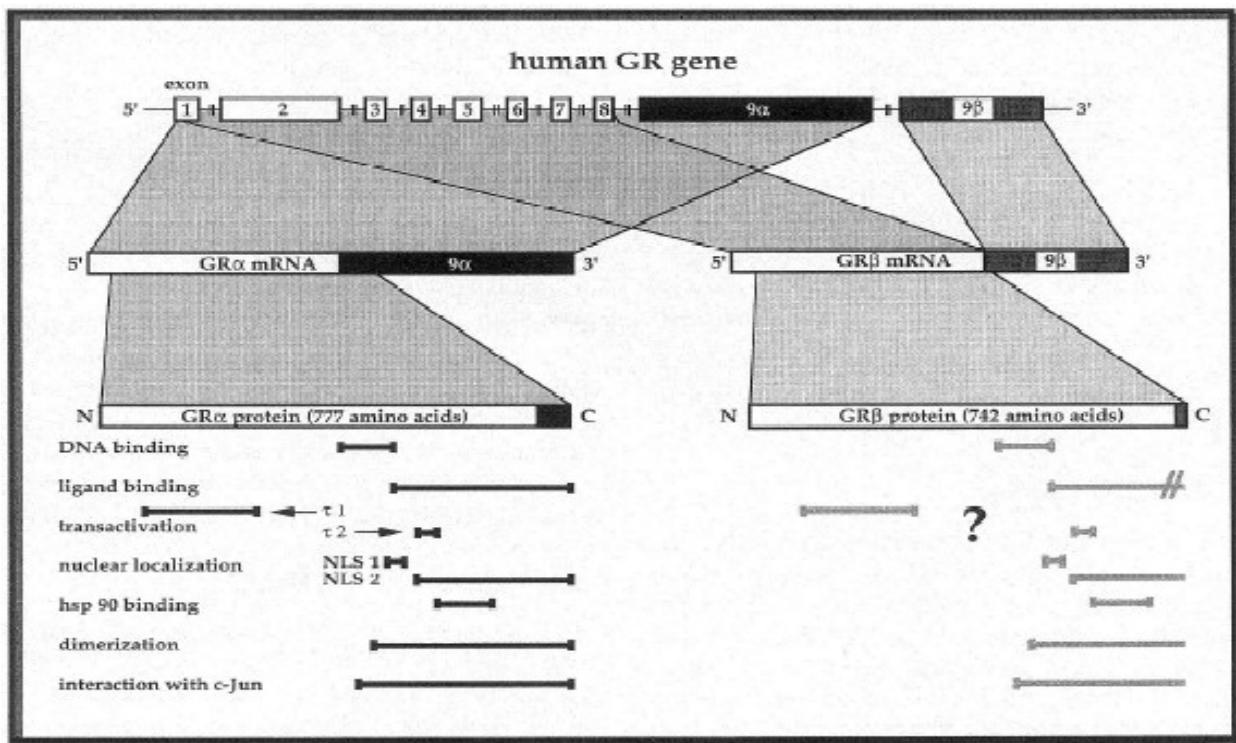
Figure 1.15: **Structures of the human GR-α and β genes and proteins. Functional sub-domains of the α-isoform are stated beneath the diagram; functional sub-domains of the β-isoform are largely undefined (Bamberger et al., 1996).**

All members of the nuclear hormone receptor super-family are organised into three structurally and functionally defined domains. Specifically, the GRα isoform has an N-terminal domain which is concerned with activation of target genes, a central DNA-binding domain involved in interactions with DNA sequences of target genes and a C-

terminal domain for ligand (glucocorticoid) binding (Oakley et al., 1996). The C-terminal domain is more complex, as it is also involved in heat shock protein binding (Dalman et al., 1991), nuclear translocation (Picard and Yamamoto, 1987), receptor dimerization (Dahlman-Wright et al., 1992) and trans-activation (Hollenberg and Evans, 1988).

Sequence analysis reveals that the GRα and β polypeptides in humans are 777 and 742 amino acids in length, respectively. The first 727 amino acids are identical in either isoform; the distinction only comes at the C-terminus with the substitution of the last 50 amino acids of GRα with a non-homologous 15 amino acid sequence in the case of GRβ (Hollenberg et al., 1985) (Figure 1.15). The two isoforms of the human GR are generated from the same gene by alternative splicing of the human GR primary transcript (Encio and Detera-Wadleigh, 1991; Oakley et al., 1996). The heterologous region of the carboxy terminal residues and the 3' untranslated regions of the two human GR isoforms are encoded separately by two different ninth exons: 9α and 9β (Encio and Detera-Wadleigh, 1991). The unique C-terminal end of human GRβ alters several key biochemical properties of this isoform which functionally distinguish it from the GRα isoform (Oakley et al., 1996). For instance, the steroid binding properties characteristic of GRα are absent in GRβ (Hollenberg et al., 1985; Bamberger et al., 1995).

In the absence of glucocorticoid, GRα is located predominantly in the cytoplasm of cells as part of a multi-protein complex (Oakley et al., 1996). The complex consists of the receptor, two molecules of hsp90 and one molecule each of hsp70 and hsp56, its main

function being to retain the receptor protein in a silent yet responsive state (Pratt, 1993) (Figure 1.16).

In contrast to GRα, GRβ in human cells is localised primarily in the nucleus, independent of the presence of glucocorticoid hormone (Oakley et al., 1996). However, as GR cDNAs that have been described in rodents are homologues of the human GRα isoform (Danielsen et al., 1986), only this isoform will be discussed further now.

1.4.3 Mechanism of action of GRα

Cognate hormone binding induces a conformational change in GRα which leads to dissociation from the heat shock complex and concomitant hyper-phosporylation of GR. Nuclear localisation signals within the C-terminal domain are unmasked and receptor molecules, with glucocorticoid bound, translocate to the nucleus (Bamberger et al., 1996). Two alternative mechanisms have been presented to describe the mechanism of hormone-activated GRα action within the nucleus (Figure 1.16).
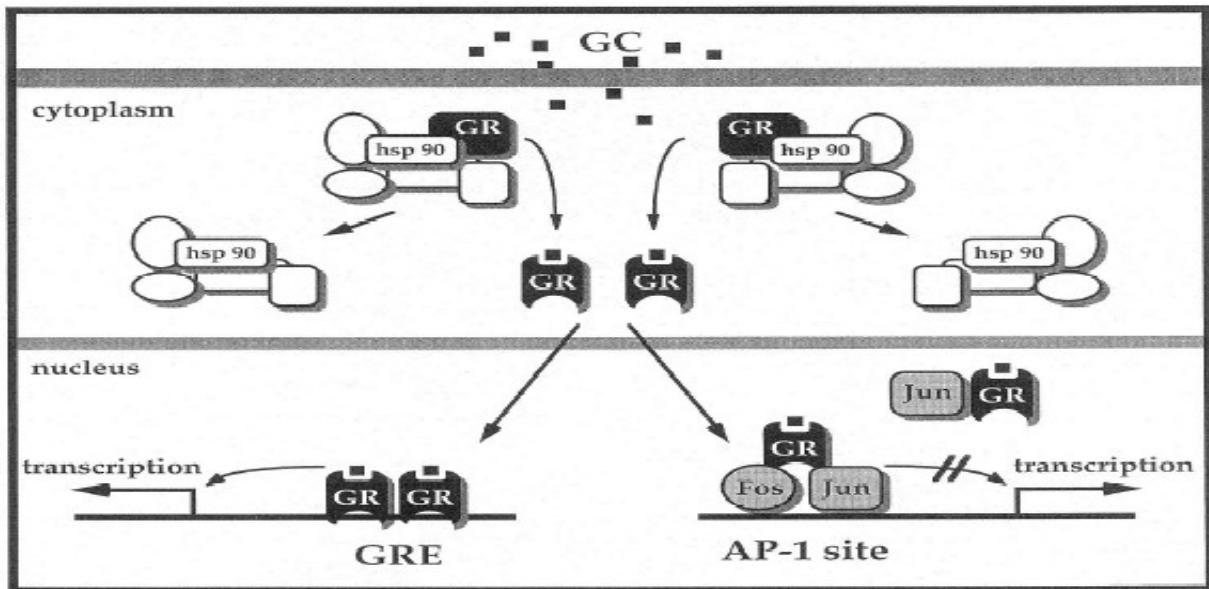
Figure 1.16: **Model of GRα-mediated transcriptional modulation. The type 1**

mechanism involves GRα homo-dimers binding to regulatory regions of target

genes and usually results in stimulation of target gene transcription, although

inhibition of transcription may occur (less frequently) by this mechanism.

The type 2 mechanism most frequently results in inhibition of transcription and

involves interactions between a GRα monomer and other transcription factors

(Bamberger et al., 1996).

Key to Figure 1.15: GC = Glucocorticoid; GRE = Glucocorticoid response element;
                  AP-1 = Activating Protein-1

Type 1 mechanism: (Figure 1.16, left hand side).

The first mechanism is the classic model of GRα action and refers to homo-dimerisation

of activated GRα molecules which enables binding of glucocorticoid responsive

elements, (GREs). These are specific palindromically arranged DNA sequence motifs in

the promoter regions of glucocorticoid target genes within the nucleus. Once bound to

the GRE, the GRα homo-dimer interacts with the basal transcription machinery directly

or via 'bridging molecules' to enhance transcription by RNA polymerase II.

Occasionally, binding of negative GREs by three active GRα molecules causes inhibition

as opposed to enhancement of transcription by this mechanism (Bamberger et al., 1996).

Thus, binding of GREs by this receptor isoform can enhance or repress transcription of

the linked gene (Oakley et al., 1996).

Type 2 mechanism: (Figure 1.16, right hand side)

As an alternative to GRE binding, the second mechanism by which GRα may mediate

glucocorticoid action is via interaction with other transcription factors. As the repression

of immune genes has an important part to play in the anti-inflammatory/immuno

-suppressive role of glucocorticoids, GRα-mediated inhibition of transcription factors for

the transcription of such target genes is of physiological significance. For example, AP-1

is a transcription factor composed of heterodimers of *Jun* and *Fos* protein which

positively regulates immune gene expression by binding to AP-1 sites within the

promoter regions of such genes. Active GRα monomers act to inhibit the transcription of

such genes by binding *Fos* and *Jun* proteins. In this way, GRα acts as a negative

regulator of the AP-1-mediated expression of immune genes, in the absence of any direct

DNA binding at the AP-1 site (Figure 1.16). Similar patterns of GRα-mediated gene

repression have been shown for other transcription factors, Nuclear Factor-kB, for

instance which is also involved in activating many immune system genes (Bamberger et

al., 1996).

1.4.4 Mineralocorticoids and the mineralocorticoid receptor

In addition to glucocorticoids, the adrenal cortex also produces the mineralocorticoid corticosteroid, aldosterone, but from the outer *zona glomerulosa* region of the adrenal cortex (Funder, 1996). However, aldosterone is secreted in much lower quantities than the glucocorticoid; glucocorticoid circulates at concentrations of 100-1000 times higher than aldosterone (Rusvai and Naray-Fejes-Toth, 1993). Mineralocorticoid receptors (MR) belong to the same subfamily of receptors as the glucocorticoid receptors (Funder, 1996). MRs are characteristically non-selective receptors; human renal MR *in vitro* binds cortisol and aldosterone with equal affinities (Arriza et al., 1987).

MRs are expressed in a wide variety of tissues which include both classic mineralocorticoid target tissues such as the kidney, parotid and colon, as well as other tissues such as the hippocampus and heart (Krozowski and Funder, 1983). In mineralocorticoid target tissues, aldosterone is involved in the regulation of plasma salt-water balance, ultimately leading to sodium retention and blood pressure homeostasis (Funder, 1996). (See aldosterone mode of action in top section of Figure 1.17).
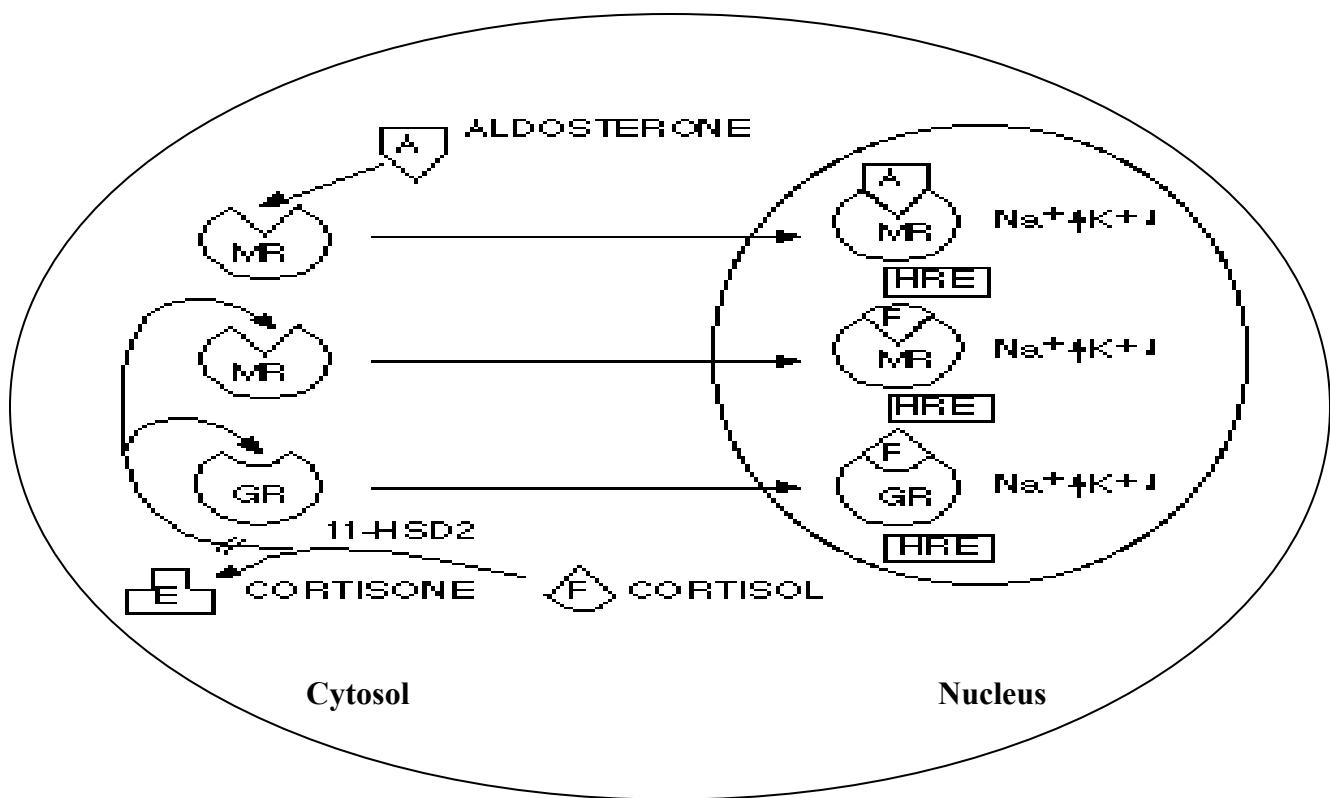
Figure 1.17: **Model of mineralocorticoid receptor activation by aldosterone in a mineralocorticoid-target cell (Funder, 1996)** [**Key**: HRE = Hormone response element]

Although corticosterone (cortisol) and aldosterone are similarly bound in the hippocampus and the heart *in vivo*, the classical mineralocorticoid target tissues are selective for aldosterone only, and show negligible corticosterone binding (Sheppard and Funder, 1987). In view of this, it was hypothesised that endogenous glucocorticoids, but not aldosterone, are inactivated by the enzyme 11 beta dehydrogenase (11β hydroxysteroid dehydrogenase type 2) in mineralocorticoid target cells which prevents glucocorticoids from acting as mineralocorticoids and binding the MR, thus allowing selective mineralocorticoid action (Funder et al., 1988; Edwards et al., 1988), (Figure 1.17 - lower section).

1.4.5 Enzymatic modulation of glucocorticoid action

11-beta hydroxysteroid dehydrogenase (11β HSD) is a microsomal enzyme complex associated with endoplasmic reticulum responsible for catalysing the inter-conversion of active cortisol and biologically inactive cortisone (Mahesh and Ulrich, 1960). Hence, the 11β HSD family of enzymes play a critical role in controlling local tissue concentrations of glucocorticoids (Edwards et al., 1996) and glucocorticoid exposure to the GR (Draper and Stewart, 2005). The enzyme complex is composed of two distinct components, one of which catalyses oxidation (the 11β-dehydrogenase) and the other responsible for reduction (the 11-oxoreductase) (Lakshmi and Monder, 1985a).

11β HSD type 1 (34 kDa) (Monder and Lakshmi, 1990) predominantly catalyses the reduction of cortisone to cortisol (Edwards et al., 1996; Funder, 1996) and is largely dependent on binding the co-factor NADP for its activity (Rusvai and Naray-Fejes-Toth, 1993). 11β HSD type 2 (40 kDa) (Gomez-Sanchez et al., 2001) exclusively catalyses the oxidation of cortisol to cortisone (Edwards et al., 1996) and depends almost totally on binding co-factor NAD which acts as a hydrogen acceptor (Rusvai and Naray-Fejes-Toth, 1993) (Figure 1.18).
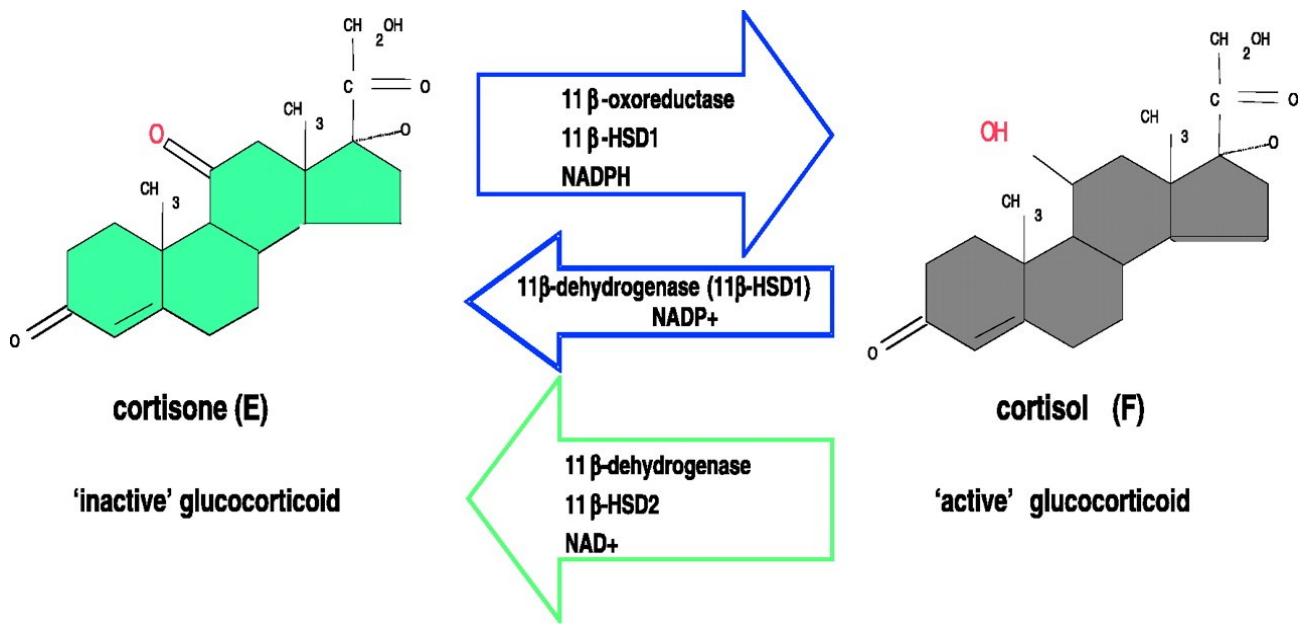
Figure 1.18: Enzymatic actions of 11β hydroxysteroid dehydrogenase on the substrates to which it binds (Draper and Stewart, 2005). **Both 11β HSD type-1 and -2 are glycosylated membrane proteins present in endoplasmic reticulum.**

The proportions of the different enzyme components present vary between different tissues; in the rat, the liver is the major site of action of 11β HSD type 1 and hence in this tissue reduction usually exceeds oxidation (Lakshmi and Monder, 1985b); other tissues where this isozyme regenerates cortisol include adipose tissue, the central nervous system and the lung (Seckl, 2004). In adipose tissue the 11β HSD type 1 activity gives rise to elevated levels of active intracellular glucocorticoid which alters a number of target genes, including leptin (Seckl, 2004).

1.4.6 Regulation of glucocorticoid exposure to the GR: a role for reductace (11β HSD type 1) activity in glucocorticoid target tissues

Expression of 11β HSD type 1 more closely parallels that of the GR than that of the MR, to regulate exposure of cortisol to the GRs (Ricketts et al., 1998). So, in glucocorticoid target tissues, 11β HSD type 1 is highly expressed and facilitates glucocorticoid exposure to the GR. Mouse 11β HSD type 1 knockout studies have highlighted the importance of hepatic 11β HSD type 1 in activating gluconeogenic enzymes and regulating hepatic glucose output (Draper and Stewart, 2005). Glucocorticoids stimulate gluconeogenesis while phosphoenolpyruvate carboxykinase (PEPCK) and glucose-6-phophatase catalyse the key steps involved. Upon starvation, these enzymes usually are induced by glucocorticoids, but in 11β HSD type 1 knockout mice there is a failure to initiate induction of these enzymes. Conversely, in fed mice liver glycogen accumulates due to a lack of glucocorticoid-induced glycogenolysis, thus such mice are able to resist the hyperglycaemia found in obese wild types (Kotelevtsev et al., 1997). In the rat kidney the predominant enzymatic conversion is in the opposite direction to the liver, i.e. in favour of oxidation (Mahesh and Ulrich, 1960; Edwards et al., 1996).

1.4.7 Protection of MR from glucocorticoids in mineralocorticoid target cells: a role for 11β dehydrogenase (11β HSD type 2) activity

The activity of the 11β dehydrogenase component of the 11β HSD enzyme complex is shown for homogenates of renal cortex, parotid, hippocampus and heart in Figure 1.19.

The highest activity was evident in the kidney with lower levels also apparent in the parotid. In contrast, in the hippocampus and heart, the enzyme activity was minimal or absent (Edwards et al., 1988; Funder et al., 1988).
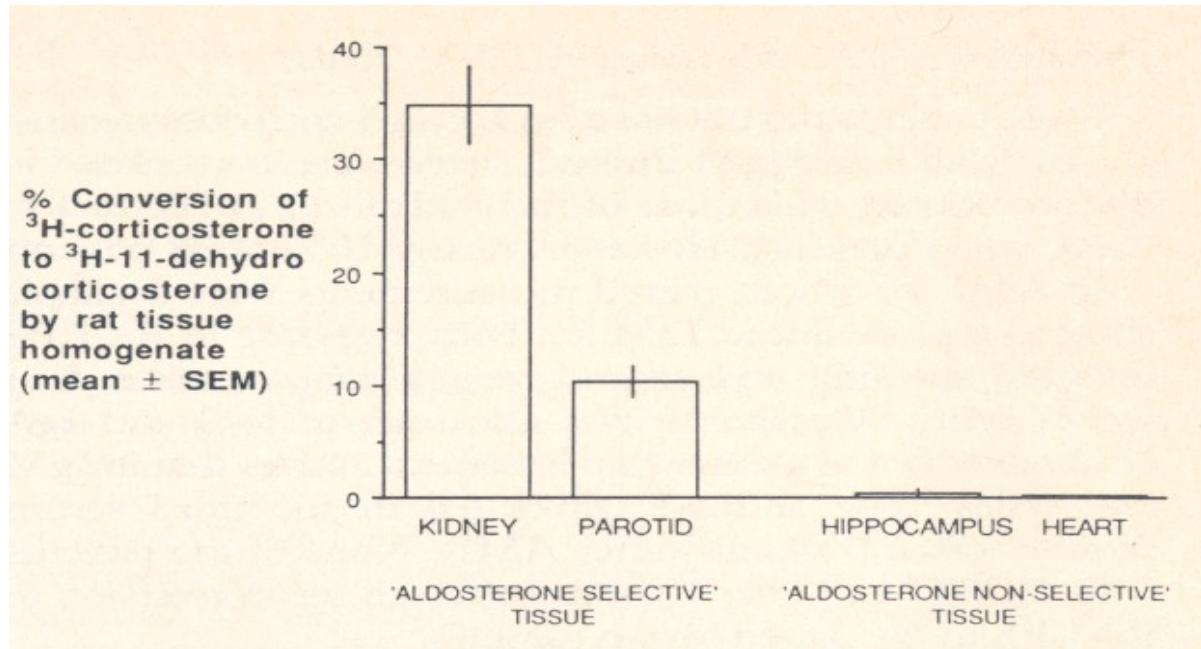
Figure 1.19: **Activity of the 11 beta dehydrogenase component of the 11β hydroxysteroid dehydrogenase enzyme in rat renal cortex, parotid, hippocampus and heart (Edwards et al., 1988). Note: corticosterone is the rodent equivalent of cortisol in humans, and 11-dehydro-corticosterone is equivalent to cortisone.**

These results are interesting because the kidney and parotid which showed significant 11β HSD activity are two major aldosterone-selective tissues. Furthermore, other organs which contain aldosterone receptors but are not aldosterone selective, such as the hippocampus and heart, show minimal levels of 11β HSD activity (Edwards et al., 1988).

Corticosterone, (the rodent equivalent of cortisol in humans) is effectively excluded from the MR to prevent inappropriate activation of MR in mineralocorticoid target tissues by

the dehydrogenase activity of 11β HSD. The inert product of the reaction does not bind

MR to any significant extent; it has only ~0.3% of the binding affinity of corticosterone

(Funder et al., 1988). The role of this dehydrogenase enzyme in conferring selectivity in

aldosterone target tissues is indicated by the use of carbenoxolone *in vivo* which inhibits

its activity. In the presence of carbenoxolone, the level of corticosterone binding to MR

markedly increases and approaches (colon) or equals (kidney and parotid) that of

aldosterone in mineralocorticoid target tissues (Funder et al., 1988). Likewise, other

studies have shown a similar loss of aldosterone selectivity in tissues such as the kidney

upon inhibition of the dehydrogenase component of 11β HSD (i.e. 11β HSD type 2)

(Edwards et al., 1988). In keeping with these observations, congenital deficiency of this

dehydrogenase activity is clinically associated with the "Syndrome of Apparent

Mineralocorticoid Excess," (SAME) characterised by severe hypertension, hypokalaemia

(abnormally low plasma potassium) and sodium retention (Edwards et al., 1988) in adult

patients (Ulick et al., 1979; Stewart et al., 1988). Symptoms of mineralocorticoid excess

have also been reproduced experimentally in rodents; rats showed an increase in blood

pressure, hypokalaemia and decreased plasma protein levels, but sodium levels were

unaffected (Campion et al., 1998).

1.4.8 Protection of the fetus *in utero* from maternal glucocorticoid: a role for 11β dehydrogenase (11β HSD type 2) activity in the placenta

The separation of the fetal circulation from glucocorticoids of maternal origin is crucial for the normal development of the fetal hypothalamic-pituitary-adrenal axis, and also ensures that the correct pattern of gene expression is followed (Chatelain et al., 1980). Normally, the fetus is protected from the higher levels of physiological glucocorticoids (cortisol in humans; corticosterone in rats) in the mother by placental 11β HSD which rapidly metabolises these to inert products (Seckl and Brown, 1994). Hence, the enzyme acts as a gatekeeper to prevent glucocorticoids from the maternal circulation from flooding the fetal system (Langley-Evans, 2001).

1.4.9 Erroneous glucocorticoid exposure to the fetus

It is hypothesised that: 'abnormally low placental 11β-dehydrogenase activity, by increasing fetal exposure to maternal glucocorticoids, leads to intrauterine growth retardation and high blood pressure in adulthood' (Edwards et al., 1993). This hypothesis is supported, in part, by the finding that in rats after a normal pregnancy, there is a strong positive correlation between placental 11β-dehydrogenase activity at term and fetal weight at term (Benediktsson et al., 1993) (Figure 1.20).
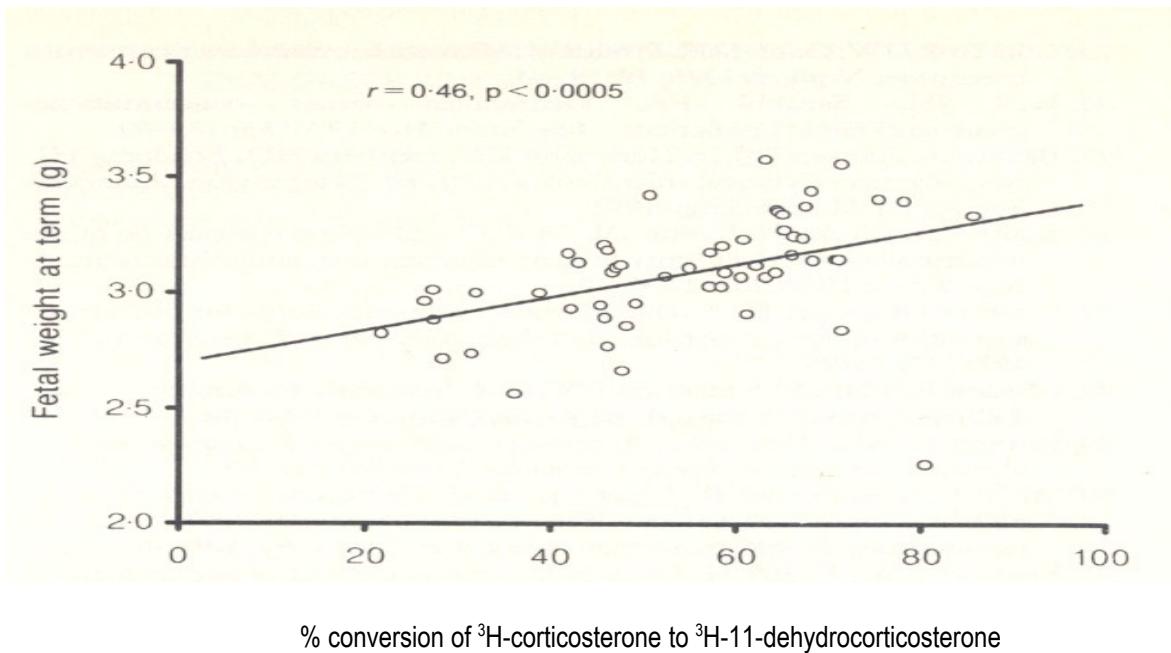
Figure 1.20: **Correlation between fetal weights at term with placental dehydrogenase activity (Benediktsson et al., 1993).**

Excess levels of glucocorticoid may also have implications for the developing fetus in terms of a disruption to the useful roles played by normal levels of glucocorticoid, e.g. in fetal liver where glucocorticoids usually control gluconeogenesis and hepatic glucose output.

1.4.10 Pharmacological manipulation of fetal exposure to glucocorticoid

Pharmacological manipulation studies in rats of fetal exposure to glucocorticoid offer further support for the hypothesis of Edwards et al (1993) that excess exposure of the fetus to maternal glucocorticoids may be the link between low birth weight and subsequent hypertension in humans, and also indicate a key role for placental 11β HSD in

controlling such fetal exposure (Lindsay et al., 1996). Analogous to the maternal low protein model, the treatment of pregnant control-fed rats with a low dose of the synthetic glucocorticoid dexamethasone (-a poor substrate for 11β HSD type 2 which crosses the placenta freely), throughout pregnancy results in a decrease in offspring birth-weight. Furthermore, the maternal dexamethasone treatment significantly increases systolic blood pressure in male and female offspring when reaching adulthood (Benediktsson et al., 1993). Similarly, maternal carbenoxylone (an inhibitor of 11β HSD type 2) treatment throughout pregnancy leads to reduced birth weight (20% mean decrease) and elevated blood pressures in male and female adult offspring of carbenoxolone-treated rats (Lindsay et al., 1996). Notably, this effect requires the presence of maternal adrenal products, as carbenoxolone treatment given to adrenalectomised mothers had no effect on offspring birth weight or blood pressure, thus supporting a role for maternal glucocorticoid in this system in mediating the observed offspring effects. Hence, further to the work of Benediktsson *et al,* 1993 described previously, these results show that in the rat model, endogenous maternal glucocorticoids may exert similar effects to synthetic glucocorticoids, once the placental enzymic barrier is inhibited (Lindsay et al., 1996).

1.4.11 Nutritional modulation of fetal corticosteroid exposure may underlie the programming effects of low protein diets *in utero*

In rats, near term activity of the placental isoform of 11β HSD was lowered by 33% by the maternal low protein diet. This was not part of an overall attenuation of placental function, as activity of other (steroid insensitive) placental enzymes was unaltered by the

diet manipulation (Langley-Evans et al., 1996a). Similarly, placental 11β HSD type 2 mRNA content has been shown to be decreased in the placentas of rats fed a low protein diet throughout pregnancy (Bertram et al., 2001). Moreover, placental activity of the glucocorticoid-inducible enzyme glutamine synthase (GSase) was elevated by 27% in rats exposed to the maternal low protein diet *in utero* which may reflect increased glucocorticoid action within the placenta as a consequence of impaired inactivation by placental 11β HSD (Langley-Evans et al., 1996a). The molecular mechanisms through which dietary protein restriction selectively lowers placental 11β HSD activity and dampens its expression remain to be elucidated. However, it is possible that an epigenetic mechanism may provide an explanation for this link (see section 1.4.12). If indeed epigenetic changes do mediate a link between the low protein diet and the expression/activity of this enzyme component, in theory other dietary interventions may also mediate its expression i.e. this phenomenon may not be exclusive to dietary protein restriction; exposure to high fat diets or global under-nutrition may also produce epigenetic alterations in the 11β HSD type 2 gene specific to the dietary intervention. Indeed in sheep, placental 11β HSD type 2 mRNA is lowered in mid-gestation placenta following global maternal nutrient restriction during early-mid gestation (Whorwood et al., 2001).

Placental deficiency of 11β HSD may be a common mechanism whereby the maternal environment (i.e. dietary protein nutrition) alters feto-placental development, and programmes hypertension (Langley-Evans et al., 1996a). Hence, a role for maternal glucocorticoids in mediating the effects of maternal low protein diet is implied.

In view of the documented effects of dexamethasone (Benediktsson et al., 1993) and

carbenoxolone (Lindsay et al., 1996) exposure to fetuses *in utero* on subsequent blood

pressure, it is likely that the decrease in placental 11β HSD in low protein diet fed rats

leads to over-exposure of their fetuses to maternal glucocorticoid hormone action

(Langley-Evans et al., 1996a) (Figure 1.21).
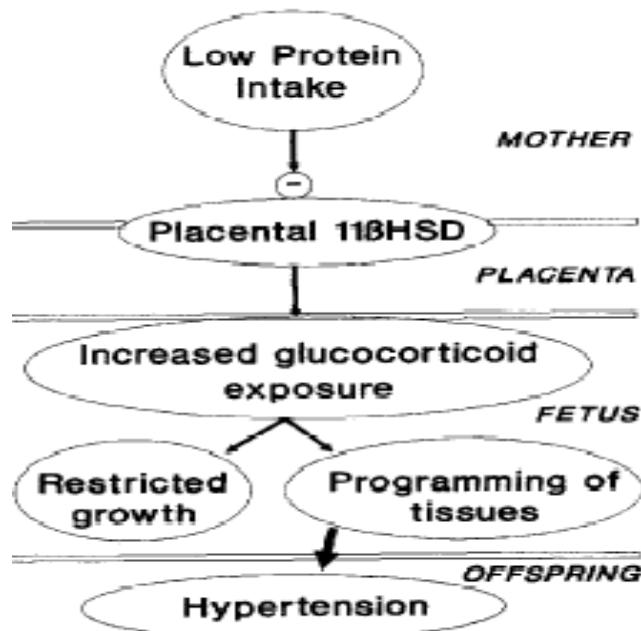
Figure 1.21: **Model of a possible mechanism linking maternal low protein diet to**

hypertension in offspring. Placental 11β HSD activity normally protects the fetus

from the programming effects of maternal glucocorticoids, but this barrier is

susceptible to modulation by nutritional factors (Langley-Evans et al., 1996b).

Interestingly, the treatment of pregnant rats fed a protein-replete control diet throughout

gestation with carbenoxolone reduced birth-weight and induced hypertension in their

offspring in a manner equivalent to that observed in the offspring from mothers fed a low

protein diet throughout pregnancy (Langley-Evans, 1997b). The offspring of the protein-replete animals were exposed to increased levels of endogenous corticosterone, through carbenoxolone inhibition of 11β HSD type 2. Both protein under-nutrition and carbenoxolone treatment in pregnancy produced effects on fetal growth, later blood pressure and body proportions of the fetus (Langley-Evans, 1997b). This further indicates that the low protein diet may initiate pathways leading to increased exposure to endogenous glucocorticoid, analogous to carbenoxolone by causing a down regulation of placental 11β HSD activity.

Metyrapone is an inhibitor of maternal glucocorticoid synthesis and effectively pharmacologically adrenalectomises treated animals. To assess the role of glucocorticoids in programming the hypertensive state in offspring from low protein diet fed mothers, metyrapone was administered for the first 14 days of pregnancy to dams consuming either low protein diet or control diet throughout gestation. The metyrapone treatment of pregnant rats fed low protein diet resulted in offspring at 8 weeks which did not develop raised blood pressure, whereas offspring from dams who received a low protein diet but no metyrapone exhibited the classical hypertensive state. Thus, the metyrapone treatment during the first 2 weeks of pregnancy had long term programming effects on alleviating the maternal-diet induced hypertension in the offspring. Hence, it appears that in the low-protein diet exposed rat fetuses, maternal corticosterone synthesis is a pre-requisite for the initiation of the hypersensitive state. However, this dietary effect was not reflected in maternal corticosterone concentrations (Langley-Evans et al., 1996b). In a follow up study, corticosterone administration to metyrapone-treated

pregnant rats fed the low protein diet restored the hypertensive effect of the diet (Langley-Evans, 1997a). Hence, nutritionally-induced hypertension depends on maternal glucocorticoid production and again it appears to be mediated through increased access of maternal glucocorticoids to fetal tissues, via the placenta (Langley-Evans, 2001). Nevertheless, the precise molecular mechanisms through which maternal dietary protein restriction selectively alters placental 11β HSD activity remain to be determined. Although the feeding of low protein diets to pregnant rats may result in an over-exposure of the fetuses to the programming effects of maternal corticosteroids, the programming of later disease states is unlikely to depend on glucocorticoids alone (Langley-Evans et al., 1996a).

1.4.12 Epigenetic regulation of transcription

It is possible that the molecular mechanism linking maternal low protein diet and decreased placental 11β HSD expression might involve epigenetics. The presence of CpG islands along the 11β HSD type 2 gene suggests that it might be regulated in part via CpG methylation. In general, hyper-methylation of normally unmethylated CpG islands correlates with transcriptional repression (Alikhani-Koopaei et al., 2004). DNA methylation of the gene encoding 11β HSD type 2 in the placenta would provide a means through which a compromised protein diet might down regulate placental expression of the enzyme.

Studies in the rat, on the DNA methylation status of the hepatic GR gene in post weaning offspring of mothers fed a low protein diet throughout pregnancy have shown that the methylation status of the GR promoter, GR exon 1 $_{10}$ was between 23% to 33% lower in these offspring relative to controls, and that the level of mRNA expression of GR was greatly increased relative to controls (Lillycrop et al., 2005; Lillycrop et al., 2007). Such findings indicate that the GR gene transcription is increased in response to maternal protein restriction and thus suggest a mechanism by which insults in early life might lead to persistent changes to offspring phenotype. Interestingly, it appears that the alterations in hepatic GR expression in the F1 offspring persist, and are passed onto the next generation in the absence of any further dietary protein restriction (F1 females received a control diet throughout their subsequent pregnancies). These data indicate that alteration in the methylation status of the GR gene promoter induced in the F1 generation by maternal protein restriction throughout pregnancy is transmitted to the F2 generation (Burdge et al., 2007). Further studies in the rat investigating how the altered epigenetic regulation of the hepatic GR promoter is induced in offspring of the protein-restricted mothers have found that DNA methyltransferase-1 (Dnmt1) transcript expression was lower in offspring from mothers fed a protein restricted diet throughout pregnancy. Thus, hypomethylation of the GR promoter may result from a reduced capacity to methylate hemimethylayted DNA during meiosis. Furthermore, histone modifications that facilitate transcription were increased at the GR promoter, and those that suppress methylation were decreased. This suggests that induction of altered epigenetic regulation of the hepatic GR promoter in the offspring may be attributed to reduced Dnmt1 expression (Lillycrop et al., 2007).

1.5 Main project objective

The overall aim of this investigation is to assess the impact of a relatively mild maternal dietary protein restriction in the mouse, imposed either throughout pregnancy or during the pre-implantation period only, on the subsequent development of the fetus.

The aim of the project will be met by studying the responses of the fetus to the maternal dietary challenge using three broadly different approaches. The response of the fetal liver to the maternal dietary challenge will be examined close to the end of gestation (at day 17) in terms of its global gene expression profile with the use of Affymetrix micro-array technology. In this way target genes of interest may be pinpointed as possible candidates for further study. The level of hepatic protein expression will also be examined at this stage by immunoblotting and densitometry of specific proteins thought to be involved in subsequent programming of growth and development. Finally, the growth phenotype of the conceptus and fetus and component tissues will be analysed at gestational day 17 after transfer at day 3.5 of embryos from 9% casein fed mothers to 18% casein fed fosters using embryo transfer surgery.

1.6 Rationale and relevance to human nutrition

Due to widespread vegetarianism in the developed world the low protein model is relevant to human nutrition. Those who opt for a vegetarian or vegan diet must take extra care to ensure that a proper nutrient balance is supplied by their diet. In particular, the diet must contain enough protein, with the correct balance of amino acids to ensure that sufficient human protein can be formed following digestion and absorption. This is particularly important during pregnancy, especially as it may not be obvious to the pregnant individual that her diet is lacking in total protein or indeed specific amino acids.

Studies have shown that amino acids have a key role in fetal growth; there appears to be a large amino acid deficiency *in utero* in growth retarded babies (Cetin et al., 1988). Amino acids are also the major factors controlling pancreatic Beta-cell growth and development in the fetus and insulin section until late in fetal life (De Gasparo et al., 1978; Snoeck et al., 1990). As the development of Beta cells usually proceeds rapidly during fetal life (Hellerstrom et al., 1988) it is possible to see how it could be vulnerable to sub standard nutrition (Hales and Barker, 1992).

Poor early development of pancreatic islets of Langerhans and Beta cells has been associated with the aetiology of Type 2 diabetes (Hales and Barker, 1992); thus it is possible to visualise links between maternal low protein diets and such metabolic disorders. However, this is not to say that other nutritional defects are excluded from contributing to the onset of these metabolic disorders.

Chapter 2

Generic Materials and Methods

2.1 Experimental design

Adult MF1 strain female mice between 7 and 8.5 weeks of age were used in this study
(mice usually reach sexual maturity from 6 weeks of age). Females were weighed prior
to mating and those falling within the weight range of 27-33 g were selected. This was to
ensure a constant body size/uterus size of the mother to avoid introducing variation into
uterine environment. Mothers were also weighed on day of plug, at 3.5 days gestation
and on day of cull (17 days gestation) to ensure no weight loss occurred during
pregnancy.

The mouse is a useful model in which to study developmental biology as mice have a
short gestation period, reach maturity quickly and have a high fertility rate. Furthermore,
the mouse and human genomes each seem to contain about 30,000 protein-
coding genes and the proportion of mouse genes with a single identifiable
orthologue in the human genome is high, approximately 80% (Waterston et al.,
2002). Finally, as the mouse is also an established transgenic model it is
possible to follow up genomics studies and analyze specific gene functions in
programming using transgenic technology.

Three dietary treatment groups were used in this study (Figure 2.1): the 18% casein diet is a control diet which provides a sufficient amount of protein to a pregnant mouse; the 9% casein diet provides half the amount of protein as the control diet as may thus be referred to as a low protein diet; the switch diet uses both types of diets and comprises the 9% casein diet for the first 3.5 days of pregnancy (i.e. during the murine pre-implantation period) and then the 18% casein diet for the remainder of pregnancy until cull (gestational day 17).
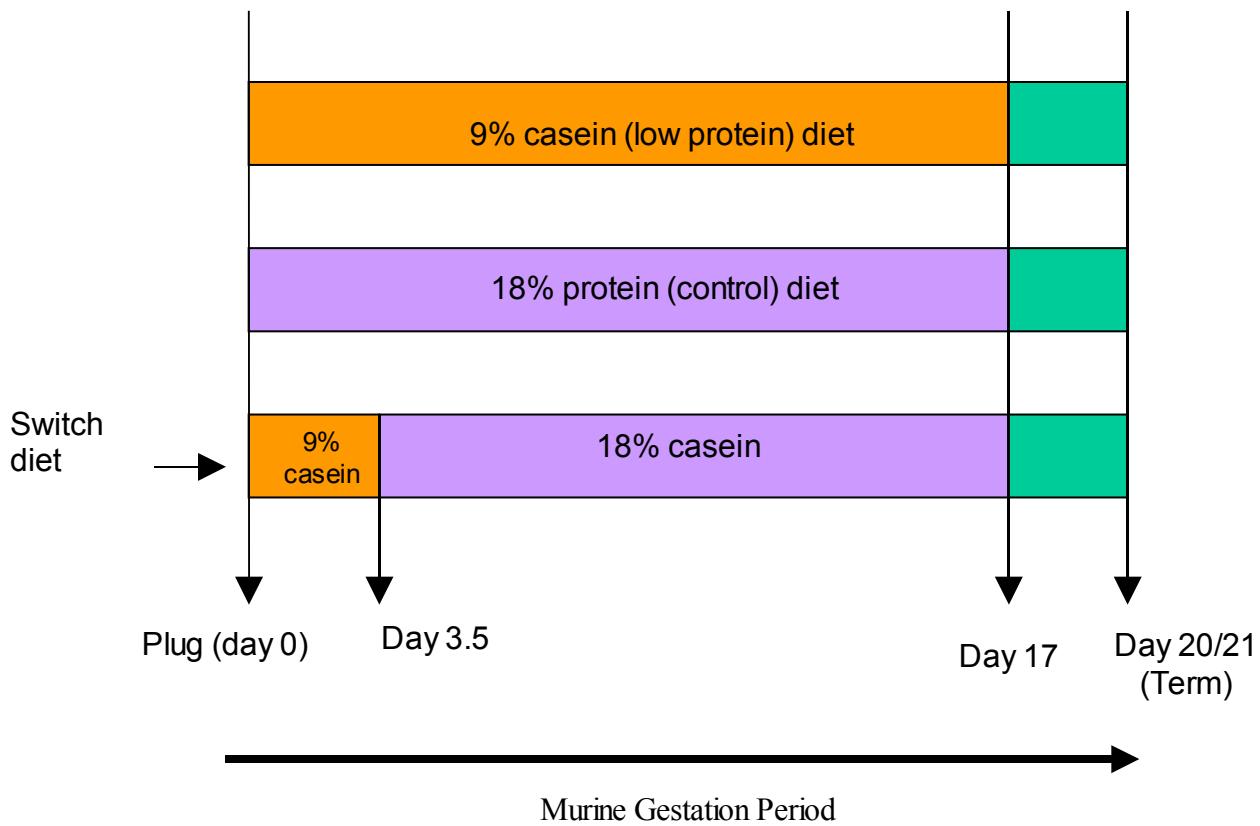
Figure 2.1: Maternal dietary treatment groups administered from day of plug

Key: <3.5 days (approx.) = during pre-implantation embryo development.

The allocation of mice to diet groups was rotated evenly to ensure that no single diet treatment is assigned all at one time. This minimises the chance that changes in environment over time might confound the results and cause false differences between diet groups.

2.2 Animal treatments

All animal experiments were conducted under Licence from the UK Home Office. Out-bred MF1 mice bred at Southampton University Biomedical Facility were used in this study. Mice were maintained under constant conditions of 24°C under a controlled light-dark cycle (lights on 0700 hours, lights off 1900 hours).

Female mice were fed a standard chow diet and tap water *ad libitum* and housed in groups of up to 12 from time of weaning at 3-4 weeks until 7 weeks of age when experimental procedures commenced. Virgin MF1 females were naturally mated overnight with individually housed male MF1 mice and mating was defined by the presence of a vaginal plug (coagulated proteins from the male seminal fluid) the following morning. Plug-positive females were then housed individually and randomly assigned to synthetic diets; diets were either prepared in-house or bought in ready made (Lillico, UK). Diet composition in either case was as outlined in Table 2.1. **All experimental data for the Genomics Analysis (Chapter 4), Protein Analysis (Chapter 5) and Embryo Transfer studies (Chapter 6) was collected using mice that were fed the bought in diets only.** Mice were fed diet *ad libitum* until day 17 of

pregnancy with free access to tap water. Note, mating was assumed to take place around midnight.

	18% casein	9% casein
Casein	18.0	9.0
Corn starch	42.5	48.5
Cellulose fibre	5.0	5.0
Sucrose	21.3	24.3
Choline chloride	0.2	0.2
DL-Methionine	0.5	0.5
Mineral mix (AIN-76)	2.0	2.0
Vitamin mix (AIN-76)	0.5	0.5
Corn oil	10.0	10.0
	=100 g	=100 g

Table 2.1: Composition of synthetic isocaloric casein diets (g per 100 g of diet) (Langley and Jackson, 1994; Langley-Evans et al., 1996a). **Ingredients supplied by Special Diet Services, Cambridge, UK.**

In house diets were provided to animals as balls (60-100 g dry weight); bought in diets were presented as smaller uniformly sized pellets. In either case the protein source was casein and all diets contained 5g//kg methionine to avoid sulphur deficiency.

The 9% casein and 18% casein diets were always of equivalent total caloric value (i.e. 4.17 kcal /g). As the proportion of the total calories contributed by casein (protein) differed, the total calories were adjusted by varying the amount of corn starch and also the sucrose content as indicated in Table 2.1; Figures 2.2 and 2.3 graphically display the difference between the compositions of the diets used. Whilst adjustments were made to the carbohydrate composition of the low protein diet to maintain an equivalent energy

content between the diets, these changes are relatively small compared to a halving of casein content.
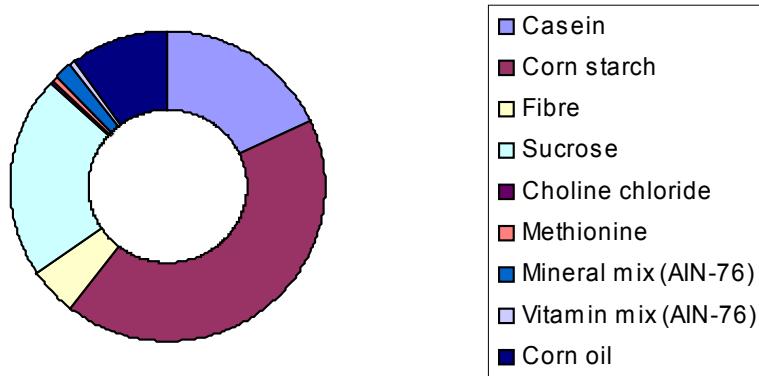
Figure 2.2: Nutrient composition of the 18% casein (control) diet.
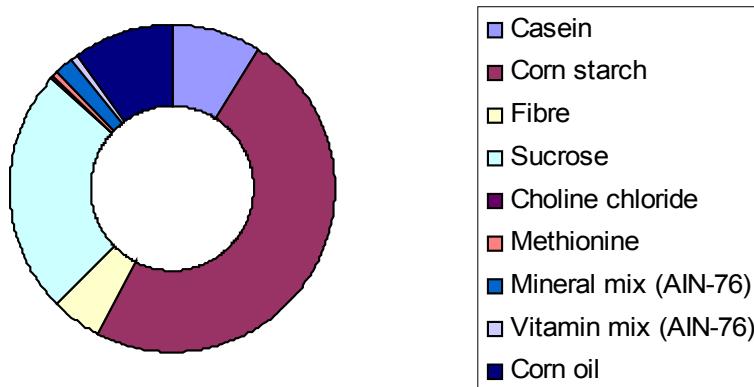
Figure 2.3: Nutrient composition of the 9% casein (low protein) diet.

2.3 Recovery of conceptuses

On gestational day 17, pregnant adults were culled by cervical dislocation of the neck and the uterus was promptly dissected out and placed in ice cold phosphate buffered saline (PBS). Conceptuses were dissected out of each of the uterine horns on ice and weighed. The conceptus weights, total litter size, and the number of conceptuses per horn were all recorded. In order to identify their position in the uterus, conceptuses were given references to denote the horn they came from and their position within that horn. For instance, the label 'R3' would identify a conceptus from the mother's right uterine horn and denote that it had been the third conceptus in the horn down from the oviduct.

2.4 Collection of gestational day 17 tissue

All conceptuses in the uterus were dissected on ice and resulting fetus, placenta, and yolk sac weights were recorded. Each fetus was then culled by decapitation and the fetal liver and kidneys were dissected on ice and weighed; fetal tails were also collected and were snap-frozen in liquid nitrogen.

2.5 Statistical analyses

Gestational day 17 weight data sets were analysed using a multilevel random effects regression model (SPSS, version 13) to account for their hierarchical structure. Model

developed by Dr. Clive Osmond, Medical Statistician, MRC Environmental Research Centre, Southampton General Hospital, University of Southampton (Kwong et al., 2004). Maternal and conceptus effects were estimated simultaneously, as both between mother and within mother variation was incorporated.

Unpaired two sample t-tests (Microsoft Excel, 2002) were used to evaluate differences in integrated density values (IDVs) for protein analysis data sets.

Changes in the expression of probe sets between diet groups in the genomics analysis were analysed using three independent downstream analyses packages: Array Assist (Stratgene), GeneSpring (Agilent), and dChip (publicly available software, Li and Wong, 2001), (see Chapter 4 section 4.2.14 for further details of these data analysis methods).

In summary, the Array Assist data analysis included comparisons between 9% casein and 18% casein treatments, switch and 18% casein treatments, and switch and 9% casein treatments. Probe sets that weren't at least 1.4 fold different between treatments were filtered out of the analysis; significant differences between filtered probe sets in each treatment were assessed using unpaired t-tests, at $p<0.05$ (Microsoft Excel, 2002) to produce candidate gene lists for each comparison.

The GeneSpring data analysis was carried out for the treatment comparisons 9% casein v 18% casein, and switch v 18% casein only. The analysis was based on probe sets that were at least 2-fold different between treatments, and that were called as "present" in at

least 3 out of the 4 arrays per treatment; significant differences in these probe sets between the treatments were assessed using ANOVA at $p<0.05$ (Microsoft Excel, 2002). The dChip analyses were conducted on the treatments: 9% casein v 18% casein, switch v 18% casein, and 9% v switch. Analyses were based on probe sets that were called as "present" on at least 1 out of the 4 arrays per treatment, and that exceeded an absolute threshold level of expression (imposed to filter out probe sets with very small expression values). The analysis parameters included two levels of stringency relating to fold change; the high stringency criteria involved filtering out probe sets that were not changing by at least 1.6 fold, whereas the low stringency criteria included probe sets that were at least 1.4 fold different between treatments. Finally, differences between the filtered probe sets for each treatment were identified using ANOVA at $p<0.05$ to produce candidate gene lists for each comparison.

Chapter 3

3.1 Introduction: Maternal Diet Effect on Gestational day 17 Tissue Weights

The DOHAD hypothesis proposed that the developing conceptus adapts to a limited

supply of maternal nutrients and permanently alters its physiology and metabolism

(Barker, 1999). Human epidemiological studies used size at birth as a marker of fetal

nutrition and related it in groups of men and women to the occurrence of several chronic

diseases in later life e.g. in the cohort in Preston, lower birth weight was used as an

indicator of reduced fetal growth and nutrition and related to evidence of the metabolic

syndrome. In both men and women, the prevalence of metabolic syndrome fell

progressively from those who had the lowest to those who had the highest birth-weights.

In addition to low birth weight, subjects with metabolic syndrome had small head

circumference and low ponderal index at birth and low weight at year 1 of age. From this

study, it was concluded that type 2 diabetes and hypertension have a common origin in

suboptimal development *in utero*, and that metabolic syndrome should be re-named *"the*

small baby syndrome" because the prevalence of metabolic syndrome was strongly

related to birth-weight (Barker et al., 1993). Unfortunately, such statements have

attracted criticism of the DOHAD hypothesis due to emphasis being placed on birth

weight as a causal marker of later disease (Huxley et al., 2002). However, the observed

relationship between birth size and risk of disease parameters such as raised systolic

blood pressure does not simply imply a causal role of being born small but rather it

reflects the sensitivity of fetal growth to adverse intrauterine influences (Gluckman and Hanson, 2004b).

Numerous rodent models have supported the notion that maternal under-nutrition during pregnancy alters early growth (reflected by alterations in birth-weight) and also the development of chronic disease indicators, such as raised systolic blood pressure, in the adult offspring (Langley-Evans et al., 1996a; Langley-Evans, 1997b; Bertram et al., 2001; Watkins et al., 2008). Furthermore, reduced cell numbers first within ICM (early blastocyst) and later within both ICM and TE (mid/late blastocyst), have been reported in rat embryos in response to maternal low protein diet (Kwong et al., 2000). This suggests that early on, the embryo adopts an altered growth profile (as indicated by a slower cellular proliferate rate) in response to the compromised maternal environment.

This chapter aims to examine whether exposure to the maternal diet manipulations imposed in this study are manifested as alterations in fetal growth (reflected by weight of fetal tissues) in late gestation.

3.2 Materials & Methods

Refer to Chapter 2 (Generic Methods), for further information on Experimental Design (section 2.1), Animal Treatments (section 2.2), Recovery of Conceptuses (section 2.3), and Collection of gestational day 17 tissue (section 2.4).

3.2.1 Collection of gestational day 17 tissue

During collection of the weight data from the gestational day 17 dissections, tissue was also specifically selected for genomics analysis (Chapter 4).

3.2.2 Storage of gestational day 17 tissue

After being weighed, the tissues from three conceptuses per uterine horn were saved and stored for further analyses. Excised tissues from the central conceptus in each uterine horn were stored appropriately for genomics analysis (Chapter 4); in addition, the same tissues from the immediate neighbours on either side of the central conceptus in each horn were snap-frozen in liquid nitrogen after collection, before being stored at -80ºC for protein analysis (Chapter 5).

<u>3.3 Results</u>

3.3.1 Growth criteria of fetal samples at gestational day 17 with respect to maternal diet (in-house diet)

Figure 3.1 indicates that 9% casein fed mothers produce significantly heavier conceptuses than mothers fed an 18% casein diet **(p= 0.04).** This difference is not reflected in the switch treatment group (p= 0.432). Total litter size has a significant negative effect on conceptus weight (independent of diet) **(p= 0.032)** and it is the 9% casein group that has

the smaller average total litter size of the three dietary groups, although litter size is not significantly different between groups (Figure 3.2).
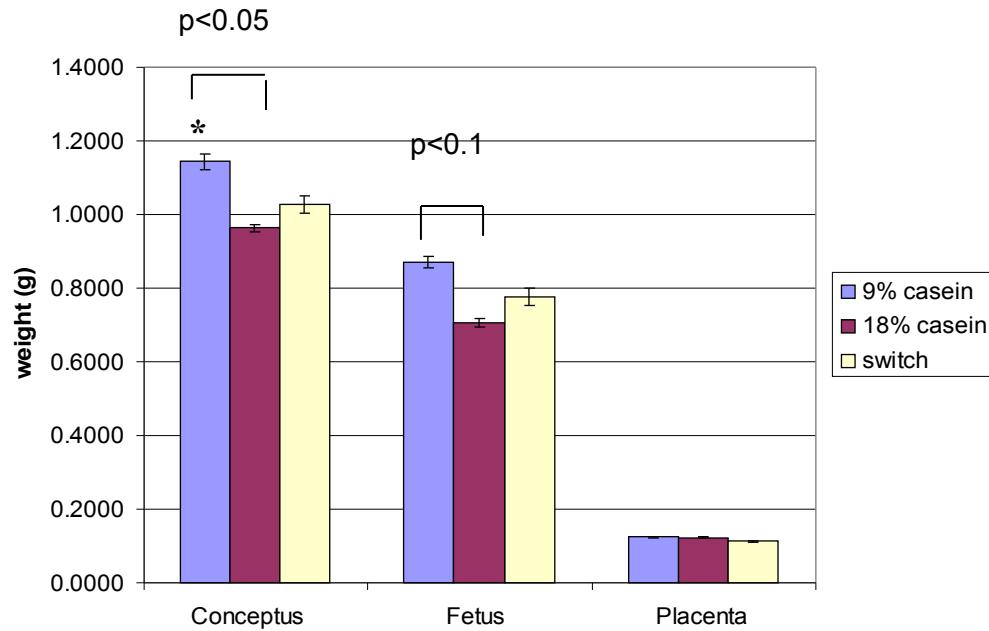
Figure 3.1: **Average conceptus, fetus and placental weights at day 17 in relation to maternal diet (in-house diet) before total litter size is incorporated into the analysis; (*p= 0.04) n= 93-99 samples and 7-8 mothers per treatment.**
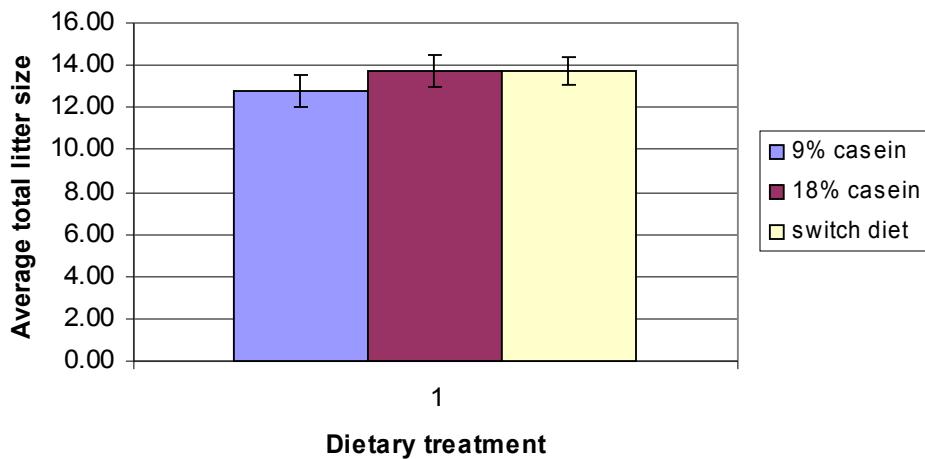
Figure 3.2: **Average total litter size for each of the dietary groups (in-house diet cohort).**

Other variables, such as the uterine horn from which conceptuses were recovered, conceptus position within a uterine horn and mother each do not significantly affect conceptus weight (independent of diet). When these other variables are incorporated in turn into the analysis of the effect of diet on conceptus weight, the significant difference in conceptus weight described above was not altered by uterine horn, position within a horn and mother. However, the significant increase in conceptus weight in the 9% casein diet group compared to the 18% casein diet group is reduced to a trend level increase when litter size is incorporated into the analysis alongside diet **(p= 0.075).** Overall, the statistics indicate that maternal diet has a significant effect on conceptus weight, but that the total litter size effect contributes to this.

Fetal weight of the 9% casein diet group is heavier at trend level **(p= 0.076)** compared to that of the 18% casein diet group, (Figure 3.1). Litter size, horn, position in a horn and

mother each had no significant effect on fetus weight. Again, this trend was not reflected in the switch treatment group (p= 0.402).
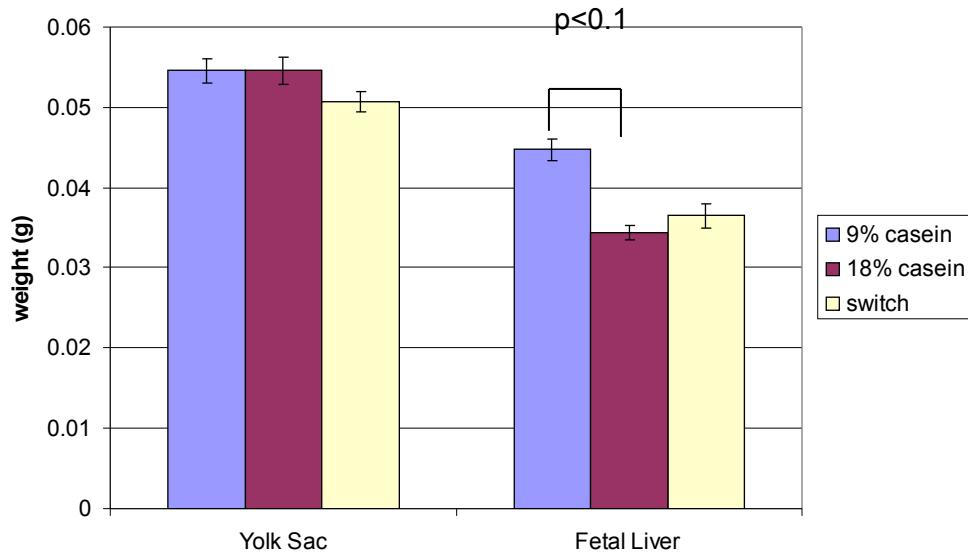
Figure 3.3: **Average yolk sac and fetal liver weights at day 17 in relation to in-house maternal diet.**

The fetal liver weights across the different dietary groups shown in Figure 3.3 reflect the trends observed in Figure 3.1. The difference in fetal liver weight between the 9% casein and 18% casein diet groups is at trend level **(p= 0.075),** and is not significant between the switch and 18% casein diet groups (p= 0.742). Fetal liver weights are normally distributed, and none of the previously mentioned variables significantly affect fetal liver weight. A similar pattern is seen for both the left and right fetal kidney weights (Figure 3.4) and there is a trend level increase in the right fetal kidney weight in the 9% casein diet group relative to the 18% diet casein group. These results indicate that the fetal

organ weights analysed are proportional to fetus weight as a whole, in each of the dietary groups.
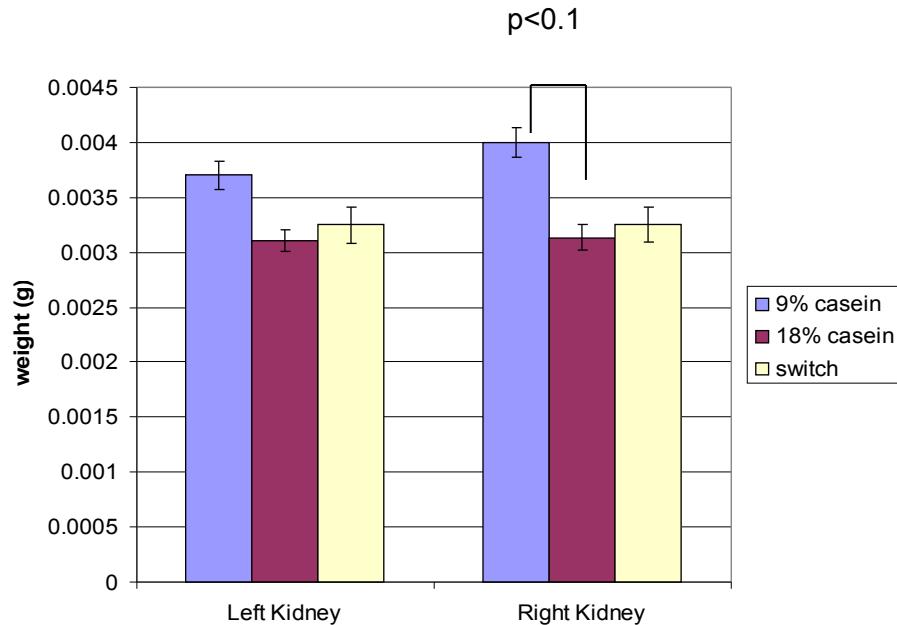
Figure 3.4: Average fetal kidney weights at day 17 in relation to in-house maternal diet.

The data shown in Figure 3.1 do not follow the pattern of previously collected gestational day 17 weight data using this diet model in mice *(Drs W. Kwong and E.Ursell, University of Southampton- unpublished-* see section 3.4.1 of Discussion). To rule out the possibility of a problem with the in-house diet used in this experiment, a further cohort of mice were fed 9% casein or 18% casein diets that had been commercially prepared (Lillico, UK) using an identical specification of ingredients.

3.3.1.2 Gestational day 17 weight data (bought in diet)
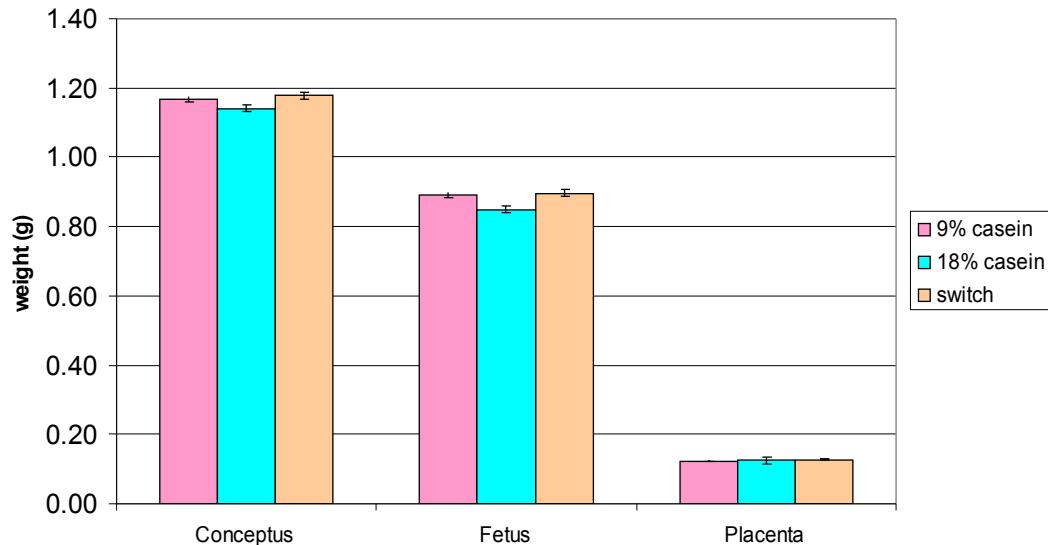
Figure 3.5: **Average weights of conceptus, fetus and placenta at day 17 in relation to maternal diet (bought in diet). n= 13-14 mothers and 151-175 samples per treatment.**

Figure 3.5 indicates that in terms of conceptus and fetus weight, a similar pattern exists in the bought in diet as was observed when the diet was made in-house i.e. the 9% casein and switch diets appear to produce slightly heavier conceptuses and fetuses than the 18% casein diet. Interestingly, the average conceptus and fetus weights produced are higher in all three treatment groups when the bought in diet was used compared to when the in-house diet was used (Table 3.1).

In-house diet	Conceptus weight (g)	SEM	Fetus weight (g)	SEM
9% casein	1.14	± 0.02	0.87	± 0.02
18% casein	0.96	± 0.01	0.70	± 0.01
switch	1.03	± 0.02	0.78	± 0.02
Bought in diet				
9% casein	1.17	± 0.008	0.89	± 0.007
18% casein	1.14	± 0.01	0.85	± 0.009
switch	1.18	± 0.01	0.90	± 0.009

Table 3.1: **Average conceptus and fetus weight data at gestational day 17 when different cohorts of mothers were fed in-house or bought in diets.**

However, for the bought in diet cohort of mice, there was no significant difference in conceptus weight between the 9% casein diet group and the 18% casein diet group (p= 0.529) or between the switch diet group and the 18% casein diet group (p= 0.338). Likewise, the extraneous variables: horn, position in horn and mother each had no significant impact on conceptus weight. Litter size however had a significant negative impact on conceptus weight **(p=0.000).** There was also no significant difference in fetal weight between the 9% casein and 18% casein groups (p= 0.169) or between the switch and 18% casein groups (p=0.150). Horn and mother each also had no significant impact on fetus weight, but litter size had a significant negative effect **(p= 0.000)** and position within the horn had a significant effect **(p= 0.004)** on fetus weight. Both conceptus and fetus weights follow a normal distribution. No significant differences existed in placental weight between the 9% casein and 18% casein groups (p= 0.469) or between the switch and 18% casein groups (p= 0.928). There is a trend level difference **(p= 0.083)** in the fetus/placenta weight ratio between the 9% casein and 18% casein dietary groups; the 9% casein group has an increased fetal:placental weight ratio relative to the 18% casein control group, which may suggest slight disproportionate growth of the fetus relative to

the placenta occurred in this treatment group. Finally, there were no significant

differences between 9% casein and 18% casein diets (p= 0.168) or between switch diet

and 18% casein diets (p= 0.149) in terms of average fetus weight per litter.
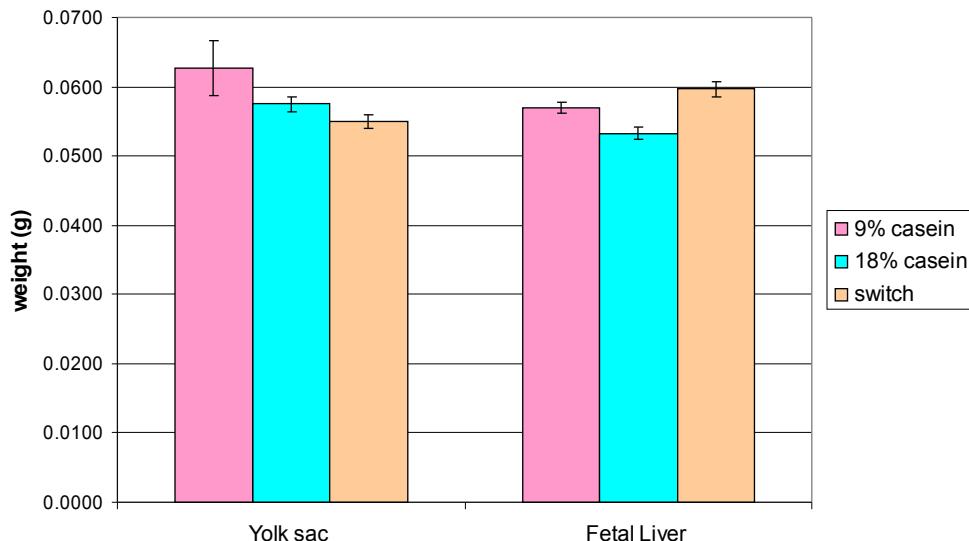
Figure 3.6: **Average yolk sac and fetal liver weights at day 17 in relation to maternal diet (bought in diet). n= 13-14 mothers and 151-175 samples per treatment.**

No significant difference exists in fetal liver weights between the 9% casein and 18%

casein diet groups (p= 0.364) or between switch and 18% casein groups (p= 0.105)

(Figure 3.6). Litter size does have a significant negative effect on fetal liver weight **(p= 0.000).** Fetal liver weight data was normally distributed. The average fetal liver weights

(Figure 3.6) and right kidney weights (Figure 3.7) reflect that of the fetus weights (Figure

3.5), indicating that these organs are largely proportional in size to the fetus in each

dietary treatment group. The pattern of the left kidney weight data is affected by the 18%

casein group which has a larger amount of variation but there was no significant
difference in the weights of the fetal kidneys (Figure 3.7).

The weight data collected for the yolk sac (Figure 3.6) is affected by a relatively large
amount of variation in the 9% casein diet group. The variation here may be due to
difficulty with weighing yolk sac tissue accurately due to the tendency for it to hold onto
fluid more than the other tissues. There was no significant difference in yolk sac tissue
weight between the 9% casein and 18% casein diets ($p= 0.312$) or between switch and
18% casein diets ($p= 0.563$). None of the extraneous variables significantly affected yolk
sac weight.
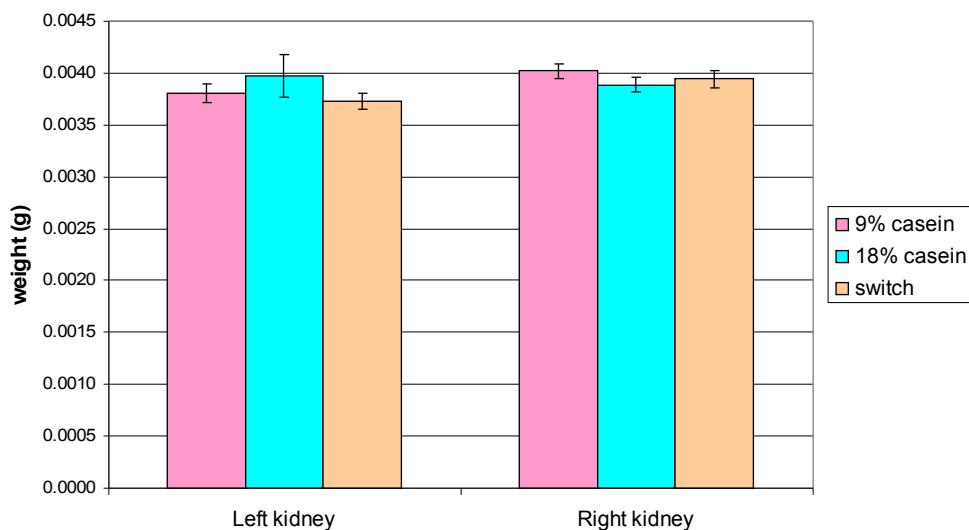
**Figure 3.7: Average fetal kidney weights at day 17 in relation to maternal diet
(bought in diet). n= 13-14 mothers and 150-173 fetal kidneys per treatment.**

3.4 Discussion

3.4.1 Gestational day 17 weight data (in-house diet cohort)

Average conceptus weights were significantly different **(p= 0.04)** between the 9% casein and 18% casein diet groups (Figure 3.1). However, the difference in conceptus weight between these diet groups was not independent of litter size. Thus it is possible that the significant increase in conceptus weight in the 9% casein diet group may be partially attributed to the smaller litters in this diet group compared to the 18% casein diet group. Nevertheless, trend level differences in average conceptus weight **(p= 0.075)** and average fetus weight **(p= 0.076)** were identified between the 9% casein and 18% casein diet treatments, and these trends were independent of the other variables identified, including litter size. Average placenta weight (Figure 3.1) and average yolk sac weight (Figure 3.2) are identical between the 9% casein and 18% casein diet groups and so do not contribute to the difference in conceptus weights. Thus, it appears that the changing weight of the fetus is the reason for the trend level difference in conceptus weights between the 9% casein and 18% casein diet groups. Finally, the average fetal liver weight also showed a trend level difference, **(p= 0.075)** (see Figure 3.2) between the 9% casein and 18% casein diets in line with the differences in the conceptus and fetus weights described above.

From these data, it appears that the 9% casein diet treatment has more of an impact on the developing conceptus than the switch diet as indicated by tissue weights at day 17.

Specifically, in the absence of any significant changes in the switch diet treatment, the 9% casein diet results in a trend level increase in the weight of the fetus compared to the controls when examined at gestational day 17. This trend does not follow the direction of published birth weight data in rodents suggesting that a lower birth weight results from protein restriction throughout pregnancy (Langley-Evans et al., 1996a; Langley-Evans et al., 1997b; Bertram et al., 2001). Furthermore, recently, Watkins et al., 2008 have shown in mice that the maternal switch diet, as was used in this study, results in a significant rise in the birth weights of pups, but the 9% casein treatment throughout gestation has no significant effect on birth weight relative to the 18% casein control treatment. Although, in the results gathered for my in house diet data set it appears that the 9% casein treatment has more of an effect on weight in late gestation than the switch diet group these results may not be wholly reliable due to questions over the diet composition made in house as alluded to previously.

Furthermore, the weight data collected at gestational day 17 from these pregnant mice fed in-house made diets also do not follow previous weight data collected in mice, specifically at gestational day 17, where maternal diet has been varied in this way and the equivalent diet recipe has been used *(Drs W. Kwong, and E.Ursell, University of Southampton- unpublished)*. Also, average weights that have been documented previously in mice at gestational day 17 were higher for the 18% casein diet than have been found in Figure 3.1 *(Drs W. Kwong, and E.Ursell, University of Southampton- unpublished)*.

In an attempt to find an explanation for the trends observed in Figure 3.1, the breeding pairs used to produce the females used in this study were analysed in order to look at the number of litters already produced (parity number) prior to the litter containing each female used as a mother in this study, (Figure 3.8).
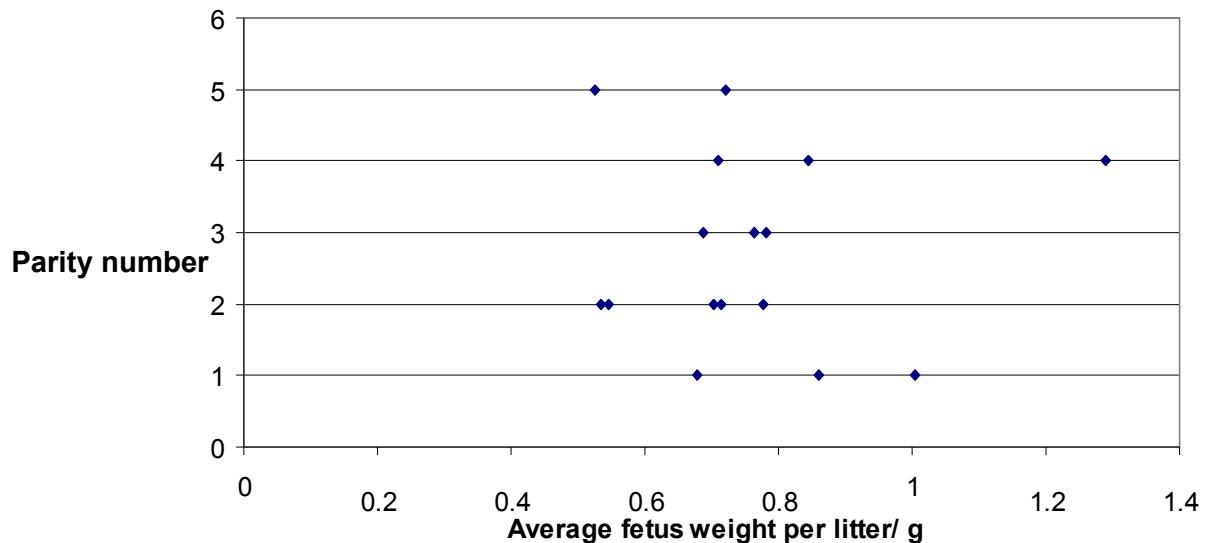
Figure 3.8: **Relationship between average fetal weight in the litter produced by a mother and the parity number of the breeding pair used to produce the litter into which mothers were born. (Note; the parity of some mothers could not be traced).**

Figure 3.8 indicates that there is no apparent correlation between the parity numbers of the litters into which mothers used in the present study were born and average fetal weight in the litters subsequently produced by these mothers in this study.

3.4.2 In-house diet versus bought in diet

Due to the unexpected nature of the weight data in Figure 3.1 mentioned previously, the quality of the in-house prepared diet, the 18% casein diet in particular, came into question. The experiment was therefore run again on a new cohort of mice which received comparable 9% casein and 18% casein diets that had been bought in ready-made rather than made in-house. An alternative remedy would be to have had the individual nutrient levels analysed for the in-house prepared diet. However this option was deemed to be less cost effective and thus not pursued.

Figure 3.5 indicates that in terms of conceptus and fetus weight a similar pattern exists in the bought in diet as was observed when the diet was made in-house i.e. the 9% casein and switch diets appear to produce slightly heavier conceptuses and fetuses than the 18% casein diet (non significant for bought in diets). However interestingly, the average conceptus and fetus weights produced at gestational day 17 are increased in all three dietary treatment groups when mice are fed the bought in diets compared to when the in-house diet was used, (Table 3.1). This lends support to the idea that something was missing or depleted in the original in-house made diets used previously. It is also noteworthy that the 18% casein diet was closer to the 9% casein diet in terms of conceptus and fetus weights when the bought in diets were used, which also is more in line with the previous findings of Drs W. Kwong, and E.Ursell, University of Southampton- unpublished.

3.4.3 Gestational day 17 weight data (bought in diet cohort)

There were no significant differences in the average weights of the gestational day 17
tissue examined in this cohort of mice. However the absence of changes in the weights
recorded does not necessarily mean that programming hasn't taken place in the tissues, as
the dietary manipulation imposed on the pregnant mice was relatively mild (Nelson and
Evans, 1953). Indeed, there is a certain amount of conflicting evidence regarding the
impact of a low protein diet on raw weights in rodents. A number of studies have
indicated changes in cardiovascular parameters in offspring in response to a diet low in
protein experienced *in utero* in the presence or the absence of changes in measured birth
weights in these offspring (Langley-Evans et al., 1996c; Kwong et al., 2000; Watkins et
al., 2008).

Litter size often had a significant negative effect on the weight data parameters measured
in this study. As the total litter size increased, conceptus, fetus, placenta and fetal liver
weights were significantly lighter; this may reflect a restriction of growth in response to
limited resources due to crowding. It is important to note here that the maternal low
protein diet has no significant effect on litter size itself in rodents (Langley-Evans, 2000;
Watkins et al., 2008; Kwong et al., 2000; *E. Ursell, University of Southampton- PhD
thesis, 2004*).

Recently in mice the maternal switch diet, as was used in my study, has been reported to
result in a significant elevation of the birth weights of pups (Watkins et al., 2008). Also

in rats, the switch treatment was found to cause significant alternations in birth weight but here the change seen is in the opposite direction, i.e. a reduction in birth weight (Kwong et al., 2000). However in my data set, the switch treatment did not result in any significant change in fetus weight at day 17 as might be expected from these birth weight results. It is possible therefore that the day 17 window is just too early for adaptations to diet treatment to have manifested themselves as changes in growth that are seen by the altered weights at birth. It may be that at day 18, changes in the weight of the gestational day 17 fetal tissues become evident.

Moreover, the reported changes in birth weight in rodents as a consequence of manipulating protein content of maternal diets are often gender specific (Kwong et al., 2000; Watkins et al., 2008). In both the aforementioned studies the significant alterations in birth weight reported as a consequence of an equivalent to the switch diet treatment, was exclusive to female offspring. As it is not possible to reliably identify fetal sex by anatomy at gestational day 17 the data set inevitably incorporates fetuses of both sexes together. This may offer another explanation for the absence of significant alterations in weight at day 17 in response to the maternal switch diet in the present study. However, as the previous aforementioned studies indicate that sex is an important factor in the response to dietary interventions during development, clearly it would have been more favourable to express the weight data on the basis of sex of the fetuses in the present study rather than group all the data for both sexes together.

Despite the absence of changes in the weights of the fetuses examined here at day 17, biochemical analyses were undertaken to examine the fetal liver tissue for evidence of programming influences in the gene and protein expression profiles (Chapters 4 and 5 respectively).

Chapter 4

4.1 Introduction: Genomics Analysis of Maternal Diet Effect on Fetal Development

It is important to identify gene pathways and specific genes influenced by maternal

dietary programming so that the mechanisms involved can be elucidated and understood.

There is minimal data currently available documenting these effects, moreover there is

currently no such information concerning the impact of the maternal switch diet on the

fetus.

Micro-array techniques provide a powerful approach to study global patterns of gene

expression. A number of studies have made use of this tool for transcript profiling during

murine pre-implantation development/embryogenesis (Hamatani et al., 2004; Wang et al.,

2004; Zeng et al., 2004). Moreover, micro-array technology has proved a useful tool in

assessing the impact of environmental manipulations during early development on global

gene expression. Thus, the short-term effects of embryo culture have been elucidated in

blastocyst stage embryos which has demonstrated alterations in the global pattern of gene

expression, and indicated the sensitivity of several gene pathways to such early

environmental programming influences (Rinaudo et al., 2004).

Affymetrix micro-arrays have also been used to understand the mechanism for the impact

of environmental insults in murine fetal liver (not related to compromised maternal diet),

including maternal perfluorooctanoic acid (PFOA) exposure, which is known to cause

growth deficits and mortality in murine neonates. Following maternal PFOA exposure,

the expression of a number of genes in the murine fetal liver at term, including those

related to fatty acid catabolism, were found to be altered in response to this treatment

(Rosen et al., 2007).

The aim of this chapter is to determine **global gene expression patterns** in gestational

day 17 murine fetal liver as a function of maternal diet using GeneChip expression

analysis probe arrays (Affymetrix) to better understand the genetic mechanisms involved

in dietary programming of the fetus.

The GeneChip Mouse Genome 430 v2.0 Array (Affymetrix) is composed of 45,101

probe sets which represent over 34,000 mouse genes. Sequences used in the design of

these arrays were selected by Affymetrix from GenBank, dbEST and RefSeq. Probe cells

are specific areas on the probe array surface that contain hundreds of thousands to

millions of copies of a given oligonucleotide probe sequence attached to the array surface

to which single stranded labeled 'target' may bind. The oligonucleotides on the surface

of the probe array are called probes because they interrogate or 'probe' the sample.

Eleven oligonucleotide probes (DNA probe cells) constitute one **probe set** and are used

to measure the level of transcription of **each mRNA sequence** represented on the array,

(Figure 4.1).
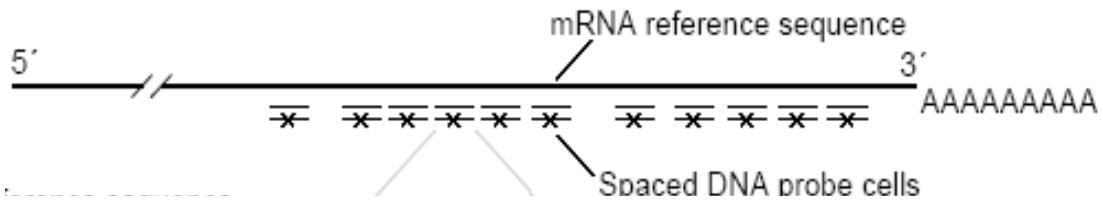
Figure 4.1: Design of probe sets on the Mouse Genome 430 2.0 arrays (provided by Dr. Geoff Scopes, Affymetrix).

All the DNA probe cells for a particular mRNA sequence are made to a similar piece of sequence close to the 3' end. Each DNA probe cell contains complementary sequence to the part of the mRNA reference sequence it represents. Individual probe cells belonging to each probe set are distributed out evenly over the array. For every probe cell containing perfect match oligo sequences, there is an adjacent probe cell containing mismatched oligo sequences which differ only by a single base (Figure 4.2). These act as controls for the specificity of target binding. Housekeeping/control genes are present on each array and include GAPDH, beta-actin, transferrin receptor and pyruvate carboxylase.

···TGTGATGGTGGGAATGGGTCAGAAGGACTCCTATGTGGGTGACGAGGCC···

TTACCCAGTCTTCCTGAGGATACAC   Perfect Match Oligo

TTACCCAGTCTTGCTGAGGATACAC   Mismatch Oligo

PM probe cells

MM probe cells
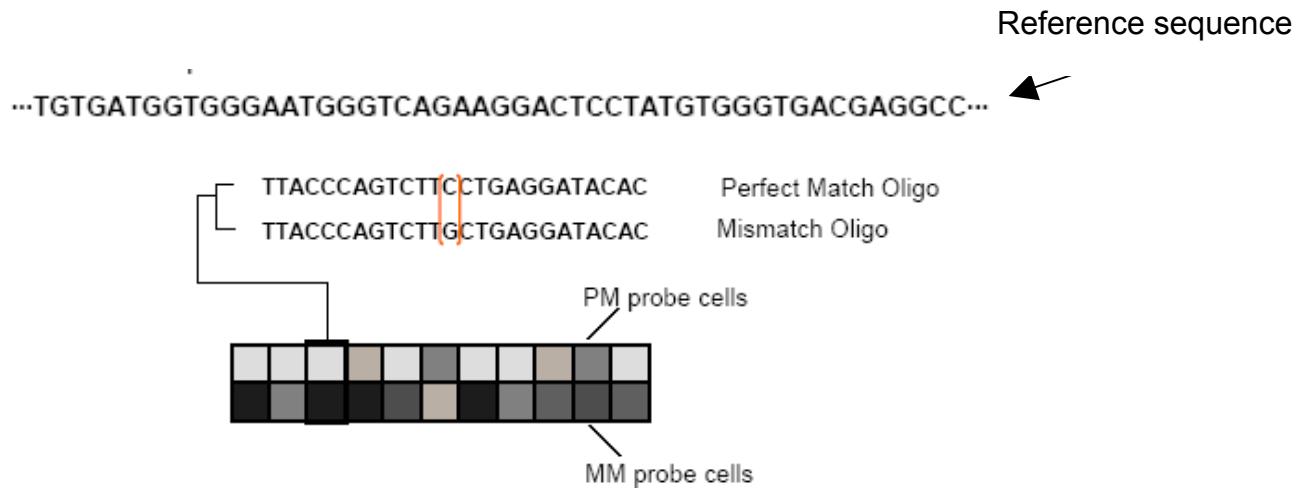
Figure 4.2: **Fluorescence intensity image of perfect match (PM) oligo sequences and mis match (MM) oligo sequences (from Dr. Geoff Scopes, Affymetrix).**

4.2 Materials & Methods

Refer to Chapter 2 on Generic Methods, sections 2.1 Experimental Design, 2.2 Animal Treatments, 2.3 Recovery of Conceptuses, and 2.4 Collection of gestational day 17 tissue.

4.2.1 Recovery of conceptuses

During the gestational day 17 dissections described in Chapter 3, the central conceptus in each uterine horn was identified as a potential candidate for use in the genomics analysis.

The central conceptus was selected in order to avoid extreme positions in the uterine horns where fetal growth may be more variable due to the nature of the uterine horn

blood supply. The blood supply to fetuses in each uterine horn in the mouse comes from offshoots of a main loop artery which is fed from both the top and the bottom ends. In such a system, the pressure of blood is greatest in the top and bottom offshoots, decreasing in the offshoots towards the middle of the horn. Thus, larger fetuses are often found at either end of the horns than in the middle. However, the topmost fetus is often, particularly in crowded horns, supplied by one limb of a bifurcated offshoot of which the other limb supplies the ovary. Therefore, this fetus is on average smaller than its neighbours in crowded horns (McLaren and Michie, 1960). The central conceptus in a uterine horn was easily identifiable where there were an odd number of conceptuses; where there was an even number, the central conceptus nearest the oviduct end of uterus was taken to be the centre.

As average fetus weight was significantly affected by position in the uterine horn in the bought-in diet data set in Chapter 3, this further supports the work undertaken to keep uterine position as constant as possible when selecting potential fetal candidates for down-stream analyses.

4.2.2 Collection of gestational day 17 tissue

Excised tissues from central conceptuses were incubated individually in 'RNA later' stabilisation reagent (QIAGEN, UK) immediately following dissection and placed on ice and then stored in the reagent overnight at 2-8°C. Each tissue was completely submerged in a minimum of ten volumes of RNA later per milligram of tissue. The following day,

tissues were removed from the RNA later and were blotted dry and transferred to -80ºC

until required.

4.2.3 PCR genotyping of fetuses

To keep biological variation in the genomics analysis to a minimum, I decided that the

genomics analysis would be conducted on tissue from one sex of fetus only (males); thus,

PCR genotyping of the central fetus in each uterine horn selected as a potential candidate

for the genomics analysis was carried out to ascertain sex. This was undertaken using

DNA extracted from fetal tail tissue (DNeasy Tissue Kit, QIAGEN UK). In addition, in

order to standardise the immediate environment experienced by each central fetus *in*

utero, the sexes of the nearest neighbours in each horn were also determined by the same

method. Thus, a central male fetus was only considered as a candidate for the micro-

array if at least one of its immediate neighbours was also a male.

The sex of the neighbouring fetuses is important information to have as hormones from

one fetus can influence the physiology and behavioural development of contiguous

fetuses in the mouse due to the close proximity in which fetuses line the uterine horns

(vom Saal, 1981). By selecting male fetuses for the genomics analysis with a maximum

of one female neighbour it was intended that the impact of hormones from nearest

neighbours of the opposite sex would be minimised. Two different primer pairs (Kunieda

et al., 1992; see below) for distinct regions of the mouse Y chromosome were used as a

check for the presence of male DNA in the samples. These primer pairs are specific for the sex-determining region of Y (*Sry*) and the Zinc-finger region of Y (*Zfy*) genes.

Y chromosome primer sequences:

SRY1, 5′GTGAGAGGCACAAGTTGGC3′;

SRY3, 5′CTCTGTGTAGGATCTTCAATC3′;

ZFY11, 5′GTAGGAAGAATCTTTCTCATGCTGG3′;

ZFY12, 5′TTTTTGAGTGCTGATGGGTGACGG3′;

A third 'micro-satellite' primer pair (Kunieda et al., 1992) specific for a locus of the mouse X-chromosome, the X-inactivation centre (*DXNds3*) (i.e. common to both sexes) was also used, namely NDS3 and NDS4 as follows:

X chromosome primer sequences:

NDS3, 5′GAGTGCCTCATCTATACTTACAG3′;

NDS4, 5′TCTAGTTCATTGTTGATTAGTTGC3′

A micro-satellite contains di-, tri- or tetra- nucleotide repeats in the DNA of the type (CA)n or (CCA)n, where n is typically between 10-30+. Here, the micro-satellite locus confirms the presence of PCR product in the reaction. It is used as a check for DNA extraction efficiency, and is a check that DNA has been added to the PCR reactions.

The conditions adopted for the PCR thermal cycling reactions are as specified in

(Kunieda et al., 1992). PCR reactions in 0.5ml PCR tubes were overlaid with mineral oil

and were incubated using a Hybaid thermal reactor. Table 4.1 shows the reagents used

per cycling reaction. The thermal cycling protocol for the PCR genotyping is also

shown; after the last cycle, samples were held at 72°C for 10 minutes.

Reagent	Volume
10 x Buffer (Invitrogen)	4.5 µl
dNTPs (10 mM each)	1 µl
$MgCl_2$ (50 mM)	1.5 µl
Primer (forward) (40 pmol/µl)	1 µl
Primer (reverse) (40 pmol/µl)	1 µl
DNA (~80 ng)	variable
Di H_2O	variable
Total volume	**45 µl**
10 x Taq Master-mix	5 µl

**Table 4.1: Example of reagents used per cycling reaction (master-mixes were made
to increase accuracy).**

94°C Denaturation (60 secs)

60°C Annealing (150 secs)   x 30 cycles

72°C Extension (150 secs)   **(Thermal cycling procedure)**
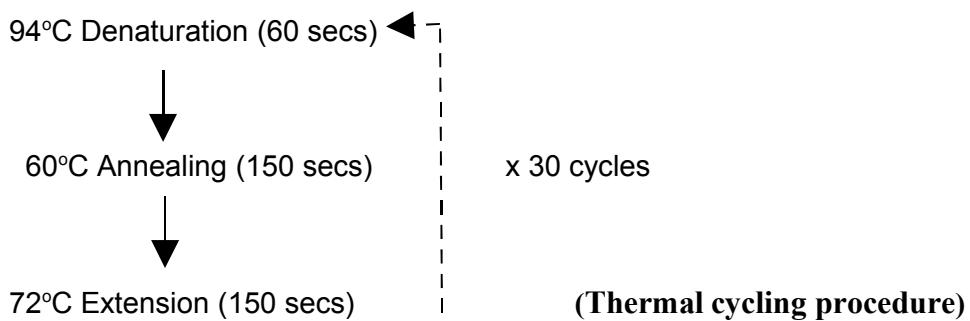
Primers pairs for *DXNds3* and *Sry* could be run together in a multiplex system while the primer pair for *Zfy* was run in a separate reaction. Despite optimisation, it was not possible to run all three sets of primers in multiplex and decipher the products reliably. In addition, as a positive control, DNA extracted from male and female adult tissue was always run alongside the DNA from the fetal tails being genotyped.

4.2.4 DNA electrophoresis and visualisation

PCR products were mixed with 6x loading dye and run alongside a 100 base-pair ladder (Invitrogen) on a 1.6% agarose gel for effective separation of multiplexed reactions, made with buffer 5 x Tris-Borate-EDTA (TBE), 1% Ethidium Bromide, and run in 5x TBE buffer at 120V for 1 hour. Gel photographs were taken using Alpha Imager technology (Alpha Innotech Corporation). For female DNA, no bands should be evident for the Y-chromosome region products; a band for the micro-satellite product only should be observed. For male DNA there should be bands evident for all three products i.e. *Sry*, *Zfy* and the micro-satellite product *DXNds3*. Expected PCR product sizes are as follows: *DXNds3* product 244bp; *Sry* product 147bp; *Zfy* product 217bp.

4.2.5 DNA sequencing of PCR products: (Sanger 'dideoxy' method)

In order to confirm PCR product identity independently of product size, *DXNds3* and the *Zfy* gene were sequenced. It was not possible to successfully sequence the *Sry* PCR product. PCR products were purified using QIAquick PCR purification kit (QIAGEN,

UK) in preparation for sequencing. The concentration of DNA recovered from the

column was assessed by running a small amount in a 1% agarose gel alongside a low

mass ladder (Invitrogen).

Sequencing (Beckman Coulter CEQ 8000 DNA analysis system)

100 fmols of template was used for the cycling step per sequencing reaction. A ratio of

40:1 primer to template was used in cycling reactions, for instance 4 pmols of primer was

used where 100 fmols (i.e. 0.1 pmols) was added to the reaction. The Beckman Coulter

Quick-start kit was used which supplies a master-mix of dye-tagged dNTPs, the 10x

Buffer, and Taq Polymerase (Table 4.2).

Reagent	Volume
DNA (100 fmols)	variable
Di H_2O	variable
Primer (4 pmol/µl)	1 µl
Beckman Coulter Mastermix	8 µl
Total volume	**20 µl**

**Table 4.2: Reagents per sequencing reaction. (Forward and reverse primers added
to separate reactions).**

Samples were transferred to a Tetrad DNA Engine for cycling. A two-step thermal

cycling protocol was adopted for sequencing *DXNds3*: 96ºC for 20 seconds

(denaturation), then 60ºC for 4 minutes (annealing and extension). This was repeated for thirty cycles. This protocol could be adopted because the melting temperatures (T^M) of the NDS primers are ~5ºC higher than the extension temperature of 60ºC. Following cycling, reactions were cleaned-up by ethanol precipitation. (For protocol see Beckman Coulter CEQ 8000 handbook). After bench drying, pellets were re-suspended in Sample Loading Solution (Beckman Coulter) transferred to a 96 well plate, overlaid with mineral oil and read by the Beckman Coulter CEQ 8000.

4.2.6 Experimental design

Twelve fetal liver samples were selected for the genomics analysis from male fetuses that had been centrally positioned within their respective uterine horns. Four biological replicates from each of three dietary treatment groups were probed with the micro-arrays (one chip per sample).

4.2.7 Total RNA extraction from fetal liver tissue

Total RNA was extracted from ~20 mg slices of RNA-preserved day 17 fetal liver samples in an RNase-restricted environment (RNeasy Mini Kit, QIAGEN, UK). RNA samples were snap frozen on dry ice and stored at -80ºC. Trial total RNA extractions using TRIzol reagent (Invitrogen) and chloroform followed by purification with RNeasy Mini Kit (QIAGEN, UK) were also attempted, but the RNeasy method alone produced much better RNA yields.

4.2.8 Qualitative analysis of total RNA extracted from fetal liver tissue

Total RNA quality extracted from fetal livers was assessed using the Agilent 2100 Bioanalyser with the RNA 6000 Nano Assay Kit (Agilent Technologies). The Agilent 2100 Bioanalyzer provides a platform that uses a fluorescent assay involving electrophoretic separation to evaluate RNA samples qualitatively. It measures the amount of fluorescence as the RNA sample is pulsed through a micro-channel over time. The Agilent Bioanalyzer software creates a graph called an electropherogram which diagrams fluorescence over time. Smaller molecules are pulsed through the separation channel more quickly than larger ones and will therefore appear on the left side of the electropherogram. For each sample the software creates a gel image to accompany the graph.

4.2.9 One-Cycle Target Labelling Assay (Affymetrix)

For more details of protocols, see Appendix I.

Poly-A-tailed *Bacillus subtilis* transcripts were spiked directly into total RNA samples to act as positive controls to monitor the target labeling process (Poly-A RNA Control Kit, Affymetrix). The poly-A RNA controls *(lys, phe, thr, and dap)* are *Bacillus subtilis* genes that are obviously not present in the eukaryotic samples. They are synthesised *in vitro* and the polyadenylated transcripts are premixed at staggered dilutions. The concentrated Poly-A Control Stock was serial diluted on ice with Poly-A Control Dil

Buffer in non-stick RNase free microfuge tubes (Ambion) and spiked directly into 5 µg

of each of the RNA samples to achieve the final dilutions. These controls were then

amplified and labelled together with the samples. Monitoring the intensities of these

controls on the arrays helps to monitor the labelling process independently of the RNA

quality of the starting material.

One-Cycle cDNA Synthesis

In the first strand cDNA synthesis reaction, 5 µg total RNA (target) per sample (with

spiked-in poly-A RNA controls) was reverse transcribed using an Oligo(dT) Primer

containing a T7 polymerase promoter binding site. RNase H-mediated second strand

cDNA synthesis followed (One-cycle cDNA Synthesis Kit, Affymetrix, Figure 4.3).
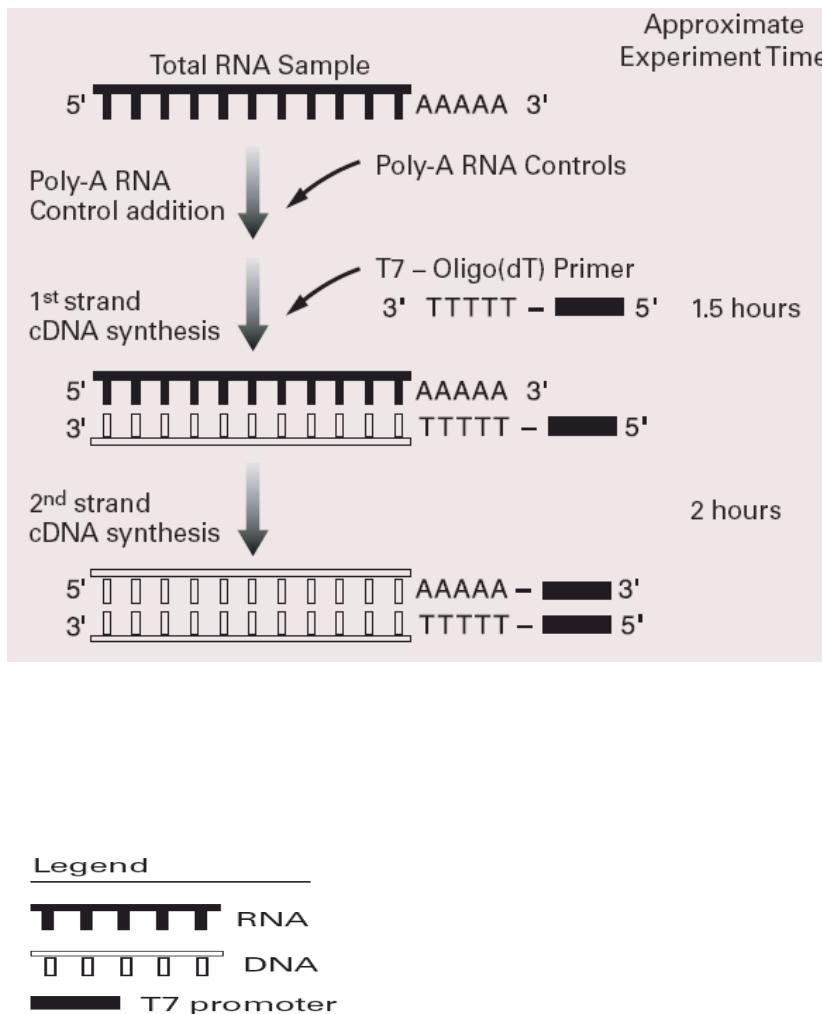
Figure 4.3: Part one of One-Cycle Target Labelling for 1-15 μg total RNA (GeneChip Expression Analysis Technical Manual, Affymetrix, http://www.affymetrix.com).

Newly synthesised double-stranded cDNA was cleaned up at room temperature using spin columns and buffers (Sample Cleanup Module, Affymetrix). The average volume of eluate recovered after cleanup was 12μl. Cleaned-up, double-stranded cDNA samples were stored at -80°C.

<u>*In Vitro* Transcription (IVT) Reaction</u>

The purified, double-stranded cDNA served as a template for the IVT reaction for the synthesis of complementary RNA. The *in vitro* transcription reaction (IVT) was carried out in the presence of T7 RNA Polymerase and a biotinylated nucleotide analog/ ribonucleotide mix for complementary RNA (cRNA) amplification and biotin labelling (IVT Labeling Kit, Affymetrix), (see top of Figure 4.4). IVT reactions were incubated for 16 hours at 37°C using a Tetrad thermal cycler.
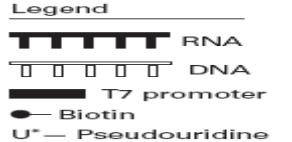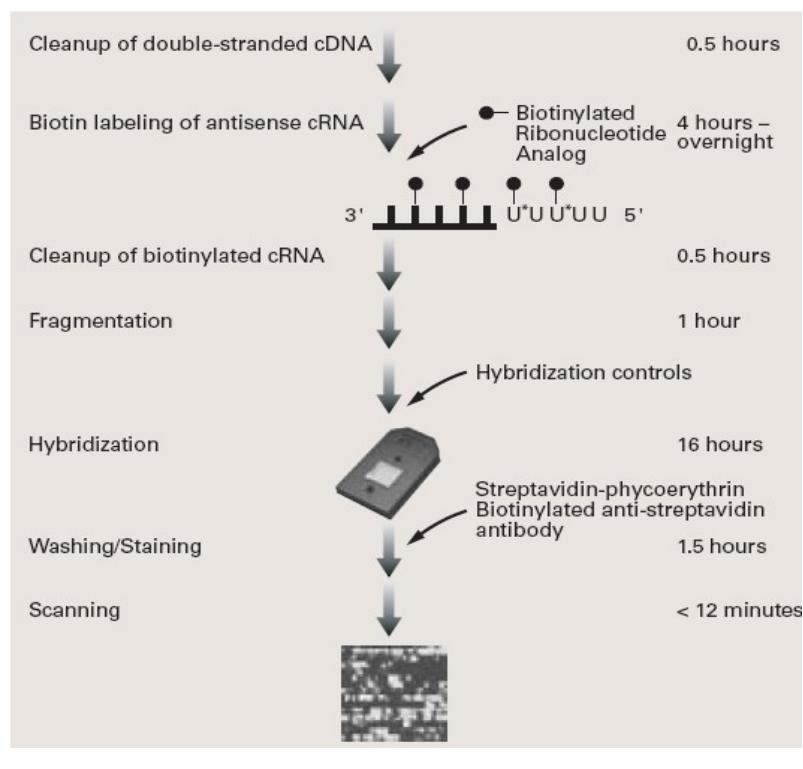
Figure 4.4: Part two of One-Cycle Target Labelling for 1-15 μg total RNA (GeneChip Expression Analysis Technical Manual, Affymetrix).

Biotinylated cRNA was cleaned up at room temperature using spin columns and buffers (Sample Cleanup Module, Affymetrix). Purified cRNA was subsequently stored at -80°C.

Quantification of cRNA yield

Spectrophotometric analysis was used to determine the cRNA yields (1 absorbance unit at 260 nm equals 40 μg/ml RNA). The A_{260}/A_{280} ratio was close to 2.0 for all purified RNA samples (acceptable levels). A_{280} represents protein content in a sample. For quantification of cRNA when total RNA was the starting material, adjusted cRNA yields were calculated to reflect carryover of unlabeled total RNA. (See Appendix I for formula).

4.2.10 cRNA fragmentation

cRNA ranges in length from 50-3000 bases and larger transcripts often contain secondary structure which can interfere with hybridisation and increase the opportunity for non-specific cross-hybridisation to the probe oligos attached to the array. The labeled cRNA makes a better target for oligo arrays once it has been fragmented to an optimal size of 50-200 bases long. This is because the structures of the fragmented targets are less complex which helps improve their specificity (Agilent Technologies, Application Note).

20 µg cRNA per sample was fragmented in a 40µl reaction to give a final concentration of 0.5 µg/µl cRNA in the fragmentation reaction (Sample Cleanup Module, Affymetrix). The fragmentation buffer breaks down full length cRNA by metal-induced hydrolysis to produce RNA fragments ranging in size from ~35 - 200 bases (average fragment size ~100bps).

4.2.11 Target (cRNA) hybridisation to probe arrays

Fragmented labelled cRNA from each sample was hybridized to individual "GeneChip Mouse Genome 430 2.0" Arrays (Affymetrix). Hybridisation cocktails were prepared at room temperature using Hybridisation, Wash and Stain Kit, Affymetrix; Eukaryotic Hybridization Control Kit, Affymetrix. Hybridization cocktails were heated at 99°C for 5 minutes and then at 45°C for 5minutes using a Tetrad thermal cycler. They were then centrifuged for 5 minutes at maximum speed in a micro-centrifuge to collect any insoluble material from the hybridization mixture. Meanwhile, each array was equilibrated at room temperature and then wet with 200 µl of Pre-Hybridization Mix by filling it with a micropipettor through one of the rubber septa. Filled probe arrays were incubated at 45°C for 10 minutes with rotation in a Hybridization Oven 640 (Affymetrix). Arrays were then removed from the hybridisation oven and the pre-hybridization mix was extracted. Finally, array cartridges were refilled with 200 µl clarified hybridization cocktail and incubated in the hybridization oven at 45°C for 16 hours with rotation at 60 rpm.

4.2.12 Washing and staining of hybridized probe arrays

The Fluidics Station 450 (Affymetrix) was used to wash and stain the probe arrays and was operated using GeneChip Operating System (GCOS) software, Affymetrix. Before inserting the probe arrays into the fluidics station modules, the lines of the fluidics station were primed with the wash buffers A (non-stringent) and B (stringent) to prepare it for use (Hybridization, Wash & Stain Kit, Affymetrix). Hybridized probe arrays were removed from the oven and the hybridization cocktails were extracted. Array cartridges were then filled with 250 µl Wash Buffer A: Non-Stringent Wash Buffer. At each of the fluidics station modules, three 1.5 ml vials containing aliquots of 600 µl of each of Stain Cocktail 1 (Streptavidin Phycoerythrin (SAPE) Stain Solution) and Stain Cocktail 2 (Biotinylated anti-streptavidin antibody solution) and 800 µl of Array Holding Buffer were positioned in the module sample holder. Stain Cocktail 1 is light-sensitive so was transferred into an amber vial (Hybridisation, Wash & Stain Kit, Affymetrix). Probe arrays were inserted into the modules of the fluidics station. The needle levers were then engaged to snap needles into position and to start the run, (Figure 4.5).

Probe array cartridge

Needle lever

Cartridge lever

Position of three vials in sample holder
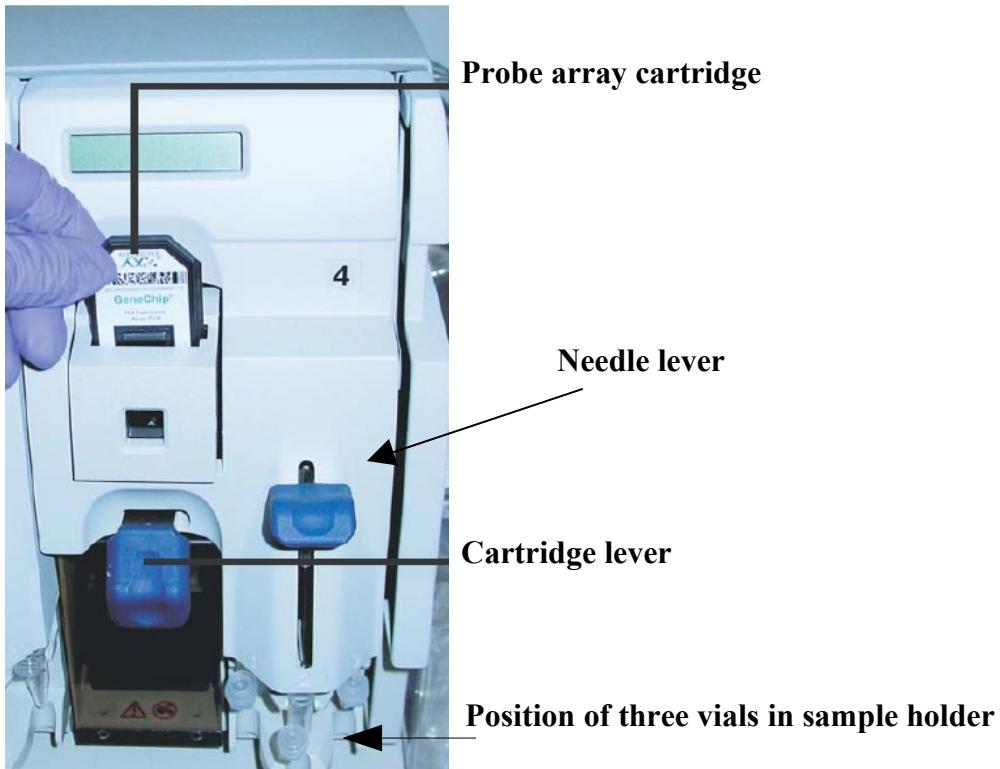
Figure 4.5: A module of the fluidics station (GeneChip Expression Analysis Technical Manual, Affymetrix).

The antibody amplification protocol used to control the washing and staining of the probe arrays can be found in Appendix I. (Note: streptavidin is a protein that binds with high affinity to the biotin-labelled cRNA target).

4.2.13 Probe array scanning

Each of the twelve hybridized probe arrays stained with the streptavidin phycoerythrin conjugate were then scanned in turn using the GeneChip Scanner 3000 (Affymetrix). The amount of light emitted at 570 nm is proportional to the bound target at each location on the probe array. Phycoerythrin, a commonly-used bright fluorescent dye, is a light

harvesting protein isolated from cyanobacteria and red algae. It has a strong emission peak at 575 +/- 10 nm.

4.2.14 Data analysis

The raw data file generated from the GeneChip scanner console was the .DAT image. This was a pixelated image of the probe array analyzed for probe intensities. .CEL files represent single (average) intensity values for each probe cell. Thus a .CEL file represents a non pixelated image whereby multiple pixel intensities are condensed to give one value for every probe cell. .CHP files are the text files generated from .CEL file data, and contain qualitative and quantitative analysis for each probe set as well as data quality assessment information. Finally, report files were generated from the .CHP file data to provide data quality information.

Data files generated were initially analyzed with the GeneChip Operating System (GCOS) software (Affymetrix) for quality control purposes. Other quality monitoring of the data was carried out using Expression Console (Affymetrix) (with thanks to Dr. Geoff Scopes, Affymetrix). Downstream analyses of .CEL file data were conducted using three separate software applications; Array Assist (Stratagene) (with help from Dr. Geoff Scopes, Affymetrix) and GeneSpring (Agilent) (with help from Dr. Nat Street, University of Southampton) and also dChip (a publicly available software package, Li and Wong, 2001) (in collaboration with Dr. Tom Papenbrock, University of Southampton), to identify genes/probe sets apparently sensitive to programming by maternal diet. The

analyses attempt to reveal differences in levels of expression between the dietary treatments.

4.2.14.1 Array Assist analysis parameters

Significance analysis (unpaired t-tests) for comparison of gene expression levels between pairs of dietary groups was carried out using after the data was filtered for Present-Absent calls to remove the genes called as absent across all samples, and so reduce noise. After filtering, the number of probe sets involved in the analysis was reduced from 45101 to 29641.

Gene lists were produced for probe sets that were at least 1.4 fold different between diet groups, with a p-value of <0.05. Three independent comparisons between the diet groups were made: 9% casein v 18% casein, switch v 18% casein and switch v 9% casein (here, the 9% casein group was the baseline for the comparison).

4.2.14.2 GeneSpring analysis parameters

For this analysis, the level of stringency was such that for a probe set to avoid being filtered out it must have been called as "present" in at least 3 out of 4 arrays per treatment group and it must also be changing by at least 2 fold in expression between treatments being compared. In generating the gene lists the data was filtered by experimental

treatment group; the 9% casein group and the switch group were each compared in turn to the 18% casein (control) group.

4.2.14.3 dChip analysis parameters

dChip, a publicly available software package (Li and Wong, 2001) was used to normalise and analyse the Affymetrix .CEL file data and for subsequent class comparison analysis between diet treatments ('classes').

The class comparison tool in dChip enables one to specify a number of filtering criteria. Two different sets of filtering criteria, termed high and low stringency were used for the class comparisons to identify differential expression of probe sets (genes) between classes/diet groups, and to eliminate signal noise.

High stringency criteria for inclusion of a probe set were as follows. The threshold for the lower bound of the 90% confidence interval for fold change was set at 1.6. We can therefore be 95% confident (median of confidence interval) that probe sets identified as being differentially expressed between groups represent differences of at least 1.6 fold. In addition, an absolute minimum expression value, equal to $^{1}/_{10}$ of the mean level of expression of all genes on every chip, was selected to exclude very small expression values from the analysis which may lead to misleading fold change information. The average expression value of genes on all chips after normalisation was found to be '89', thus the absolute expression value was set to 8.9. Finally, the p-value (ANOVA) to

assess likelihood of there being no significant difference in expression for a particular probe set between classes had to be 0.05 or less. Only probe sets that met these criteria were included on candidate lists generated from the class comparisons.

The low stringency comparison criteria were identical to the above, except that the lower bound of the 90% confidence interval for fold change was set at 1.4.

In order to control for multiple testing error, multiple (50) random permutations were made for each class comparison to determine the false discovery rate (FDR) in each case. The number of false discoveries generated empirically from non-meaningful comparisons was determined and the non-meaningful gene lists were used to give an indication of the average number of candidates that might be generated by chance due to **multiple testing**. This gives us an insight into the level of error that may be present in gene lists produced from the meaningful class comparisons. The average number of probe sets reportedly differentially expressed based upon the arbitrary comparisons obtained empirically was expressed as a percentage of the number of probe sets apparently differentially expressed when actual class comparisons were made. This gives a percentage for false discoveries specifically based upon those samples involved in each actual class comparison.

Gene ontology enrichment analysis was performed on lists of candidate genes generated from the class comparisons in order to find biological meaning and clues about the transcriptional response to treatments. Enrichment analysis is most effective when carried out on a large pool of candidates as it is used to determine gene ontologies that

are over-represented relative to an appropriate background. The gene ontology tools used to identify enriched/over-represented categories on a given gene list were Gene Ontology Tree Machine (GOTM) http://bioinfo.vanderbilt.edu/gotm and the Database for Annotation, Visualisation and Integrated Discovery (DAVID) http://david.abcc.ncifcrf.gov/. In order to generate a background list against which the candidates on the gene lists could be compared, the background was defined as the Affymetrix chip used in the study i.e. Mouse 430v2.0 Array. The representation of probe sets was thus equivalent between the background and the gene lists analysed for enrichment.

To identify enriched categories of probe sets for a given candidate list[+], the gene ontology tools group similar probe sets from the list into categories and compare the observed number found in each category to the calculated number of probe sets expected to be present in each category based on the background list. If the observed value is greater than the expected value the category is said to be enriched in the gene list being analysed. Based on the observed and expected numbers an enrichment factor (R) is calculated; the higher the number of observed probe sets relative to the number expected for a given category, the greater the enrichment of that category in the gene list being analysed. For all enrichment factors, the p-value to assess the likelihood of there being no true enrichment was $p<0.01$.

[+]Probe sets on a given gene list were separated into those that were up-regulated and those that were down-regulated and analysed separately for enrichment.

4.3 Results

4.3.1 Genotyping of centrally positioned fetuses and the immediate neighbours by PCR

Figure 4.6 is a representative photograph of PCR products run on an agarose gel. It shows the sexes of six fetuses collected for genotyping from an 18% casein diet fed mother (three fetuses from each horn of the uterus). Known adult male DNA: *'m liv'* shows bands for all three PCR products as expected, and known adult female DNA *'f liv'* shows just one band in the first lane at ~244 bp which is indicative of the *DXNds3* product from the X-chromosome primer pair NDS3/NDS4, as expected.
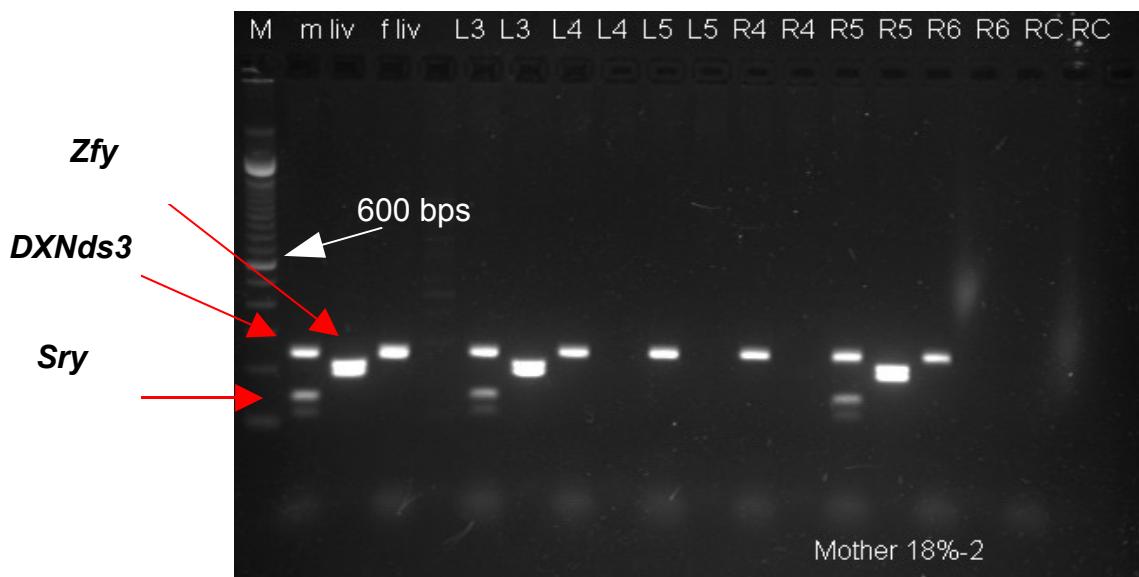
Figure 4.6: DNA electrophoresis. 'M' refers to a 100 base-pair size marker ladder (Invitrogen). 'm-liv' refers to the positive control male liver tissue and 'f-liv' refers to known female liver tissue. 'RC' refers to reagent control (i.e. no DNA added to the reaction).

The fetuses are denoted by their uterine position references L3, L4, L5 etc. For each fetus there are two lanes on the gel. The first lane for each fetus represents a reaction containing NDS and SRY primers in multiplex and the second lane represents a reaction containing the ZFY primers only. For fetus 'L3,' there are two bands at the corresponding sizes to *DXNds3* (244 bp) and *Sry* (147 bp) in the first lane, and there is one band corresponding to the size of *Zfy* (217 bp) in the second lane, hence it is concluded that this fetus is male. Conversely, for fetus 'L4,' there is one band only evident at ~244bp (*DXNds3*) in the first lane, and there is no band evident in the second lane, hence it may be concluded that this fetus is female. Table 4.3 shows potential fetal candidates identified by PCR genotyping that met the genotyping criteria for the micro-array samples as laid out in section 4.2.3.

9-n16	9-n17	9-n19	9-n20	9-n22
R4 (0) 8	R2 (1) 5	L4 (1) 7	R2 (0) 5	R4 (1) 8
R5 (0) 8	L3 (0) 7		R3 (1) 5	
L4 (1) 9	L4 (1) 7			

Litter/mother references

18-n10	18-n11	18-n14	18-n20	18-n18
R5 (1) 9	R5 (1) 9	R2 (1) 4	R2 (1) 5	R3 (1) 7
L2 (1) 5			R3 (0) 5	L4 (1) 7
L3 (0) 5			L5 (1) 8	

sw-n10	sw-n11	sw-n12	sw-n20	sw-n22
R3 (1) 6	R5 (1) 10	L4 (0) 9	L3 (1) 6	R3 (1) 6
R4 (0) 6		L5 (1) 9		L2 (1) 5
				L3 (1) 5

Table 4.3: Results from PCR genotyping: fetuses are denoted by their uterine position references e.g. R3, L2. Male fetuses with a maximum of one female neighbour (see number in brackets) are shown. The numbers in red indicate the corresponding horn litter size for each fetus.

The fetuses listed in Table 4.3 all refer to male fetuses with a maximum of one female nearest neighbour fetus. *Results not shown include where the central fetus was female or where there were two females neighboring a central male fetus.*

Of the twenty-nine male fetuses listed in Table 4.3, the twenty-one which had one female neighbour (and therefore also one male neighbour) were selected for RNA extraction and qualitative analysis (see section 4.3.4). These are the samples with a (1) in brackets after

the fetal reference in Table 4.3. Thus, for each dietary treatment there are five possible

mothers (biological replicates) with at least one fetus available which had a single female

neighbour. Quality RNA from one fetal liver sample from each of four biological

replicates per treatment is required for the genomics analysis study.

4.3.2 Sequencing of PCR products

Confirmation of the identity of the band at ~244 bp as *DXNds3* is achieved from

analyzing the sequence generated from NDS4 (reverse primer) shown in Figure 4.7.
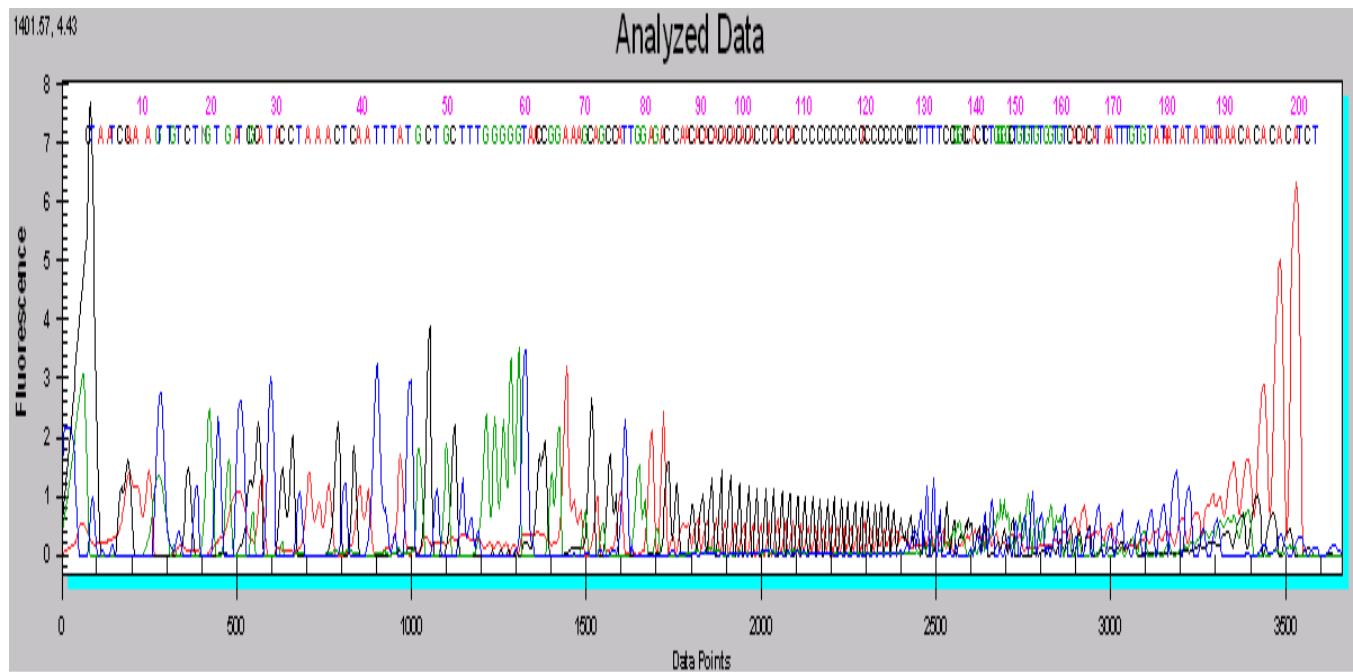
Figure 4.7: Sequence retrieved with the NDS4 (reverse) primer using *Beckman Coulter* CEQ 8000

The *DXNds3* product is rich in GT/CA base repeats in its middle region, which made it difficult to sequence the entire product. Regions with long strings of repeats often cause secondary structure to form during amplification and prevent the DNA polymerase making the complete product. As shown in Figure 4.7, the sequence is read successfully up until the highly repeated region beginning around base 90. At this point the sequence degenerates and thereafter it is no longer possible to gain any useful sequence data. However, upon blasting this sequence (NCBI, BLAST), 73 bases out of 244 matched the known sequence for the X-inactivation centre *(DXNds3)* and hence it can be assumed with reasonable confidence that the primers are amplifying the appropriate product. The sequence retrieved from the reverse primer ZFY12 confirms that the Zinc-finger region of the Y-chromosome was also amplified successfully (Figure 4.8).
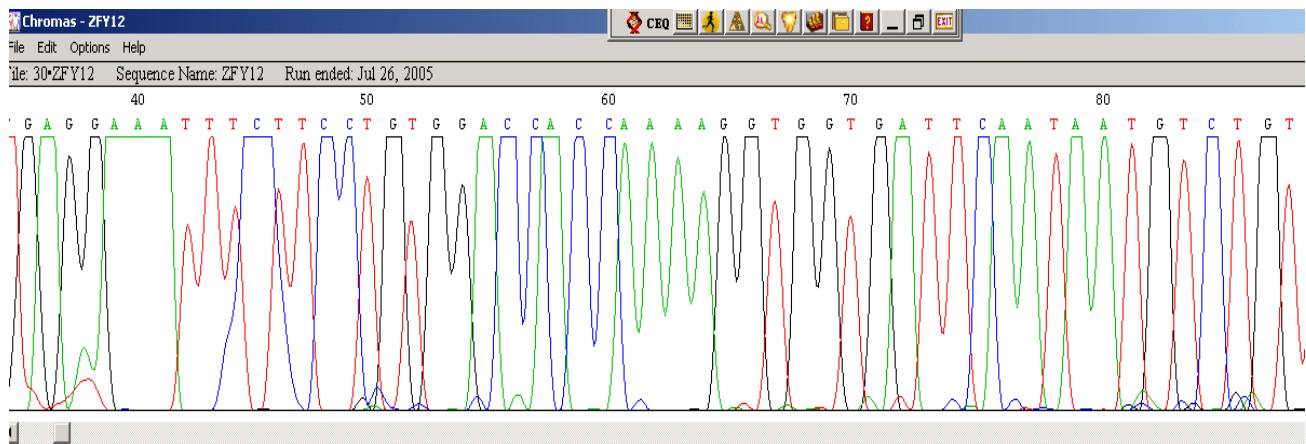
Figure 4.8: **Sequence obtained with the ZFY12 (reverse) primer using the ABI377 sequencing system**

4.3.3 Qualitative analysis of total RNA using Agilent Bioanalyser
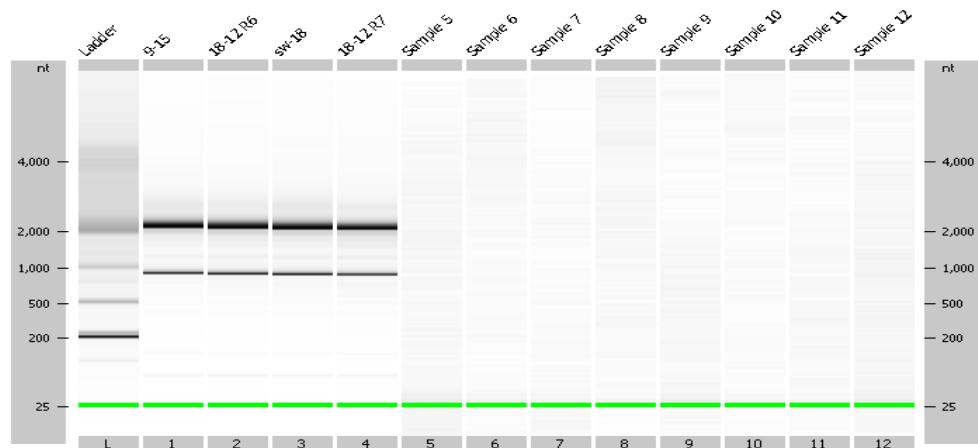
Figure 4.9: Gel of ribosomal RNA bands for 28S and 18S subunits shows high quality non-degraded total RNA.
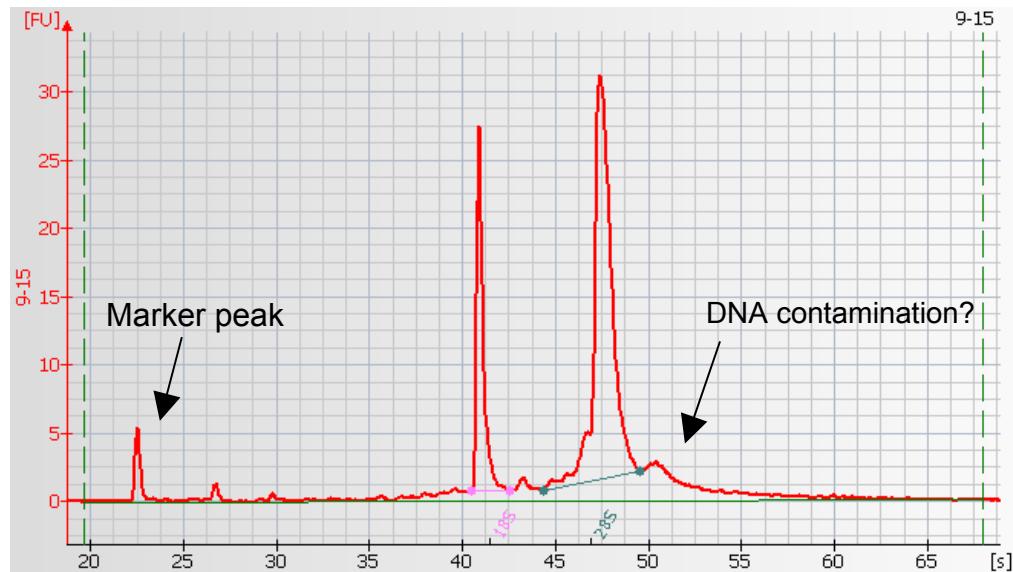
Figure 4.10: Electropherogram of clearly defined 18S and 28S ribosomal RNA peaks.

Figures 4.9 and 4.10 respectively are representative examples of the gel images and electropherograms produced for four trial total RNA samples of fetal liver (~200 ng RNA loaded per sample). The electropherogram shows clearly defined 18S and 28S ribosomal RNA subunit peaks with low inter-peak noise, and minimal low molecular weight contamination. The distinctive marker peak is detectable at the left hand side of the trace in Figure 4.10. It is possible that there is genomic DNA contamination present within the samples as indicated by the small bump just after the 28S ribosomal peak on the electropreogram. The peak ratios achieved for the trail samples were all between 2.4-2.6. A peak ratio of around 2.0 is desirable (i.e. the 28S ribosomal RNA subunit should be present with approximately twice the intensity of the 18S ribosomal RNA subunit). This indicates that the sample handling and preparation and the RNA extraction procedure employed were effective at maintaining good quality total RNA with minimal degradation.

4.3.4 Qualitative analysis of total RNA extracted from the twenty-one selected male fetal liver samples

In the selection of the final twelve fetal liver RNA samples for the micro-array experiment it was also important to take account of the following variables:

-the RNA quality of fetal liver samples
-horn and total litter sizes from which fetuses were taken
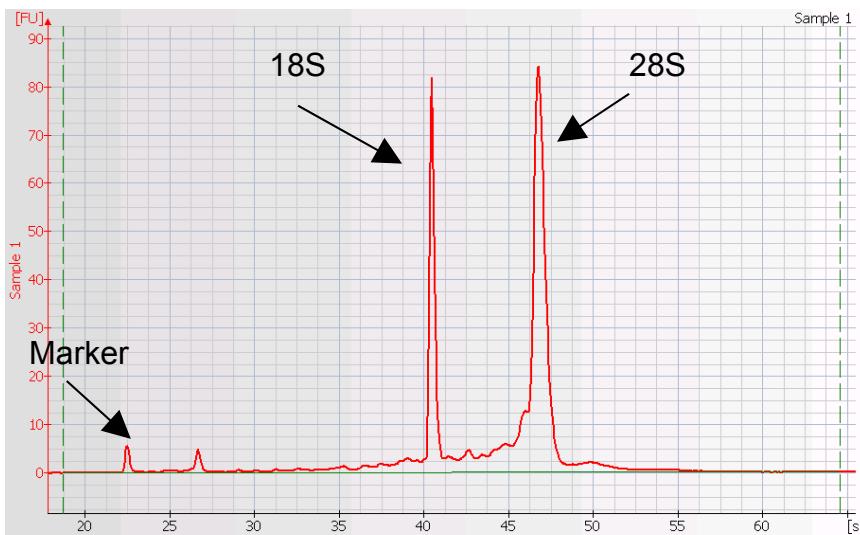
Figure 4.11: **Representative electropherogram of the total RNA quality of one of the 21 selected fetal liver samples showing low baseline, minimal low molecular weight noise, low inter-peak noise, well defined 18S and 28S peaks, 28S/18S ribosomal peak area ratio 2:1 with 28S peak taller than 18S peak.**

Figure 4.11 is an electropherogram of the total RNA of one of the twenty-one selected fetal liver samples that were assessed for RNA quality using the Agilent Bioanalyser. The electropherograms for most of the twenty-one samples resembled this graph.
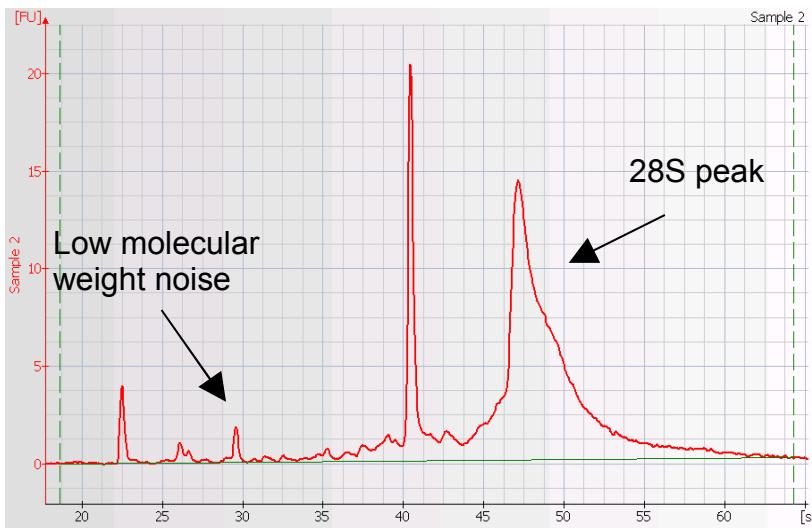
Figure 4.12: **Electropherogram example of total RNA quality from one of the 21 selected fetal liver samples showing apparent degradation (this sample was discarded from the selection on the basis of poor RNA quality).**

Figure 4.12 was an exception and shows poor quality RNA with moderate degradation. Consequently this sample was excluded from the selection.

4.3.5 Final sample selection of fetal liver RNA

From the twenty-one male fetuses selected from Table 4.3, twelve fetal liver samples were chosen to be used in the micro-array study. The final twelve fetal samples were selected on the basis of total RNA quality (28S/18S peak ratios for the selected twelve samples were between 1.5 and 2.1), as well as on the sizes of the litters from which the fetuses were taken (see Table 4.4).

9% casein	Horn/total	28s/18s ratio	18% casein	Horn/total	28s/18s ratio	Switch	Horn/total	28s/18s ratio
9-n16 L4	9/17	2.1	18-n10 R5	9/14	2.0	SW-n10 R3	6/10	1.5
9-n17 L4	7/12	2.1	18-n11 R5	7/13	2.0	SW-n11 R5	10/11	1.6
9-n19 L4	7/16	1.7	18-n20 L5	8/13	1.9	SW-n12 L5	9/10	2.1
9-n22 R4	8/13	2.0	18-n18 R3	7/14	1.6	SW-n20 L3	6/13	2.0
Means	(7.75/14.5)			(7.75/13.5)			(7.75/11)	

Table 4.4: References of the final twelve male fetal liver samples selected for genomics analysis, four biological replicates per dietary treatment group. Numbers in red indicate the horn litter size and the total litter size respectively from which each fetus came.

As described in Chapter 3, (section 3.3.1.2) the total size of the litter (i.e. total number of conceptuses in both uterine horns) from which a conceptus is taken has a significant negative effect on the weight of the conceptus, fetus, placenta and fetal liver when measured at day 17. In addition, left horn litter size had a significant negative effect on left horn fetus weights **(p= 0.000)** and on left horn placenta weights **(p=0.025)** in the same cohort of samples. Similarly, right horn litter size had a significant negative effect on right horn fetus weights **(p=0.000).** Note that horn (i.e. left or right) did not have a significant effect on the weight data at day 17.

In view of the above, and in order to minimize any potential effects of litter size on the genomics analysis, the total and in particular, the horn litter sizes of fetuses were taken into account when selecting the final fetal samples for the micro-array study so that these parameters could be kept as constant as possible between the dietary treatments. Mean total litter size and mean horn litter size for the final twelve samples selected are shown at

the bottom of Table 4.4. It was possible to standardize the average horn litter sizes across

all treatment groups in the samples, however total litter sizes were more variable.

4.3.6 Comparison of total RNA yields (µg) from final fetal liver samples
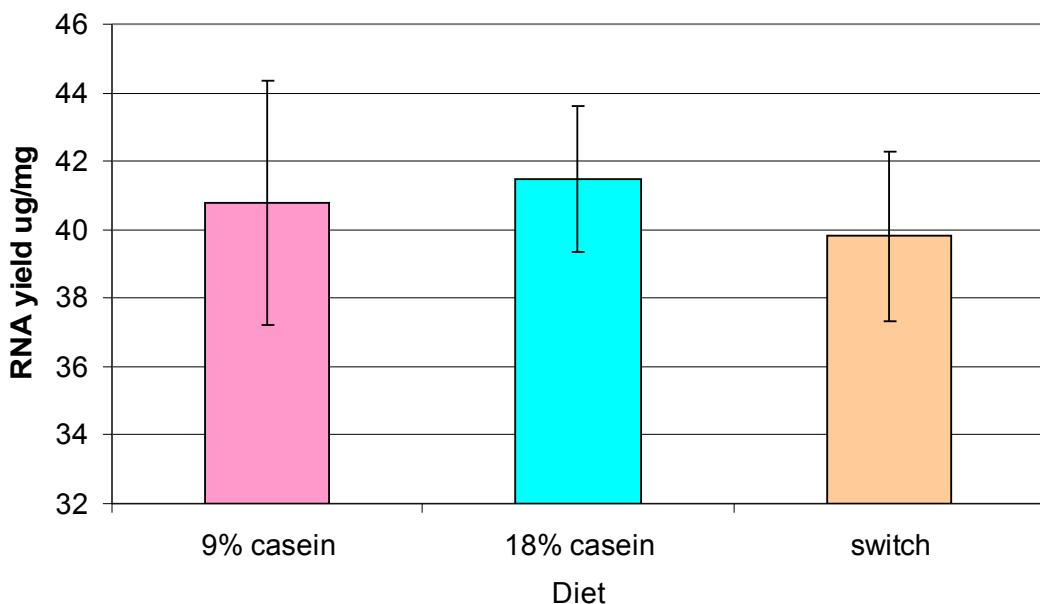
Figure 4.13: **Average RNA yield (µg/mg) from fetal liver tissue for final 12 micro-**

array samples. (n = 4 livers per group).

Figure 4.13 indicates that the average amount of RNA extracted from fetal liver tissue

(µg/mg) was broadly similar between dietary treatments for the twelve selected samples.

There was a large amount of variation around the means due to the low number of

replicates in each dietary treatment group (n = 4).

4.3.7 Adjusted cRNA yields

Yields of biotinylated cRNA recovered after clean up were above average. The yields

ranged from ~49 µg to ~85 µg across all samples, (Table 4.5).

9-16 L4	60.84		18-10 R5	85.42		SW-10 R3	71.81
9-17 L4	49.60		18-11 R5	59.03		SW-11 R5	83.31
9-19 L4	82.20		18-20 L5	48.81		SW-12 L5	57.72
9-22 R4	67.75		18-18 R3	57.34		SW-20 L3	64.00

Table 4.5: Adjusted cRNA yields (µg) for the twelve micro-array samples

4.3.8 Monitoring cRNA fragmentation

Figure 4.14 is a representative example of an electropherogram produced with the newly

fragmented cRNA. Migration of the fragmented cRNA at ~25 seconds correlates with an

average fragment size of above 25 bps (migrates at 22.5 seconds) but below 200 bps

(migrates at about ~29 seconds). Average cRNA fragment size was estimated as ~90 bp

in all samples, similar to expected.
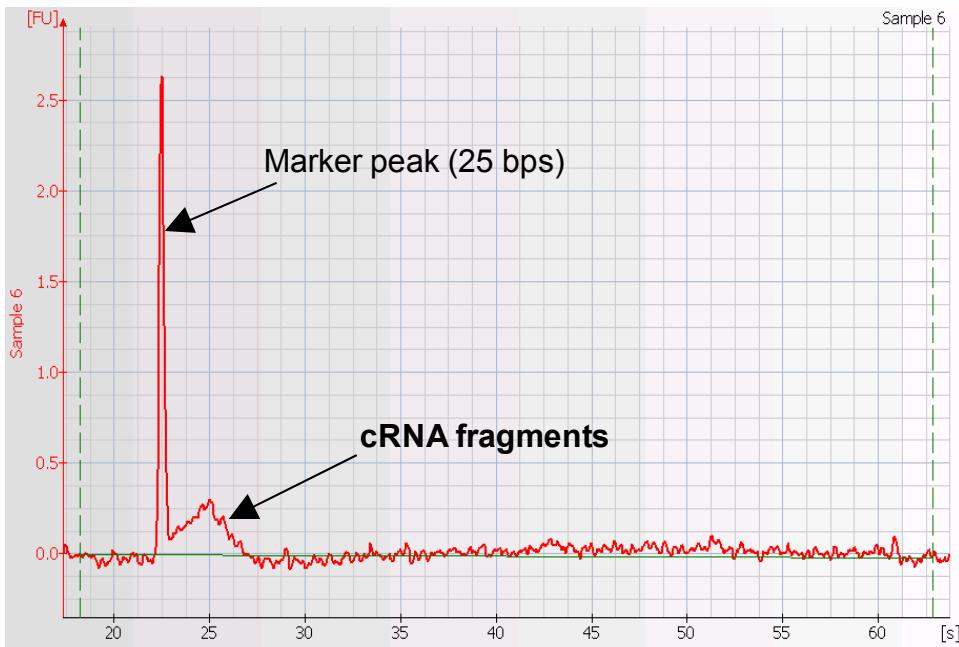
Figure 4.14: Example electropherogram of fragmented cRNA. Peak height relates to quantity of fragmented cRNA. Only 38.5 ng of fragmented cRNA was loaded here, hence the small cRNA peak reflects the small quantity of cRNA fragments loaded. Note the change of fluorescence scale (y-axis) compared to previous electropherograms which explains large marker peak here.

4.3.9 Scanned probe array images

Figures 4.15 to 4.18 show some images obtained from the GeneChip Scanner 3000 (Affymetrix). Images are of scanned probe arrays and show raw (.DAT file) data and averaged (.CEL file) data. By eye, all the .DAT files showed a high degree of similarity to one another amongst the chips for twelve samples which is desirable (i.e. no gross differences in staining/fluorescence were apparent at this stage).
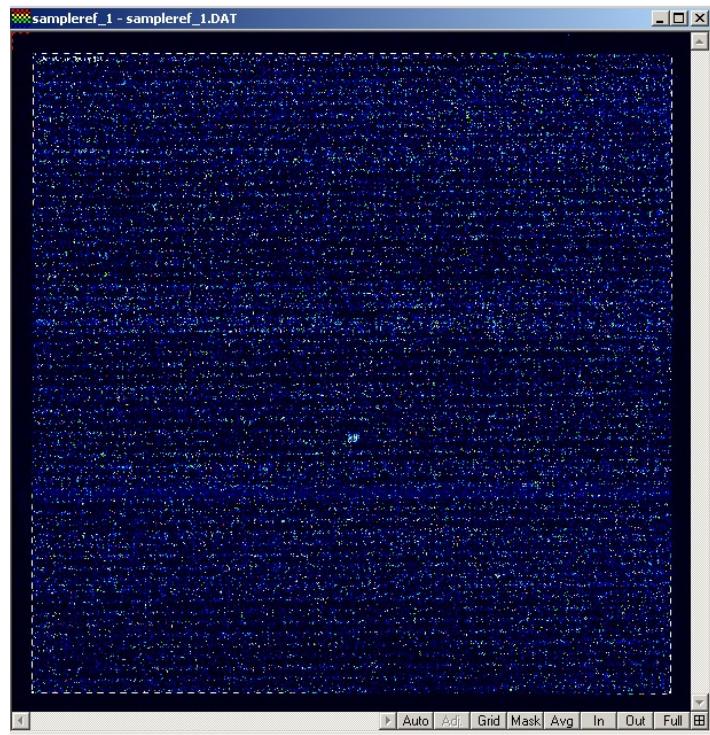
Figure 4.15: Raw .DAT file image of a scanned probe array generated from the GeneChip Scanner 3000.

The B2 Oligo serves as a positive hybridisation control and it is used by the GCOS software to place a grid over the image. Grid alignment is indicated by a checkerboard pattern at each corner of the array, and the pattern of intensities on the borders as well as by the central cross (Figure 4.16).
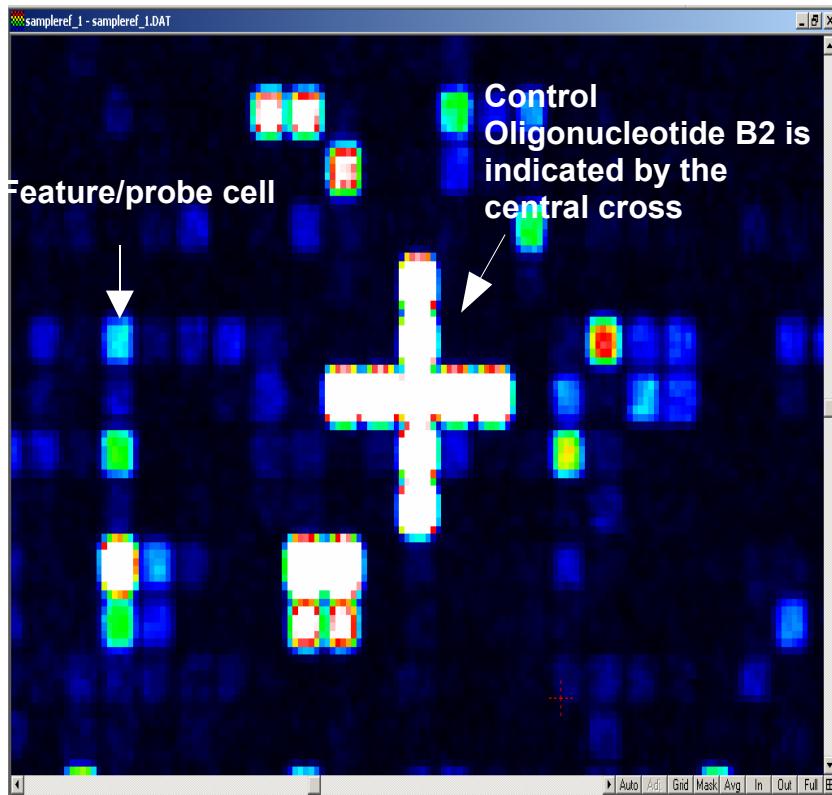
Figure 4.16: **Zoomed in example .DAT file image from a scanned probe array of pixel intensities in each probe cell. Here, the central cross on the array formed by the Oligo B2 indicates that the grid has been correctly aligned for image analysis. This was the case for all twelve scanned arrays.**

.CEL files were generated from the .DAT file data. .CEL files contain a single intensity value for each probe cell delineated by the grid (Figure 4.17, 4.18).
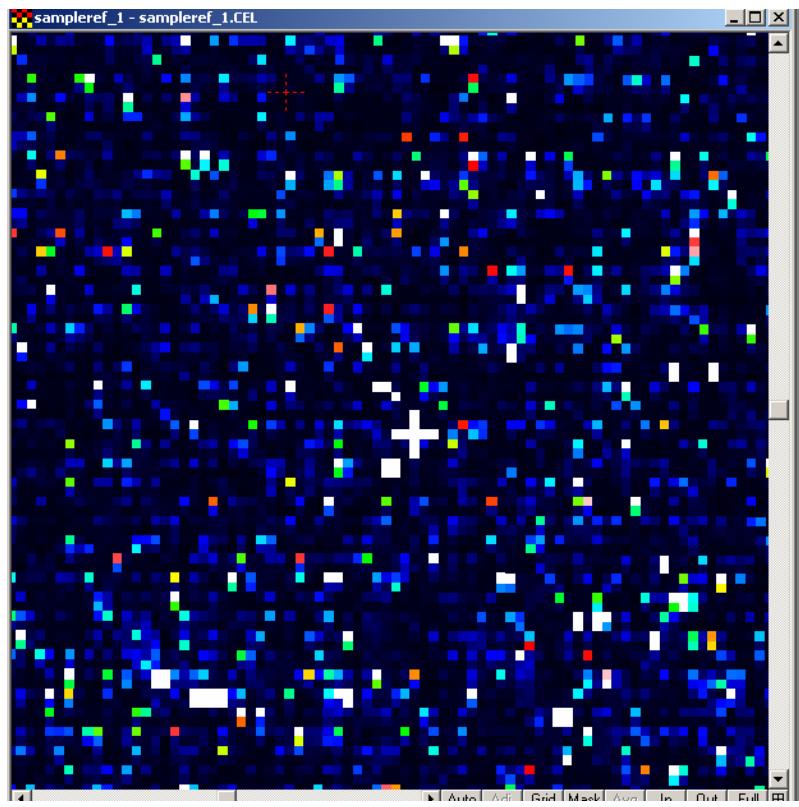
Figure 4.17: Example .CEL file image from a scanned probe array. Single (average)

intensity values for each probe cell are calculated here.

Figure 4.18: Zoomed in example .CEL file image

4.3.10 Data quality control parameters (GCOS)

Before conducting downstream analyses of array data, the quality of the array images was

assessed using the GCOS software (Affymetrix). From the report files (generated

from .CHP file data), a number of quality control parameters were assessed using the

poly-A controls, hybridization controls and house keeping/control probe sets.

For the purposes of reliable array-array comparison, a global scaling strategy was

employed. Thus, the average signal intensity of all the arrays was set to a default Target

Signal (TGT) value of 500. The key assumption here is that a relatively small subset of

transcripts will be changing amongst the arrays being analyzed. In this case, since the majority of transcripts will not be changing amongst samples, the overall intensities of the arrays should be similar. The overall intensity for each array is determined and compared to the target intensity value in order to calculate an appropriate scaling factor to make the different arrays comparable. The resulting scaling factors should be similar amongst all arrays, i.e. within two or three-fold of one another, as larger discrepancies here may indicate significant assay variability or sample degradation leading to noisier data (personal communication from Dr. Geoff Scopes, Affymetrix).

Overall Intensity x Scaling Factor = Target Intensity

For all twelve arrays, the scaling factors were within 2 fold of one another, the range of scaling factors for all the samples was between 3.792 and 5.137.

The number of probe sets called as "present" relative to the total number of probe sets on the array is shown as a percentage. The percentage detected should be similar amongst the replicates in each treatment (Table 4.6). Very low percent present can indicate poor sample quality.

Replicate	9% casein	18% casein	switch
1	50.30%	48.30%	48.80%
2	46.80%	49%	47.10%
3	47.40%	50.40%	51.20%
4	50.50%	49.10%	49.60%

Table 4.6: The percentage of probe sets called as "present" in samples from each dietary treatment showed similarity amongst replicates.

Table 4.6 indicates that around 50% of probe sets were detected across all samples in each of the three treatment groups which indicate there is a relatively high expression profile, (personal communication from Dr. Geoff Scopes, Affymetrix). Thus, the probe arrays contained genes which were relevant and appropriate for the samples used.

The poly-A RNA controls are internal control genes used to monitor the target labeling process for each sample and should be called "present" with increasing signal values in the order of *lys, phe, thr, dap.* In all cases, the poly-A controls were all present and were generally called in the expected order of detection although some minor exceptions were present at the lower end of detection.

The hybridisation controls *bioB, bioC, bioD* and *cre* (1.5pM, 5pM, 25pM and 100pM respectively) were spiked into the hybridization cocktail and hence are independent of RNA sample preparation, and thus can be used to measure sample hybridization efficiency on the expression arrays. *BioB* is at minimum level of assay sensitivity and hence may not always be called present. However *BioC*, *BioD* and *cre* should always be called "present" with increasing signal intensity. For all twelve arrays used, *BioC*, *BioD*, and *cre* were detectable with increasing intensity. Furthermore, *BioB* was also detectable on all of the arrays indicating that the detection was as good as it could be within the limitations of the assay.

Finally, the internal control genes on each array, β-actin and GAPDH, were used to indicate RNA sample and assay quality. Signal values of the 3' probe sets for actin and

GAPDH are compared to the signal values of the corresponding 5' probe sets. The ratio of the 3' probe set to the 5' probe set is usually no more than 3.0. The Affymetrix expression assay used has a strong 3' bias because this is where transcription started (in IVT reactions). Anti-sense cRNA was transcribed from the **sense** strand of the double-stranded cDNA via the T7 promoter. A higher 3' to 5' ratio indicates degraded RNA or inefficient transcription of the double-stranded cDNA or biotinylated cRNA. For all twelve arrays, actin and GAPDH were detected and the 3'/5' ratios for both genes were close to 1.0 in all cases. This indicates that RNA samples were of sufficient quality (non-degraded) and the cDNA synthesis and cRNA labelling assays worked optimally for all samples producing full-length transcripts.

4.3.11 Quality control monitoring with Expression Console

Expression Console is able to confirm many of the quality control measures that were analysed in GCOS, as well as provide some novel qualitative analyses of the array data gathered. Micro-array signals were normalised and quantified using Micro-array Analysis Suite 5.0 (MAS 5.0), Affymetrix before examining the Expression Console metrics.
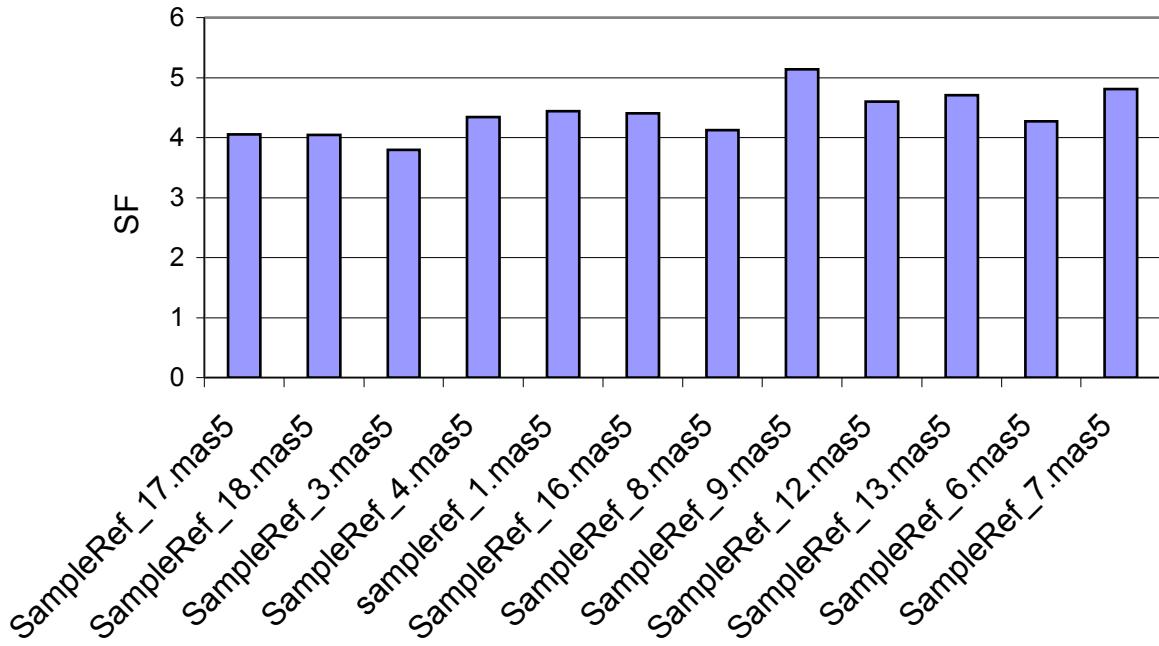
Figure 4.19: Comparison of Scale Factors (SF) across all micro-array samples.

Figure 4.19 confirms the GCOS results for this metric. The sample references denote the

array samples in the three treatment groups as shown in Table 4.7.

Diet treatment:	9% casein	18% casein	switch diet
Sample References:	1	3	6
	8	4	7
	9	17	12
	16	18	13

Table 4.7: Sample references of the twelve micro-array samples and the dietary

treatment groups to which they belong.
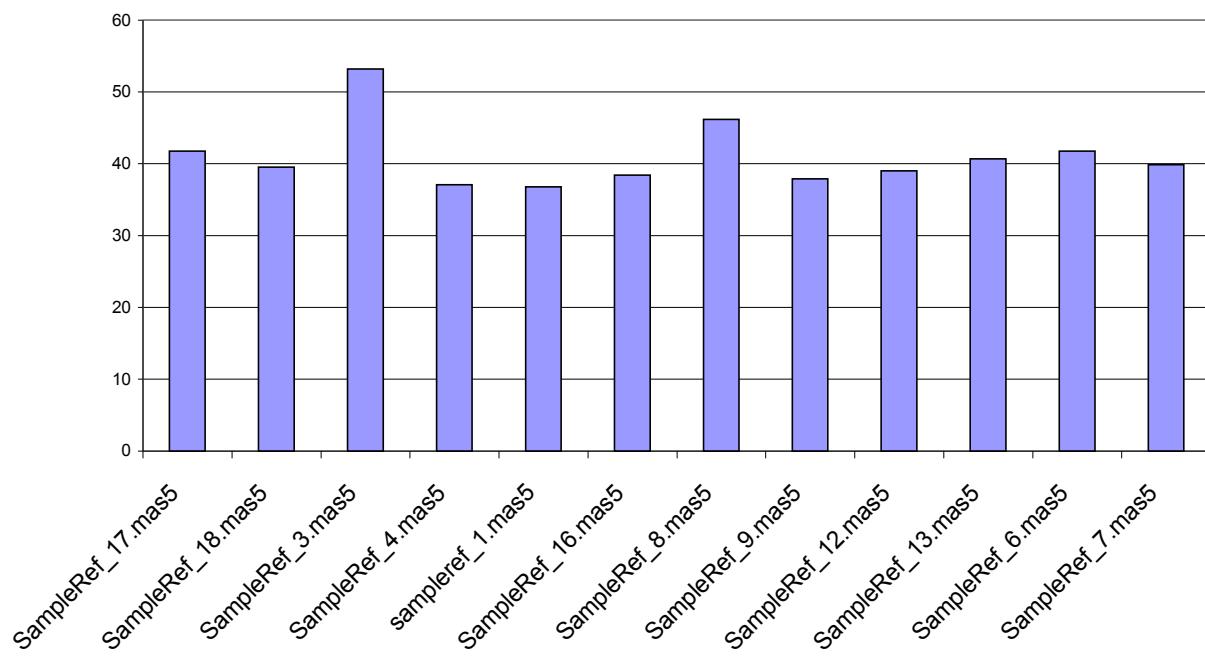
Figure 4.20: Background average intensity across all micro-array samples.

Figure 4.20 indicates that there were no extreme outliers in terms of the background level of fluorescence detected on the arrays across all diet groups.
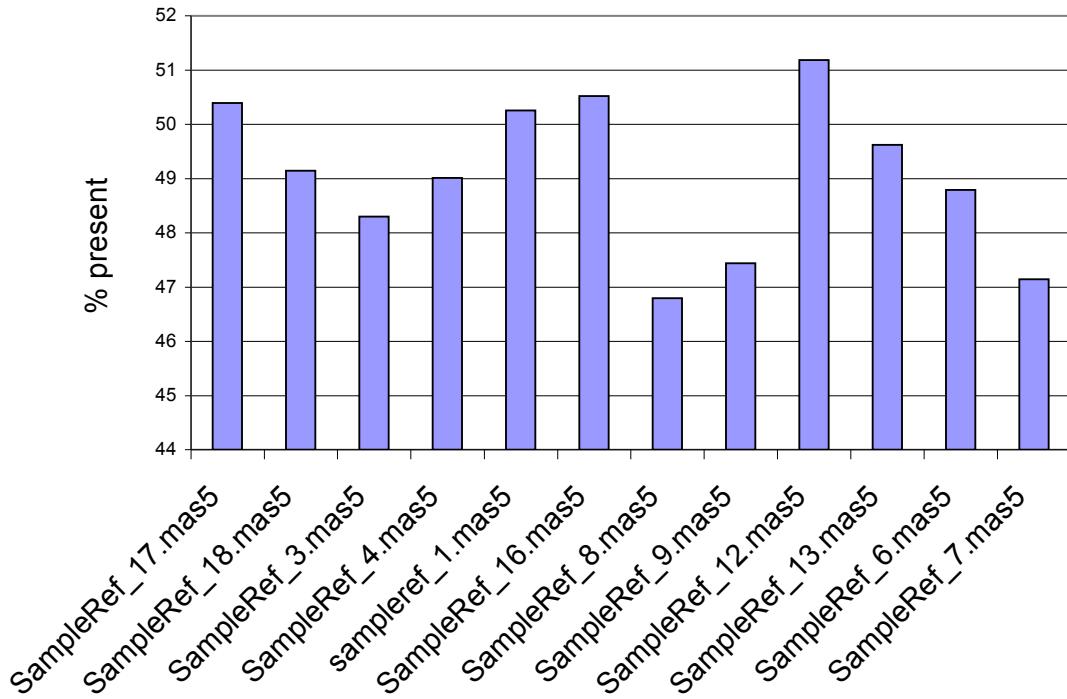
Figure 4.21: The percentage of probe sets called as "present" in each micro-array fetal liver sample.

Again, Figure 4.21 confirms the GCOS analysis of this parameter i.e. approximately 46-50% of the probe sets on the micro-array are detected in the fetal liver samples.
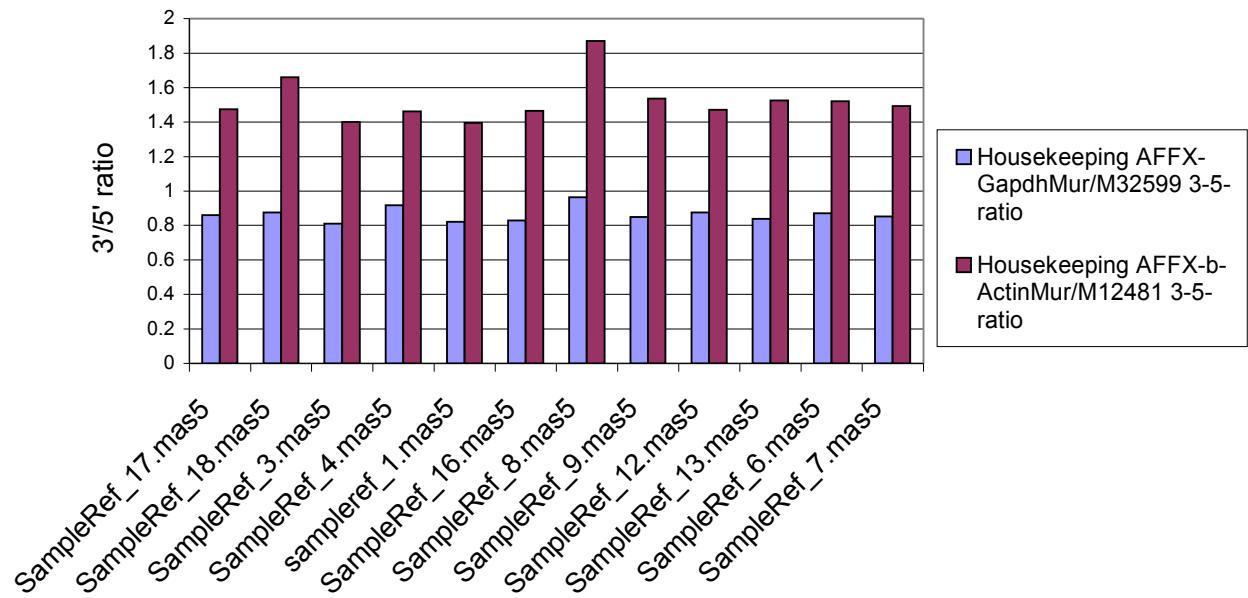
Figure 4.22: 3` to 5` ratios of housekeeping genes GAPDH and β-Actin across all micro-array samples.

Figure 4.22 indicates that the 3` to 5` ratios for the house keeping genes are close to 1.0 across all array samples which confirms the results obtained from GCOS.

Using the Expression Console software, a Pearson Correlation plot was generated from the .CEL file data. Figure 4.23 and Table 4.8 indicates the strength of the correlations of signals amongst samples of the same treatment group and between samples in different treatment groups.

Figure 4.23: (Overleaf) Pearson's Correlation plot showing the correlations in signals amongst all samples after analysing the .CEL files normalised with the MAS 5.0 algorithms. The strength of correlation between any two samples is indicated by the sliding colour scale from red (perfect correlation, 1.0) to dark blue (weakest correlation coefficient, 0.985).
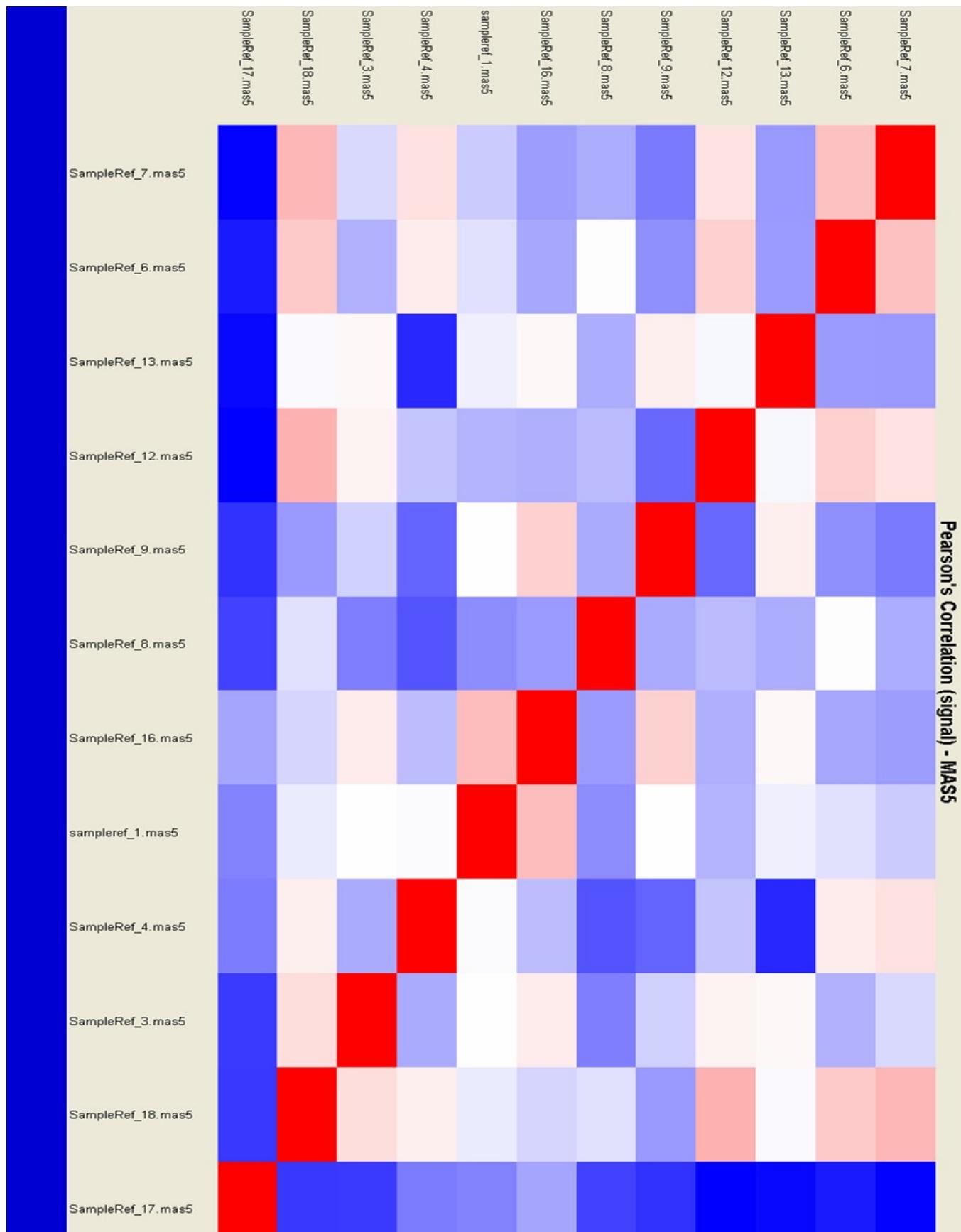
Correlation
coefficient
sliding scale

Mean of samples 17,18,3,4 (18% casein diet treatment)	0.9922988
Mean of samples 1,16,8,9 (9% casein diet treatment)	0.9917677
Mean of samples 12, 13, 6, 7 (switch diet treatment)	0.9899321
Mean of 18% casein samples Vs 9% casein samples	0.9907692
Mean of 18% casein samples Vs switch samples	0.9906570
Mean of 9% casein samples Vs switch samples	0.9902044

Table 4.8: Mean correlation coefficients of signals for array samples within and between treatment groups (MAS 5.0 normalised data).

Figure 4.23 and Table 4.8 indicate that all the array samples, from whichever treatment group, show a very high degree of similarity. This suggests that there are no appreciable differences in the correlation coefficients within groups compared to between groups. Therefore, changes in expression that are due to treatment may be difficult to distinguish from background biological variation.

RMA normalisation algorithm

A Pearson Correlation plot and table of mean correlations was also created for correlations between the sample arrays when the .CEL files were analysed using the RMA algorithm (see Appendix I). In general, the strength of these correlations appeared to be stronger compared to that in Figure 4.23, where data were normalised with MAS 5.0 algorithm. However, it is still the case that in general there does not seem to be much higher correlation coefficients of signals amongst samples of the same treatment group compared to between samples of different groups (see also Figure 4.24).
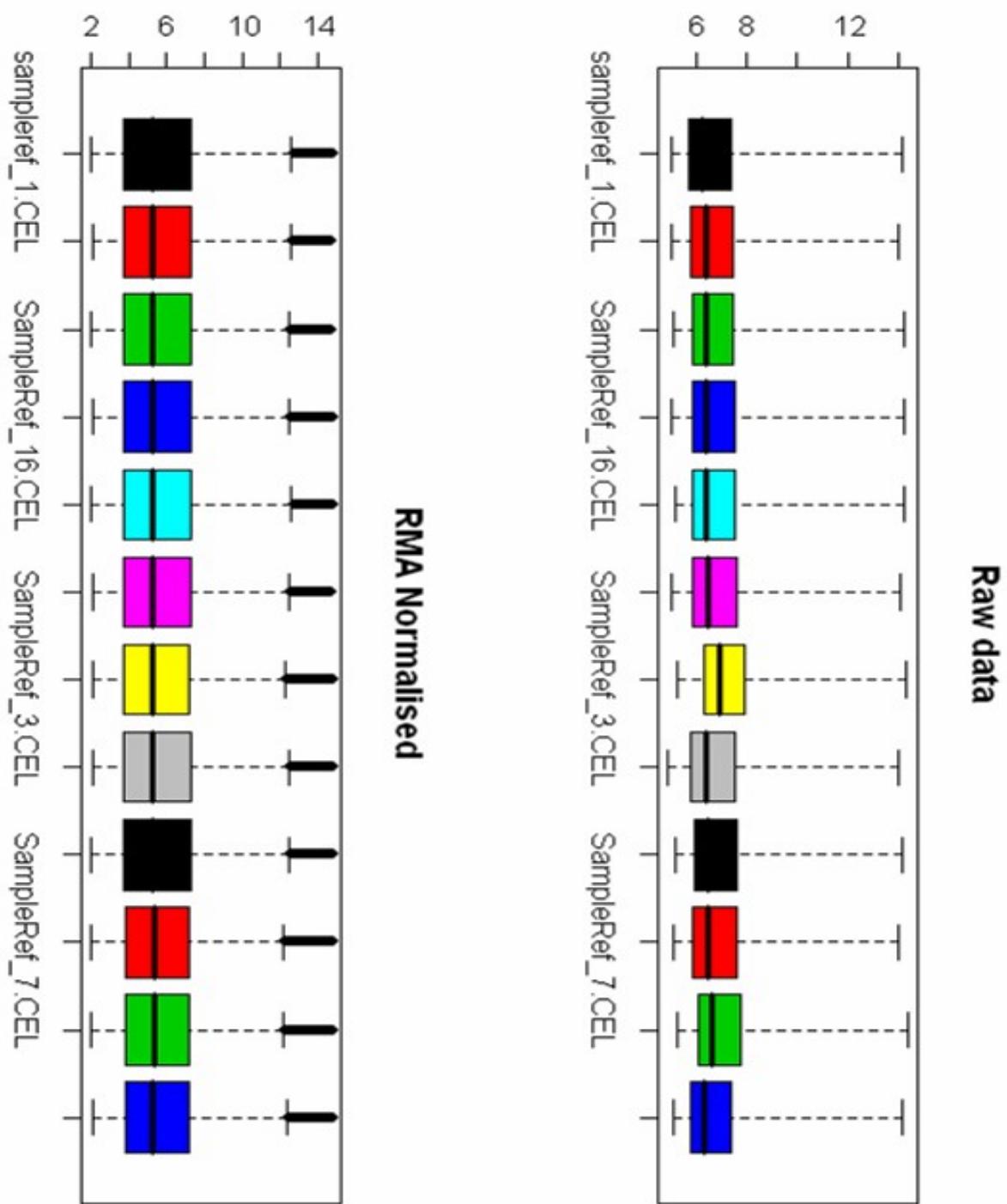
Figure 4.24: RMA normalized log expression signal data compared to raw log expression signal data. After RMA normalization, all twelve array samples are comparable and no real differences in expression signals are apparent overall.

4.3.12 Downstream analysis using Array Assist (using RMA normalised data).

The .CEL file data were converted into expression levels and Principal Component Analysis was used to visualize the separation between the different treatment groups of samples when the array data had been normalised with the RMA algorithm. However, there is not a clear-cut separation of samples into the three treatment groups, (Figure 4.25). Indeed, as described earlier many of the samples show a higher correlation between different diet groups than within groups of replicates.
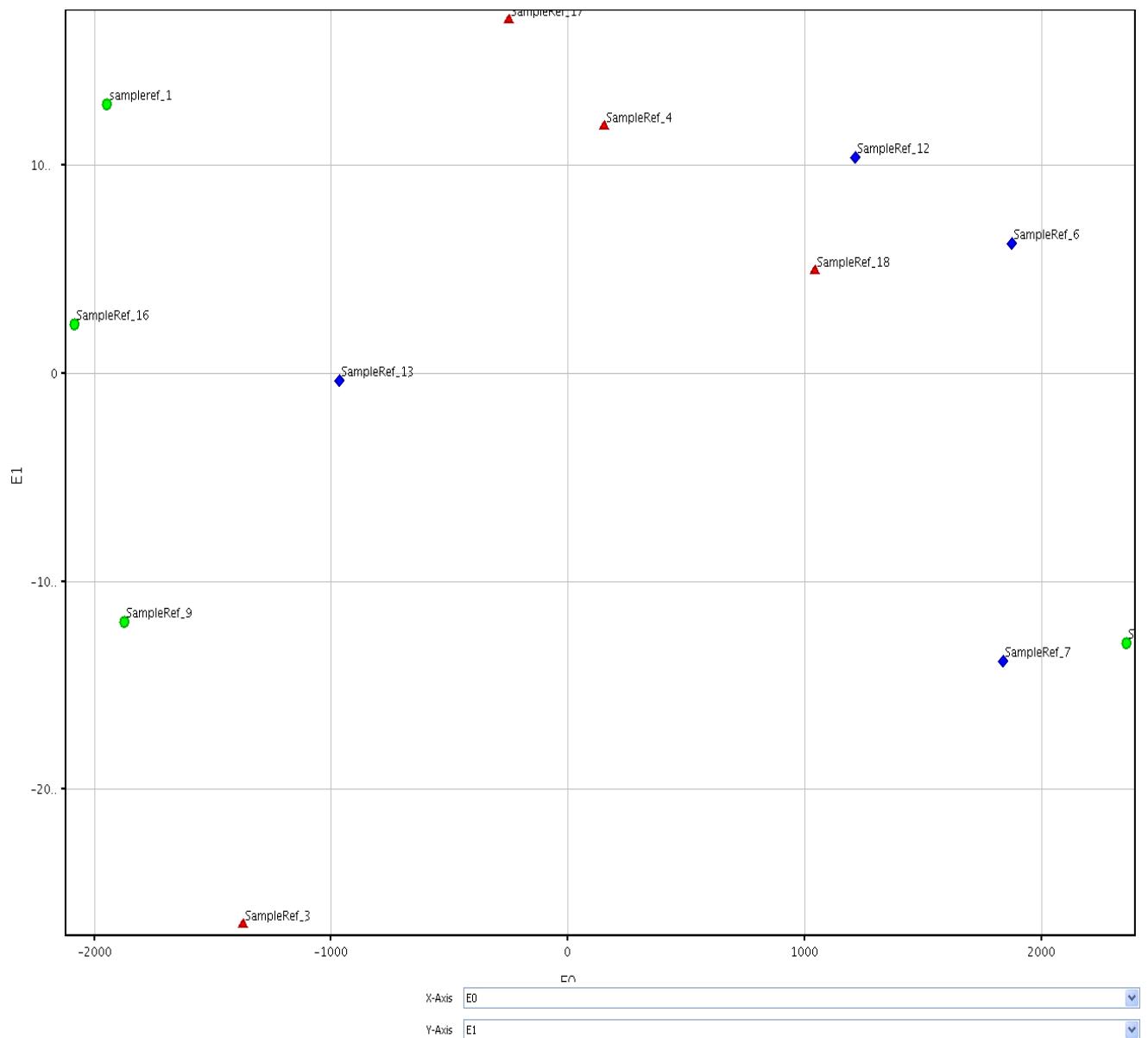
Figure 4.25: Principal Component Analysis Scores for array data when normalised with RMA. The three dietary groups are identified by the different coloured shapes. Ideally, there should be a good separation between the control group and the two treatment groups, but this is not the case.

In Figure 4.25, samples 1, 9 and 16 in the 9% casein diet group all look fairly closely related, but sample 8 is a strong outlier from this group on the opposite side of the plot. Similarly, for the 18% casein diet group samples 4, 17, and 18 are closely related but sample 3 is a strong outlier. In the switch diet group samples 6, 7, 12 are fairly close to one another, but sample 13 is further away from its group. Thus, it appears that samples 3, 8 and 13 are outliers to their respective diet groups. One possibility would be to exclude these outliers from the further analysis; however, this would also mean a loss of information. Thus the analysis proceeded with all samples included.

Table 4.9 displays the results of the significance analysis for each of three comparisons made between the diet groups. The number of changed genes at different p-values, combined with different sized fold changes is shown for each comparison. The bottom row of each comparison indicates the number of changed genes expected to arise by chance at each p-value, which is quite concerning.

Table 4.9: (overleaf) Results of differential expression analyses between pairs of diet groups (unpaired t-tests). Key to nomenclature used in this table: T1 (9% casein), T2 (switch), Ctrl (18% casein), FC (Fold change).

	P all	P < 0.05	P < 0.02	P < 0.01
FC all	29641	1556	635	
FC > 1.1	8041	1377	581	
FC > 1.5	152	38	19	
FC > 2.0	37	11	6	
FC > 3.0	6	3	2	
Expected by chance		1482	592	

Select group or pair [T2] Vs [Ctrl]

	P all	P < 0.05	P < 0.02	P < 0.01
FC all	29641	1182	430	
FC > 1.1	7130	992	379	
FC > 1.5	140	25	8	
FC > 2.0	21	4	2	
FC > 3.0	3	1	0	
Expected by chance		1482	592	

Select group or pair [T2] Vs [T1]

	P all	P < 0.05	P < 0.02	P < 0.01
FC all	29641	2172	876	
FC > 1.1	9448	1964	812	
FC > 1.5	287	121	65	
FC > 2.0	53	20	13	
FC > 3.0	13	4	2	
Expected by chance		1482	592	

Using the least stringent criteria in Table 4.9, i.e. p<0.05 and fold change 1.1< (a very small change in expression), the results indicate that for the 9% casein v 18% casein comparison 1377 probe sets changed; for the switch v 18% casein comparison 992 probe sets changed and for the switch v 9% casein comparison 1964 probe sets were changed. Thus, it appears that the greatest number of changes in probe set expression was between the switch and 9% casein diet groups. However, the expected number of changes identified by chance at this significance level was 1482! If gene lists were produced of the probe sets identified in the first two comparisons using the above criteria they would include non-meaningful results as the numbers of probe sets identified by chance is greater than the number of probe sets identified as changing in each of these comparisons. Using these criteria, only the switch v 9% casein comparison is likely to include meaningful probe sets changes, not generated by chance, but even then the rate of false discovery stands at 75%!

Despite the high likelihood of false discoveries, analysis was carried out to detect probe sets apparently changing between the diet groups with a fold change of **1.4<** and a p-value of <0.05, and gene lists were produced (Tables 4.10 to 4.12). The gene lists indicate that the largest number of changes again results from the switch v 9% comparison. For all comparisons the number of up-regulated genes was greater than the number down-regulated: 9% casein v 18% casein = 73 probe sets changed, 29 down; 44 up; switch v 18% casein = 53 probe sets changed, 13 down, 40 up; switch v 9% casein 227 probe sets changed, 109 down, 118 up.

Probe Set ID	Gene Title	p-value	FC
1455869_at	**Calcium/calmodulin-dependent protein kinase II, beta**	1.41E-06	**(-)14.20**
1431213_a_at	RIKEN cDNA 1300007C21 gene ///	7.15E-05	(-)11.52
1436296_x_at	Similar to dynein, axonemal, intermediate polypeptide 2	0.04	(-)3.51
1455773_at	Phosphatidylinositol binding clathrin assembly protein	0.02	(-)2.32
1448406_at	CREBBP/EP300 inhibitory protein 1	0.001	(+)2.31
1423257_at	cytochrome P450, family 4, subfamily a, polypeptide 14	0.01	(+)2.23
1416460_at	myo-inositol oxygenase	0.03	(-)2.21
1452975_at	alanine-glyoxylate aminotransferase 2-like 1	0.02	(+)2.19
1458609_at	Adult male bone cDNA, RIKEN full-length enriched library,	0.03	(+)2.17
1457458_at	cDNA sequence BC057627	0.04	(+)2.10
AFFX-18SRNAMur		0.02	(+)2.03
1438644_x_at	COMM domain containing 9	0.03	(+)1.98
1438763_at	dynein, axonemal, heavy chain 2 /// dynein heavy chain domain 3	0.01	(+)1.92
1429351_at	kelch-like 24 (Drosophila)	0.01	(+)1.92
1436735_at	NOL1/NOP2/Sun domain family 3	0.04	(+)1.86
1450459_at	RIKEN cDNA 2010106G01 gene	0.05	(+)1.86
1451920_a_at	replication factor C 1	0.05	(-)1.80
1451793_at	kelch-like 24 (Drosophila)	0.01	(+)1.78
1419127_at	neuropeptide Y	0.02	(+)1.75
1435378_at	RIKEN cDNA 2210020M01 gene	0.03	(-)1.67
1425451_s_at	chitinase 3-like 3 /// chitinase 3-like 4	0.03	(+)1.65
1419039_at	cytochrome P450, family 2, subfamily d, polypeptide 22	0.02	(+)1.64
1421031_a_at	RIKEN cDNA 2310016C08 gene	0.02	(+)1.63
1417273_at	pyruvate dehydrogenase kinase, isoenzyme 4	0.03	(+)1.63
1423566_a_at	heat shock protein 110	0.03	(-)1.62
1419764_at	chitinase 3-like 3	0.01	(+)1.61
1416521_at	selenoprotein W, muscle 1	0.01	(+)1.61
1449051_at	peroxisome proliferator activated receptor alpha	0.02	(+)1.60
1423062_at	insulin-like growth factor binding protein 3	0.03	(-)1.59
1426037_a_at	regulator of G-protein signaling 16	0.02	(+)1.59
1428923_at	protein phosphatase 1, regulatory (inhibitor) subunit 3G	0.02	(+)1.57
1434278_at	X-linked myotubular myopathy gene 1	0.02	(-)1.54
1436795_at	RIKEN cDNA 9630058J23 gene	0.01	(+)1.54
1436948_a_at	RIKEN cDNA 6430550H21 gene	0.03	(+)1.54
1436355_at	fatty acid desaturase domain family, member 6	0.01	(-)1.53
1419314_at	tubulointerstitial nephritis antigen	0.04	(-)1.53
1418936_at	v-maf musculoaponeurotic fibrosarcoma oncogene family,	0.04	(+)1.51
1437497_a_at	heat shock protein 90kDa alpha (cytosolic), class A member 1	0.02	(-)1.51
1421163_a_at	nuclear factor I/A	0.02	(+)1.50
1426743_at	Dip3 beta	0.003	(+)1.49
1429530_a_at	sphingomyelin phosphodiesterase 4	0.02	(-)1.48
1451355_at	N-acylsphingosine amidohydrolase 3-like	0.03	(+)1.48
1458268_s_at	insulin-like growth factor binding protein 3	0.02	(-)1.48
1453457_at	RIKEN cDNA 2900070H08 gene	0.04	(+)1.48
1460328_at	bromodomain containing 3	0.03	(-)1.48
1425993_a_at	heat shock protein 110	0.04	(-)1.48
1417707_at	RIKEN cDNA B230342M21 gene	0.03	(+)1.47
1421198_at	integrin alpha V	0.03	(+)1.47

1441915_s_at	RIKEN cDNA 2310076L09 gene	0.01	(+)1.47
1427347_s_at	tubulin, beta 2a /// tubulin, beta 2b /// similar to tubulin, beta 3	0.01	(-)1.46
1434405_at	RIKEN cDNA A730024A03 gene	0.01	(+)1.46
1428682_at	zinc finger CCCH type containing 6	0.03	(+)1.46
1446807_at	ubiquitin specific peptidase 8	0.03	(-)1.45
1428870_at	nucleolar and coiled-body phosphoprotein 1	0.04	(-)1.45
1433772_at	stress 70 protein chaperone, microsome-associated, human homolog	0.003	(-)1.45
1424937_at	RIKEN cDNA 2310076L09 gene	0.005	(+)1.44
1444036_at	Protein phosphatase 2, regulatory subunit B (B56), alpha isoform	0.05	(+)1.43
1439516_at	RIKEN cDNA 2610201A13 gene	0.02	(-)1.43
1453008_at	RIKEN cDNA 2300002D11 gene	0.01	(+)1.43
1453080_at	RIKEN cDNA 9130022K13 gene ///	0.03	(+)1.43
1424843_a_at	growth arrest specific 5	0.03	(-)1.43
1450900_at	expressed sequence AW011752	0.01	(+)1.43
1425632_a_at	PQ loop repeat containing 2	0.02	(+)1.42
1437959_at	zinc finger protein 324	0.02	(-)1.42
1456991_at	Cobl-like 1	0.04	(+)1.42
1453954_a_at	mitochondrial ribosomal protein S5	0.03	(-)1.42
1421260_a_at	spermidine synthase	0.002	(-)1.42
1448277_at	polymerase (DNA directed), delta 2, regulatory subunit	0.002	(-)1.41
1426657_s_at	3-phosphoglycerate dehydrogenase ///	2.58E-04	(-)1.41
1428869_at	nucleolar and coiled-body phosphoprotein 1	0.04	(-)1.41
1421009_at	radical S-adenosyl methionine domain containing 2	0.04	(+)1.41
1425503_at	glucosaminyl (N-acetyl) transferase 2, I-branching enzyme	0.03	(+)1.40
1421002_at	angiopoietin-like 2	0.01	(+)1.40

Table 4.10: Gene list of 73 probe sets identified as up or down-regulated in expression in the 9% casein treatment group relative to 18% casein control group. The +/- sign in the FC (fold change) column indicates the direction of the change in expression of that gene. The largest fold change identified here is for probe set 1455869 which represents the Camk2b gene. This analysis suggests that Camk2b is heavily down regulated by the 9% casein treatment.

Probe Set ID	Gene Title	p-value	FC
1448406_at	CREBBP/EP300 inhibitory protein 1	0.02	(+)1.98
1429809_at	transmembrane and tetratricopeptide repeat containing 2	0.01	(-)1.44
1457484_at	hypothetical D930050J11	9.53E-04	(+)1.42
1438644_x_at	COMM domain containing 9	0.002	(+)2.60
1435378_at	RIKEN cDNA 2210020M01 gene	0.04	(-)1.59
1436296_x_at	Similar to dynein, axonemal, intermediate polypeptide 2	0.04	(-)3.59
1457458_at	cDNA sequence BC057627	0.03	(+)2.23
1426737_at	G1 to S phase transition 1	0.02	(-)1.46
1440443_at	RIKEN cDNA E030016H06 gene	0.04	(+)1.90
1443852_at	Transcribed locus	0.04	(+)1.51
1446160_x_at	transmembrane protein 69	0.05	(+)1.48
1436944_x_at	RIKEN cDNA 4933439C20 gene	0.02	(+)1.49
1435371_x_at	carboxylesterase 3	0.05	(+)1.45
1442255_at	RIKEN cDNA 5033414D02 gene	0.04	(+)1.73
1438508_at	Jumonji domain containing 1B	0.02	(+)1.49
1436766_at	LUC7-like 2 (S. cerevisiae)	0.05	(+)1.48
1421258_a_at	pyruvate kinase liver and red blood cell	0.02	(-)1.42
1439319_at	E74-like factor 1	0.04	(+)1.62
1429478_at	RIKEN cDNA 6720463M24 gene	0.04	(+)1.82
1417079_s_at	lectin, galactose-binding, soluble 2	0.02	(-)1.61
1451798_at	interleukin 1 receptor antagonist	0.03	(-)1.46
1458505_at	hypothetical LOC552901	0.01	(+)1.50
1436898_at	splicing factor proline/glutamine rich (polypyrimidine tract binding protein associated)	0.004	(+)1.48
1457605_at	Ataxin 1	0.03	(+)1.45
1421869_at	tripartite motif-containing 44	0.03	(-)1.54
1445402_at	Adenosine kinase	0.03	(+)1.56
1420901_a_at	hexokinase 1	0.03	(-)1.45
1438244_at	nuclear factor I/B	0.02	(+)1.62
1443056_at	Protein tyrosine phosphatase, receptor type, D	0.05	(+)1.45
1435163_at	RIKEN cDNA 9030612M13 gene	0.01	(+)1.44
1445695_at	Ataxin 1	5.25E-04	(+)1.62
1424737_at	thyroid hormone responsive SPOT14 homolog (Rattus)	0.02	(+)1.64
1429701_at	RIKEN cDNA 2410003J06 gene	0.03	(+)1.63
1442109_at		0.02	(+)1.82
1449556_at	histocompatibility 2, T region locus 23 /// RIKEN cDNA C920025E04 gene	0.03	(-)1.41
1430404_at	RIKEN cDNA 4833416J08 gene	0.05	(+)1.46
1440365_at	Actin, beta, cytoplasmic	0.04	(+)1.43
1418604_at	arginine vasopressin receptor 1A	0.03	(-)1.69
1446284_at	metastasis suppressor 1	0.004	(+)2.02
1441988_at	protein phosphatase 1K (PP2C domain containing)	0.05	(+)1.41
1417015_at	Ras association (RalGDS/AF-6) domain family 3	0.01	(-)1.45
1429882_at	RIKEN cDNA 2610005L07 gene	0.03	(+)1.55
1437862_at	RIKEN cDNA 2600011C06 gene	0.04	(+)1.49
1457770_at	solute carrier family 39 (zinc transporter), member 14	0.04	(+)1.50
1441653_at	RIKEN cDNA D030022P06 gene	0.01	(+)1.52
1430622_at	RIKEN cDNA 4833423F13 gene	0.04	(+)1.44
1427052_at	acetyl-Coenzyme A carboxylase beta	0.02	(+)1.58
1443512_at	Spermatogenesis associated 5	0.01	(+)1.42

1431096_at	integrator complex subunit 8	0.03	(-)1.47
1450332_s_at	flavin containing monooxygenase 5	0.02	(+)1.40
1438265_at		0.04	(+)1.41
1457554_at	apolipoprotein B	0.01	(+)1.59
1451577_at	zinc finger and BTB domain containing 20	0.02	(+)1.41

Table 4.11: **Gene list of 53 probe sets identified as up or down-regulated in expression in the switch treatment group relative to 18% casein control group.**

Probe Set ID	Gene Title	p-value	FC	(+/-)
1434062_at	RAB GTPase activating protein 1-like	5.01E-04	1.55	down
1429809_at	transmembrane and tetratricopeptide repeat containing 2	6.12E-04	1.78	down
1453365_at	RAB GTPase activating protein 1-like	6.78E-04	1.40	down
1422833_at	forkhead box A2	6.89E-04	1.43	up
1444406_at	Mitogen-activated protein kinase kinase kinase kinase 3	7.82E-04	1.41	up
1457528_at	solute carrier family 4, sodium bicarbonate cotransporter, member 7	8.38E-04	1.54	up
1422906_at	ATP-binding cassette, sub-family G (WHITE), member 2	8.39E-04	1.40	down
1416286_at	regulator of G-protein signaling 4	8.44E-04	1.86	down
1449252_at	RIKEN cDNA 9030611O19 gene	9.42E-04	1.42	down
1422100_at	cytochrome P450, family 7, subfamily a, polypeptide 1	0.002	1.53	up
1424864_at	homeodomain interacting protein kinase 2	0.002	1.60	down
1437360_at	protocadherin 19	0.002	1.51	down
1416521_at	selenoprotein W, muscle 1	0.002	1.43	down
1449936_at	RIKEN cDNA 8430419L09 gene	0.002	1.45	down
1415899_at	Jun-B oncogene	0.002	2.56	down
1429882_at	RIKEN cDNA 2610005L07 gene	0.002	1.62	up
1416913_at	esterase 1	0.002	1.81	up
1427347_s_at	tubulin, beta 2a /// tubulin, beta 2b ///	0.002	1.64	up
1456359_at	peptidylprolyl isomerase domain and WD repeat containing 1	0.003	1.55	down
1444538_at	Expressed sequence AL033314	0.003	1.55	up
1441653_at	RIKEN cDNA D030022P06 gene	0.003	1.56	up
1426721_s_at	TCDD-inducible poly(ADP-ribose) polymerase	0.003	1.74	down
1437878_s_at	coiled-coil domain containing 39 /// tetratricopeptide repeat domain 14	0.003	1.41	up
1443512_at	Spermatogenesis associated 5	0.003	1.43	up
1429433_at	BAT2 domain containing 1	0.003	1.55	up
1431235_at		0.004	1.50	up
1427052_at	acetyl-Coenzyme A carboxylase beta	0.004	1.62	up
1416460_at	myo-inositol oxygenase	0.004	2.23	up
1417079_s_at	lectin, galactose-binding, soluble 2	0.004	1.90	down
1430622_at	RIKEN cDNA 4833423F13 gene	0.004	1.40	up
1424962_at	transmembrane 4 superfamily member 4	0.004	1.49	down
1446284_at	metastasis suppressor 1	0.004	1.89	up
1421163_a_at	nuclear factor I/A	0.004	1.61	down
1439970_at	WNK lysine deficient protein kinase 1	0.005	1.41	up
1443505_at	Prokineticin 1	0.005	3.34	up
1449335_at	tissue inhibitor of metalloproteinase 3	0.01	1.41	down
1438037_at	hect domain and RLD 5	0.01	1.72	up
1448852_at	regucalcin	0.01	1.45	up
1438763_at	dynein, axonemal, heavy chain 2 /// dynein heavy chain domain 3	0.01	2.01	down
1451240_a_at	glyoxalase 1	0.01	1.47	up
1440490_at	Membrane protein, palmitoylated 6 (MAGUK p55 subfamily member 6)	0.01	1.54	down
1440573_at	Erbb2 interacting protein	0.01	2.44	down
1424108_at	glyoxalase 1	0.01	1.42	up
1457554_at	apolipoprotein B	0.01	1.59	up
1449005_at	solute carrier family 16 (monocarboxylic acid transporters), member 3	0.01	1.45	down
1417231_at	claudin 2	0.01	1.78	up
1418918_at	insulin-like growth factor binding protein 1	0.01	1.45	down

1459984_at	melanoma inhibitory activity 3	0.01	2.00	up
1423663_at	folliculin	0.01	1.41	down
1439933_at	RIKEN cDNA B430316J06 gene	0.01	1.42	up
1419149_at	serine (or cysteine) peptidase inhibitor, clade E, member 1	0.01	6.87	down
1450387_s_at	adenylate kinase 3 alpha-like 1	0.01	1.64	down
1441228_at	apolipoprotein L domain containing 1	0.01	1.45	down
1426037_a_at	regulator of G-protein signaling 16	0.01	1.75	down
1421031_a_at	RIKEN cDNA 2310016C08 gene	0.01	1.98	down
1416921_x_at	aldolase 1, A isoform	0.01	1.47	down
1433831_at	RIKEN cDNA 4833418A01 gene	0.01	1.52	down
1434278_at	X-linked myotubular myopathy gene 1	0.01	1.69	up
1417766_at	cytochrome b5 type B	0.01	1.49	up
1416667_at	phenylalkylamine Ca2+ antagonist (emopamil) binding protein	0.01	1.51	up
1455186_a_at	RIKEN cDNA 1190003J15 gene	0.01	1.59	up
1458268_s_at	insulin-like growth factor binding protein 3	0.01	1.73	up
1431786_s_at	RIKEN cDNA 1190003J15 gene	0.01	1.54	up
1452973_at	protein phosphatase 1K (PP2C domain containing)	0.01	1.50	down
1427213_at	6-phosphofructo-2-kinase/fructose-2,6-biphosphatase 1	0.01	1.55	up
1438244_at	nuclear factor I/B	0.01	1.48	up
1423062_at	insulin-like growth factor binding protein 3	0.01	1.88	up
1419647_a_at	immediate early response 3	0.01	1.68	down
1438663_at	BAT2 domain containing 1	0.01	1.43	up
1439825_at	deltex 3-like (Drosophila)	0.01	1.66	up
1441438_at	glypican 6	0.01	1.47	up
1437355_at	zinc finger, CCHC domain containing 5	0.01	1.42	down
1416895_at	ephrin A1	0.01	2.33	down
1444036_at	Protein phosphatase 2, regulatory subunit B (B56), alpha isoform	0.01	1.69	down
1449846_at	eosinophil-associated, ribonuclease A family, member 2	0.01	1.41	up
1457760_at	RIKEN cDNA A930004J17 gene	0.01	1.65	up
1419103_a_at	abhydrolase domain containing 6	0.01	1.48	down
1442109_at		0.01	2.03	up
1441272_at		0.01	1.60	up
1423244_at	RIKEN cDNA 9030012A22 gene	0.01	1.69	up
1434799_x_at	aldolase 1, A isoform	0.01	1.47	down
1438167_x_at	Folliculin	0.01	1.47	down
1442015_at	RIKEN cDNA 2500002B13 gene	0.01	1.47	down
1451756_at	FMS-like tyrosine kinase 1	0.01	1.45	down
1439038_at	RIKEN cDNA 9130227C08Rik gene	0.01	1.52	down
1440461_at	RIKEN cDNA 0910001A06 gene	0.02	1.46	up
1419039_at	cytochrome P450, family 2, subfamily d, polypeptide 22	0.02	1.63	down
1454229_a_at	exonuclease domain containing 1	0.02	1.41	down
1426805_at	SWI/SNF related, matrix associated, actin dependent regulator of chromatin,	0.02	1.86	up
1429351_at	kelch-like 24 (Drosophila)	0.02	1.63	down
1445381_at		0.02	1.70	down
1441947_x_at	cDNA sequence BC033915	0.02	1.56	down
1446007_at	Bone morphogenetic protein 1	0.02	1.40	up
1448510_at	ephrin A1	0.02	2.54	down
1418787_at	mannose binding lectin (C)	0.02	2.76	up
1459687_x_at	Cleavage and polyadenylation specific factor 6	0.02	1.41	up

1457449_at	Longevity assurance homolog 6 (S. cerevisiae)	0.02	1.46	up
1451798_at	interleukin 1 receptor antagonist	0.02	1.64	down
1448340_at	transmembrane protein 30A	0.02	1.54	up
1460052_at	Acyl-CoA synthetase medium-chain family member 1	0.02	1.64	down
1430566_at	RIKEN cDNA 4733401A01 gene	0.02	1.85	up
1454617_at	arrestin domain containing 3	0.02	1.48	down
1459497_at	Farnesyl diphosphate farnesyl transferase 1	0.02	1.42	up
1441102_at	prolactin receptor	0.02	2.15	up
1418936_at	v-maf musculoaponeurotic fibrosarcoma oncogene family, protein F (avian)	0.02	1.79	down
1434025_at		0.02	1.42	down
1419322_at	FYVE, RhoGEF and PH domain containing 6	0.02	1.40	down
1448009_at	UDP-glucose ceramide glucosyltransferase-like 1	0.02	1.41	up
1426958_at	ribosomal protein S9 /// similar to ribosomal protein S9	0.02	1.47	up
1420774_a_at	RIKEN cDNA 4930583H14 gene	0.02	2.99	down
1437638_at	serine/arginine repetitive matrix 2	0.02	1.55	up
1421830_at	adenylate kinase 3 alpha-like 1	0.02	1.58	down
1426810_at	jumonji domain containing 1A	0.02	1.43	down
1436538_at	ankyrin repeat domain 37	0.02	3.21	down
1459141_at	RIKEN cDNA 1810008I18 gene	0.02	1.62	up
1448792_a_at	cytochrome P450, family 2, subfamily f, polypeptide 2	0.02	2.00	up
1438743_at	cytochrome P450, family 7, subfamily a, polypeptide 1	0.02	1.87	up
1433604_x_at	aldolase 1, A isoform	0.02	1.49	down
1427070_at	RIKEN cDNA 5730407K14 gene	0.02	1.85	down
1438265_at		0.02	1.40	up
1428923_at	protein phosphatase 1, regulatory (inhibitor) subunit 3G	0.02	1.56	down
1451355_at	N-acylsphingosine amidohydrolase 3-like	0.02	1.61	down
1449347_a_at	X-linked lymphocyte-regulated 4B /// 4A /// 4E	0.02	1.59	up
1437417_s_at	glypican 6	0.02	1.48	up
1443838_x_at	fatty acid desaturase 2	0.02	1.42	up
1458601_at	RIKEN cDNA 8030447M02 gene	0.02	1.41	up
1434465_x_at	very low density lipoprotein receptor	0.02	1.73	down
1442679_at	Mitogen activated protein kinase kinase 4	0.02	2.21	up
1458832_at	Growth hormone receptor	0.02	1.52	up
1420678_a_at	interleukin 17 receptor B	0.02	1.40	down
1435866_s_at	histone 3, H2a	0.03	1.56	down
1434958_at	sacsin	0.03	1.43	up
1425632_a_at	PQ loop repeat containing 2	0.03	1.41	down
1426356_at	RIKEN cDNA 6330578E17 gene	0.03	1.48	down
1424794_at	ring finger protein 186	0.03	1.51	down
1453189_at	ubiquitin-conjugating enzyme E2I	0.03	1.73	up
1439173_at	hook homolog 1 (Drosophila)	0.03	1.43	up
1459627_at	Sterol-C4-methyl oxidase-like	0.03	1.44	up
1456974_at	one cut domain, family member 1	0.03	2.75	up
1420934_a_at	serine/arginine repetitive matrix 1	0.03	1.42	up
1453009_at	carboxypeptidase M	0.03	1.99	down
1440926_at	FMS-like tyrosine kinase 1	0.03	1.41	down
1442549_at	muscleblind-like 3 (Drosophila)	0.03	1.45	up
1421076_at	SERTA domain containing 3	0.03	1.74	down
1418662_at	RIKEN cDNA 2210012G02 gene	0.03	1.81	down

1453776_at	RIKEN cDNA 5730407K14 gene	0.03	1.45	down
1441573_at	Sex comb on midleg homolog 1	0.03	1.49	down
1435018_at	RIKEN cDNA 5930434B04 gene	0.03	1.40	up
1421946_at	C-reactive protein, pentraxin-related	0.03	1.44	up
1451261_s_at	expressed sequence AW049765	0.03	1.51	up
1454904_at	X-linked myotubular myopathy gene 1	0.03	1.61	up
1418028_at	dopachrome tautomerase	0.03	1.58	up
1424737_at	thyroid hormone responsive SPOT14 homolog (Rattus)	0.03	1.85	up
1416514_a_at	fascin homolog 1, actin bundling protein (Strongylocentrotus purpuratus)	0.03	1.50	down
1437862_at	RIKEN cDNA 2600011C06 gene	0.03	1.56	up
1447046_at	DnaJ (Hsp40) related, subfamily B, member 13	0.03	1.57	up
1440373_at	ELAV (embryonic lethal, abnormal vision, Drosophila)-like 1 (Hu antigen R)	0.03	1.41	up
1457635_s_at	nuclear receptor subfamily 3, group C, member 1	0.03	1.44	down
1457357_at	tousled-like kinase 2 (Arabidopsis)	0.03	1.43	up
1419523_at	cytochrome P450, family 3, subfamily a, polypeptide 13	0.03	1.63	up
1460242_at	CD55 antigen	0.03	1.42	down
1417273_at	pyruvate dehydrogenase kinase, isoenzyme 4	0.03	1.61	down
1445695_at	Ataxin 1	0.03	1.50	up
1426008_a_at	solute carrier family 7 (cationic amino acid transporter, y+ system),	0.03	1.67	down
1448239_at	heme oxygenase (decycling) 1	0.03	3.70	down
1418946_at	ST3 beta-galactoside alpha-2,3-sialyltransferase 1	0.03	1.84	down
1418453_a_at	ATPase, Na+/K+ transporting, beta 1 polypeptide	0.03	1.43	down
1453290_at	high mobility group box 2-like 1	0.03	1.87	up
1450109_s_at	ATP-binding cassette, sub-family C (CFTR/MRP), member 2	0.03	1.56	up
1457483_at	AT rich interactive domain 5B (Mrf1 like)	0.03	1.41	up
1431170_at	ephrin A3	0.03	1.75	down
1428141_at	golgi associated, gamma adaptin ear containing, ARF binding protein 2	0.03	1.41	down
1424148_a_at	expressed sequence AW049765	0.03	1.49	up
1455904_at	growth arrest specific 5	0.03	1.40	up
1458719_at	Transcribed locus	0.03	1.42	up
1437218_at	Fibronectin 1	0.04	1.73	up
1430165_at	serine/threonine kinase 17b (apoptosis-inducing)	0.04	1.61	down
1419251_at	epidermal growth factor receptor pathway substrate 15	0.04	1.44	down
1460328_at	bromodomain containing 3	0.04	1.53	up
1439036_a_at	ATPase, Na+/K+ transporting, beta 1 polypeptide	0.04	1.46	down
1425031_at	Fukuyama type congenital muscular dystrophy homolog (human)	0.04	1.54	up
1440439_at	Expressed sequence AI591476	0.04	1.42	up
1423828_at	fatty acid synthase	0.04	1.54	up
1451577_at	zinc finger and BTB domain containing 20	0.04	1.41	up
1453080_at	RIKEN cDNA 9130022K13 gene ///	0.04	1.44	down
1442277_at	choline kinase alpha	0.04	1.46	up
1424733_at	purinergic receptor P2Y, G-protein coupled, 14	0.04	1.50	down
1451263_a_at	fatty acid binding protein 4, adipocyte	0.04	1.41	down
1426812_a_at	RIKEN cDNA 9130404D14 gene	0.04	1.44	down
1444330_at	DNA segment, Chr 2, ERATO Doi 173, expressed	0.04	1.60	up
1457987_at	RIKEN cDNA 6030458C11 gene	0.04	2.07	up
1418736_at	UDP-GalNAc:betaGlcNAc beta 1,3-galactosaminyltransferase, polypeptide 1	0.04	1.40	down

1416432_at	6-phosphofructo-2-kinase/fructose-2,6-biphosphatase 3	0.04	1.45	down
1422797_at	mitogen activated protein binding protein interacting protein	0.04	1.48	down
1416833_at	kidney expressed gene 1	0.04	1.50	up
1455265_a_at	regulator of G-protein signaling 16	0.04	1.45	down
1418370_at	troponin C, cardiac/slow skeletal	0.04	1.43	down
1418813_at	serine (or cysteine) peptidase inhibitor, clade A, member 5	0.04	2.04	up
1424273_at	cytochrome P450, family 2, subfamily c, polypeptide 70	0.04	1.42	up
1429093_at	DNA-damage inducible protein 2	0.04	1.53	up
1439255_s_at	G protein-coupled receptor 137B ///	0.04	1.47	down
1439231_at		0.04	1.68	up
1418603_at	arginine vasopressin receptor 1A	0.04	1.44	down
1418601_at	aldehyde dehydrogenase family 1, subfamily A7	0.04	1.62	up
1456094_at	ubiquitin specific peptidase 36	0.04	1.49	up
1422710_a_at	calcium channel, voltage-dependent, T type, alpha 1H subunit	0.04	1.41	down
1437100_x_at	proviral integration site 3	0.04	1.51	down
1448453_at	hydroxy-delta-5-steroid dehydrogenase, 3 beta- and steroid delta-isomerase 1	0.04	1.53	up
1424140_at	galactose-4-epimerase, UDP	0.04	1.42	up
1448873_at	occludin	0.04	1.54	down
1424981_at	neurolysin (metallopeptidase M3 family)	0.04	1.45	down
1455818_at	RIKEN cDNA 4930427A07 gene	0.04	1.43	up
1418835_at	pleckstrin homology-like domain, family A, member 1	0.05	1.65	up
1415965_at	stearoyl-Coenzyme A desaturase 1	0.05	1.54	up
1417388_at	brain expressed X-linked 2	0.05	1.54	down
1429847_a_at	RIKEN cDNA 4833418A01 gene	0.05	1.45	down
1435926_at	RIKEN cDNA E030003F13 gene	0.05	1.41	up
1433837_at	RIKEN cDNA 8430408G22 gene	0.05	1.60	down
1449233_at	basic helix-loop-helix domain containing, class B, 8	0.05	1.42	up
1451456_at	RIKEN cDNA 6430706D22 gene	0.05	1.45	up
1449047_at	2-hydroxyacyl-CoA lyase 1	0.05	1.54	up
1434486_x_at	UDP-glucose pyrophosphorylase 2	0.05	1.46	down
1421198_at	integrin alpha V	0.05	1.43	down
1417900_a_at	very low density lipoprotein receptor	0.05	1.85	down
1428329_a_at	intraflagellar transport 80 homolog (Chlamydomonas)	0.05	1.43	down
1450876_at	complement component factor h	0.05	1.79	up
1416687_at	procollagen lysine, 2-oxoglutarate 5-dioxygenase 2	0.05	1.99	down

Table 4.12: **Gene list of 227 probe sets identified as up or down-regulated in expression in the switch treatment group relative to 9% casein treatment group.**

4.3.13 Downstream analysis using GeneSpring (using RMA normalized data).

Initial analysis of the data using GeneSpring suggested there was a considerable amount of biological variation amongst replicates from within the same diet group, thus making it difficult to distinguish changes in expression that are due to the diet treatment.

Log signal intensity plots created from RMA normalized data are shown in Figures 4.26 to 4.29; the vertical blue grid lines on the plots represent the four biological replicates within each of the diet groups. If minimal biological variation in gene expression was present, the zigzagged lines on these plots would appear more linear across replicate samples from the same diet group. Each coloured line on the grid represents the expression pattern of a single probe set/gene that appears to be changing in relation to diet under the analysis parameters selected (section 4.2.14.2). The line colours are dictated by comparison to the level of expression in the 18% casein diet group for the particular gene (a sliding scale of line colour denotes the relative level of expression relative to the 18% casein diet).
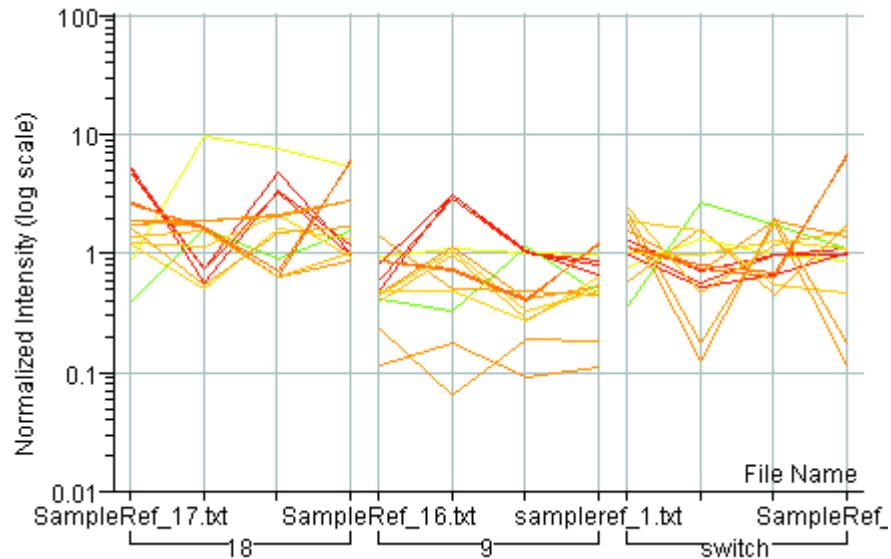
Figure 4.26: Data filtered for two-fold decreases in gene expression in the 9% casein diet treatment compared to the 18% casein diet treatment.
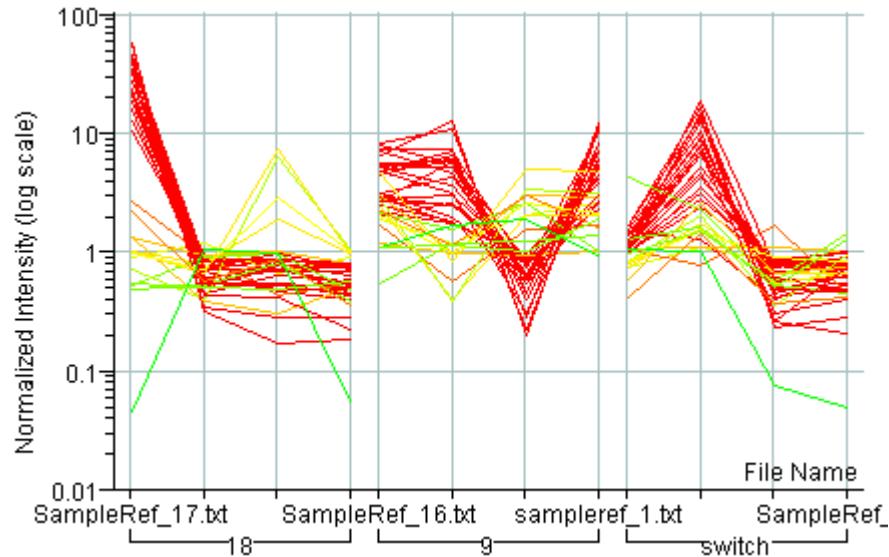
Figure 4.27: Data filtered for two-fold increases in gene expression in the 9% casein diet treatment compared to the 18% casein diet treatment.

In Figure 4.27 there appears to be multiple genes following the same pattern of expression amongst the replicates within the diet groups being compared; this may be because these genes are all associated with a common pathway. Notably, in this comparison, one sample from the 18% casein diet group appears to be markedly different in terms of probe set expression levels relative to the other three replicates within that group.
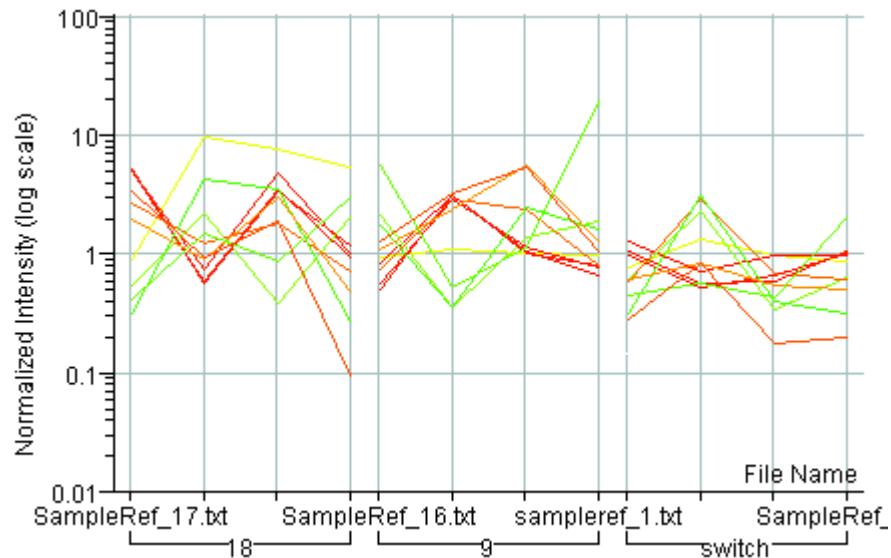
Figure 4.28: Data filtered for two-fold decreases in the switch diet treatment compared to the 18% casein diet treatment.
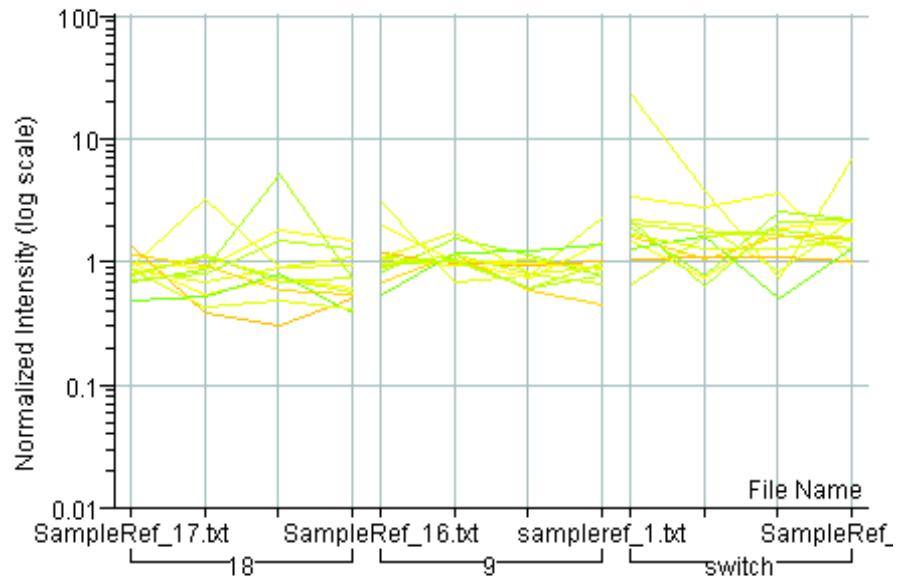
Figure 4.29: **Data filtered for two-fold increases in the switch diet treatment compared to the 18% casein diet treatment.**

Gene lists were generated from the log signal intensity plots in Figures 4.26 to 4.29 detailing the gene name/description of the genes identified as increasing or decreasing in expression in each of the treatment groups relative to the control group (Tables 4.13 to 4.16). However, no significant differences were up held in the level of probe set expression between the dietary treatments (ANOVA, $p<0.05$).

9% casein (down)

Gene	Number pass	Description
1431213_a_at	4	RIKEN cDNA 1300007C21 gene;
1455869_at	**4**	**Calcium/calmodulin-dependent protein kinase II, beta (Camk2b),** mRNA 82; G1/S transition of mitotic cell cycle; protein amino acid phosphorylation; calcium ion transport; protein amino acid autophosphorylation;
1436296_x_at	4	Transcribed locus
1452388_at	3	heat shock protein 1A 723 ; telomere maintenance; DNA repair; protein folding; response to unfolded protein; response to heat;
1452318_a_at	3	heat shock protein 1B 723 ; telomere maintenance; inhibition of caspase activation; DNA repair; protein folding; anti-apoptosis; response to unfolded protein; response to heat;
1457987_at	3	RIKEN cDNA 6030458C11 gene
1455773_at	3	
1452705_at	3	expressed sequence AA415817 6520; amino acid metabolism;
1427126_at	3	heat shock protein 1B 723; telomere maintenance; inhibition of caspase activation; DNA repair; protein folding; anti-apoptosis; response to unfolded protein; response to heat;
1418129_at	3	24-dehydrocholesterol reductase 188; inactivation of MAPK activity; cholesterol biosynthesis; electron transport;
1416460_at	3	myo-inositol oxygenase 9992 ; cellular osmoregulation; membrane organization and biogenesis; myo-inositol catabolism; inositol phosphate-mediated signaling;
1436823_x_at	3	hemoglobin Y, beta-like embryonic chain 6810 ; transport ; oxygen transport;
1436717_x_at	3	hemoglobin Y, beta-like embryonic chain 6810 ; transport; oxygen transport;
1433876_at	3	RIKEN cDNA 6430402H13 gene 7155; cell adhesion;

Table 4.13: Gene list of 14 probe sets down-regulated in expression in the 9% casein treatment group relative to 18% casein control group. Interestingly, the Camk2b gene was also identified as being down regulated in the 9% casein group relative to controls in the gene lists produced by analysis using Array Assist (section 4.3.12).

9% casein (up)

Gene	Number pass	Description
1427451_a_at	4	cDNA sequence BC018473
1438763_at	3	
1436240_at	3	RIKEN cDNA 1500010G04 gene (1500010G04Rik), mRNA
1438612_a_at	3	colipase, **pancreatic** 7586 ; digestion; lipid catabolism;
1437326_x_at	3	elastase 3B, **pancreatic** 6508 ; proteolysis;
1433459_x_at	3	protease, serine, 2 6508; proteolysis; digestion;
1431743_a_at	3	solute carrier family 4 (anion exchanger), member 1 6810; transport; ion transport; anion transport;
1435611_x_at	3	elastase 3B, **pancreatic** 6508; proteolysis;
1435012_x_at	3	elastase 3B, **pancreatic** 6508; proteolysis;
1450689_at	3	protease, serine, 3 ; trypsinogen 16 ; similar to trypsinogen 12 6508; proteolysis;
1450459_at	3	RIKEN cDNA 2010106G01 gene 6508; proteolysis;
1458609_at	3	Adult male bone cDNA, RIKEN full-length enriched library, clone:9830162N06 product:unclassifiable,
1454623_at	3	similar to Carboxypeptidase A2 precursor
1448406_at	3	CREBBP/EP300 inhibitory protein 1 122; negative regulation of transcription from RNA polymerase II promoter;
1448220_at	3	chymotrypsinogen B1 6508; proteolysis; digestion;
1448107_x_at	3	kallikrein 6 6508; proteolysis;
1448281_a_at	3	elastase 2 6508; proteolysis;
1448239_at	3	heme oxygenase (decycling) 1 6788; heme oxidation; response to stimulus;
1416523_at	3	ribonuclease, RNase A family, 1 **(pancreatic)**
1415954_at	3	trypsin 4 ; trypsinogen 16 ; RIKEN cDNA 1810049H19 gene 6508; proteolysis;
1420774_a_at	3	RIKEN cDNA 4930583H14 gene
1417257_at	3	carboxyl ester lipase 16042; lipid catabolism; ceramide catabolism; cholesterol catabolism; fatty acid catabolism; protein amino acid esterification; intestinal lipid catabolism;
1415837_at	3	kallikrein 6 6508 ; proteolysis;
1415805_at	3	colipase, **pancreatic** 7586; digestion; lipid catabolism;
1415884_at	3	elastase 3B, **pancreatic** 6508 ; proteolysis;
1415883_a_at	3	elastase 3B, **pancreatic** 6508 ; proteolysis;
1415777_at	3	**pancreatic** lipase related protein 1 6629 ; lipid metabolism; lipid catabolism;
1428062_at	3	carboxypeptidase A1 6508 ; proteolysis;
1425642_at	3	similar to centrosome protein cep290
1428359_s_at	3	RIKEN cDNA 1810010M01 gene
1428102_at	3	carboxypeptidase B1 (tissue) 6508; proteolysis;
1422434_a_at	3	RIKEN cDNA 2210010C04 gene 6508; proteolysis; digestion;
1421866_at	3	nuclear receptor subfamily 3, group C, member 1 6350; transcription; regulation of transcription, DNA-dependent; glucocorticoid receptor signaling pathway;
1423257_at	3	cytochrome P450, family 4, subfamily a, polypeptide 14 6118; electron transport;
1422682_s_at	3	protease, serine, 3 ; trypsinogen 16; similar to trypsinogen 12 6508; proteolysis;
1421077_at	3	SERTA domain containing 3 6350; transcription; regulation of transcription, DNA-dependent;

Table 4.14: Gene list of 36 probe sets up-regulated in expression in the 9% casein treatment group relative to 18% casein control group. This condition revealed the largest number of apparent gene expression changes of the comparisons that were made here. However, there are a number of pancreatic transcripts identified in this list which may suggest an element of tissue contamination at the dissection stage.

Switch (down)

Gene   Number pass   Description

1427126_at   4   heat shock protein 1B 723; telomere maintenance; inhibition of caspase activation; DNA repair; protein folding; anti-apoptosis; response to unfolded protein; response to heat

1427127_x_at 4   heat shock protein 1B 723; telomere maintenance; inhibition of caspase activation; DNA repair; protein folding; anti-apoptosis; response to unfolded protein; response to heat

1452388_at   4   heat shock protein 1A   723; telomere maintenance; DNA repair; protein folding; response to unfolded protein; response to heat;

1436296_x_at 4   Transcribed locus

1449526_a_at 3   glycerophosphodiester phosphodiesterase domain containing 3   6071; glycerol metabolism;

1439483_at   3   expressed sequence AI506816

1419149_at   3   serine (or cysteine) peptidase inhibitor, clade E, member 1   45765; regulation of angiogenesis;

1420491_at   3   eukaryotic translation initiation factor 2, subunit 1 alpha   6412; protein biosynthesis; regulation of protein biosynthesis; regulation of translation; protein biosynthesis;

1436538_at   3   Lrp2 binding protein

1455213_at   3   RIKEN cDNA 4930488E11 gene   7010; cytoskeleton organization and biogenesis;

Table 4.15: Gene list of 10 probe sets down-regulated in expression in the switch treatment group relative to 18% casein control group.

```
Switch (up)
Gene        Number pass      Description
1438644_x_at  4             COMM domain containing 9
1427451_a_at  4             cDNA sequence BC018473
1442679_at    3             Mitogen activated protein kinase kinase 4 (Map2k4), mRNA     165 ; MAPKKK cascade; protein
                            amino acid phosphorylation;
1457680_a_at  3             transmembrane protein 69
1446284_at    3             metastasis suppressor 1    7015 ; actin filament organization; actin filament polymerization; cell
                            motility; cell adhesion; transmembrane receptor protein tyrosine kinase signaling pathway;
                            microspike biogenesis; actin cytoskeleton organization and biogenesis; nervous system
                            development; muscle development;
1450459_at    3             RIKEN cDNA 2010106G01 gene          6508; proteolysis;
1442109_at    3             Far upstream element (FUSE) binding protein 1 (Fubp1), mRNA      6350; transcription; regulation
                            of transcription, DNA-dependent; phosphate transport;
1423866_at    3             serine (or cysteine) peptidase inhibitor, clade A, member 3K
1423556_at    3             aldo-keto reductase family 1, member B7     44255; cellular lipid metabolism;
1440443_at    3             RIKEN cDNA E030016H06 gene
1429478_at    3             RIKEN cDNA 6720463M24 gene
1419094_at    3             cytochrome P450, family 2. subfamily c, polypeptide 37 ; cytochrome P450, family 2, subfamily c,
                            polypeptide 50 ; cytochrome P450    6118; electron transport;
```

Table 4.16: Gene list of 12 probe sets up-regulated in expression in the switch

treatment group relative to 18% casein control group.

4.3.14 Downstream analysis using dChip

In order to obtain lists of candidate probe sets that appear to be differentially expressed, class comparisons were made of the expression of all individual probe sets between diet groups. These comparisons were made for all three possible pair-wise combinations of the diet groups, i.e. switch and 9% casein; switch and 18% casein; 9% casein and 18% casein. The 9% casein group may be seen as a type of control for the switch group, as the low protein treatment is maintained throughout gestation.

The class comparison tool in dChip (Li and Wong, 2001) was used with two different sets of comparison criteria- a 'high' and a 'low' stringency setting (see section 4.2.14.3).

A positive average fold change for a probe set in a gene list generated from a class comparison indicates an up-regulation/higher level of expression of the probe set in the experimental diet group relative to the baseline diet group. Likewise, a negative average fold change indicates a down-regulation/lower level of expression relative to the baseline group. Percentage FDRs were analysed for each class comparison to give an indication of the reliability of the gene lists produced from the actual class comparisons versus random permutations of the samples between the two classes.

4.3.14.1 Class comparison analyses using all samples in each treatment group

Results from the high stringency analyses are shown in Tables 4.18 to 4.20. A summary of the high stringency results is given in Table 4.17.

Class (treatment group) comparison	No. probe sets changed	Median FDR (probe sets)
switch v 9% casein	10	50% (5)
switch v 18% casein	6	50% (3)
9% casein v 18% casein	4	75% (3)

Table 4.17: Summary of class comparison results including all samples in each class, using the high stringency comparison criteria. The numbers of apparently differentially expressed probe sets and the median FDRs are given in each case.

Affx probe set	Gene information	p-value	Fold change
1415899_at	Junb: Jun-B oncogene	0.015699	-3.08
1416913_at	Es1: esterase 1	0.000463	2.09
1417079_s_at	Lgals2: lectin, galactose-binding, soluble 2	0.013999	-2.09
1417461_at	Cap1: CAP, adenylate cyclase-associated protein 1 (yeast)	0.015394	2.45
1418787_at	Mbl2: mannose binding lectin (C)	0.024216	3.14
1420774_a_at	4930583H14Rik: RIKEN cDNA 4930583H14 gene	0.046268	-3.79
1441573_at	Scmh1: Sex comb on midleg homolog 1	0.030059	-2.31
1443505_at	Transcribed locus	0.03639	3.28
1444330_at	D2Ertd173e: DNA segment, Chr 2, ERATO Doi 173, expressed	0.026757	2.56
1457987_at	6030458C11Rik: RIKEN cDNA 6030458C11 gene	0.036347	2.94

Table 4.18: Candidate probe sets with apparent differential expression for switch versus 9% casein (baseline) class comparison using high stringency criteria. The median FDR from random permutations of these samples was 50%.

Affx probe set	Gene information	p-value	Fold Change
1438644_x_at	Commd9: COMM domain containing 9	0.002046	2.75
1440443_at	E030016H06Rik: RIKEN cDNA E030016H06 gene	0.030419	3.28
1442255_at	Mm.132067.1	0.047928	3.22
1445826_at	Ankrd17: ankyrin repeat domain 17	0.006859	2.18
1446284_at	Mtss1: metastasis suppressor 1	0.003451	2.19
1457458_at	Zc3h4: zinc finger CCCH-type containing 4	0.024002	2.66

Table 4.19: Candidate probe sets with apparent differential expression for switch versus 18% casein (baseline) class comparison using high stringency criteria. Median FDR was 50%.

Affx probe set	Gene information	p-value	Fold change
1431213_a_at	LOC100041156 /// LOC100041932	0.001615	-16.44
1448406_at	Eid1: EP300 interacting inhibitor of differentiation 1	0.032715	2.67
1431220_at	LOC100040353 /// LOC100046169: similar to splicing coactivator subunit SRm300 ///	0.001555	2.27
1438763_at	Dnahc2: dynein, axonemal, heavy chain 2	0.013813	2.48

Table 4.20: Candidate probe sets with apparent differential expression for 9% casein versus 18% casein (baseline) class comparison using high stringency criteria. Median FDR was 75%.

Across all class comparisons few probe sets were identified as apparently diet responsive and the apparent differential expression identified had a high likelihood of being due to chance, as indicated by the high FDRs. The largest numbers of candidate genes were identified when the switch and 9% casein diet treatments were compared (Table 4.18), but even that comparison only yielded ten possible candidates.

The average fold changes for the candidate probe sets identified in Tables 4.18 to 4.20 were all more than 2-fold up or down, raising the possibility that some important candidate genes with slightly weaker fold changes may have been eliminated by the stringent filtering criteria. Thus, further class comparison analyses were made using low stringency criteria (see section 4.2.14.3 for details). Here, the lower bound of the 90% confidence interval for fold change had to be at least 1.4. All other filtering criteria remained the same as before, and fifty random comparisons were made so that the FDR could be established for each class comparison. Again, FDRs were determined empirically by class comparison on random permutations of sample allocation to classes.

Table 4.21 summarises the findings from these reduced stringency analyses; the detailed

results for each class comparison are shown in Tables 4.22 to 4.24.

Class comparison	No. probe sets changed	Median FDR (probe sets)
switch v 9% casein	35	37.1% (13)
switch v 18% casein	8	100% (8)
9% casein v 18% casein	9	88.9% (8)

Table 4.21: Summary of class comparison results including all samples in each class,

using the low stringency comparison criteria. The numbers of apparently

differentially expressed probe sets and the median FDRs are shown.

Affx probe set	Gene information	p-value	Fold change
1415899_at	Junb: Jun-B oncogene	0.015699	-3.08
1416913_at	Es1: esterase 1	0.000463	2.09
1417079_s_at	Lgals2: lectin, galactose-binding, soluble 2	0.013999	-2.09
1417461_at	Cap1: CAP, adenylate cyclase-associated protein 1 (yeast)	0.015394	2.45
1418787_at	Mbl2: mannose binding lectin (C)	0.024216	3.14
1420774_a_at	4930583H14Rik: RIKEN cDNA 4930583H14 gene	0.046268	-3.79
1420934_a_at	Srrm1: serine/arginine repetitive matrix 1	0.014744	1.97
1423062_at	Igfbp3: insulin-like growth factor binding protein 3	0.012875	2.12
1426721_s_at	Tiparp: TCDD-inducible poly(ADP-ribose) polymerase	0.030553	-1.83
1426805_at	Smarca4: matrix associated, actin dependent regulator of chromatin	0.042023	2.14
1434062_at	Rabgap1l: RAB GTPase activating protein 1-like	0.000734	-1.62
1434278_at	Mtm1: X-linked myotubular myopathy gene 1	0.009015	1.78
1438167_x_at	Flcn: Folliculin	0.000896	-1.67
1438743_at	Cyp7a1: cytochrome P450, family 7, subfamily a, polypeptide 1	0.02487	2.15
1429809_at	Tmtc2: transmembrane and tetratricopeptide repeat containing 2	0.002183	-1.76
1429882_at	6820431F20Rik: RIKEN cDNA 6820431F20 gene	0.00617	1.76
1430566_at	4733401A01Rik: RIKEN cDNA 4733401A01 gene	0.022219	2.04
1438763_at	Dnahc2: dynein, axonemal, heavy chain 2	0.018764	-2.32
1441272_at	Matr3: Matrin 3	0.009433	1.89
1441573_at	Scmh1: Sex comb on midleg homolog 1	0.030059	-2.31
1443505_at	Transcribed locus	0.03639	3.28
1444036_at	Transcribed locus	0.013603	-1.88
1444330_at	D2Ertd173e: DNA segment, Chr 2, ERATO Doi 173, expressed	0.026757	2.56
1444538_at	Mm.182679.1	0.022366	1.83
1445826_at	Ankrd17: ankyrin repeat domain 17	0.012525	1.87
1446284_at	Mtss1: metastasis suppressor 1	0.006739	1.89
1447258_at	Mm.210555.1	0.002793	1.86
1453189_at	Ube2i: ubiquitin-conjugating enzyme E2I	0.00708	2
1453776_at	Snx21: sorting nexin family member 21	0.020045	-1.9
1454649_at	Srd5a1: steroid 5 alpha-reductase 1	0.004672	1.7
1455933_at	Tra2a: transformer 2 alpha homolog (Drosophila)	0.025982	2.06
1457554_at	Apob: apolipoprotein B	0.001648	1.72
1457987_at	6030458C11Rik: RIKEN cDNA 6030458C11 gene	0.036347	2.94
1459734_at	Mm.212401.1	0.003337	1.75
1459984_at	Mia3: melanoma inhibitory activity 3	0.009647	2.13

Table 4.22: Candidate probe sets with apparent differential expression for switch versus 9% casein (baseline) class comparison using low stringency criteria. The median FDR was 37.1%.

Affx probe set	Gene information	p-value	Fold Change
1438644_x_at	Commd9: COMM domain containing 9	0.002046	2.75
1440443_at	E030016H06Rik: RIKEN cDNA E030016H06 gene	0.030419	3.28
1442255_at	Mm.132067.1	0.047928	3.22
1445695_at	0 day neonate lung cDNA, RIKEN full-length enriched library,	0.017914	1.86
1445826_at	Ankrd17: ankyrin repeat domain 17	0.006859	2.18
1446284_at	Mtss1: metastasis suppressor 1	0.003451	2.19
1457458_at	Zc3h4: zinc finger CCCH-type containing 4	0.024002	2.66
1457554_at	Apob: apolipoprotein B	0.000831	1.91

Table 4.23: Candidate probe sets with apparent differential expression for switch versus 18% casein (baseline) class comparison using low stringency criteria. Median FDR was 100%.

Affx probe set	Gene information	p-value	Fold Change
1415777_at	Pancreatic lipase related protein 1	0.032647	-2.45
1423114_at	Ubiquitin-conjugating enzyme E2D 3	0.04101	-1.89
1423257_at	Cyp4a14: cytochrome P450,	0.03825	2.35
1431213_a_at	LOC100041156 /// LOC100041932	0.001615	-16.44
1448406_at	EP300 interacting inhibitor of differentiation 1	0.032715	2.67
1429351_at	Klhl24: kelch-like 24 (Drosophila)	0.023692	2.04
1431220_at	LOC100040353 /// LOC100046169:	0.001555	2.27
1438763_at	Dnahc2: dynein, axonemal, heavy chain 2	0.013813	2.48
1455773_at	0 day neonate kidney cDNA, RIKEN full-length enriched library,	0.04721	-2.55

Table 4.24: Candidate probe sets with apparent differential expression for 9% casein versus 18% casein (baseline) class comparison using low stringency criteria. Median FDR was 88.9%.

For the class comparison switch versus 9% casein, the low stringency criteria identifies a larger number of gene candidates as differentially expressed and there is a lower proportion of FDRs compared to when the higher stringency filtering criteria was adopted (Table 4.22). However, when class comparisons were made for the other two possible combinations of diet group with the low stringency filtering criteria it became apparent

that the FDRs were very high, and the number of probe sets identified did not increase markedly (Tables 4.23 and 4.24). Thus, it is difficult to have any confidence in these gene lists.

The lower stringency criteria only appear to improve upon the results obtained for the switch versus 9% casein class comparison. For this comparison, a list of thirty-five probe-sets was produced, of which all are above the lower limit of the 90% confidence interval for 1.4 fold change (Table 4.22). The smaller percentage FDR helps us to have more confidence in the reliability of candidates produced by the meaningful comparison. Thus, the gene list in Table 4.22 mostly contains candidates that are meaningful and truly changing in the class comparison, but also contains some candidates that are not and appear on the list by chance.

Of the thirty-five probe sets identified in Table 4.22 as apparently differentially expressed, twenty-four probe sets were expressed at a higher level in the switch group relative to the 9% group. Up-loading these twenty-four probe sets into GOTM indicated that in terms of biological processes, enriched categories were growth, cellular lipid metabolism and steroid metabolism (Figure 4.30).
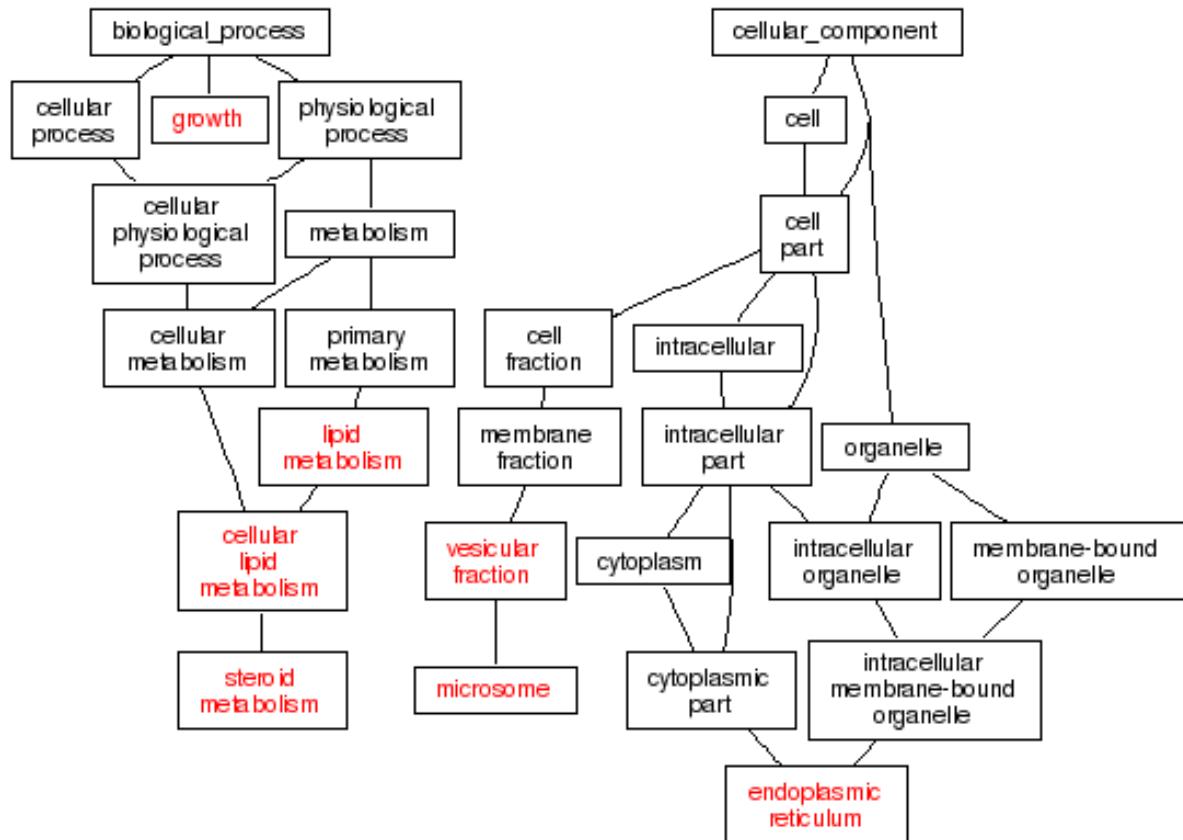
Figure 4.30: **GOTM tree produced for the twenty-four probe sets that were expressed at a higher level in the switch group relative to the 9% casein group from the gene list shown in Table 4.22. Enriched categories are shown in red.**

Analysis of the tree in Figure 4.30, based on the twenty-four up regulated probe sets shown in Table 4.22, indicates that the enriched growth category is based on the two observed transcripts: Igfbp3: insulin-like growth factor binding protein 3 (1423062_at) and Smarca4: matrix associated, actin dependent regulator of chromatin (1426805_at). The expected number of transcripts for this category based on the background list was 0.15, thus the enrichment factor (R) was 13.33. The enriched steroid metabolism category (R= 20) is composed of two observed probe sets Cyp7a1: cytochrome P450,

family 7, subfamily a, polypeptide 1 (1438743_at) and Srd5a1: steroid 5 alpha-reductase

1 (1454649_at). Finally, the enriched cellular lipid metabolism category (R=7.69) is also

composed of probe set (1438743_at) and (1454649_at) as well as ApoB: apolipoprotein

B (1457554_at). In terms of cellular components the over-represented categories were:

the endoplasmic reticulum (R= 8.7), vesicular fraction (R= 18.18) and microsomes (R=

20).

Similarly using DAVID, gene ontology analysis was carried out on the same twenty-four

probe sets as in Figure 4.30 (Table 4.25).

Gene Report
GOTERM_BP_ALL:GO:0044237~cellular metabolic process
Current Gene List: 4E>4L_1.4fold

12 Gene(s)

AFFY_ID	Gene Name
1444538_at	expressed sequence al033314
1457554_at	apolipoprotein b
1454649_at	steroid 5 alpha-reductase 1
1438743_at	cytochrome p450, family 7, subfamily a, polypeptide 1
1446284_at	metastasis suppressor 1
1434278_at	x-linked myotubular myopathy gene 1
1445826_at	ankyrin repeat domain 17
1426805_at	swi/snf related, matrix associated, actin dependent regulator of chromatin, subfamily a, member 4
1453189_at	ubiquitin-conjugating enzyme e2i
1420934_a_at	serine/arginine repetitive matrix 1
1418787_at	mannose binding lectin (c)
1423062_at	insulin-like growth factor binding protein 3

Gene Report

GOTERM_BP_ALL:GO:0044255~cellular lipid metabolic process
Current Gene List: 4E>4L_1.4fold

4 Gene(s)

AFFY_ID	Gene Name
1457554_at	apolipoprotein b
1454649_at	steroid 5 alpha-reductase 1
1438743_at	cytochrome p450, family 7, subfamily a, polypeptide 1
1434278_at	x-linked myotubular myopathy gene 1

Table 4.25: DAVID gene ontology analysis of twenty-four probe sets expressed at a higher level in the switch group versus the 9% casein group (see Table 4.22).

The DAVID analysis shown in Table 4.25 identifies two enriched categories: cellular metabolic process, and cellular lipid metabolic process. These enriched categories include the same five probe sets as were identified the enriched GTOM categories for biological process in Figure 4.30, as well as a number of others.

Eleven of the probe sets in gene list in Table 4.22 were expressed at a lower level in the switch group relative to the 9% casein group; enrichment analysis carried out with GOTM (Figure 4.31).
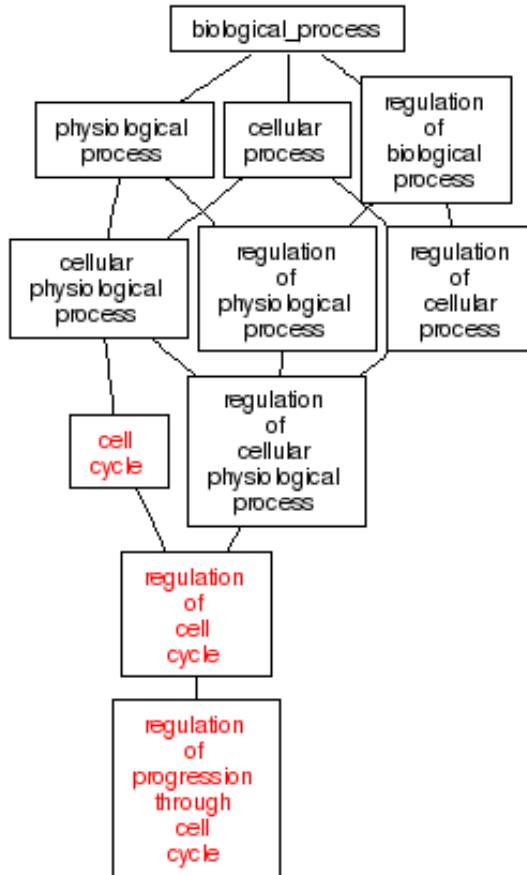
Figure 4.31: **GOTM tree produced for probe sets that were expressed at a lower level in the switch group relative to the 9% casein group in the gene list shown in Table 4.22. Enriched categories are shown in red.**

Closer examination of the tree in Figure 4.31, based on the eleven down regulated probe sets in Table 4.22, indicates that in terms of biological process enriched categories are cell cycle (R= 11.76), regulation of cell cycle (R= 20) and the regulation of progression through cell cycle (R= 20). All the enriched categories consist of the two probe sets, Junb: Jun-B oncogene (1415899_at) and Flcn: Folliculin (1438167_x_at).

Too few probe sets were identified as being expressed at a lower level in the switch versus 9% casein class comparison in Table 4.22 for DAVID gene ontology analysis to be carried out on these candidates.

4.3.14.2 Hierarchical clustering analysis

In view of the fact that there are approximately 45,000 probe sets on the Mouse 430_v2 chip used, and approximately 50% of the probe sets were detected and called as present in each of the samples across all the treatment groups (Table 4.6), relatively few probe sets appeared to be diet sensitive, even when the lower stringency analysis criteria was adopted for the class comparisons (see section 4.2.14.3). One possible explanation for this is that responsiveness to maternal dietary treatment is being obscured by another factor, such as the presence of outlier samples within treatment groups (biological variation). Thus, after obtaining expression values from the dChip model, high-level hierarchical clustering analysis (Eisen et al., 1998) was performed. Unsupervised sample clustering using probe sets obtained by filtering* was used to identify the separation of samples between classes/treatment groups, so that unexpected clustering could be identified (Li and Wong, 2001) (Figure 4.32).

*Clustering analysis was performed on the normalised expression of probe sets which had a coefficient of variation of 0.5< across all twelve samples from the three diet groups, and which had Affymetrix "present" calls in at least 20% of the twelve samples. This

excludes background probe set noise and prevents it from being incorporated into the

cluster analysis.
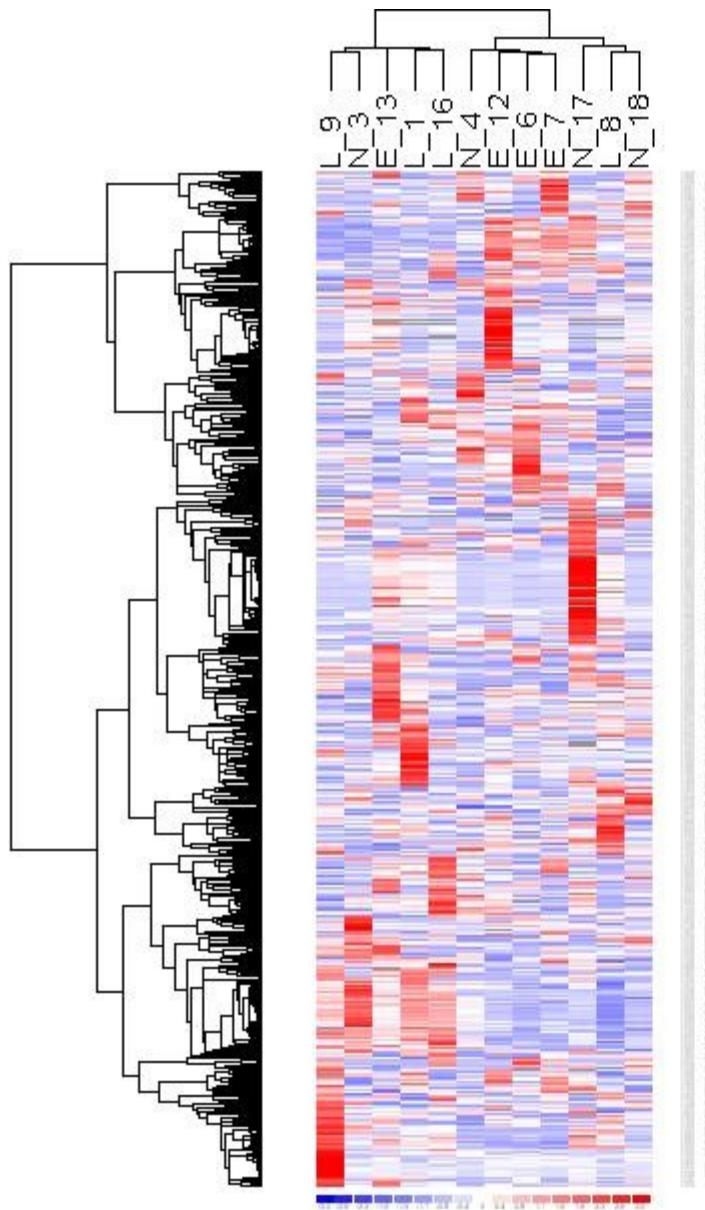
Figure 4.32: **Cluster diagram for the 508 probe sets called as "present" in at least 20% of the twelve samples and which have a coefficient of variation of 0.5< across all samples. Different samples with similar probe set/gene expression profiles to one another are clustered together (on horizontal axis); different genes/probe sets with similar expression profiles to each other are clustered (on vertical axis).**
Samples are coded as follows: N= 18% casein diet treatment, L= 9% casein diet treatment, E= switch diet treatment. Red= higher, blue= lower expression of probe sets.

Using the horizontal axis in Figure 4.32, outlier samples from within classes/treatment groups may be identified. Whilst three out of the four samples in each of the three classes appear to cluster together, each class contains one member that did not cluster with the remainder of their group, indicating that these samples (N 3, L 8, and E 13) might be outliers. Likewise, clustering analysis performed on the normalised expression of probe sets which had a coefficient of variation of 0.2< across all twelve samples from the three diet groups, and which had Affymetrix "present" calls in at least 20% of the twelve samples also produced similar results (Figure 4.33). Interestingly, the same three samples were also identified as possible outliers in the analysis using Array Assist in section 4.3.12 (Figure 4.25).

In view of the concordant evidence presented above, further class comparisons were made excluding the presumed outlier samples N 3, L 8, and E 13 from their respective classes (refer to next section 4.3.14.3).
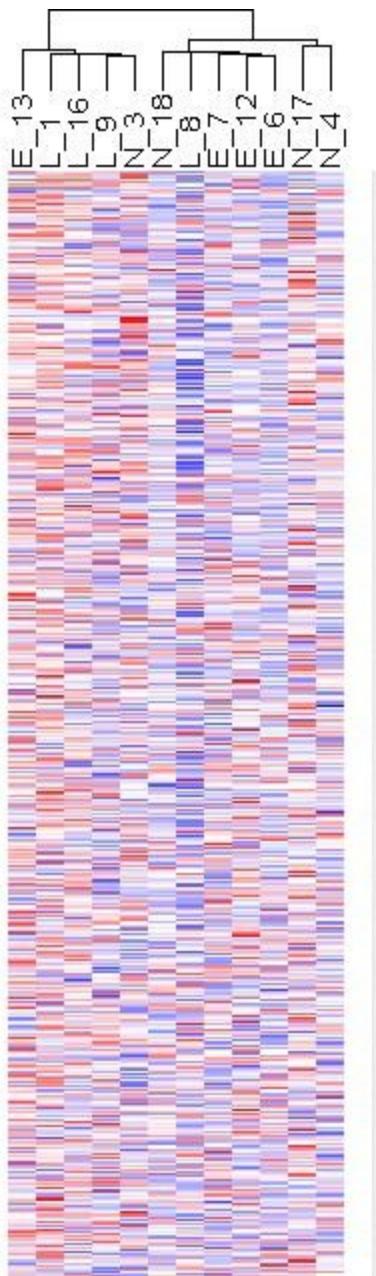
Figure 4.33: Cluster diagram (cropped) for the 7475 probe sets called as "present" in at least 20% of the twelve samples and which have a coefficient of variation of 0.2< across all samples. Different samples with similar probe set/gene expression profiles to one another are clustered together on the horizontal axis.

4.3.14.3 Class comparison analyses using three out of four samples from each treatment group/class

To examine the possibility of diet effects on global fetal liver gene transcription in the majority but not all, of the experimental fetuses, class comparisons were conducted with only the three most closely clustered samples in each treatment group (Figures 4.32, 4.33). Otherwise, these class comparisons were performed in the same way as those in section 4.3.14.1.

Comparing the results summary for the high stringency analysis given in Table 4.26 with the summary given in Table 4.17 illustrates the effect of removing the outlier samples, as both tables display the results of class comparisons performed at the high stringency level (refer to section 4.2.14.3 for details). The largest effect of removing outlier samples was on the switch versus 9% casein class comparison, where elimination of the respective outliers raised the returned probe set number from 10 to 136, with a lower percentage FDR of just 4.4%. Conversely, the number of probe sets returned from the switch versus 18% casein class comparison remained the same whether the respective outlier samples were included in the analysis or not. For the 9% casein versus 18% casein class comparison, exclusion of the appropriate outlier samples resulted in an increase from 4 to 26 probe sets obtained. Refer to Appendix I, Tables AI.12 to AI.14 for the gene lists generated by each of the high stringency class comparisons summarised in Table 4.26, when outlier samples were excluded from the analyses.

Class comparison	No. probe sets changed	Median FDR (probe sets)
switch v 9% casein	136	4.4% (6)
switch v 18% casein	6	100% (6)
9% casein v 18% casein	26	23.1% (6)

Table 4.26: Summary of class comparison results when excluding one outlier samples per class, using the high stringency comparison criteria. The numbers of apparently differentially expressed probe sets and the median FDRs are shown. Outlier samples excluded from the class comparison analyses were: samples 3 (18% casein group), 8 (9% casein group), and 13 (switch group).

Further class comparison analyses excluding the outlier samples were made using low stringency criteria (see section 4.2.14.3). Table 4.27 summarises the findings for the low stringency analyses; the gene lists generated from each class comparison are shown in Appendix I Tables AI.15 to AI.17. Comparison of the results summarised in Table 4.21 and Table 4.26 indicates the impact of removing the outlier samples from the class comparisons performed at low stringency. Again, the largest effect of removing the outlier samples was seen for the switch versus 9% casein class comparison. Elimination of the respective outliers from each class raised the number of probe sets returned from 35 to 344! In addition, the number of finds for the 9% versus 18% comparison increased from 9 to 76. However, as was the case for the high stringency criteria, removal of the outliers did not markedly improve upon the number of probe sets returned for the switch versus 18% class comparison.

Class comparison	No. probe sets changed	Median FDR (probe sets)
switch v 9% casein	344	4.9% (17)
switch v 18% casein	18	83.3% (15)
9% casein v 18% casein	76	23.7% (18)

Table 4.27: **Summary of class comparison results when excluding one outlier samples per class, using the low stringency comparison criteria. The numbers of apparently differentially expressed probe sets and the median FDRs are shown.**

Gene ontology analysis using GOTM (Figures 4.34 to 4.36) was performed on the gene list produced from the low stringency switch versus 9% class comparison excluding the outlier samples, (see gene list in Appendix I, Table AI.15). This comparison returned the largest number of probe sets (344) and had a very low FDR (4.9%) which means we can be confident that the gene list generated for the comparison (Table AI.15) represents candidates that are truly changing.
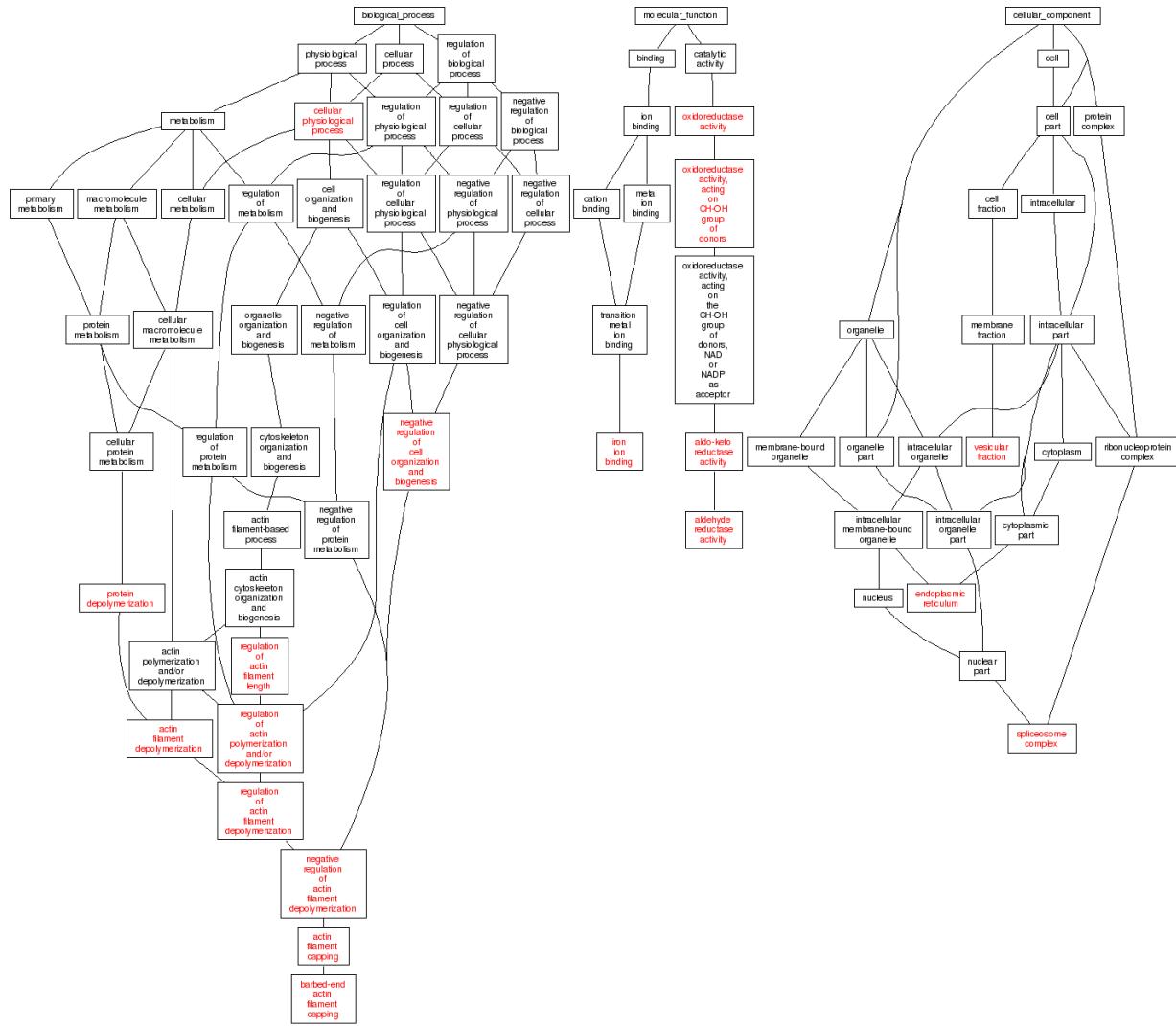
Figure 4.34: General overview of the GOTM tree produced for the 99 probe sets over expressed in the switch group relative to the 9% casein group from the gene list in Appendix I, Table AI.15 for the low stringency comparison when outliers were excluded from the analysis. Enriched categories are shown in red. Biological processes, molecular functions and cellular components all contained enriched categories.
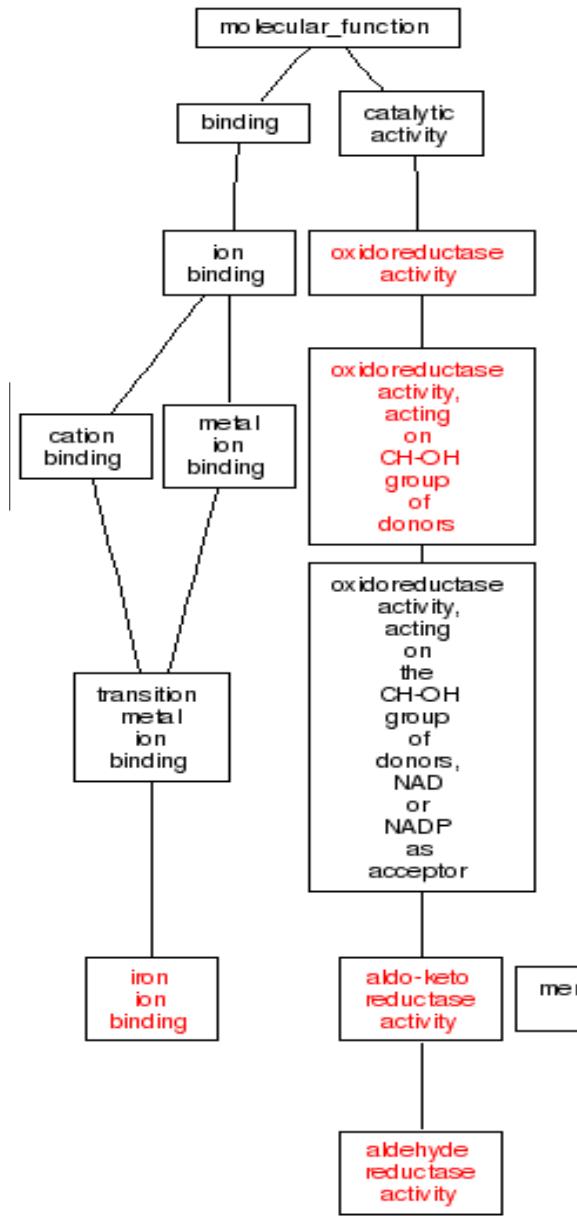
Figure 4.35: Enlarged section of Figure 4.34 to illustrate the enriched categories (shown in red) of molecular function which include oxidoreductase activity (R= 2.93), aldehyde reductase activity (R= 100) and iron ion binding (R= 4.5) for the 99 probe sets over expressed in the switch group relative to the 9% casein group from the gene list in Appendix I, Table AI.15.

Enriched categories in terms of molecular function are shown in the GOTM tree in Figure 4.35 for the probe sets over expressed in the switch versus the 9% casein diet group (from gene list in Table AI.15 in Appendix I). The most highly enriched of these categories was aldehyde reductase activity (R= 100). This category is composed of three probe sets representing two genes; Akr1b3: aldo-keto reductase family 1, member B3 (aldose reductase) (1437133_x_at), (1456590_x_at) and Akr1b7: aldo-keto reductase family 1, member B7 (1423556_at). In terms of cellular components, the enriched categories shown in the GOTM tree in Figure 4.34 are vesicular fraction (R= 8.51), endoplasmic reticulum (R= 3.4) and spliceosome complex (R= 11.54).

Figure 4.36 illustrates an overview of the GOTM tree and enriched categories (shown in red) for probe sets down regulated in the switch group relative to the 9% casein group (from gene list in Table AI.15 in Appendix I).
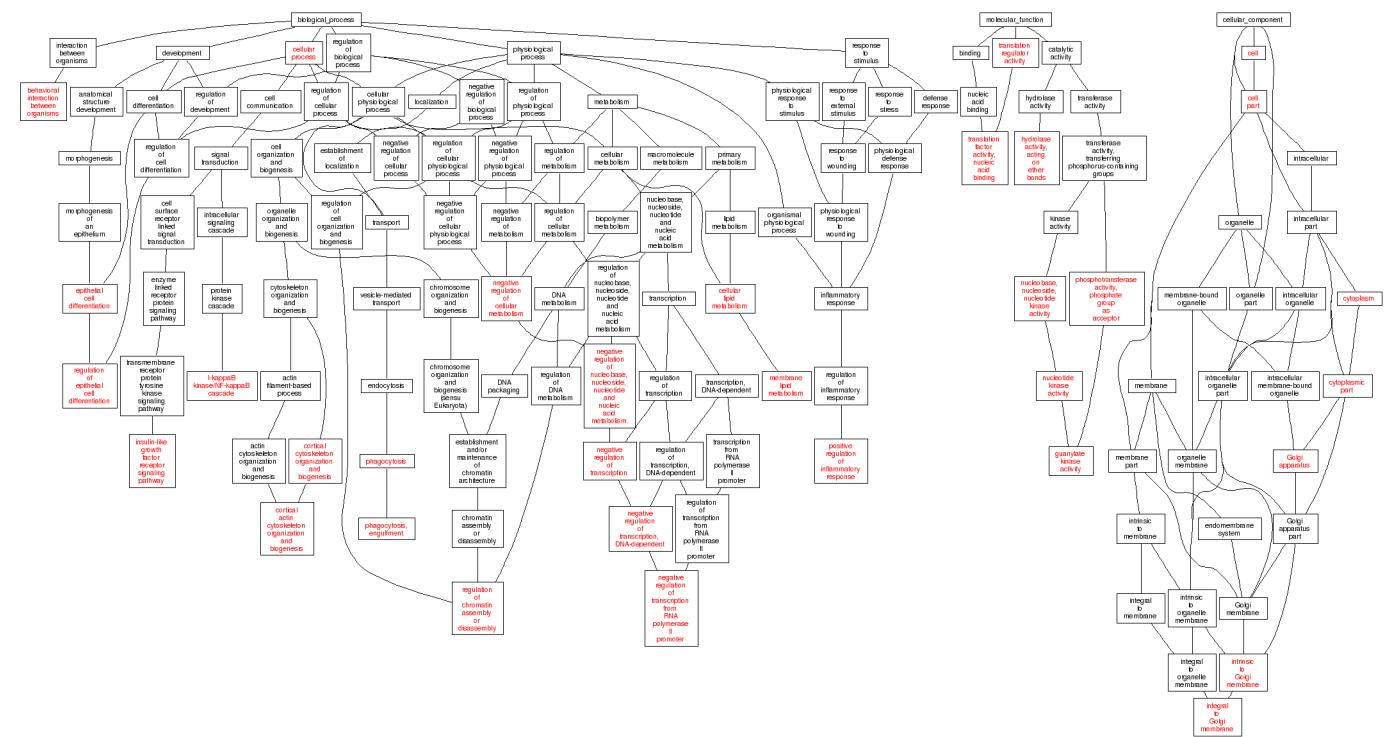
Figure 4.36: General overview of the GOTM tree produced for the 245 probe sets down regulated in the switch group relative to the 9% casein group from the gene list in Appendix I, Table AI.15 for the low stringency comparison when outliers were excluded from the analysis. Enriched categories are shown in red. Biological processes, molecular functions and cellular components all contained enriched categories.

In Figure 4.36, in terms of molecular function, enriched categories include translation factor activity/ nucleic acid binding (R= 4.11) and nucleotide kinase activity (R= 13.64). Enriched cellular components shown in the GOTM tree are related to the golgi apparatus (R= 3.09).

4.4 Discussion

4.4.1 Basis for experimental design regarding gender of fetuses

In an attempt to keep biological variation to a minimum, male fetuses only were used in the genomics analysis, and the gender of the nearest neighbours *in utero* was also monitored. This is because secreted fetal hormones are thought to pass either through the amniotic fluid or uterine blood vessels to neighbouring littermates. For instance, it has been observed that as a result of prenatal exposure to testosterone, female fetuses that were situated between two males *in utero* ('2M females') display a number of traits as adults that distinguish them from female fetuses which were next to two other females in the uterus (Figure 4.37).
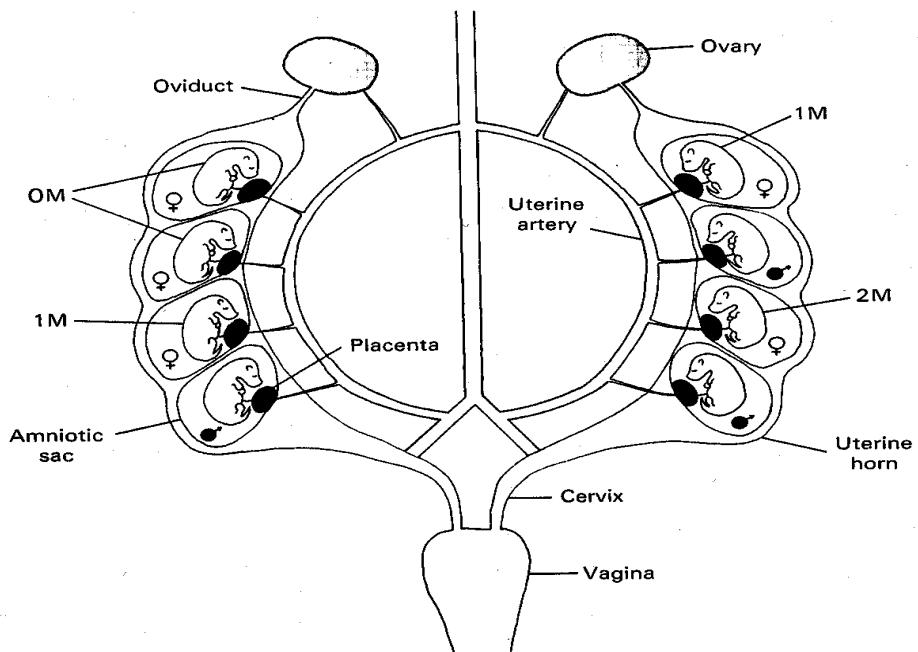
Figure 4.37: Schematic diagram of pregnant mouse uterus. Fetuses develop within individual amniotic sacs in the uterine horns. Positions of female fetuses are

depicted in relation to male fetuses; e.g. '1M female'= a female fetus with one male neighbour and one female neighbour (vom Saal, 1981).

These traits include 2M females being less attractive to males, more aggressive to female intruders, marking of a novel environment at an increased rate, and having longer and more irregular estrous cycles (vom Saal and Bronson, 1978; vom Saal and Bronson, 1980a; vom Saal and Bronson, 1980b). Similarly, the adult behaviour of male mice is thought to be affected in a similar way by intrauterine estrogen secreted by the ovary and found in relatively high concentrations in female fetuses. Males which develop *in utero* between two male fetuses ('2M males') tend to exhibit parental behaviour as adults when presented with newborn pups, whereas males that develop between two female fetuses often will kill the newborn. Differential exposure to testosterone is not responsible for this as testosterone concentrations in blood and amniotic fluid of both these types of male fetuses do not differ (vom Saal, 1983).

4.4.2 Micro-array data analyses

The GCOS software and Expression Console metrics (Affymetrix) indicate that the
micro-array data generated for the twelve fetal liver samples is of high quality. However,
a considerable amount of biological variation is present between samples from within the
same diet group making it quite difficult to reliably identify genes that are changing due
to diet treatment.

4.4.2.1 Array Assist analysis

By far the largest number of gene candidates was identified for the comparison between
the switch and 9% casein diet groups (Table 4.12). However, these analyses were all
coupled with high FDRs which weaken the reliability of the gene candidates identified by
the comparison of the treatments.

4.4.2.2 GeneSpring analysis

The GeneSpring analysis of the micro-array data identified a relatively large number of
genes that appeared to be altered in expression in fetal liver by at least two-fold in
response to dietary treatment. However, none of the probe sets identified were
significantly different the between dietary treatments (ANOVA at $p<0.05$).

The gene lists created using GeneSpring are grouped according to dietary treatment (9%
casein or switch) relative to control (18% casein) and according to whether the change is
an increase or decrease in the level of expression relative to the control treatment. From

these comparisons, the largest number of changes in gene expression relative to control was attributed to the 9% casein dietary treatment.

Despite problems surrounding the validity and reliability of candidates included on the gene lists produced by the Array Assist and GeneSpring analyses, both analyses suggest that probe set **1455869_at** may be heavily down-regulated in the 9% casein treatment group relative to the control 18% casein group (Tables 4.10 and 4.13). As shown in the aforementioned tables, the Affymetrix annotation for this probe set at the time the gene lists were generated implicated it as representing the Camk2b gene.

CaM kinases (calcium/calmodulin-dependent protein kinases) are important proteins as they catalyse phosphorylations on serine or threonine residues in selected proteins which mediate most of the actions of calcium in animal cells. CaM-kinase II is a multifunctional CaM-kinase found in all animal cells, but especially enriched in the nervous system, and has been implicated in some types of learning and memory in the vertebrate nervous system (Alberts et al., 1994).

However, closer investigation into this probe set (Ensembl) reveals that it is in fact located within an intron present in the Camk2b gene; hence the probe set is not directed against the mRNA for Camk2b. Indeed, the probe set sequence hits the mouse genome in 348 locations, one of which is within the Camk2b gene, in 46 separate sites throughout the genome, and thus it would appear to be a repeated element. Moreover, blasting this probe set (NCBI) reveals that the sequence the probe set best matches encodes for a viral

poly-protein. Thus, the Camk2b gene is just one of numerous elements possessing

integration sites for a retrovirus. Affymetrix has since updated the annotation for this

probe set and no longer attributes it to Camk2b mRNA.

4.4.2.3 dChip analyses

Due to the difficulties with high probability for false discoveries with the Array Assist

and GeneSpring analyses further analysis of the data was undertaken using an alternative

software package, dChip.

Class comparison analyses using all samples in each treatment group

The biological effect on transcription appeared to be the greatest for the switch versus 9%

casein class comparison using the low stringency criteria (Table 4.22). This reflects a

meaningful difference between these classes, but the reason for this was not clear. One

would expect that, if diet was the main contributor the other class comparisons may also

show a similar report, but they do not. Thus, some other factor/s in the dataset may be

overshadowing the dietary treatment effect here.

Enrichment analyses were only performed on the gene list in Table 4.22 produced from

the low stringency switch versus 9% casein class comparison. This was due to the small

number of probe sets returned for the other comparisons, at both stringencies, and the

difficulties with the associated high FDRs.

The GOTM tree shown in Figure 4.30 indicates that genes involved in **growth, steroid metabolism and cellular and lipid metabolism** are expressed more highly in the switch group relative to the 9% casein group. One interesting candidate gene upon which the enriched cellular lipid metabolism category in Figure 4.30 was based is ApoB. ApoB is expressed more highly in fetal livers of fetuses from the maternal switch diet group than in those from the 9% casein group. APOB protein levels are positively correlated with coronary heart disease and are a strong predictor of risk of myocardial infarction (McQueen et al., 2008). Indeed, mice over-expressing the ApoB gene have an increased level of low-density lipoprotein (LDL) also termed "harmful cholesterol" and decreased levels of high density lipoprotein (HDL) ("beneficial cholesterol") (McCormick et al., 1996). However, ApoB heterozygous knockout mice containing only one functional copy of the ApoB gene show the opposite effect, being resistant to diet-induced plasma hypercholesterolemia (Farese Jr et al., 1995). This information, together with the observation that the ApoB gene is more highly expressed in my switch group relative to my 9% casein group, is consistent with findings in rodents that male offspring from switch fed mothers tend to develop cardiovascular risk factors i.e. raised systolic blood pressure (relative to 18% casein offspring) (Watkins et al., 2008; Kwong et al., 2000) and may represent a tentative mechanism through which post natal defects in cardiovascular function are programmed before birth, possibly due to increased circulating LDL cholesterol associated with raised hepatic ApoB expression in the fetus.

Furthermore, the GOTM tree shown in Figure 4.31 indicates that genes for **cell cycle**; cell cycle regulation and regulation of progression through cell cycle are expressed at a lower

level in the switch group relative to the 9% casein group. The Folliculin (Flcn) gene is an interesting candidate being one of two genes upon which all of the aforementioned enriched categories in Figure 4.31 were based. There are three probe sets representing Folliculin transcript on the Mouse 430_v2 arrays used in this study, one of which appeared diet-sensitive in this class comparison. FLCN is a tumour suppressor protein encoded for by the BHD gene, with otherwise unknown function. Homozygous loss of BHD may initiate renal tumorigenesis in the mouse (Baba et al., 2008). Indeed, patients with Birt-Hogg-Dubé (BHD) syndrome have germ line mutations in the BHD tumor suppressor gene that are associated with an increased risk for kidney cancer. FLCN may interact with the energy- and nutrient-sensing 5'-AMP-activated protein kinase-mammalian target of rapamycin (AMPK-mTOR) signaling pathways (Baba et al., 2006). Targeted BHD knockout leads to activation of Akt-mTOR pathways in the kidneys and increased expression of cell cycle proteins and cell proliferation (Baba et al., 2008).

In fetuses from the switch diet group, the Flcn probe set was expressed at lower levels than in those from the 9% casein group, which may indicate increased cell proliferation is taking place in the tissues of the switch fetuses, coupled with activation of mTOR signaling. This hypothesis might lend support to the elevated birth weights of pups born to switch fed mothers relative to pups born to 9% casein or 18% casein fed mothers in the mouse (Watkins et al., 2008) and may suggest an elevation of the fetal growth trajectory takes place in these fetuses during gestation.

The dChip analysis of the micro array data thus far had indicated that relatively few probe sets in the fetal liver were diet sensitive. It is possible that the reason for this is that the maternal dietary treatment is a mild intervention which does not manifest itself as a vast number of transcriptional changes at this stage in hepatic fetal tissue. However, it was also possible that some other factor in the dataset was obscuring the diet response from being observed in its entirety. To this end, hierarchical clustering analysis was performed to examine the tightness of the dataset, with a view to potential excluding outliers in the biological replicates.

<u>Class comparison analyses using only the three most closely related (clustered) samples from each treatment group</u>

Table 4.27 shows that when outlier samples 3, 13 and 8 were excluded from the data and class comparisons were re run at low stringency, the greatest benefit was seen in the switch versus 9% casein comparison. When the switch and 9% casein outlier samples were removed from the respective classes the returned number of probe sets returned for this comparison rocketed to from 35 to 344, with a very low FDR (4.9%).

The GOTM trees in Figures 4.34 and 4.36 produced from the list of candidates given in Table AI.15 indicate that a larger number of probe sets were down regulated in the switch versus 9% casein comparison, than were up regulated. The most highly enriched category of probe sets that were over expressed in the switch group relative to the 9% casein was for aldehyde reductase activity (Figure 4.35). This category comprised three

probe sets representing two genes in aldo-keto reductase family 1 (Akr); Akr1b3:

member B3 (aldose reductase) and Akr1b7: member B7.

Aldo-keto reductases (AKRs) catalyze NADPH-dependent reduction of various aliphatic

and aromatic aldehyde and ketones. Aldehyde reductase (AKR1A) and aldose reductase

(AKR1B) have been extensively investigated, and the gene regulation of AKR1B has

been noted to be heavily influenced by the hyperglycemic state and high glucose

ambience in various culture systems. AKR1B catalyzes the conversion of glucose to

sorbitol with a coenzyme, NADPH (Danesh et al., 2003). Thus over-expression of this

gene may result in disturbed glucose metabolism which might have implications for

stabilizing blood sugar in the pathobiology of diabetes mellitus.

The reason why the switch versus 9% casein comparison alone was so strongly affected

by the removal of the outlier samples appeared to be a mystery. Indeed, it would be

expected that, if diet was the main contributor the other class comparisons may also show

a similar report in the absence of biological variation confounding the results, but they

did not. This raised the question as to whether some other factor unrelated to maternal

diet treatment or to biological variation within groups was driving the difference between

the switch and 9% casein classes. Indeed, this unknown factor may also help to explain

the reason for the main branching of the twelve samples into a group of five and a group

of seven observed in the clustering analyses (Figure 4.38).

Figure 4.38: Samples cluster broadly into two branches composed of a group of five samples and a group of 7 samples, (Figure taken from the hierarchical clustering analysis across all samples for 7475 probe sets with a coefficient of variation of 0.2 or more, shown in Figure 4.33).

Table 4.28 illustrates that the main branching of samples into a group of five and a group of seven appears to be due to a significant difference in the total litter sizes of the '5' group and the '7' group (p= 0.0189). Horn litter size was not significantly different in either group.

In order to minimize the potential effects of litter size on the genomics analysis, the total and in particular, the horn litter sizes of fetuses were taken into account when selecting the twelve fetal samples so that these parameters could be kept as constant as possible between the dietary treatments. The horn litter size was standardised across all litters from which samples were selected and thus the effects of local crowding in the uterus were controlled for (average horn litter size for all diet groups was 7.75 fetuses). Total litter size was standardised as far as possible but compromises were made in this parameter, and thus the average total litter sizes varied from 11 for the switch group to 14.5 for the 9% casein group.

Horn litter size was standardised in preference to total litter size due to information relating to the blood supply to fetuses in crowded uterine horns in the mouse. Blood supply comes from offshoots of a main loop artery which is fed from both the top and the bottom ends of the uterine horns. However, in crowded horns, growth of fetuses in the horn may be more variable because some of the fetuses may be supplied by one limb of a bifurcated offshoot of which the other limb supplies the ovary (McLaren and Michie, 1960).

Array code	Sample ref	Horn litter size	Total litter size	
E_13	Sw-20 L3	6	13	
L_1	9-16 L4	9	17	
L_16	9-22 R4	8	13	
L_9	9-19 L4	7	16	
N_3	18-10 R5	9	14	
N_18	18-18 R3	7	14	
L_8	9-17 L4	7	12	
E_7	Sw-11 R5	10	11	
E_12	Sw-12 L5	9	10	
E_6	Sw-10 R3	6	10	
N_17	18-20 L5	8	13	
N_4	18-11 R5	7	13	
ANOVA	"5" v "7"	P = 0.916	**P = 0.0189**	
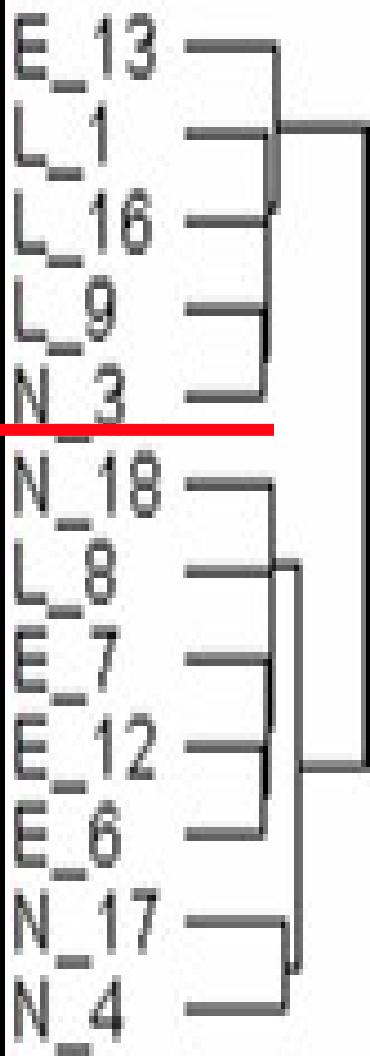
Table 4.28: The main branching of samples into a group of 5 and a group of 7 shown in relation to the horn and total litter sizes of the samples.

Table 4.28 indicates that the total litter size from which fetal samples were harvested for micro-array analysis has a significant effect on probe set expression and thus explains the division of samples into a group of five and a group of twelve. Also this may explain

why the switch versus 9% class comparison produces more differentially expressed candidates when the outlier samples 13 and 8 are removed. After removal of these outliers the average total litter sizes for the three 9% casein samples versus the three switch samples become more different to one another; average total litters size after outlier exclusion are 10.3 for the switch group compared to 15.3 for the 9% casein group.

Thus, the switch group has a smaller total litter size than the 9% casein group before removal of outliers and removal of outliers widens the gap. Hence, rather than the maternal diet, it appears that the total stress on the mother, as reflected by the total number of fetuses she must support, is the driving force for the differences in gene transcription between the switch and 9% casein classes. Gene expression differences may still be generated by the manipulation of maternal diet, but in this case it is not possible to elucidate this effect separately from the effect of the maternal capacity to support a large litter. Further, as the 9% casein group had the larger total litter sizes which might have resulted in intra-uterine growth restriction due to a limited access to the mother's resources/nutrients in the blood, it makes it difficult to distinguish whether effects on gene expression are related to the low protein manipulation or the larger litters as both parameters may have a similar effect on growth.

The strength of the effect of total litter size on probe set expression is indicated by a Peason's correlation test which indicates that the expression of 356 probe sets out of the 7475, which have a coefficient of variation of 0.2< across all samples (Figure 4.33) correlate to total litter size ($p<0.01$). (The mean FDR based on multiple random allocations of total litter size information to samples was 20%). Hence, the apparent

effect of total litter size on probe set expression represents a true correlation between these parameters.

In summary, initial analyses of the micro-array data using dChip highlighted some interesting candidates at the level of transcription that appeared to offer, in part explanations for mechanisms of programming of post natal phenotypes in response to maternal diet for the switch versus 9% class comparison. However, further analysis of the class comparisons suggested that a factor unrelated to diet might be driving the differences in gene expression, particularly between the switch and 9% classes. Thus, it appears that the mother's capacity to support her litter is sensed by individual fetuses in the uterus, and indeed this seems to manifest in alterations in fetal heptic gene expression.

4.4.2.4 Analyses overview

The downstream analyses described in section 4.4.2.1 to 4.4.2.3 all indicated that the level of biological variation in the data set made drawing comparisons between treatment groups more challenging. The biological variation between fetal liver samples of the same treatment group may be explained in a number of ways. For instance, the MF1 strain used in this study is an out bred stock which inevitably shows a measure of genetic variability. This may well have caused major differences in the response to environmental conditions, including maternal dietary restriction, between the experimental fetuses. Furthermore, the mice were housed under non specific-antigen free conditions in a non-barrier biomedical facility. Thus, the incidence of sub-clinical

infection/inflammation in some animals is a possibility and may be another factor affecting the response to environmental manipulation.

Other explanations for the biological variation between replicates may be related to the developmental model used in this study; variability in the stage of fetal liver development at day 17 could not be controlled amongst replicates. Similarly, as gestational day 17 murine fetal liver does not have clearly defined lobes, as in the adult, there was no way to standardise the anatomical portion of liver tissue selected for the genomics analysis amongst different fetuses. In terms of the tissue dissections, there is a possibility that some contamination of the hepatic tissue may have occurred from closely associated tissues in any number of samples to a greater or lesser extent (suggested in Table 4.14, of GeneSpring analysis) although every care was taken to preclude this.

As micro-arrays are largely explorative tools, it is important that candidates which appear to be differentially expressed are confirmed by means of another method, such as real-time PCR, before any firm conclusions are drawn. Unfortunately, it was not possible to validate any of the micro-array candidates due to time constraints. However, it may prove difficult to show relatively small fold changes in gene expression conclusively amid a background of high variability within treatments using this type of technique.

Chapter 5

5.1 Introduction: Effect of Maternal Diet on Fetal Protein Expression

The glucocorticoid system of receptors and enzymes mediate directly the action of the glucorticoids. Glucocorticoids have been widely implicated in mammalian fetal growth control (Bertram and Hanson, 2002; Reinisch et al., 1978; Novy and Walsh, 1983; Ikehami et al., 1997) and in organ maturation *in utero* (Thompson et al., 2004; Liggins, 1994; Cole et al., 1995; Langley-Evans, 2001). In addition, glucocorticoids have a variety of physiological roles in mammalian fetal tissues such as blood pressure control (Tangalakis et al., 1992; Benediktsson et al., 1993; Lindsay et al., 1996; Langley-Evans, 1997b), regulation of salt-water homeostasis, immunological responses and metabolism (Bertram and Hanson, 2002).

Evidence suggests that the glucocorticoid system is sensitive to nutritional modulation during pregnancy (Langley-Evans et al., 1996a; Langley-Evans, 1997b; Bertram et al., 2001; Kwong et al., 2007; Lillycrop et al., 2005; Lillyccrop et al., 2007; Burdge et al., 2007). Thus, the glucocorticoid system was selected as an interesting target to study the effects of the maternal low protein diet in the fetus, with a view to understanding potential mechanisms for programming of adult cardiovascular and metabolic diseases such as hypertension and type 2 diabetes mellitus as outlined in the DOHAD hypothesis.

5.1.1 Glucocorticoid receptor

The GR is an intracellular steroid hormone receptor belonging to the super-family of

nuclear hormone receptors (Mangelsdorf et al., 1995; Funder, 1996). Two

phenotypically distinct isoforms of GR have been identified in humans: GRα, (the

predominant physiological isoform) and GRβ (Hollenberg et al., 1985) of molecular

weight 94 kDa and 90 kDa, respectively (Oakley et al., 1996). Rodent GR cDNAs that

have been identified are homologues of the human GRα isoform, (Danielsen et al., 1986).

The GRα isoform is organised into defined domains. It has an N-terminal domain which

is concerned with activation of target genes, a central DNA-binding domain involved in

interactions with DNA sequences of target genes and a C-terminal domain for ligand

(glucocorticoid) binding (Oakley et al., 1996) (Figure 5.1).
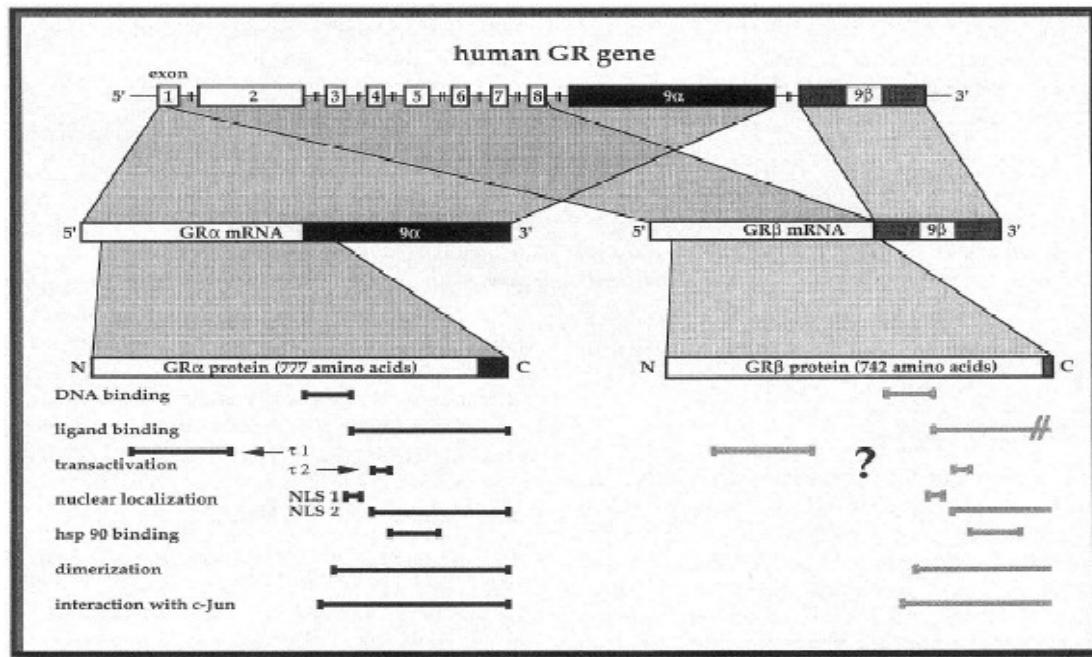
Figure 5.1: Structure of the human GR-α and β genes and proteins; functional sub-

domains of the α-isoform are also stated (Bamberger et al., 1996).

In the absence of glucocorticoid, GRα is located predominantly in the cytoplasm of cells as part of a multi-protein complex (Oakley et al., 1996). Cognate hormone binding induces a conformational change in GRα which leads to dissociation from the heat shock complex and concomitant hyper-phosporylation of GR. Nuclear localisation signals within the C-terminal domain are unmasked and receptor molecules, with glucocorticoid bound, translocate to the nucleus (Bamberger et al., 1996).

5.1.2 Enzymatic modulation of glucocorticoid action

11-beta hydroxysteroid dehydrogenase (11β HSD) is a microsomal enzyme complex associated with endoplasmic reticulum responsible for catalysing the inter-conversion of active cortisol and biologically inactive cortisone (Mahesh and Ulrich, 1960). Hence, the 11β HSD family of enzymes play a critical role in controlling local tissue concentrations of glucocorticoids (Edwards et al., 1996) and glucocorticoid exposure to the GR (Draper and Stewart, 2005). The enzyme complex is composed of two distinct components, one of which catalyses oxidation (the 11β-dehydrogenase) and the other responsible for reduction (the 11-oxoreductase) (Lakshmi and Monder, 1985a).

The proportions of the different enzyme components present vary between different tissues, e.g. in the rat, the liver is the major site of action of 11β HSD type 1 and hence in this tissue reduction usually exceeds oxidation (Lakshmi and Monder, 1985b).

The aim of this chapter was to quantify protein expression of the Glucocorticoid Receptor (GR) and 11β hydroxysteroid dehydrogenase (11β HSD) in fetuses at day 17 of gestation as a function of maternal diet.

5.2 Materials & Methods

Refer to Chapter 2 for Generic Methods on Experimental Design (section 2.1), Animal Treatments (section 2.2), Recovery of Conceptuses (section 2.3), and Collection of gestational day 17 tissue (section 2.4).

5.2.1 Collection of gestational day 17 tissue and total protein extraction

During the gestational day 17 dissections described in Chapter 3, tissues from the nearest neighbours on either side of the central conceptus in each horn were collected, snap frozen in liquid nitrogen and stored at -80°C for protein analysis. For analysis of the 11β HSD type 1 enzyme and the GR, the fetal liver was used as this organ is the target tissue for these proteins.

Day 17 fetal liver tissue was homogenised in 1% weight per volume of the strong anionic detergent, sodium dodecyl sulphate (SDS) in PBS (extraction buffer) using a motorised homogeniser, PowerGen 125 (Fisher Scientific). SDS denatures proteins and gives them net negative charges proportional to their masses. 10 µl of extraction buffer was used per mg of tissue. The resultant lysate was heated at 100 °C for 10 minutes and centrifuged at

10,000 g for 10 minutes at 4 °C. The supernatant was removed from the pellet and assessed for total protein content.

5.2.2 Protein assay

Calculation of total protein content in samples was made using the *DC* Lowry Protein Assay (BIORAD, UK). Four serial dilutions of samples were prepared in 1% SDS-PBS as well as four serial dilutions of 2 mg/ml Bovine Serum Albumin (BSA) protein standard, which were assayed alongside samples to generate a standard curve from which total protein content could be related to light absorbance. Light absorbance was read at 630 nm. As a result, the concentration of total protein in all sample lysates was calculated.

5.2.3 Gel electrophoresis (SDS-PAGE)

To each sample lysate, 4 x NuPAGE LDS sample buffer (Invitrogen) and 0.05M DTT (reducing agent to break the covalent disulphide bonds in proteins) were added and samples were heated at 100°C for 3 minutes. A known quantity (μg) of total protein from each sample lysate was loaded into the wells of a 1.0 mm pre-cast 4-12% BIS-TRIS polyacrylamide SDS gel (Invitrogen) alongside a protein standard marker (Precision Plus Protein Standards, All blue, BIORAD, UK). Gels were run in 20 x NuPAGE (MOPS) SDS running buffer (Invitrogen) diluted with deionised H_2O. NuPAGE Anti-oxidant (Invitrogen) was added to the running buffer in the inner part of the gel tank to maintain

proteins reduced by DTT in a reduced state and prevent re-oxidation of the –SH groups on cysteine amino acids that are juxtaposed in space during the gel electrophoresis. Gels were run for ~1 hour at 200 volts (maximum current). Following gel electrophoresis, proteins were electro-blotted from the gel onto low fluorescence Immobilon-FL PVDF (0.45 μm) membranes (Millipore) overnight (16 hours) in transfer buffer (Appendix II) at 300 mA with maximum voltage.

Pre-treatment of the PVDF is required before transfer of proteins from the gel: the membrane was wet in 100% methanol for 15 seconds, soaked in deionised water for 2 minutes and finally placed in transfer buffer to equilibrate for at least 5 minutes. Post-transfer, the PVDF membranes were rinsed in deionised water and bench dried on Whatman 3MM paper, for 2 hours at room temperature.

5.2.4 Protein detection

Abundance of the target protein is quantified as a percentage of the abundance of appropriate non-diet sensitive loading controls also present in the target tissues. For 11β HSD type 1 (34 kDa,) and GR (94 kDa), Actin (42 kDa) was used as such a control.

5.2.5 Western blotting

PVDF membranes were re-wet i.e. by soaking in 100% methanol and rinsed in double-distilled water before being incubated in PBS only. Prepared membranes were then

blocked for 1 hour in PBS-5% non-fat milk powder on a moving surface to prevent non-specific antibody binding. Primary antibodies specific for proteins of interest were then diluted in blocking buffer and incubated with membranes overnight at 4ºC on a moving surface. Primary antibodies used included: **Rabbit polyclonal anti-11β HSD1** {Cayman Chemical, USA}; **Mouse monoclonal anti-Actin** {Sigma Aldrich, USA}; **Rabbit polyclonal anti-Actin** {Sigma Aldrich, USA}; **Rabbit polyclonal anti-GR** {Santa-Cruz Biotechnology, USA}. After incubation with primary antibody, membranes were given 4 x 5 minute washes in PBS, with gentle shaking to remove any unbound antibody, and then incubated for 1 hour with appropriate fluorescently-labelled secondary antibodies diluted in blocking buffer and protected from the light (Goat anti-Rabbit 680 nm {Molecular Probes, UK}; Goat anti-Mouse 778 nm {Rockland, USA}). Membranes were then given 4 x 5 minute washes in PBS with gentle shaking, before being scanned using the Licor Odyssey infra-red imaging system (680 nm tagged antibodies give a red signal when scanned, 778 nm tagged antibodies give a green signal). Membranes were scanned with the default intensity setting (+ 5.0) for both 680 nm and 778 nm channels unless otherwise stated.

5.2.6 Densitometry

Integrated density values (IDVs) were obtained from the Odyssey infrared imaging system (Licor Biosciences), enabling quantification of the signal intensities of bands representing the target proteins present in each sample. Rectangular boxes were fitted

around the perimeter of each band and IDVs were automatically calculated for the area

inside the boxes (Figure 5.2).
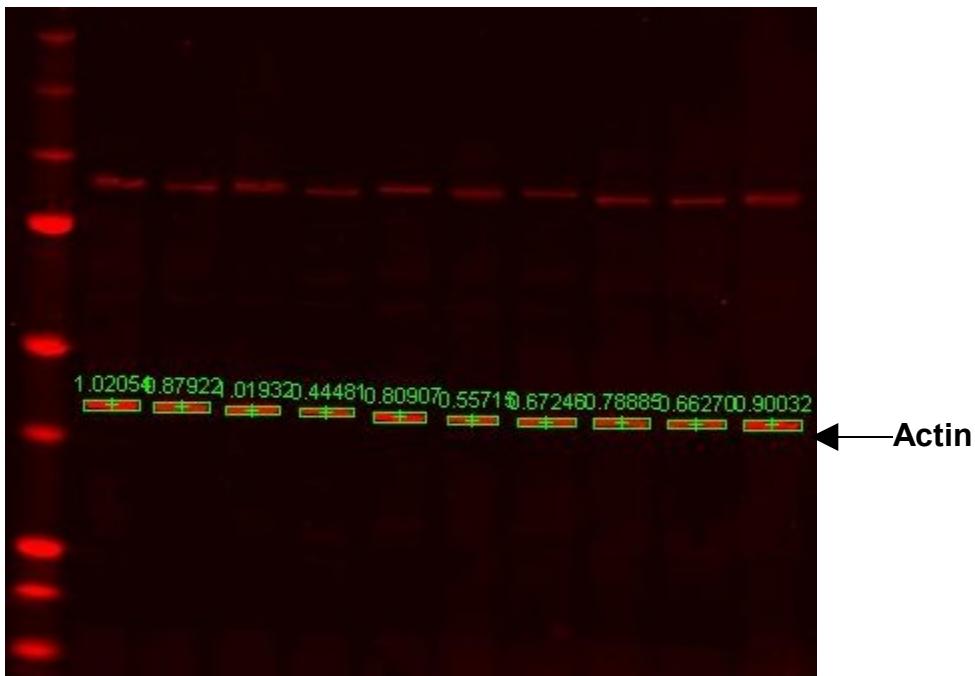
Figure 5.2: Example of IDV calculation. The bands for actin are quantified here by fitting boxes to the bands and recording the automated integrated density value produced for each signal.

5.2.7 Signal correction using gel standards

For the final GR and 11β HSD type 1 experiments, the same standard sample of fetal

liver was loaded once onto every gel in each experiment to act as a gel standard to control

for any variations in the blotting process of the different membranes within either

experiment. All the samples within each experiment were then corrected by comparison to this standard sample in order to make sure all blots were comparable with one another.

5.2.8 Design of final experiments

The protein expression of six different fetal livers (from six different mothers) from each dietary group was analysed. Each sample lysate was loaded a total of three times across different gels and in different positions on each gel. The average expression of the protein of interest relative to actin from each of the three loadings of one lysate was then taken as a representative level of expression of the protein relative to actin for that fetal liver sample. The fetal liver samples from each dietary group were coded A-F and then loaded in parallel across each gel. An example layout of samples is shown in Figure 5.3.

9A 18A SWA 9B 18B SWB 9C 18C SWC

Figure 5.3: **Example of layout of samples across a gel. The different diets are loaded in parallel in all cases. In this example, fetal samples A-C from the three dietary groups are each loaded once on the gel.**

5.3 Results

5.3.1 Initial antibody optimisation
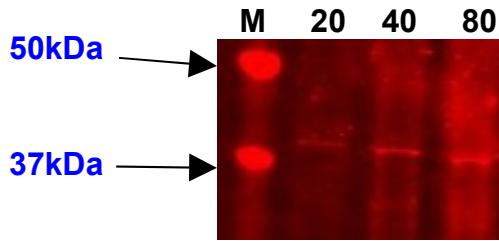
Figure 5.4: **Detection of 11β HSD type 1 in gestational day 17 fetal liver.**

M= Protein Standard Marker (BIORAD, Precision Plus). 20, 40 and 80 μg total

protein loaded as shown. Primary antibody conditions used: 1:250 (shown in

figure), 1:500 and 1:1000 conditions produced no detectable bands (not shown),

secondary antibody concentration 1:10,000 in all cases.

Figure 5.4 shows that at 20 μg and 40 μg, faint but well defined bands representing 11β

HSD type 1 are evident at ~37 kDa using a primary antibody concentration of 1:250. At

80 μg, the lane appears overloaded at this antibody concentration. Higher primary

antibody concentrations between 1:30 and 1:100 were also trialled with the same

secondary antibody conditions but did not produce such satisfactory bands for 11β HSD

type 1 due to signal saturation.

In order to distinguish reliably between the signals for 11β HSD type 1 (~34 kDa) and actin (42 kDa) when the blots are double-labelled for quantification, a Mouse anti-actin primary antibody was trialled so that a different fluorescently-labelled secondary antibody (Goat anti-Mouse 778 nm) could be used to produce a signal for actin at a different wavelength to that produced for 11β HSD type 1 (i.e. at 778 nm rather than 680 nm).

M   20   40   80   M   20   40   80

37kDa →
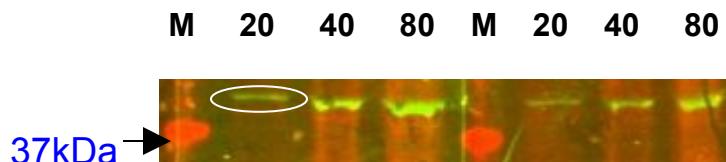
Figure 5.5: Detection of Actin in gestational day 17 fetal liver (as a loading control for 11β HSD type 1). M= Protein Standard Marker (BIORAD, Precision Plus). 20, 40 and 80 µg total protein loaded as shown. Primary antibody conditions used: Mouse anti-actin 1:500 (not shown) 1:300 (right three wells); 1:200 (left three wells). In all conditions 1:10,000 secondary antibody concentration was used.

Figure 5.5 shows that the 1:200 concentration of primary antibody produces a well defined band for actin detectable at ~42 kDa with 20 µg of total protein loaded (see circled band in Figure 5.5).

To further optimise the signals for 11β HSD type 1 and actin at a loading of 20 μg of total

protein the primary antibody conditions for both proteins were manipulated (Figure 5.6).
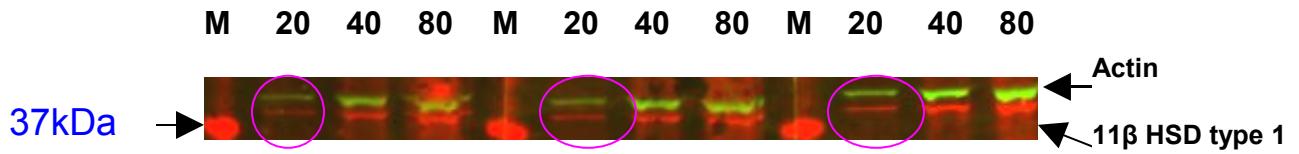
Figure 5.6: Primary antibody concentrations used to optimise the signals of 11β

HSD type 1 and actin at 20 μg of total protein loaded- see bands in circles. Left

circle, Mouse anti-actin 1:200 and Rabbit anti-11β HSD1 1:250 - as tried previously,

Middle circle, Mouse anti-actin 1:150 and Rabbit anti-11β HSD1 1:200, Right circle,

Mouse anti-actin 1:100 and Rabbit anti-11β HSD1 1:150. In all cases, appropriate

secondary antibodies were used at concentrations of 1:10,000.

As a result of the above optimisation results, the antibody conditions selected were those

for the right hand circle shown in Figure 5.6. At these antibody concentrations loading

20 μg of total protein enables both proteins to be clearly and independently visualised

without overloading.

Figure 5.7 indicates that the glucocorticoid receptor is present and detectable in day 17

fetal liver. Subsequent optimisation of the GR signal indicated that lower amounts of

total protein loaded, i.e. <10 μg, produced a crisper signal with minimal non-specific

bands using the same antibody conditions.

M   10   20   40   80

Figure 5.7: Detection of GR in gestational day 17 fetal liver. 10, 20, 40, 80 μg total protein loaded as indicated. Primary antibody concentration 1:250, secondary antibody concentration 1:10,000.

Figure 5.8 shows that, as was the case for GR, the lower amount of total protein loaded produces a more defined, less saturated band for Rabbit anti-actin.

M   10   10   10   20   20   20
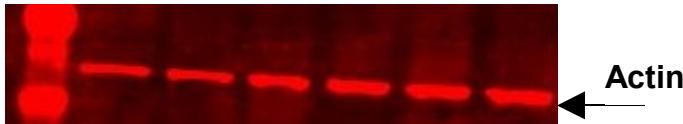
Actin

Figure 5.8: Detection of Actin in gestational day 17 fetal liver (as a loading control for GR). 10 and 20 μg of fetal liver total protein loaded; primary antibody 1:250 Rabbit anti-actin, secondary antibody 1:10,000.

A summary of the above antibody optimisations is given in Figure 5.9.

Detection of 11β HSD type 1 protein in the fetal liver at 20- 40 µg total protein using 1:250 dilution of primary antibody, secondary antibody dilution 1:10,000 (Figure 5.4).

Detection of actin in the fetal liver (using a Mouse anti-actin primary antibody) at 20 µg total protein using 1:200 dilution of primary antibody, secondary antibody dilution 1:10,000 (Figure 5.5)

20 µg total protein selected as the amount with which to optimise anti-11β HSD type 1 and Mouse anti-actin antibody concentrations further.

Double-labelling of 11β HSD type 1 and actin using different fluorescently-tagged secondary antibodies with 20 µg total protein loaded (Figure 5.6). Optimal signal detection was at the following primary antibody dilutions: Mouse anti-actin 1:100, anti-11β HSD type 1 1:150.

Detection of GR protein in the fetal liver at 10 µg total protein using 1:250 dilution of primary antibody, secondary antibody dilution 1:10,000 (Figure 5.7)

Detection of actin in the fetal liver (using a Rabbit anti-actin primary antibody) at 10µg total protein using 1:250 dilution of primary antibody, secondary antibody dilution 1:10,000 (Figure 5.8)

Double-labelling of GR and actin with 10 µg total protein loaded (Figure 5.10). Primary antibody dilutions: Rabbit anti-actin 1:250, anti-GR 1:250.

Figure 5.9: Summary of initial antibody optimisation of signals from target proteins

in the fetal liver

In summary, the initial antibody optimisations for the proteins of potential study indicate that GR and 11β HSD type 1 are present and detectable in day 17 fetal liver tissue. The optimum amount of total protein loaded and optimum antibody dilutions found for GR and for 11β HSD type 1 according to the degree of detection is shown in the following Table 5.1.

	Total protein (µg)	Primary antibody	Secondary antibody
GR	10	1 in 250	1 in 10,000
Actin	10	1 in 250	1 in 10,000
11β HSD type 1	20	1 in 150	1 in 10,000
Actin	20	1 in 100	1 in 10,000

Table 5.1: Summary of optimum amount of total protein and optimum antibody concentrations for detection of target proteins

5.3.2 Linear signal detection for GR and Actin

Prior to commencing experiments, several attempts were made to identify a linear range of detection for both GR and Rabbit anti-actin signals. To optimise the conditions so that a linear phase of both proteins could be detected, integrated density values were taken for each protein in blots where doubling amounts of total protein had been loaded under various antibody conditions. In the linear phase of signal detection it is expected that with a doubling of total protein loaded, the IDVs for the proteins being detected should also approximately double. Note that, for double labelling the optimal amount of total protein loaded must be equivalent for both proteins. Thus, antibody conditions were then varied in an attempt to bring ranges of detection in parallel (Table 5.2).

	2.5 μg	5 μg	Ratio	10 μg	20 μg	Ratio
GR (9% casein)	0.74	1.49	**2.01**	6.44	---------	
GR (18% casein)	0.99	2.08	**2.10**	8.13	---------	
GR (switch)	0.91	1.71	**1.88**	6.57	---------	
ACTIN (9% casein)	0.25	1.31	**5.24**	10.63	19.36	**1.82**
ACTIN (18% casein)	0.41	1.26	**3.07**	9.74	18.21	**1.87**
ACTIN (switch)	0.80	1.02	**1.28**	13.94	24.48	**1.76**

Table 5.2: IDVs for anti-GR and Rabbit anti-actin signals and the IDV signal ratios across increasing amounts of total protein loaded. Primary antibodies: 1:250 (Rabbit anti-GR; Rabbit anti-actin), secondary antibody 1:10,000 *(blots not shown)*. Note; the 2.5 and 5 μg lanes were loaded on a different gel to the 10 and 20 μg lanes, thus the 5 μg and 10 μg IDVs are not directly comparable so ratios were not calculated.

Table 5.2 shows that between 2.5 and 5 μg of total protein, the signal for GR in all the diet lysates is approximately doubling. Although this was not the case for actin, here the signal for the three diet lysates appears closer to a doubling between 10 and 20 μg of total protein loaded. Therefore further optimisation was required to bring the linear range of both proteins in line with one another.

As the IDVs for 2.5 μg actin loaded shown in Table 5.2 are relatively low, the following primary antibody dilutions were used in an attempt to boost the signal for actin, again with 2.5 and 5 μg total protein loaded: 1:200, 1:150, 1:120, 1:100, 1:50 (all with 1:10,000 secondary antibody concentrations). The best results were achieved using the 1:150 primary antibody dilutions; IDVs for this blot are shown in Table 5.3.

	2.5 µg	5 µg	Ratio
ACTIN (9% casein)	0.83	1.50	1.81
ACTIN (18% casein)	0.87	1.08	1.24
ACTIN (switch)	0.89	--------	

Table 5.3: IDVs obtained for actin signal with 1:150 Rabbit anti-actin primary antibody *(blot not shown),* and the IDV signal ratios obtained.

Table 5.3 shows a slight improvement in linearity for the actin signal between 2.5 and 5 µg total protein loaded compared to that shown for actin in Table 5.2. However, as the detection spectrum with the Licor scanner is extremely sensitive it will be able to reliably detect changes in signal which are outside a broadly linear part of the signal detection for a particular protein. This means that it is no longer necessary to first find linear ranges of proteins being immuno-blotted when using this detection system *(Personal communication from Licor Odyssey Technical Services).* Therefore, the amount of total protein loaded and the antibody dilutions for the GR and actin were selected according to the degree of detection of the bands rather than the degree of linearity obtained for each protein. Thus, conditions selected for further experiments into GR expression in fetal liver were as follows: anti-GR 1:250 primary antibody (1:10,000 secondary), anti-actin 1:250 primary antibody (1:10,000 secondary); 10 µg total protein loaded (Figure 5.10).
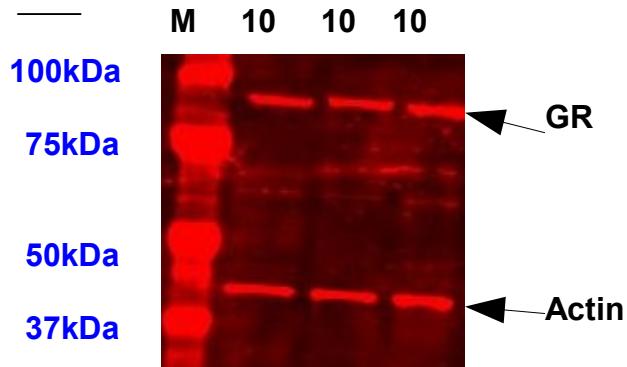
Figure 5.10: M= Protein Standard Marker (BIORAD, Precision Plus).

10 μg of fetal liver total protein loaded; primary antibody dilutions: 1:250 Rabbit anti-GR; 1:250 Rabbit anti-actin; secondary antibody 1:10,000.

5.3.3 Experimental: negative antibody controls

Use of secondary antibodies Goat anti-Rabbit 680, Goat anti-Mouse 778 in the absence of primary antibodies for 11βHSD type 1, GR and Actin resulted in clean blots, (Figure 5.11). The faint bands present at 25 kDa result from the anti-Mouse 778 secondary antibody binding the light chains of mouse antibody present in the sample of mouse tissue lysate.
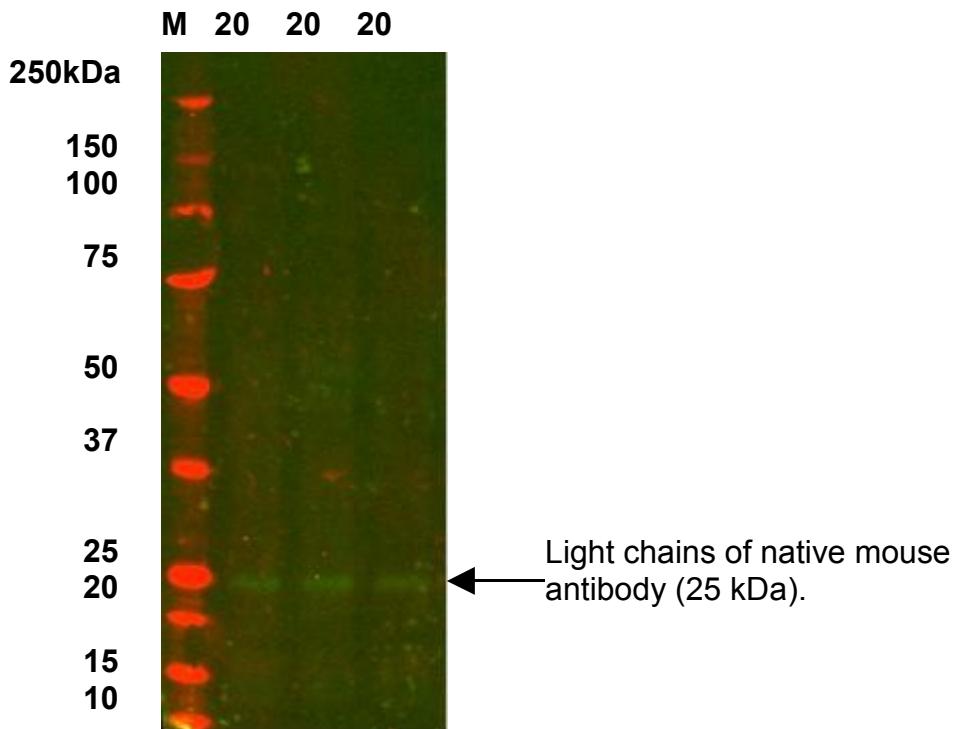
Figure 5.11: Negative primary antibody control. M= Protein Standard Marker (BIORAD, Precision Plus). 20 μg total protein from fetal liver lysate was loaded in each lane. Blot incubated with secondary antibodies only: Goat anti-Mouse 778, Goat anti-Rabbit 680, each at a dilution of 1:10,000. Membrane scanned at intensity + 5.5 for both channels.

5.3.4 Sample selection

Six fetal liver samples were selected from each dietary treatment group (one per litter). In terms of the sex of the fetuses from which fetal livers used in this study were harvested, PCR genotyping showed that at least 50% of the fetal livers in each of the dietary groups came from male fetuses. (The samples selected for protein analysis were nearest neighbours in the uterus to the central fetuses identified in the day 17 dissections in Chapter 3, bought in diet cohort. The nearest neighbours had their sexes determined as

described in Chapter 4, section 4.2.3). Horn litter size and total litter size were not significantly different between the dietary groups from which fetal livers were selected for protein analysis (Figure 5.12).
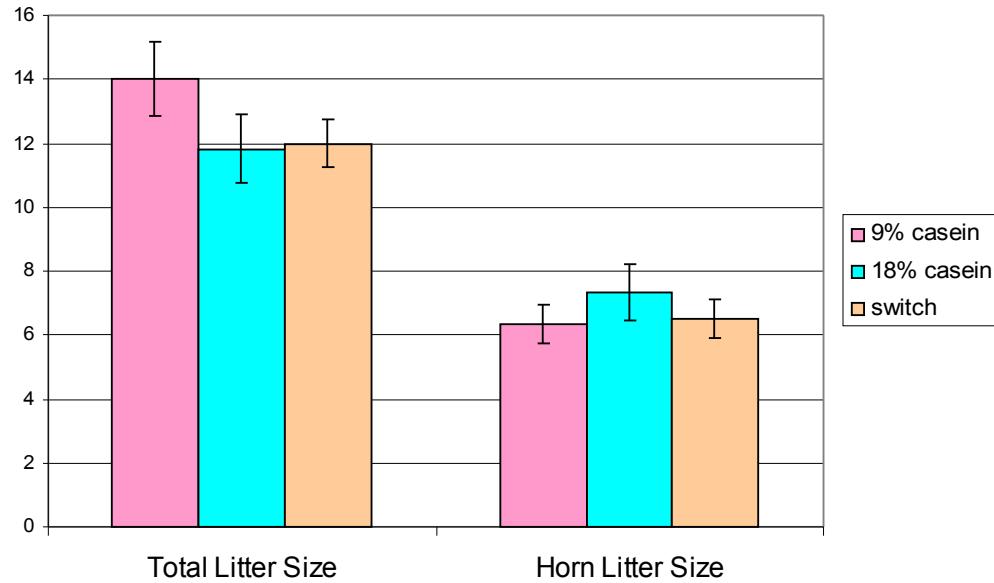
Figure 5.12: **Total and horn litter sizes from which fetal livers were selected for protein analysis.**

Figure 5.13 shows the comparison between the dietary groups in terms of amounts of total protein extracted per tissue weight. The amount of total protein extracted per milligram of fetal liver tissue was not significantly different between the dietary groups.
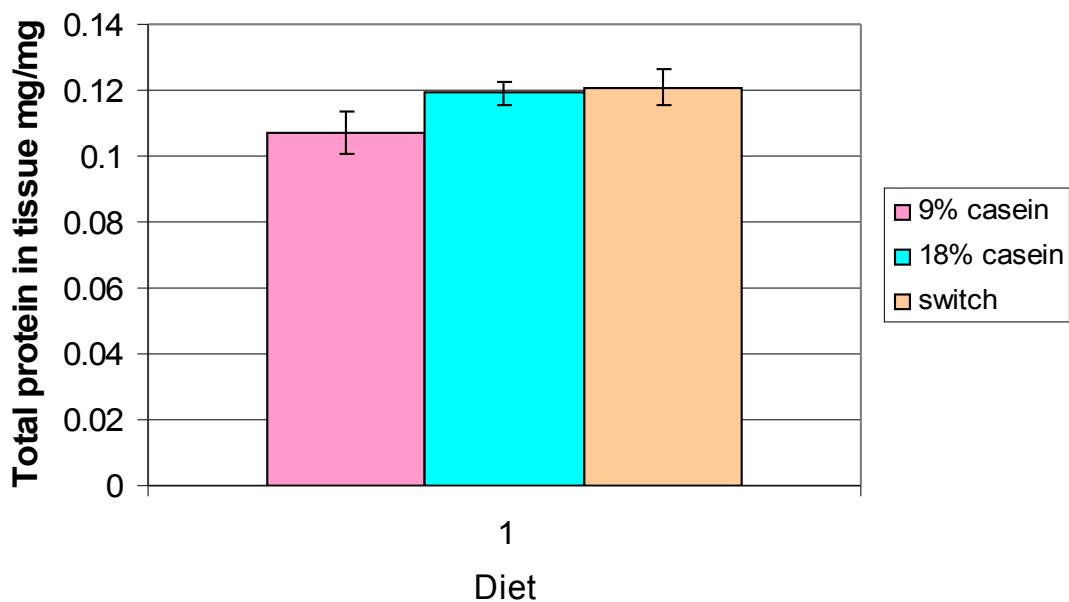
Figure 5.13: **Comparison of average amount of total protein extracted between the dietary groups from fetal liver tissues selected for protein analysis.**

For continuity, and to enable valid comparisons to be drawn, the same fetal liver lysates were used in both western blotting Experiments 1 and 2.

5.3.5 Experiment 1: Quantification of level of expression of glucocorticoid receptor in gestational day 17 fetal liver in relation to maternal diet.

An example of a blot from the experiment to determine the level of expression of the GR protein in samples of fetal liver from each of the dietary treatments is shown in Figure 5.14.

M 9 18 sw 9 18 sw 9 18 sw S

←GR (94 kDa)

←Actin (42 kDa)
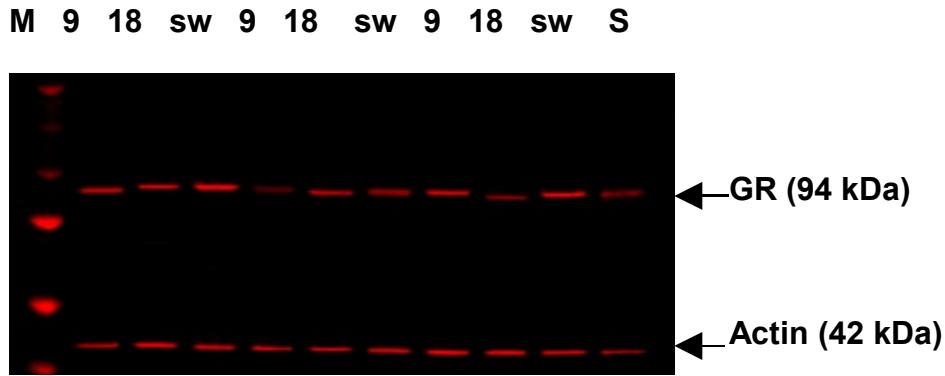
Figure 5.14: Experiment 1: analysis of GR expression levels in fetal liver in relation to maternal diet. M= Protein Standard Marker (BIORAD, Precision Plus). S= Standard fetal liver sample (same sample loaded onto all gels). Fetal liver lysates from each dietary treatment were loaded in parallel as indicated, (9% casein, 18% casein and switch/sw). 10 µg total protein was loaded in each well, primary antibody dilutions: 1:250 Rabbit anti-GR; 1:250 Rabbit anti-Actin; secondary antibody 1:10,000. Note; for the final experiment membranes were all scanned with the following intensities: L 2.0 (Actin) and + 1.5 (GR).

Figure 5.15 displays the results from this experiment. It illustrates that the level of protein expression of GR in fetal liver is significantly increased in the switch dietary treatment group compared to the control (18% casein) group ($p < 0.05$).

p<0.05
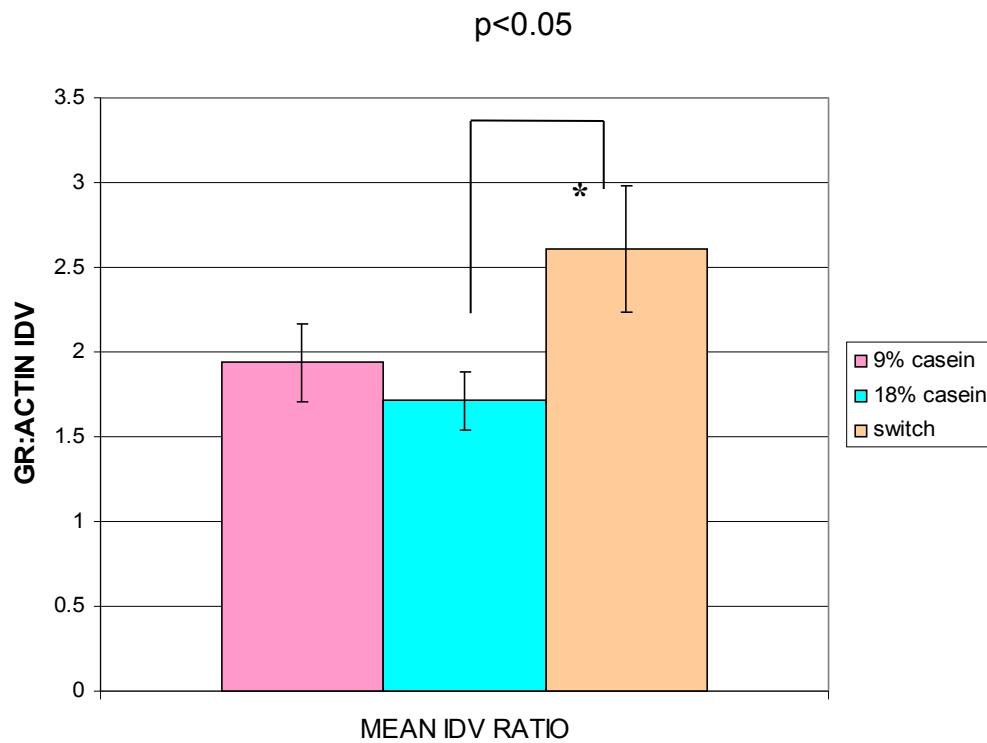
Figure 5.15: **Protein expression of GR relative to Actin in day 17 fetal liver in respect to maternal diet. *p=0.03, one-tailed two sample t-test, n= 6 livers per treatment group.**

Importantly, the level of average actin expression alone in the fetal livers did not change significantly between the diets (Figure 5.16).
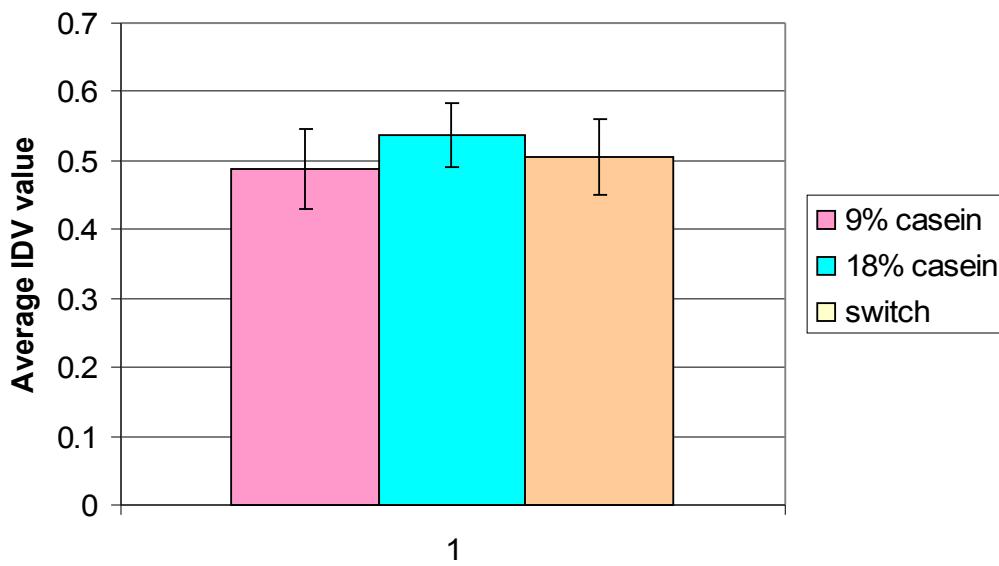
Figure 5.16: **Raw IDV averages for actin in the fetal livers from each of the maternal dietary groups.**

5.3.6 Experiment 2: Quantification of level of expression of 11β HSD type 1 in gestational day 17 fetal liver in relation to maternal diet.

An example of a blot from the experiment to determine the level of expression of the 11β HSD type 1 protein in samples of fetal liver from each of the dietary treatments is shown in Figure 5.17.

| 9 | 18 | sw | 9 | 18 | sw | 9 | 18 | sw | S |

ACTIN (42 kDa)

11β HSD type 1 (34 kDa)
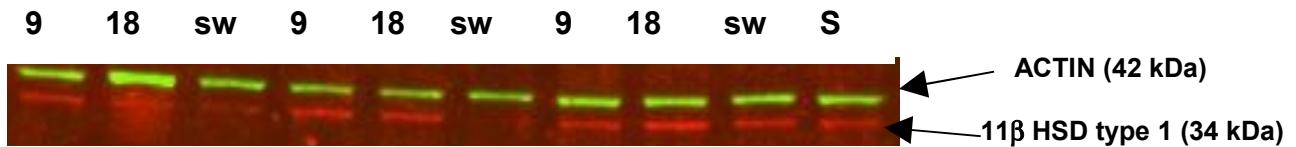
Figure 5.17: Experiment 2: analysis of 11β HSD type 1 expression levels in fetal liver in relation to maternal diet. S= Standard fetal liver sample (same sample loaded onto all gels). Fetal liver lysates from each dietary treatment were loaded in parallel as indicated (9% casein, 18% casein and switch/sw). 20 μg total protein loaded, primary antibody dilutions: 1:150 Rabbit anti-11β HSD 1; 1:100 Mouse anti-Actin; secondary antibodies 1:10,000. Note; for the final experiment membranes were all scanned with the following intensities: + 1.5 (Actin) and + 5.5 (11β HSD type 1).

Figure 5.18 shows the results from this experiment and indicates that there is a significant reduction in the level of expression of the 11β HSD type 1 protein in the fetal liver in response to the switch diet relative to controls ($p<0.05$). Decreased 11β HSD type 1 expression in the fetal liver may result in a lower availability of active glucocorticoid in the fetus.
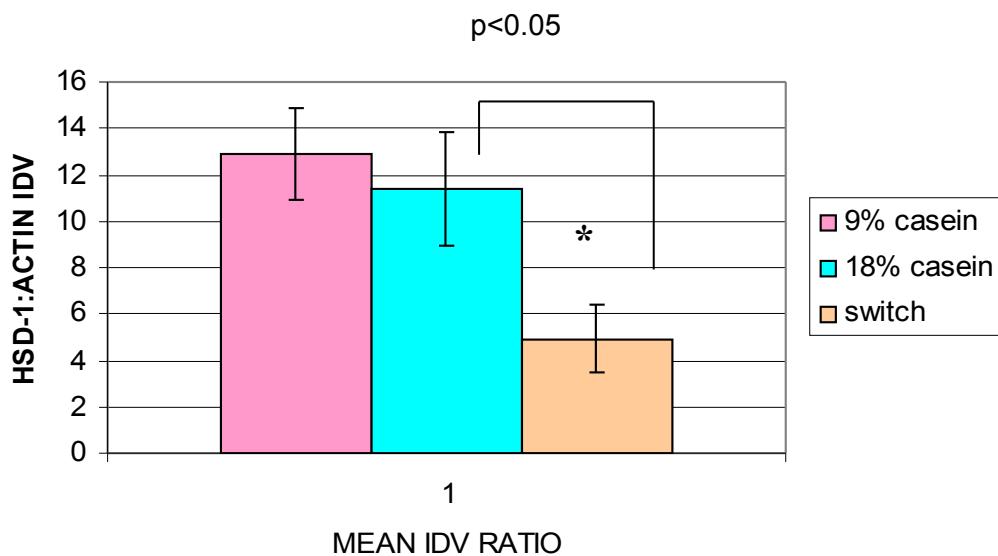
Figure 5.18: Protein expression of 11β HSD type 1 relative to Actin in day 17 fetal liver with respect to maternal diet. *p=0.026, one-tailed two sample t-test, n= 6 livers per treatment group.

5.4 Discussion

The results obtained from the experiments to determine the level of protein expression of
GR and 11β HSD type 1 in the fetal liver in relation to maternal diet suggest that the
switch diet is sufficient to invoke changes in the expression of both these proteins in the
fetal liver, but that the low protein diet maintained throughout pregnancy does not induce
any significant changes relative to controls. The increased expression of GR in fetal
livers from fetuses of switch diet fed mothers suggests that there may be a heightened
level of glucocorticoid action in these livers, due to the increased receptor availability.
Decreased 11β HSD type 1 expression in the exact same tissues suggests there may be a
lower abundance of the active form of the glucocorticoid hormone in these switch fetal
livers compared with the control group.

The decreased expression of 11β HSD type 1 may be a compensatory response to the
increased GR expression present in the switch group fetal livers because, as described
previously in rodents and in humans, increases in active glucocorticoid *in utero* may
result in alterations to growth (Reinisch et al., 1978; Novy and Walsh, 1983) and changes
to blood-pressure control and thus propensity to cardiovascular disease (Benediktsson et
al., 1993; Lindsay et al., 1996; Edwards et al., 1993; Langley-Evans, 1997a,b).

Although the data collected for the 9% casein diet treatment here do not mirror the
findings documenting significantly raised hepatic GR mRNA expression relative to
controls in rat offspring as a result of maternal low protein fed throughout gestation

(Lillycrop et al., 2005; Lillycrop et al., 2007) these studies did not examine expression at the protein level as mine did. However, the results I obtained showing elevated GR protein expression in the switch treatment group does support other more closely related work using mouse liver tissue from 28-week old offspring from mothers fed the same switch diet as was used in my experiments. This has shown DNA methylation of the GR promoter was significantly decreased relative to controls (Lillycrop, K, Watkins, A, Fleming, T; unpublished data). Such hypomethylation may result in less restriction of the promoter's activity and elevated expression of the GR gene. This idea lends support to the raised protein expression of GR in the fetal liver of fetuses from switch fed mothers shown in the protein analysis data above. It may be that in the fetus too there is this alteration to the methylation status of the promoter for the GR gene, which may in turn contribute to raise expression of the gene and thus the GR protein levels. The elevated GR protein expression profile in the fetal liver is also supported by a trend towards raised GR gene expression in mouse day 17 fetal livers (although only female fetuses were analysed) from a switch dietary treatment relative to controls measured by Real-time PCR (Lillycrop, K, Watkins, A, Fleming, T; unpublished data).

In both the aforementioned studies, in the 28 week post-natal murine liver of males and females and the *female* day 17 murine fetal liver, the Dnmt1 gene was found to be significantly elevated in the switch treatment group relative to controls (Lillycrop, K, Watkins, A, Fleming, T; unpublished data). In contrast, previous work in the rat has indicated that Dnmt1 transcript expression is reduced in offspring in response to a maternal low protein diet throughout gestation (Lillycrop et al., 2007). Thus, the

maternal protein restriction throughout pregnancy versus the switch treatment may work through different epigenetic mechanisms in rodents. It appears that the low protein diet throughout pregnancy leads to reduced capacity for methylation by Dnmt1 in the offspring, whereas the switch diet group seems to invoke an enhanced capacity for methylation by Dnmt1. However, Dnmt1 is just one methyl transferase; expression of others may not necessarily reflect these patterns.

A recent study in mice using the same maternal switch dietary treatment has found that the switch diet causes an elevation in recorded birth weight of pups at term (Watkins et al., 2008) indicating that there has been an up-regulation of fetal growth. However, the increased level of hepatic glucocorticoid receptor expression found in the present study in the fetus at day 17 may indicate an increased action of glucocortoid in fetal tissues, which is known to have an inhibitory effect on fetal growth (Ikegami et al., 1997; Bertram and Hanson, 2002, Novy and Walsh, 1983). Thus, the findings appear contradictory. Although in rats, it has been previously reported that the equivalent switch diet treatment results in a significant reduction of measured birth weights of pups at term (Kwong et al., 2000) which may lend support to an attenuation of fetal growth taking place in late gestation. However, the rat model may represent a slightly different mechanism in this species and thus the results obtained by Watkins *et al,* 2008 in the mouse may be more relevant to this study. Although, as the effects on birth weight documented by Watkins *et al,* 2008 and also Kwong *et al,* 2000 are gender specific (the switch dietary treatment only resulted in a significant alteration of birth weight in female pups), and the present study incorporated fetuses of both sexes, these data may not be directly comparable to my

study. In hindsight, it would have been beneficial to know the level of target protein expression based on the sex of the fetuses in the present study so that gender-specific differences could be identified and more specific conclusions drawn.

The depression in 11β HSD type 1 expression found in the fetuses from the maternal switch group might result in a reduction in the level of glucocorticoid action in the fetus and thus might lend support to there being an up-regulation of fetal growth, due to the reduction of a growth retarding influence in the form of active glucocorticoid, thus resulting in elevated birth weights at term.

If indeed the decrease in 11β HSD type 1 expression compensates for the elevation in GR expression, the net effect may be a slightly dampened expression of 11β HSD type 1 in the fetal liver, and hence a small reduced capacity of the fetus to transform inactive glucocorticoid into physiologically active forms. This may manifest itself as a reduced capacity for glucocorticoid action in these fetuses. In contrast to my findings at the protein level, increased levels of hepatic 11β HSD type 1 mRNA have been reported in female rat fetuses at late gestation in an equivalent of the switch diet group relative to controls (Kwong et al., 2007). However, as mentioned earlier, my protein analysis of the fetal liver did not distinguish between fetal sexes comprehensively and thus may include fetal liver from both males and females in the analysis. Thus, my results cannot be directly compared to reports of gender-specific changes.

Programming responses are likely to be multi-factorial; glucocorticoids represent just one hormone of a pool of important signals in the fetus which are relevant for fetal growth and development. Thus, these hormones alone cannot explain the bounds of fetal programming, but instead may explain a small part of the complex picture in the fetus in which adaptations to the environment *in utero* are made.

Further work

Further work on the GR protein might involve the selective detection of the phosphorylated form of the protein only. This would enable specific analyses of the level of activated receptor to be made i.e. receptor that has bound its hormone ligand (Bamberger et al, 1996), and thus give a more specific indication of glucocorticoid presence in the tissue. However, at the time of writing, the phospho-GR antibodies available were all raised against phosphorylations present on the human form of the GR protein (Serotec Database). An additional possibility for further work on the glucocorticoid theme might involve analysis of the level of expression of the IGF-II protein in the same fetal liver tissues. As IGF-II is a negative downstream target of glucocorticoids involved in stimulating fetal cell growth and differentiation (Fowden, 2003), it may be that levels are reduced in those tissues where there is heightened glucocorticoid activity. Indeed in the rat fetal liver, it has been reported that an equivalent to the maternal switch diet used in my study has resulted in reduced hepatic *Igf2* gene expression in male fetuses (Kwong et al., 2006).

Finally, further work might involve investigation of the protein expression/activity of 11β HSD type 2 in the placenta at day 17 to analyze the level of maternal glucocorticoid crossing the placenta and entering fetal circulation at this time.

Chapter 6

6.1 Introduction: The Influence of Pre-implantation Embryo Environment on Fetal

Development

Studies in a variety of animal models have demonstrated that the environment to which

the early embryo is exposed has lasting implications for its later development. A striking

example of the sensitivity of the early embryo to its environment is documented by the

phenomenon of Large Offspring Syndrome (LOS). LOS has been illustrated in sheep and

cattle after *in vitro* culture of embryos in the presence of serum. The LOS phenotype is

characterised by increased birth weight, increased muscle mass, cerebellar dysplasia,

skeletal and facial malformations, and changes in the size and weight of internal organs.

Furthermore, these animals die peri-natally (Thompson et al., 1995; Sinclair et al., 1999;

Holm et al., 1996; Young et al., 1998). Long-term effects of pre-implantation embryo

culture and transfer documented in mice include adverse alterations to post natal

behaviour, memory and growth (Ecker et al., 2004; Fernandez-Gonzalez et al., 2004) and

elevated post natal blood pressure in female offspring (Watkins et al., 2007). Similarly,

in vivo manipulations to the pre-implantation embryo environment, mediated by altered

maternal diet in rodents has demonstrated reduced blastocyst cell numbers in the short

term, first within ICM (in early blastocyst) and later within both ICM and TE (in mid/late

blastocyst), induced by a slower rate of cellular proliferation (Kwong et al., 2000) and

altered birth weight, post natal growth and hypertension in the long term (Kwong et al.,

2000; Watkins et al., 2008).

Thus, the pre-implantation stage of development represents an important window during which the embryo is sensitive to programming brought about through manipulations in its immediate environment.

Blastocyst stage embryo transfers were conducted at 3.5 days from low protein and control fed donor mothers to control fed pseudo-pregnant foster mothers, also at 3.5 days post plug in order to determine the influence of the *in vivo* low protein environment exclusively during the pre-implantation period. Post-transfer, embryos were allowed to develop inside foster mothers until gestational day 17, when fetal growth was examined through weight analyses.

This experiment isolates the importance of the period during the pre-implantation window of embryo development (0-3.5 days) without altering uterine environment. This is in contrast to the switch diet described in Chapter 2 which effects both maternal physiology and the embryo. In this way it is possible to determine the relative maternal and fetal contributions for potential fetal programming in response to diet, and to investigate the potential for predictive adaptive responses (PARs) to be made by the embryo in response to its early environment (Gluckman and Hanson, 2004a, c).

6.2 Materials & Methods

Also refer to Chapter 2 on Generic Methods, sections 2.1 Experimental Design, 2.2 Animal Treatments, 2.3 Recovery of Conceptuses, and 2.4 Collection of gestational day 17 tissue.

6.2.1 Experimental design

Pseudo pregnant mothers fed a control (18% casein) diet since day of plug surgically received blastocysts from both low protein (9% casein) and control (18% casein) diet fed donor mothers. Six blastocysts from a low protein diet fed donor were transferred into one horn of the pseudo pregnant uterus, and six blastocysts from a control diet fed donor were transferred into the other horn (Figure 6.1). In this way it was intended that litters of up to twelve fetuses would be produced, representing average total litter sizes of naturally-mated females (see Chapter 3, Figure 3.2). The transfer of blastocysts from 18% casein fed donors, into the same foster mother as blastocysts from low protein (9% casein) diet donors acted as an internal control to account for the effects of the transfer procedure on the foster mother.

To avoid horn bias the transfer of blastocysts of one diet type to either the left and right uterine horns was alternated during the experiment. The order in which embryos of each diet were transferred was also alternated i.e. embryos from 9% casein diet fed donors

were not always transferred before embryos from 18% casein diet fed donors and vice versa.
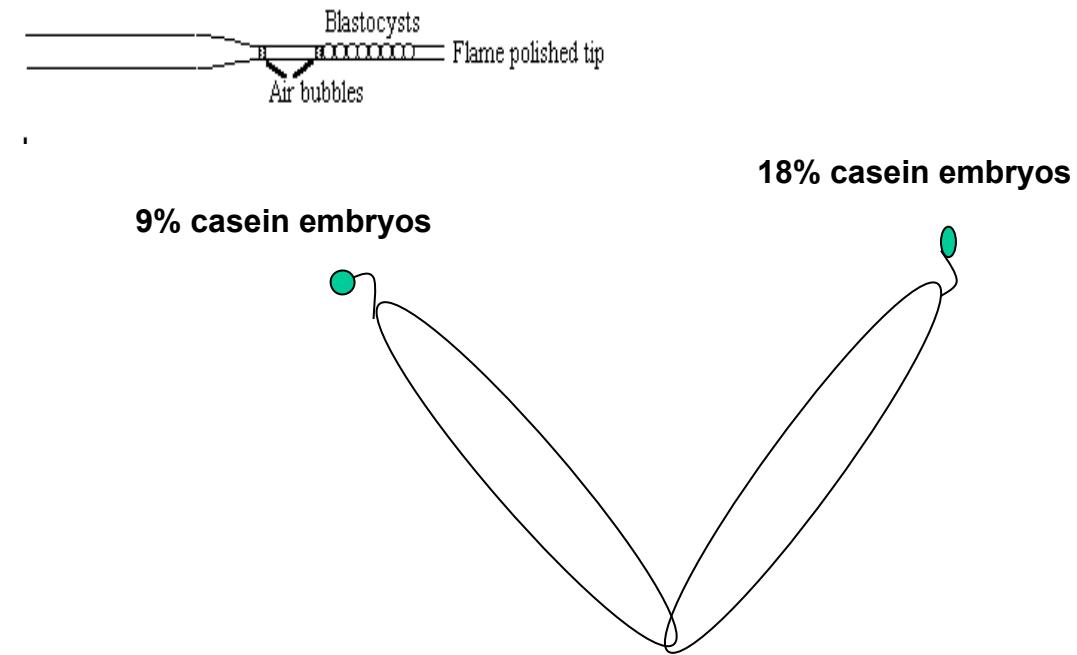
Figure 6.1: **Schematic representation of the pseudo pregnant mouse uterus at blastocyst transfer; also the loaded transfer pipette. Adapted from** http://wheat.pw.usda.gov

Importantly, it is worth noting at this stage that trans-uterine migration does not appear to occur in mice (Rulicke et al., 2006). Trans-uterine migration is the movement of embryos from one uterine horn into the other and is a phenomenon that has been described for animals of different species with a bicornuate type of uterus, as is present in the mouse. The separation of the uterine body and the pre-vaginal portion of the uterine cervix into two canals by a septum seem to be the main reason for the absence of successful trans-uterine migration in mice (Rulicke et al., 2006).

6.2.2 Stud vasectomies

Surgery was carried out under general anaesthesia following an intra-peritoneal injection of a Ketamine based anaesthetic (see Appendix III) to vasectomise ten 6-week old MF1 studs which had been fed a standard chow diet from weaning. After preparation of the skin area, the vasectomy was carried out by making a ventral incision at knee height, and locating the fat pad associated with the testis on either side. The vas deferens were then located and cut and the ends cauterized.

Vasectomised males were housed individually, fed a standard chow diet and tap water *ad libitum* and allowed two weeks to recover from the procedure under standard conditions (refer to Chapter 2, section 2.2). After recovery, mating commenced to generate pseudo pregnant females in which the signal of mating is sufficient to generate a uterus receptive to receiving embryos, in the absence of any fertilization.

To check the effectiveness of the surgery before the experiment began, vasectomised males were allowed to mate two females each. Plug-positive females were then observed for the following 21 days to ensure no weight gain, indicative of a pregnancy, was evident.

6.2.3 Animal treatments

Plug-positive embryo donor females were fed either the 9% casein or 18% casein (control) diet from day of plug until day 3.5 of pregnancy, at which point they were culled and their embryos collected. At 3.5 days, surgery took place in order to transfer embryos from the donors into 18% casein fed pseudo pregnant mothers at the equivalent stage of pseudo pregnancy. After mating with vasectomised males, plug positive pseudo pregnant foster mothers were fed the 18% casein diet from day of plug until day 17 when they were sacrificed.

6.2.4 Uterine dissection at day 3.5

Pregnant embryo donor females were culled by cervical dislocation after 3.5 days gestation. The uterus was dissected out by cuts made just posterior to the oviduct at the isthmus region of each uterine horn and a cut anterior to the cervix and was placed in saline warmed to 37 °C. Excess fat and mesometrial tissue was removed from the uterus at this point.

6.2.5 Embryo collection and short term culture

At 3.5 days post plug, embryos were flushed from each of the uterine horns of pregnant donors. A needle puncture near the oviduct end of each uterine horn was made under a

dissecting microscope and Hepes-buffered (H6 PVP) culture media (see Appendix III) pre-warmed to 37 °C was flushed through and expelled with blastocysts at the cervix. Blastocyst stage embryos were selected and collected using a mouth pipette and transferred to ~20 µl drops of CO_2 equilibrated T6 PVP culture media (see Appendix III) warmed to 37 °C, covered with a layer of equilibrated mineral oil. Blastocysts flushed from either horn of the donor uterus were pooled, as were blastocysts recovered from different donors of the same dietary treatment. T6 PVP drops containing embryos were placed in a CO_2 incubator at 37 °C and gassed at 5% CO_2 until required for transfer to a pseudo pregnant female. To keep embryo culture time to a minimum, a 'flush-transfer-flush-transfer' routine was adopted i.e. as soon as six embryos of one diet type were flushed and collected from the donor/s, these were transferred into the pseudo pregnant uterus before the donor/s of the other type of diet were flushed.

6.2.6 Embryo transfer surgery

Pseudo pregnant animals were given an intra-peritoneal injection of a Ketamine-based anaesthetic which incorporated analgesic (see Appendix III). A maximum dose equivalent to 1% body weight was administered (weight vol $^{-1}$). The lower dorsal region of the mouse was shaved and the skin covered with iodine solution. A small skin incision was made followed by an incision into the body wall over the region of the ovary. The fat pad covering the ovary was located, clamped and rested across the mouse's back to hold the uterus in place (Figure 6.2).
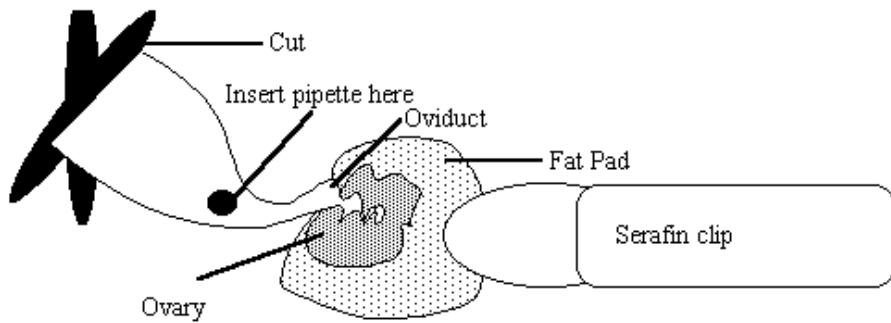
Figure 6.2: Schematic showing how ovarian fat pad is easily visible and provides an anchor from which the delicate uterine horn may be accessed; taken from http://wheat.pw.usda.gov.

The uterus was located by easing the ovary, oviduct and part of the uterus out through the incision in the body wall. Under a dissecting microscope, a puncture was made to the top of each uterine horn into the lumen of the uterus using a 25 gauge needle and embryos loaded in a fine flame-polished transfer pipette were expelled into each horn in turn (Figure 6.3). Six embryos were transferred per horn with a small amount of T6 PVP (avoiding mineral oil from the culture).
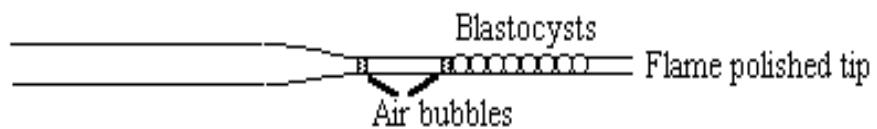
Figure 6.3: Schematic of a loaded transfer pipette; taken from http://wheat.pw.usda.gov.

To minimise risk of infection, care was taken during surgery to keep instruments for cutting the skin separate from instruments used for working inside the mouse.

All foster mothers were housed individually following surgery and were allowed to recover post-operatively in a quiet, warm room (~33 °C) to minimise onset of hypothermia brought about by the anaesthesia (Bagis et al., 2004) and to aid recovery.

6.2.7 Recovery of conceptuses

On gestational day 17 (i.e. 14 days post-embryo transfer surgery), pregnant foster mothers were culled by cervical dislocation of the neck, and the uterus was dissected out and placed in ice cold PBS. Conceptuses were dissected out of each of the uterine horns and weighed, and conceptus weights and horn litter sizes recorded.

6.3 Results

Uterine horn litters from six different foster mothers for each of the embryo donor diet groups were collected at day 17, uterine horns containing just a single conceptus at day 17 were excluded from the analysis as being anomalous.

6.3.1 Embryo development and horn litter sizes at day 17

Following the transfer of six embryos per uterine horn into the pseudo pregnant uterus, on average 3.5 conceptuses were recovered from a single uterine horn at day 17 for both types of diet embryos i.e. the average horn litter sizes were equivalent between diet groups. As mentioned in Section 6.2.1, the design of this experiment was drawn up to enable conceptuses from both embryo diet treatments, to be recovered at day 17 in the same foster mother thus there would be an internal control for the effects of the transfer procedure on a particular foster mother. However, only in 20% of foster mothers did two or more embryos develop successfully in both horns of the uterus. In the majority of foster mothers the pregnancy was unilateral and restricted to just one of the uterine horns, despite both horns being transferred into (Table 6.1).

No. foster mothers with fetuses recovered from **both** 9% & 18% casein diet embryo donors	2
No. foster mothers with fetuses recovered from 9% casein diet embryo donors **only**	4
No. foster mothers with fetuses recovered from 18% casein diet embryo donors **only**	4
Total number of foster mothers pregnant at day 17 (with 2+ conceptuses per horn)	10

Table 6.1: Numbers of foster mothers where conceptuses were recovered at day 17 in one or both uterine horns.

6.3.2 Weight data at gestational day 17 after embryo transfer into 18% casein diet foster mothers at day 3.5

It appears that the dietary environment of the embryo <3.5 days has a significant effect on conceptus weight when measured at day 17. Figure 6.4 indicates that the 9%-18% group

(i.e. embryos from 9% casein diet fed donors transferred into 18% casein fed fosters)

develop into significantly heavier conceptuses than the 18%-18% group (i.e. embryos

from 18% casein diet fed donors transferred into 18% casein fed fosters).
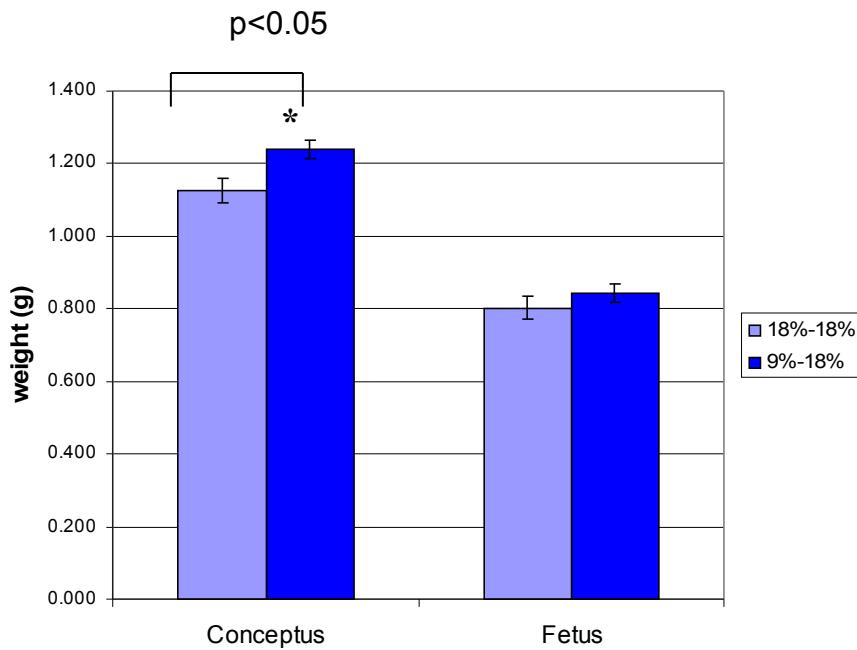
Figure 6.4: **Average conceptus and fetus weights after embryo transfer into 18%**

casein diet fed foster mothers, (*p =0.048) n= 6 mothers, 19-21 samples for each type

of transfer.

Conceptus weight measured at day 17 indicates that embryos derived from 9% casein diet

fed donor mothers give rise to larger conceptuses than embryos from 18% casein diet fed

donors when both types of embryo develop within the same type of environment post 3.5

days **(p= 0.048).** However, when horn litter size is incorporated into the analysis, the

effect of embryo donor diet on conceptus weight remains **(p= 0.013)** but there is a

significant effect of horn litter size also **(p= 0.024).**

Similar patterns to that shown in Figure 6.4 were also observed in the fetus and a number of the other tissues examined, i.e. placenta and fetal kidneys, although not significant (Figures 6.5 and 6.6). This indicates there may be a proportionate increase in growth of these components; the conceptus:placenta and fetal:placental weight ratios were unchanged between diet groups.
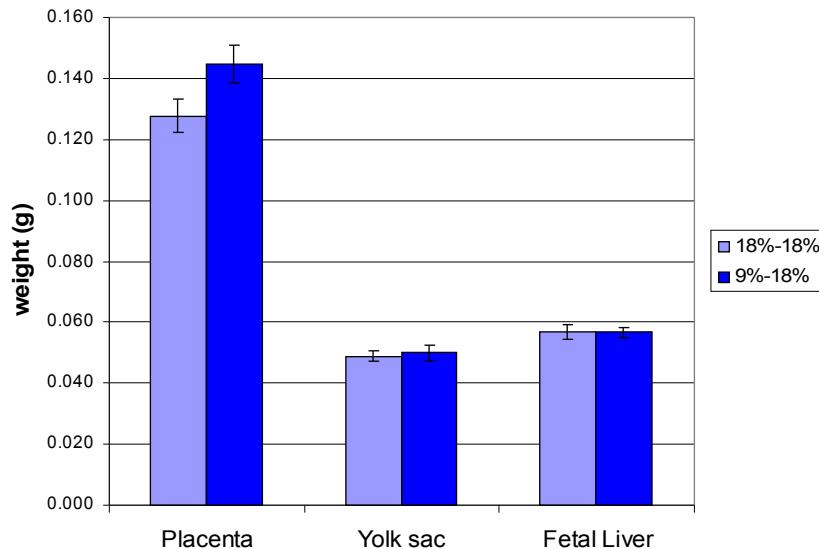
Figure 6.5: **Average placenta, yolk sac and fetal liver weights after embryo transfer into 18% casein diet fed foster mothers.**

No significant differences were found between embryo donor diets in terms of the average placenta, yolk sac and fetal liver and fetal kidney weights of conceptuses recovered from 18% casein diet fed foster mothers at day 17, (Figures 6.5, 6.6).
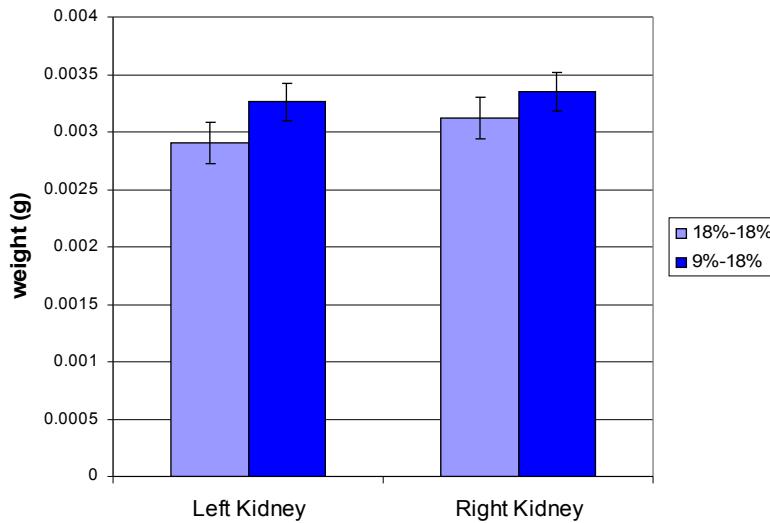
Figure 6.6: **Average fetal kidney weights after embryo transfer into 18% casein diet fed foster mothers.**

6.3.3 Modifications to embryo transfer method

In an attempt to find ways to improve upon the pregnancy rate and average number of embryos recovered per horn, a number of modifications were implemented in a series of initial trials. The first modification involved incorporating a day delay into the synchronicity of the developmental stage of the embryos being transferred (3.5 days) and the stage of pseudo pregnancy of the foster mother's uterus. Here, day 3.5 blastocysts were flushed from embryo donors as before but instead were transferred into foster mothers that were at 2.5 days of pseudo pregnancy. In doing this it was intended to give embryos more chance to recover from the short term culture before the pseudo pregnant uterus was receptive to implantation at ~4.5 days post plug. Other modifications to the method included increasing the number of embryos transferred into each uterine horn to

ten so that even if only ~50% implanted and developed this would represent a more natural horn litter size.

A new cohort of twelve foster mothers was transferred into using this method, and the pregnancy rate increased (a pregnancy was counted as the presence of at least one fetus in the uterus). However the average number of fetuses recovered per horn (of either diet) was just $^{2.6}/_{10}$ which represents a lower proportion of the total number transferred per horn than in the main experiment (data not shown). This may indicate that the day delay helps with getting at least one embryo to implant and develop after transfer but there may still be problems with the method which restrict the number of embryos that are able to develop successfully post transfer.

6.4 Discussion

Comparison of conceptuses that have been transferred as embryos from 9% casein to 18% casein diet fed mothers at day 3.5 with those transferred from 18% casein to 18% casein diet fed mothers, seeks to answer the question as to whether a restricted protein uterine environment for the first 3.5 days of development can programme embryos such that their development does not benefit from a normal maternal protein environment after this time. If such conceptuses were comparable it may suggest that embryo fate is somewhat dependent on the maternal environment post 3.5 days and is not permanently programmed by the pre-implantation environment. If, however the conceptuses showed differences it might indicate that 9% casein embryos have been programmed by the low

protein uterine environment during the pre-implantation window and their development thereafter is largely independent of continued maternal environmental cues, as the developmental path has been determined. Indeed it appears that the latter is the case in terms of the growth of the conceptus as a whole entity.

Figure 6.4 showed that conceptuses that developed from 9% casein embryos were significantly heavier than those that developed from 18% casein embryos when each were transferred into 18% casein diet fed foster mothers at day 3.5, which may be an indication that over-compensatory modifications to growth occurred within the early embryo at the blastocyst stage. This argument is supportive of an adaptation in embryonic development having taken place prior to day 3.5, which is then manifested itself as an increased weight phenotype at day 17 in the embryos from the 9% casein donors. The significant difference in conceptus weight shown in Figure 6.4 in the absence of significant changes in the weights of component tissues: fetus, placenta, yolk sac, may suggest a cumulative effect of smaller changes to each component, notably the placenta, amounting to a significant change in conceptus weight. Alternatively, a change in the volume of amniotic fluid surrounding the fetus may contribute to the difference in conceptus weight observed.

As the significant effect of dietary treatment on conceptus weight was accompanied by a significant effect of horn litter size on conceptus weight, it is difficult to make conclusions about the relative impact of each factor on the resulting change in conceptus weight. Furthermore, it is important to highlight that only 20% of the foster mothers

contributed data at day 17 for both the 9% casein and 18% casein diet embryos. The remainder of the data came from fosters mothers where only the 9% casein or the 18% casein embryos could be retrieved at day 17. Thus, in the majority of cases there was no internal control. However, this effect was evident equally in both diet treatments and therefore does not account for the change in weight gain observed.

These data indicate that the initial low protein environment was sensed by the 9% casein embryos prior to their transfer and suggest these embryos increased their nutrient uptake or altered their metabolism to maximize use of all available nutrients in a restricted environment to protect future growth and development; once transferred to an environment of normal protein levels, such adaptations would have been inappropriate and thus may have caused embryos to overshoot the control (18% casein diet) conceptus weight at day 17. This argument is supportive of the PARS hypothesis (Gluckman and Hanson, 2004 a, c) described previously in which the embryo 'makes predictions' about the environment in which it will develop and adapts its development accordingly. The 9% casein embryos may have been programmed by their protein restricted environment <3.5 days of development and thus made adaptations to enable themselves to best prepare for coping with a protein-restricted environment in the future, which were rendered inappropriate after the embryo transfer procedure into a non-restricted uterine environment.

The 9%-18% transfer group is somewhat similar to the switching diet group (Chapter 2, section 2.1) in that the uterine environment experienced by the embryo changes from day

3.5 of gestation onwards. However, in the present study the transition is more immediate and is independent of maternal physiology. Birth-weight data in the mouse using a maternal low protein model has shown that weights of pups at term can be significantly elevated if the maternal diet was switched at day 3.5 from 9% casein to 18% casein. Although not an embryo-transfer model, this finding may lend support to the apparent changes in growth *in utero* found here, due to similarities in principle between the switch diet treatment and the 9%-18% transfer group in terms of the types of uterine environment experienced by the embryo during its *in utero* development. Furthermore, parameters of post-natal health were also affected by the maternal protein diet during the pre-implantation period in this study (Watkins et al, 2008).

Extra embryonic lineages segregated at the blastocyst stage are likely to be contributors of pre implantation responses to maternal diet as they control the maternal-fetal nutrient transport capacity (Watkins et al., 2008). The yolk sac (derived from blastocyst ICM) functions in part, in nutrition through endocytic uptake and lysosomal digestion of maternal proteins and delivery of release amino acids for fetal growth (Beckman et al., 1998). Indeed, yolk sacs from late gestation murine conceptuses exposed to a low protein environment *in vivo* have been studied and suggest that yolk sac function changes to promote an elevated rate of endocytosis in response to the low protein surroundings (Watkins et al., 2008). Thus, the altered yolk sac function may represent a physiological adaptation to dietary conditions *in utero,* and provide a mechanism for the up regulated growth at term described in mice exposed to a maternal switch diet if the altered rate for endocytic uptake is programmed in the blastocyst by the environmental conditions

experienced during the early pre implantation stage of embryo development. Further, if this is the case it might offer some explanation for the elevated conceptus weight found in my study after embryo transfer.

Further work

Biochemical investigation of the tissues from the conceptuses produced by the embryo transfer procedure may reveal some explanations for the difference found in overall conceptus weight at gestational day 17.

Further investigation of this area might involve analysis of the conceptuses at a later stage of gestation, such as day 18. It is possible that day 17 does not capture the time frame when the differences between the embryos from each type of donor are the most apparent. As there was a consistent pattern of tissue weights for the different embryo-donor diets across most of the tissues analyzed it is possible that a slightly later stage of development those differences would have become more marked and reflected the significant difference in conceptus weight described at gestational day 17.

Chapter 7

General Summary

In this project I have examined the impact of maternal low protein diet on the subsequent development of the fetus. I have collected data on gene and protein expression in day 17 fetal liver and have also examined the growth phenotype of the fetus as a whole at day 17 in response to a maternal dietary challenge. A brief summary of my findings from the work in each of the aforementioned areas follows:

Genomics analysis data

The downstream analyses from all three of the programmes used to analyse the micro-array data set (discussed in sections 4.4.2.1 to 4.4.2.3) indicated that the level of biological variation in the data set made drawing comparisons between treatment groups more challenging.

In summary, initial analyses of the micro-array data using dChip highlighted some interesting candidates at the level of transcription that appeared to offer, in part explanations for mechanisms of programming of post natal phenotypes in response to maternal diet for the switch versus 9% class comparison. However, further analysis of the class comparisons suggested that a factor unrelated to diet might be driving the differences in gene expression, particularly between the switch and 9% classes. Thus, it appeared that it was the mother's capacity to support her litter (determined by total litter

size) more than her level of protein intake, which was sensed by individual fetuses in the uterus, and indeed this seems to manifest in alterations in fetal hepatic gene expression.

Protein analysis data

The results obtained from the experiments to determine the level of protein expression of GR and 11β HSD type 1 in the fetal liver in relation to maternal diet suggest that the switch diet is sufficient to invoke changes in the expression of both these proteins in the fetal liver, but that the low protein diet maintained throughout pregnancy does not induce any significant changes relative to controls. The increased expression of GR in switch fetal liver suggests that there may be a heightened level of glucocorticoid action in these livers, due to the increased receptor availability. Decreased 11β HSD type 1 expression in the same tissues suggests there may be a lower abundance of the active form of the glucocorticoid hormone in these switch fetal livers compared with the control group. The decreased expression of 11β HSD type 1 may thus be a compensatory response to increased GR expression.

Embryo transfer data

These data indicate that the initial low protein environment was sensed by the 9% casein embryos prior to their transfer and suggest these embryos adapted their nutrient uptake or altered their metabolism to maximize use of all available nutrients in the restricted environment to protect future growth and development; once transferred to an

environment of sufficient protein levels, such adaptations would have become inappropriate and thus may have caused embryos to overshoot the control (18% casein diet) conceptus weight at day 17. This argument is supportive of the PARS hypothesis (Gluckman and Hanson, 2004 a, c) described previously in which the embryo 'makes predictions' early on about the environment in which it will develop and adapts its development accordingly.

Overall, the data I have collected show that switching the maternal diet from low to adequate protein at the end of the pre implantation period of embryo development has the most striking impact on fetal development observed at day 17; evidenced by elevated conceptus weight after natural mating (in house diet) and significantly altered hepatic expression of two glucocorticoid related proteins. Furthermore, data collected from the embryo transfers performed at gestational day 3.5 support this idea; it appears that exposure to a low protein environment for the pre implantation period exclusively, programs the embryo to follow a different developmental pathway which is not reversed by subsequent exposure to an *in utero* environment of adequate nutrition after 3.5 days.

Appendices

Appendix I

DNA Sequencing of PCR Products (Sanger 'dideoxy' method)

The Sanger chain termination method of DNA sequencing involves synthesis of a new DNA strand using a single stranded DNA template from the gene being sequenced. Synthesis of the new strand can be stopped at any of the four bases by adding the corresponding dideoxy (dd) derivative of the deoxyribonucleoside phosphates, e.g. by adding ddATP the synthesis terminates at an adenosine base. The fragments are separated by electrophoresis according to their chain length and the dideoxy terminators are detected by fluorescence spectroscopy. A computer generated printout of the corresponding base sequence from the bottom of the gel towards the top is produced.

Calculation of 100 fmols for 244 bp *DXNds3* product:

330 (D) x (244 x 2) = 161040 Daltons

1×10^{-13} moles $(100 \times 1 \times 10^{-15})$ x 161040 D = Equivalent weight (g) i.e. 1.6×10^{-8} g (16 ng)

16 ng of *DXNds3* PCR product = 100 fmols

Sequencing with ABI377 automated sequencer

Due to a number of technical difficulties with the Beckman Coulter system, the ABI377 system was used as an alternative method for sequencing of the *Zfy* gene product. The protocol for preparing sequencing reactions for the ABI system is similar to the Beckman Coulter system. However the cycling sequencing chemistry used for the ABI377 automated sequencer is *BigDye Terminators*.

Detailed Affymetrix Methods

Target Labelling

Preparation of Poly-A RNA Controls for One-Cycle cDNA Synthesis

Poly-A RNA Spike	Final Dilution (estimated ratio of copy number)
lys	1:100,000
phe	1:50,000
thr	1:25,000
dap	1:6,667

Table AI.1: Final dilutions of Poly-A RNA controls in samples (GeneChip Expression Analysis Technical Manual, Affymetrix).

(Each probe array contains probe sets for the bacterial genes: *lys, phe, thr, dap*).

First strand cDNA synthesis

For each sample, the total RNA, diluted poly-A RNA controls, and T7-Oligo(dT) Primer were mixed together in 0.2 ml thin walled PCR tubes.

Component	Volume
Sample RNA	variable
Diluted poly-A RNA controls	2 µL
T7-Oligo(dT) Primer, 50 µM	2 µL
RNase-free Water	variable
Total Volume	12 µL

Table AI.2: RNA/T7-Oligo(dT) primer mix preparation for 1-8 µg RNA

(GeneChip Expression Analysis Technical Manual, Affymetrix).

Tubes were flick mixed, pulse centrifuged and incubated at 70°C for 10 minutes, and then cooled for 2 minutes (minimum) at 4°C. A first strand master-mix was assembled on ice in a separate RNase-free tube, sufficient for all RNA samples.

Component	Volume
5X 1st Strand Reaction Mix	4 µL
DTT, 0.1M	2 µL
dNTP, 10 mM	1 µL
Total Volume	7 µL

Table AI.3: Components of first-strand master-mix per reaction (GeneChip

Expression Analysis Technical Manual, Affymetrix).

To each RNA/Primer mix, 7µl of the first-strand master-mix was added to make a final volume of 19 µl. Reactions were mixed and incubated at 42°C for 2 minutes. 1 µl of Superscript II reverse transcriptase was then added to each reaction and reactions were

incubated for 1 hour at 42°C, and were then cooled for 2 minutes (minimum) at 4°C.

Second strand synthesis followed immediately.

70°C	10 minutes
4°C	hold
42°C	2 minutes
42°C	1 hour
4°C	hold

Table AI.4: Summary of incubations for first strand cDNA synthesis reaction (one cycle only). Heated lids were used to prevent evaporation. All incubations were performed in a Tetrad thermal cycler.

Second strand cDNA synthesis

Sufficient second strand master-mix was prepared on ice for all samples in a separate tube.

Component	Volume
RNase-free Water	91 µL
5X 2nd Strand Reaction Mix	30 µL
dNTP, 10 mM	3 µL
E. coli DNA ligase	1 µL
E. coli DNA Polymerase I	4 µL
RNase H	1 µL
Total Volume	130 µL

Table AI.5: Components of second strand master-mix per reaction (GeneChip Expression Analysis Technical Manual, Affymetrix).

To each first-strand synthesis reaction 130 µl of second strand master-mix was added to make a total volume of 150 µl. These reactions were incubated for 2 hours at 16ºC. Finally, 2 µl of T4 DNA Polymerase was added to each sample and samples were incubated for 5 minutes at 16ºC. After this incubation, 10 µl of 0.5M EDTA was added to each reaction. Cleanup followed immediately.

16°C	2 hours
4°C	hold
16°C	5 minutes
4°C	hold

Table AI.6: Summary of incubations for one cycle second strand cDNA synthesis (using Tetrad thermal cycler).

In Vitro Transcription (IVT) Reaction

11 µl of each of the double-stranded cDNA samples synthesised was added to each IVT reaction. Reactions were assembled in 0.2 ml thin-walled PCR tubes at room temperature. Sufficient IVT master-mix was prepared for all samples. Reactions were incubated for 16 hours at 37ºC using a Tetrad thermal cycler.

Component	Volume
Template cDNA*	~~variable (see Table 2.17~~) ← **11µl**
RNase-free Water	variable (to give a final reaction volume of 40 µL)
10X IVT Labeling Buffer	4 µL
IVT Labeling NTP Mix	12 µL
IVT Labeling Enzyme Mix	4 µL
Total Volume	40 µL

Table AI.7: Components of IVT master-mix per reaction (GeneChip Expression Analysis Technical Manual, Affymetrix).

Calculating an adjusted cRNA yield

Assuming an estimate of 100% carryover, the formula below was used to determine adjusted cRNA yields:

adjusted cRNA yield = RNAm – (total RNAi) (y)

RNAm = amount of cRNA measured after IVT (µg)

Total RNAi = starting amount of total RNA (µg)

y = fraction of cDNA reaction used in IVT

Formula for calculating adjusted cRNA yields (GeneChip Expression Analysis Technical Manual, Affymetrix).

For each cRNA sample the adjusted yield was calculated as above. Adjusted cRNA concentrations were subsequently used for the cRNA fragmentation step. Expected average yields of cleaned up cRNA are between 30-50 μg + (personal communication Geoff Scopes, Affymetrix).

cRNA Fragmentation Reaction

Component	49/64 Format
cRNA	20 μg (1 to 21 μL)
5X Fragmentation Buffer	8 μL
RNase-free Water (variable)	to 40 μL final volume
Total Volume	40 μL

Array format used (← pointing to 49/64 Format header)

Table AI.8: Sample fragmentation reaction (GeneChip Expression Analysis Technical Manual, Affymetrix).

Fragmentation reactions were prepared on ice in 0.2 ml thin-walled PCR tubes and incubated for 35 minutes at 94°C with a Tetrad thermal cycler. Following the incubation, reactions were placed on ice and fragmented cRNA was subsequently stored at -80°C.

Fragmentation of the cRNA was monitored with the Agilent 2100 Bioanalyser using the RNA 6000 Nano Assay Kit (Agilent Technologies) to determine whether the sample was of the length required for optimal micro-array performance.
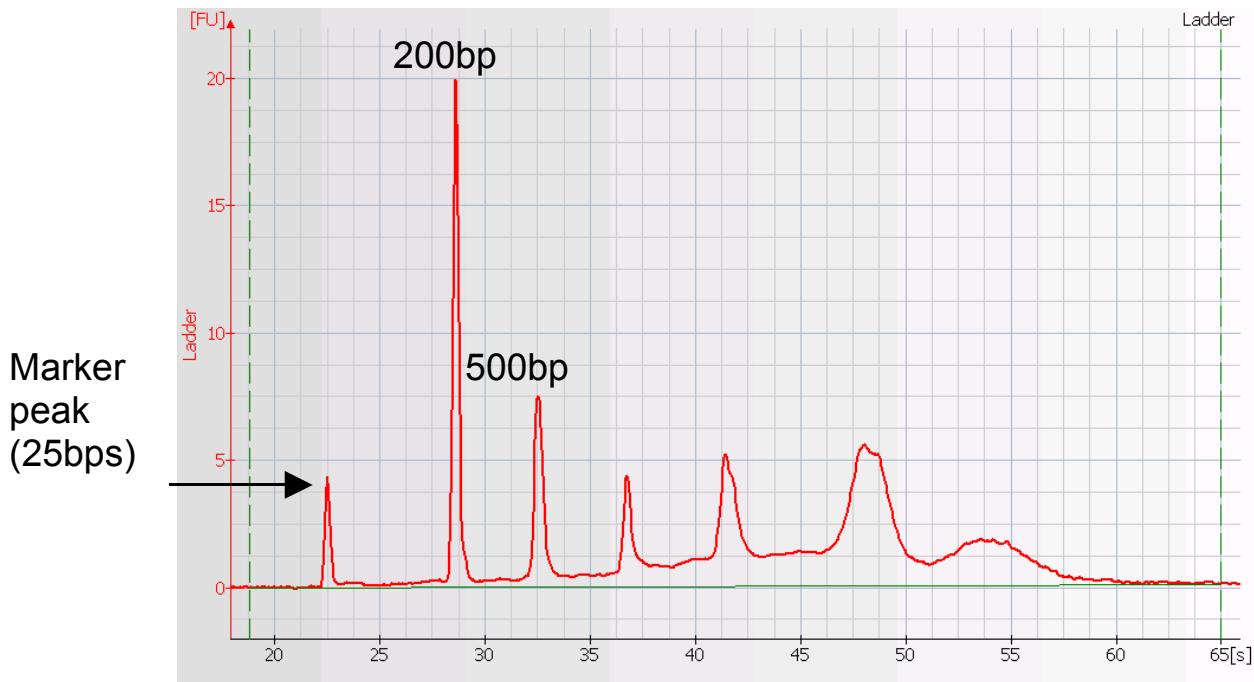
Figure AI.1: RNA Ladder (Agilent Bioanalyser). The marker peak and first 5 ladder peaks define a correlation between migration time and sizing; the marker peak is set at a migration time of 22.5 seconds.

Target (cRNA) Hybridisation

Component	49 Format (Standard) / 64 Format Array	Final Dilution
Fragmented and Labeled cRNA†	15 µg	0.05 µg/µL
Control Oligonucleotide B2 (3 nM)	5 µL	50 pM
20X Eukaryotic Hybridization Controls (*bioB, bioC, bioD, cre*)	15 µL	1.5, 5, 25, and 100 pM respectively
2X Hybridization Mix	150 µL	1X
DMSO	30 µL	10%
Nuclease-free Water	to final volume of 300 µL	
Total Volume	300 µL	

Table AI.9: Hybridization cocktail for a single probe array; 30 µl of the 0.5 µg/µl fragmented labelled cRNA stock per sample was used. Hybridization controls are ready made biotinylated and fragmented cRNA of *bioB, bioC*, and *bioD* from *E. coli, and cre* from P1 from bacteriophage premixed at staggered concentrations. Probes detecting these controls are present on the probe arrays. Control Oligo B2 was used to provide control and alignment signals for subsequent image analysis (GeneChip Expression Analysis Technical Manual, Affymetrix).
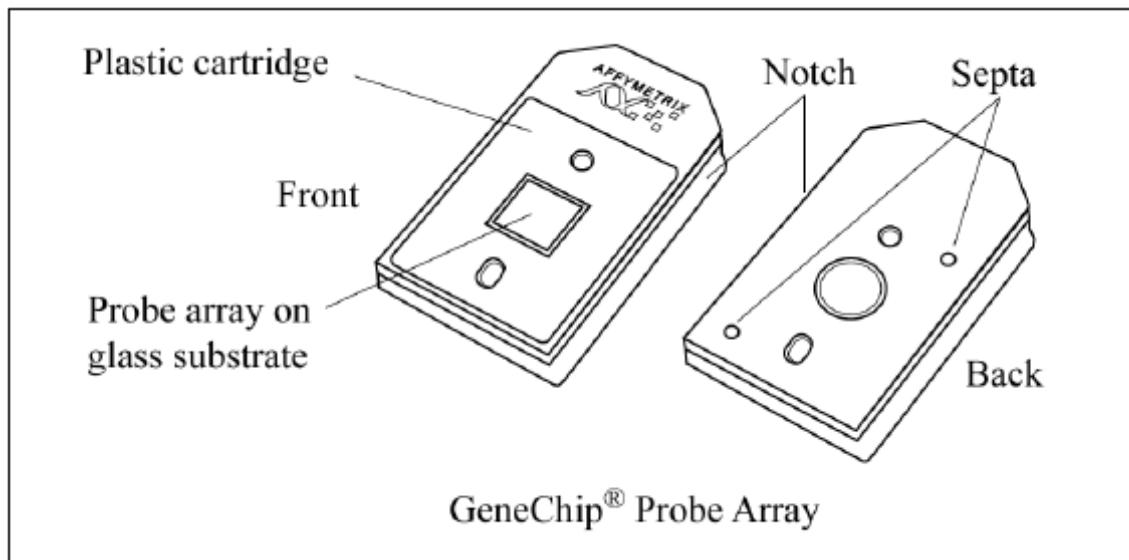
Figure AI.2: Cartridge structure of the probe arrays (GeneChip Expression Analysis Technical Manual, Affymetrix). The array chamber must be first vented through one of the septa before filling or draining. The glass substrate consists of an array of oligonucleotides on its inner surface.

Washing and Staining of Hybridised Probe Arrays

The Fluidics Station Bleach Protocol was run prior to use of the Fluidics Station. This involved running 500 ml 0.525% sodium hypochlorite solution through the station, followed by a rinse cycle with deionised water. For bleach protocol, refer to GeneChip Expression Analysis Technical Manual, Affymetrix.

	FS450_0001 FS450_0002
Post Hyb Wash #1	10 cycles of 2 mixes/cycle with Wash Buffer A at 30°C
Post Hyb Wash #2	6 cycles of 15 mixes/cycle with Wash Buffer B at 50°C
1st Stain	Stain the probe array for 5 minutes with Stain Cocktail 1 at 35°C
Post Stain Wash	10 cycles of 4 mixes/cycle with Wash Buffer A at 30°C
2nd Stain	Stain the probe array for 5 minutes with Stain Cocktail 2 at 35°C
3rd Stain	Stain the probe array for 5 minutes with Stain Cocktail 3 at 35°C
Final Wash	15 cycles of 4 mixes/cycle with Wash Buffer A at 35°C.
Array Holding Buffer	Fill the probe array with Array Holding Buffer

Stain Cocktail 1

Table AI.10: **Antibody amplification fluidics protocol (GeneChip Expression Analysis Technical Manual, Affymetrix).**
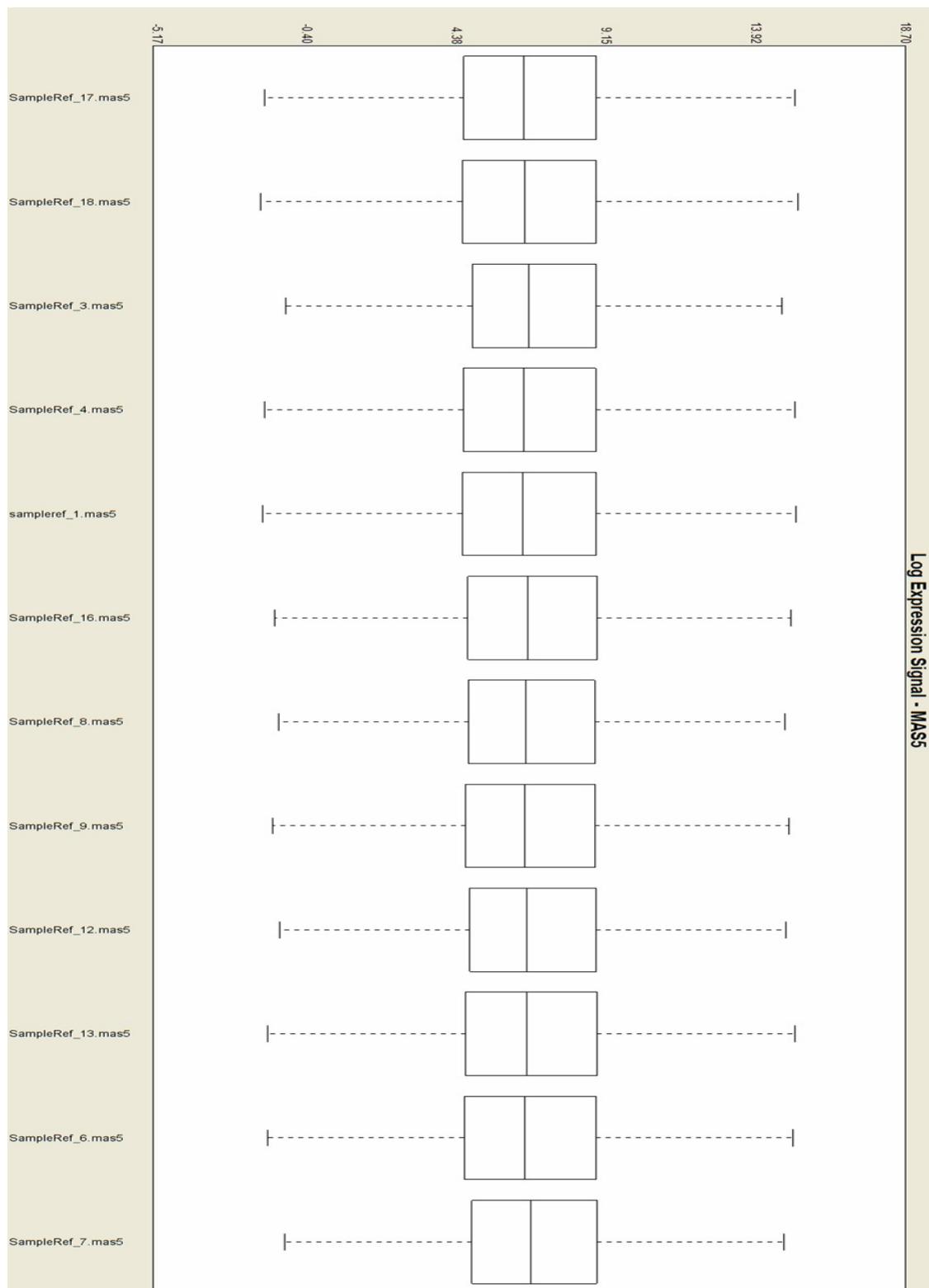
Figure AI.3: MAS 5.0 normalized log expression signal data was similar for all twelve arrays across all treatments.
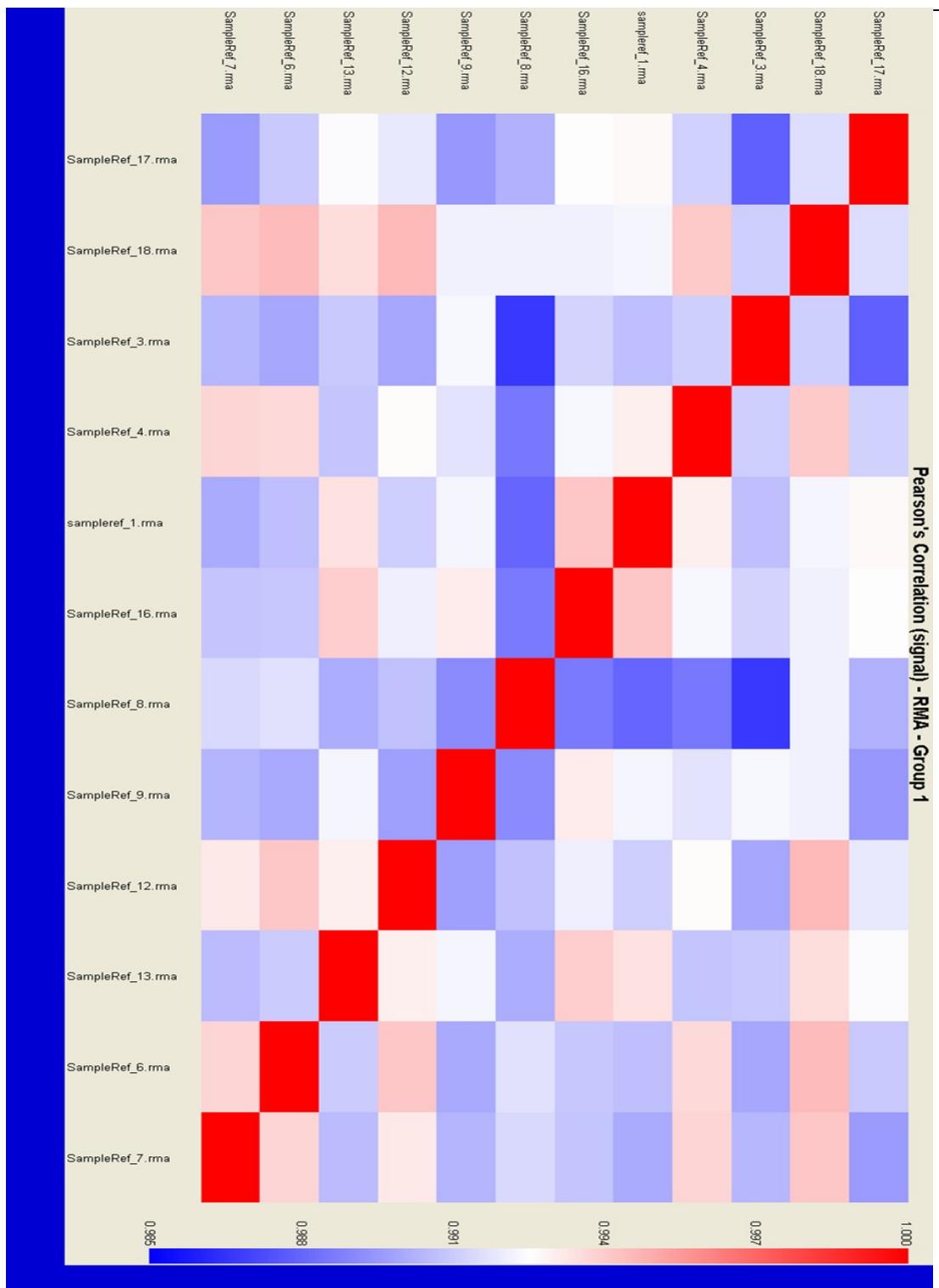
Pearson's Correlation (signal) - RMA - Group 1

Figure AI.4: Pearson correlation plot showing the correlations in signals amongst all samples after analysing the .CEL files with the RMA algorithm. All correlation are ~0.985 and above.

Mean of samples 17,18,3,4 (18% casein diet treatment)	0.991335
Mean of samples 1,16,8,9 (9% casein diet treatment)	0.9910763
Mean of samples 12, 13, 6, 7 (switch diet treatment)	0.9927703
Mean of 18% casein samples Vs 9% casein samples	0.9914352
Mean of 18% casein samples Vs switch samples	0.99228
Mean of 9% casein samples Vs switch samples	0.9913881

Table AI.11: Mean correlation coefficients for array samples within and between treatment groups (RMA normalised data).

Affx probe set	Gene information	Fold change	p-value
1415773_at	Ncl: nucleolin	-2.57	0.001249
1415784_at	Vps35: vacuolar protein sorting 35	-2.26	0.002003
1416157_at	Vcl: vinculin	-2.21	0.016113
1416180_a_at	Rdx: radixin	3.56	0.004056
1416388_at	Pip4k2c: phosphatidylinositol-5-phosphate 4-kinase, type II, gamma	-1.89	0.001527
1416656_at	Clic1: chloride intracellular channel 1	-2.17	0.000526
1416660_at	Eif3s10: eukaryotic translation initiation factor 3, subunit 10 (theta)	-2.1	0.010294
1416686_at	Plod2: procollagen lysine, 2-oxoglutarate 5-dioxygenase 2	-2.5	0.030153
1416691_at	Gtpbp2: GTP binding protein 2	-1.98	0.003956
1416794_at	Arl6ip2: ADP-ribosylation factor-like 6 interacting protein 2	-1.91	0.001552
1416837_at	Bax: Bcl2-associated X protein	-2.04	0.002074
1416913_at	Es1: esterase 1	2.23	0.003057
1417238_at	Ewsr1: Ewing sarcoma breakpoint region 1	-1.84	0.002141
1417576_a_at	Otub2: OTU domain, ubiquitin aldehyde binding 2	-2.33	0.007124
1417900_a_at	Vldlr: very low density lipoprotein receptor	-2.68	0.000589
1418020_s_at	Cpd /// LOC100046781: carboxypeptidase D /// similar to carboxypeptidase D	-1.87	0.005103
1418231_at	Lims1: LIM and senescent cell antigen-like domains 1	-2.04	0.013542
1418685_at	Tirap: toll-interleukin 1 receptor (TIR) domain-containing adaptor protein	3.02	0.00666
1418787_at	Mbl2: mannose binding lectin (C)	2.92	0.025395
1418946_at	St3gal1: ST3 beta-galactoside alpha-2,3-sialyltransferase 1	-2.21	0.031563
1419029_at	Ero1l: ERO1-like (S. cerevisiae)	-1.94	0.02372
1419030_at	Ero1l: ERO1-like (S. cerevisiae)	-2.45	0.002844
1419098_at	Stom: stomatin	-2.86	0.000481
1419099_x_at	Stom: stomatin	-2.4	0.000538
1419256_at	Spnb2: spectrin beta 2	2.75	0.031929
1420420_at	Hao1: hydroxyacid oxidase 1, liver	1.88	0.019711
1420620_a_at	Rnf13: ring finger protein 13	-1.84	0.000767
1420904_at	Il17ra: interleukin 17 receptor A	-2.26	0.005163
1420973_at	Arid5b /// LOC100044968: AT rich interactive domain 5B (Mrf1 like) ///	2.45	0.00453
1421011_at	Hsd17b11: hydroxysteroid (17-beta) dehydrogenase 11	-1.95	0.002402
1421077_at	Sertad3: SERTA domain containing 3	-2.08	0.003372
1421534_at	Dfna5h: deafness, autosomal dominant 5 homolog (human)	-1.99	0.013375

1421600_a_at	Trim26: tripartite motif protein 26	-2.91	0.008922
1421839_at	Abca1: ATP-binding cassette, sub-family A (ABC1), member 1	-1.96	0.002918
1421866_at	Nr3c1: nuclear receptor subfamily 3, group C, member 1	-3.12	0.010773
1421890_at	St3gal2: ST3 beta-galactoside alpha-2,3-sialyltransferase 2	-2.48	0.014365
1422102_a_at	Stat5b: signal transducer and activator of transcription 5B	-1.94	0.00265
1422512_a_at	Ogfr: opioid growth factor receptor	-2.01	0.002948
1422966_a_at	Tfrc: transferrin receptor	-2.17	0.028869
1422967_a_at	Tfrc: transferrin receptor	-4.25	0.031933
1423556_at	Akr1b7: aldo-keto reductase family 1, member B7	3.12	0.00072
1423601_s_at	Tcof1: Treacher Collins Franceschetti syndrome 1, homolog	2.1	0.020039
1423652_at	Isca1: iron-sulfur cluster assembly 1 homolog (S. cerevisiae)	-1.79	0.000272
1424684_at	Rab5c: RAB5C, member RAS oncogene family	1.91	0.00641
1425457_a_at	Grb10: growth factor receptor bound protein 10	-3.48	0.004811
1425515_at	Pik3r1: phosphatidylinositol 3-kinase, regulatory subunit, polypeptide 1 (p85 alpha)	-2.45	0.032447
1425576_at	Ahcyl1: S-adenosylhomocysteine hydrolase-like 1	-1.89	0.001966
1425617_at	Dhx9: DEAH (Asp-Glu-Ala-His) box polypeptide 9	-2.84	0.002422
1425644_at	Lepr: leptin receptor	-3.33	0.00165
1425713_a_at	Rnf146: ring finger protein 146	-2.12	0.007326
1425732_a_at	Mxi1: Max interacting protein 1	-2.3	0.00104
1425803_a_at	Mbd2: methyl-CpG binding domain protein 2	-1.9	0.000775
1426519_at	P4ha1: procollagen-proline, 2-oxoglutarate 4-dioxygenase (proline 4-hydroxylase), alpha 1 polypeptide	-3.18	0.001533
1426576_at	Sgms1: sphingomyelin synthase 1	-1.86	0.002219
1426805_at	Smarca4: SWI/SNF related, matrix associated, actin dependent regulator of chromatin, subfamily a, member 4	2.5	0.006415
1427070_at	Snx21: sorting nexin family member 21	-2.55	0.033775
1427359_at	Jhdm1d: jumonji C domain-containing histone demethylase 1 homolog D (S. cerevisiae)	-2.23	0.004561
1427471_at	Fbxl3 /// LOC100044862: F-box and leucine-rich repeat protein 3 /// similar to Fbxl3 protein	-2.56	0.001351
1429492_x_at	Ptdss2: phosphatidylserine synthase 2	-2.81	0.025099
1430692_a_at	Sel1l: sel-1 suppressor of lin-12-like (C. elegans)	-1.99	0.001872
1431030_a_at	Rnf14: ring finger protein 14	-2.34	0.01264
1431170_at	Efna3 /// LOC100046031: ephrin A3 /// similar to Ephrin A3	-4.17	0.03907
1431645_a_at	Gdi2: guanosine diphosphate (GDP) dissociation inhibitor 2	-1.91	0.001702

1432344_a_at	Aplp2: amyloid beta (A4) precursor-like protein 2	-2.31	0.00582
1433491_at	Epb4.1l2: erythrocyte protein band 4.1-like 2	-1.92	0.001775
1434020_at	Pdap1: PDGFA associated protein 1	2.31	0.011171
1434357_a_at	Kpnb1: karyopherin (importin) beta 1	-2.23	0.007152
1434370_s_at	Faf1: Fas-associated factor 1	-1.84	0.003088
1434419_s_at	Tardbp: TAR DNA binding protein	-1.77	0.000683
1434465_x_at	Vldlr: very low density lipoprotein receptor	-1.91	0.000398
1437133_x_at	Akr1b3: aldo-keto reductase family 1, member B3 (aldose reductase)	2.17	0.004414
1438743_at	Cyp7a1: cytochrome P450, family 7, subfamily a, polypeptide 1	2.61	0.028814
1439120_at	BC010304: cDNA sequence BC010304	-1.93	0.001818
1448009_at	LOC100044322: similar to UDP-glucose ceramide glucosyltransferase-like 1	1.89	0.000855
1448127_at	Rrm1: ribonucleotide reductase M1	-1.81	0.000918
1448239_at	Hmox1: heme oxygenase (decycling) 1	-6.01	0.000075
1449051_at	Ppara: peroxisome proliferator activated receptor alpha	-2.03	0.004285
1449262_s_at	Lin7c: lin-7 homolog C (C. elegans)	-2.49	0.002731
1449341_a_at	Stom: stomatin	-1.92	0.00229
1449931_at	Cpeb4: cytoplasmic polyadenylation element binding protein 4	-2.51	0.022915
1450006_at	EG627557 /// Ncoa4: nuclear receptor coactivator 4 /// predicted gene, EG627557	-1.86	0.003071
1450007_at	1500003O03Rik /// LOC100048622: RIKEN cDNA 1500003O03 gene ///	-2.15	0.005709
1450104_at	Adam10: a disintegrin and metallopeptidase domain 10	-1.96	0.001934
1450113_at	Mpp5: membrane protein, palmitoylated 5 (MAGUK p55 subfamily member 5)	-1.98	0.002464
1450368_a_at	Ppp3r1: protein phosphatase 3, regulatory subunit B, alpha isoform (calcineurin B, type I)	-2.24	0.023175
1450392_at	Abca1: ATP-binding cassette, sub-family A (ABC1), member 1	-2.93	0.001511
1450703_at	Slc7a2: solute carrier family 7 (cationic amino acid transporter, y+ system), member 2	-2.75	0.014162
1451456_at	6430706D22Rik: RIKEN cDNA 6430706D22 gene	2.09	0.004218
1451658_a_at	Polr3c: polymerase (RNA) III (DNA directed) polypeptide C	-2.47	0.003352
1452315_at	Kif11: kinesin family member 11	-2.13	0.001605
1452427_s_at	Ptplad1: protein tyrosine phosphatase-like A domain containing 1	-2.24	0.000256
1452527_a_at	P2rx4: purinergic receptor P2X, ligand-gated ion channel 4	-2.15	0.008256
1453604_a_at	Hbs1l: Hbs1-like (S. cerevisiae)	-2.15	0.001737
1454120_a_at	Pcgf6: polycomb group ring finger 6	-2.28	0.048782
1454174_a_at	C330007P06Rik: RIKEN cDNA C330007P06 gene	-2.14	0.003745
1456080_a_at	Serinc3: serine incorporator 3	-1.81	0.007701

1456494_a_at	AI451617 /// Trim30: tripartite motif protein 30 /// expressed sequence AI451617	2.97	0.011689
1460521_a_at	Obfc2a: oligonucleotide/oligosaccharide-binding fold containing 2A	-2.5	0.008642
1429413_at	Cpm: carboxypeptidase M	-2.89	0.001247
1429545_at	EG546265 /// F830028O17Rik /// LOC100044900 /// Ube2i: ubiquitin-conjugating enzyme E2I ///	2.75	0.00401
1429809_at	Tmtc2: transmembrane and tetratricopeptide repeat containing 2	-1.92	0.002831
1430566_at	4733401A01Rik: RIKEN cDNA 4733401A01 gene	2.56	0.001863
1430697_at	Ammecr1: Alport syndrome, mental retardation, midface hypoplasia and elliptocytosis	2.72	0.004264
1430981_s_at	Gpbp1: GC-rich promoter binding protein 1	-2.19	0.012382
1430984_at	Azin1: antizyme inhibitor 1	-3.02	0.006748
1431061_s_at	Peli1: pellino 1	-2.32	0.00346
1431197_at	Arl6ip2: ADP-ribosylation factor-like 6 interacting protein 2	-2.26	0.000657
1431430_s_at	LOC630539 /// Trim59: tripartite motif-containing 59 /// similar to mouse RING finger 1	-2.42	0.000373
1432304_a_at	9030624J02Rik: RIKEN cDNA 9030624J02 gene	-2.46	0.005099
1433633_at	Irf2bp2: interferon regulatory factor 2 binding protein 2	-2.3	0.01103
1436070_at	Glo1: glyoxalase 1	2.18	0.005461
1437638_at	Srrm2: serine/arginine repetitive matrix 2	2.12	0.036937
1438410_at	Prtg: protogenin homolog (Gallus gallus)	-2.33	0.006175
1438433_at	Whdc1: WAS protein homology region 2 domain containing 1	2.78	0.008947
1442109_at	Activated spleen cDNA, RIKEN full-length enriched library, clone:F830222N19 product:	2.82	0.002018
1443522_s_at	Phip: pleckstrin homology domain interacting protein	-2.25	0.003737
1444330_at	D2Ertd173e: DNA segment, Chr 2, ERATO Doi 173, expressed	3.45	0.001175
1444436_at	9630030I15Rik /// Hsf2: heat shock factor 2 /// RIKEN cDNA 9630030I15 gene	2.83	0.001263
1446284_at	Mtss1: metastasis suppressor 1	2.17	0.03126
1447063_at	Sept14: septin 14	3.15	0.011794
1452906_at	Meg3: maternally expressed 3	2.18	0.002968
1453009_at	Cpm: carboxypeptidase M	-2.54	0.002255
1453041_at	Tmem16j: transmembrane protein 16J	-2.39	0.001034
1453140_at	9030612M13Rik: RIKEN cDNA 9030612M13 gene	2.15	0.000222
1453189_at	Ube2i: ubiquitin-conjugating enzyme E2I	2.31	0.008989
1453290_at	Hmgb2l1: high mobility group box 2-like 1	3.11	0.006481
1453760_at	Mier1: mesoderm induction early response 1 homolog (Xenopus laevis	-2.66	0.016102
1454003_at	Afg3l2: AFG3(ATPase family gene 3)-like 2 (yeast)	-3.77	0.000099
1455876_at	Slc4a7: solute carrier family 4, sodium bicarbonate cotransporter, member 7	2.58	0.006464

1455933_at	Tra2a: transformer 2 alpha homolog (Drosophila)	2.34	0.013907
1455998_at	LOC667118: similar to Zinc finger BED domain containing protein 4	2.29	0.006551
1456596_at	6430550H21Rik: RIKEN cDNA 6430550H21 gene	-3.53	0.001931
1457987_at	6030458C11Rik: RIKEN cDNA 6030458C11 gene	5.02	0.000052
1458609_at	14 days embryo liver cDNA, RIKEN full-length enriched library, clone:I530025F13 product:	-5.29	0.000046
1458685_at	Garnl1: GTPase activating RANGAP domain-like 1	3.52	0.00907
1459734_at	Mm.212401.1	1.93	0.002868

Table AI.12: Candidate probe sets with apparent differential expression for switch versus 9% casein (baseline) class comparison using high stringency criteria and excluding one sample outlier from each class. Median FDR was 4.4%

Affx probe set	Gene information	Fold change	p-value
1423556_at	Akr1b7: aldo-keto reductase family 1, member B7	2.6	0.006555
1438644_x_at	Commd9: COMM domain containing 9	2.69	0.011373
1452677_at	LOC100044383 /// Pnpt1: polyribonucleotide nucleotidyltransferase 1 ///	3.03	0.032029
1435770_at	Txndc13: thioredoxin domain containing 13	2.42	0.044705
1440443_at	E030016H06Rik: RIKEN cDNA E030016H06 gene	3.68	0.004556
1457458_at	Zc3h4: zinc finger CCCH-type containing 4	3.03	0.031387

Table AI.13: Candidate probe sets with apparent differential expression for switch versus 18% casein (baseline) class comparison using high stringency criteria and excluding one sample outlier from each class. Median FDR was 100%

Affx probe set	Gene information	Fold change	p-value
1415773_at	Ncl: nucleolin	1.96	0.002835
1415784_at	Vps35: vacuolar protein sorting 35	1.94	0.002317
1416656_at	Clic1: chloride intracellular channel 1	2.05	0.001959
1418129_at	Dhcr24: 24-dehydrocholesterol reductase	-3.45	0.013174
1419098_at	Stom: stomatin	2.16	0.005589
1419099_x_at	Stom: stomatin	2.21	0.003188
1420904_at	Il17ra: interleukin 17 receptor A	2.16	0.005609
1421077_at	Sertad3: SERTA domain containing 3	2.1	0.002635
1421600_a_at	Trim26: tripartite motif protein 26	3.43	0.015389
1421866_at	Nr3c1: nuclear receptor subfamily 3, group C, member 1	2.2	0.012703
1422797_at	Mapbpip: mitogen activated protein binding protein interacting protein	1.93	0.002532
1422967_a_at	Tfrc: transferrin receptor	2.48	0.040924
1425457_a_at	Grb10: growth factor receptor bound protein 10	2.47	0.01139
1426519_at	P4ha1: procollagen-proline, 2-oxoglutarate 4-dioxygenase (proline 4-hydroxylase), alpha 1 polypeptide	1.98	0.004679
1431213_a_at	LOC100041156 /// LOC100041932:	-12.4	0.020197
1448239_at	Hmox1: heme oxygenase (decycling) 1	4.7	0.00011
1450703_at	Slc7a2: solute carrier family 7 (cationic amino acid transporter, y+ system), member 2	2.21	0.020347
1438763_at	Dnahc2: dynein, axonemal, heavy chain 2	2.8	0.013799
1444330_at	D2Ertd173e: DNA segment, Chr 2, ERATO Doi 173, expressed	-2.36	0.030702
1444436_at	9630030I15Rik /// Hsf2: heat shock factor 2 /// RIKEN cDNA 9630030I15 gene	-2.35	0.006199
1447757_x_at	Inpp5f: inositol polyphosphate-5-phosphatase F	-2.36	0.013168
1452906_at	Meg3: maternally expressed 3	-2.25	0.038167
1453290_at	Hmgb2l1: high mobility group box 2-like 1	-2.55	0.013424
1454003_at	Afg3l2: AFG3(ATPase family gene 3)-like 2 (yeast)	2.37	0.015738
1455773_at	0 day neonate kidney cDNA, RIKEN full-length enriched library, clone:D630004N14 product	-2.9	0.00904
1458609_at	14 days embryo liver cDNA, RIKEN full-length enriched library, clone:I530025F13 product	3.49	0.006039

Table AI.14: Candidate probe sets with apparent differential expression for 9% casein versus 18% casein (baseline) class comparison using high stringency criteria and excluding one sample outlier from each class. Median FDR was 23.1%

Affx Probe set	Gene information	Fold change	p-value
1415771_at	Ncl: nucleolin	-1.59	0.000754
1415773_at	Ncl: nucleolin	-2.57	0.001249
1415784_at	Vps35: vacuolar protein sorting 35	-2.26	0.002003
1415800_at	Gja1: gap junction protein, alpha 1	-1.66	0.00127
1415810_at	Uhrf1: ubiquitin-like, containing PHD and RING finger domains, 1	1.66	0.021671
1415957_a_at	Rrp1: ribosomal RNA processing 1 homolog (S. cerevisiae)	-1.93	0.031635
1415964_at	Scd1: stearoyl-Coenzyme A desaturase 1	2.52	0.033312
1416157_at	Vcl: vinculin	-2.21	0.016113
1416162_at	Rad21: RAD21 homolog (S. pombe)	-1.62	0.003416
1416180_a_at	Rdx: radixin	3.56	0.004056
1416388_at	Pip4k2c: phosphatidylinositol-5-phosphate 4-kinase, type II, gamma	-1.89	0.001527
1416514_a_at	Fscn1: fascin homolog 1, actin bundling protein (Strongylocentrotus purpuratus)	-1.77	0.00669
1416656_at	Clic1: chloride intracellular channel 1	-2.17	0.000526
1416660_at	Eif3s10: eukaryotic translation initiation factor 3, subunit 10 (theta)	-2.1	0.010294
1416686_at	Plod2: procollagen lysine, 2-oxoglutarate 5-dioxygenase 2	-2.5	0.030153
1416691_at	Gtpbp2: GTP binding protein 2	-1.98	0.003956
1416794_at	Arl6ip2: ADP-ribosylation factor-like 6 interacting protein 2	-1.91	0.001552
1416837_at	Bax: Bcl2-associated X protein	-2.04	0.002074
1416881_at	LOC632101 /// Mcl1: myeloid cell leukemia sequence 1 ///	-1.58	0.006713
1416913_at	Es1: esterase 1	2.23	0.003057
1417023_a_at	Fabp4: fatty acid binding protein 4, adipocyte	-1.76	0.013645
1417033_at	Ube2g2: ubiquitin-conjugating enzyme E2G 2	-1.97	0.04656
1417079_s_at	Lgals2: lectin, galactose-binding, soluble 2	-2.08	0.045964
1417238_at	Ewsr1: Ewing sarcoma breakpoint region 1	-1.84	0.002141
1417388_at	Bex2: brain expressed X-linked 2	-1.82	0.025224
1417576_a_at	Otub2: OTU domain, ubiquitin aldehyde binding 2	-2.33	0.007124
1417707_at	B230342M21Rik: RIKEN cDNA B230342M21 gene	-1.94	0.035774
1417752_at	Coro1c: coronin, actin binding protein 1C	-1.9	0.035375
1417766_at	Cyb5b: cytochrome b5 type B	1.78	0.013101
1417900_a_at	Vldlr: very low density lipoprotein receptor	-2.68	0.000589
1418020_s_at	Cpd /// LOC100046781: carboxypeptidase D /// similar to carboxypeptidase D	-1.87	0.005103
1418231_at	Lims1: LIM and senescent cell antigen-like domains 1	-2.04	0.013542

1418470_at	Yes1: Yamaguchi sarcoma viral (v-yes) oncogene homolog 1	-1.98	0.016232
1418604_at	Avpr1a: arginine vasopressin receptor 1A	-2.28	0.023481
1418685_at	Tirap: toll-interleukin 1 receptor (TIR) domain-containing adaptor protein	3.02	0.00666
1418787_at	Mbl2: mannose binding lectin (C)	2.92	0.025395
1418889_a_at	Csnk1d: casein kinase 1, delta	-1.71	0.012703
1418898_at	Lin7c: lin-7 homolog C (C. elegans)	-1.67	0.013382
1418946_at	St3gal1: ST3 beta-galactoside alpha-2,3-sialyltransferase 1	-2.21	0.031563
1419029_at	Ero1l: ERO1-like (S. cerevisiae)	-1.94	0.02372
1419030_at	Ero1l: ERO1-like (S. cerevisiae)	-2.45	0.002844
1419094_at	Cyp2c37: cytochrome P450, family 2. subfamily c, polypeptide 37	2.25	0.015508
1419098_at	Stom: stomatin	-2.86	0.000481
1419099_x_at	Stom: stomatin	-2.4	0.000538
1419103_a_at	Abhd6: abhydrolase domain containing 6	-1.74	0.009894
1419236_at	Helb: helicase (DNA) B	2.28	0.019125
1419256_at	Spnb2: spectrin beta 2	2.75	0.031929
1419322_at	Fgd6: FYVE, RhoGEF and PH domain containing 6	-1.75	0.019566
1419382_a_at	Dhrs4: dehydrogenase/reductase (SDR family) member 4	-1.73	0.009271
1420420_at	Hao1: hydroxyacid oxidase 1, liver	1.88	0.019711
1420620_a_at	Rnf13: ring finger protein 13	-1.84	0.000767
1420629_a_at	Dnaja3: DnaJ (Hsp40) homolog, subfamily A, member 3	-1.78	0.006157
1420899_at	Rab18: RAB18, member RAS oncogene family	-1.77	0.005357
1420901_a_at	Hk1: hexokinase 1	-1.74	0.0142
1420904_at	Il17ra: interleukin 17 receptor A	-2.26	0.005163
1420934_a_at	Srrm1: serine/arginine repetitive matrix 1	2.04	0.01154
1420951_a_at	Son: Son cell proliferation protein	-1.8	0.014015
1420966_at	Slc25a15: solute carrier family 25 (mitochondrial carrier ornithine transporter), member 15	-1.82	0.019793
1420970_at	Adcy7: adenylate cyclase 7	-1.79	0.015584
1420973_at	Arid5b /// LOC100044968: AT rich interactive domain 5B (Mrf1 like) ///	2.45	0.00453
1421011_at	Hsd17b11: hydroxysteroid (17-beta) dehydrogenase 11	-1.95	0.002402
1421013_at	Pitpnb: phosphatidylinositol transfer protein, beta	-1.75	0.022539
1421027_a_at	Mef2c: myocyte enhancer factor 2C	2	0.024058
1421076_at	Sertad3: SERTA domain containing 3	-1.87	0.010405
1421077_at	Sertad3: SERTA domain containing 3	-2.08	0.003372

1421156_a_at	Dsc2: desmocollin 2	-1.82	0.015919
1421218_at	Bche: butyrylcholinesterase	-1.78	0.007625
1421491_a_at	Tmem49: transmembrane protein 49	-1.57	0.004085
1421534_at	Dfna5h: deafness, autosomal dominant 5 homolog (human)	-1.99	0.013375
1421600_a_at	Trim26: tripartite motif protein 26	-2.91	0.008922
1421830_at	Ak3l1 /// LOC100047616: adenylate kinase 3 alpha-like 1 /// similar to adenylate kinase 4	-1.77	0.025935
1421839_at	Abca1: ATP-binding cassette, sub-family A (ABC1), member 1	-1.96	0.002918
1421845_at	Golph3: golgi phosphoprotein 3	-1.63	0.006705
1421866_at	Nr3c1: nuclear receptor subfamily 3, group C, member 1	-3.12	0.010773
1421890_at	St3gal2: ST3 beta-galactoside alpha-2,3-sialyltransferase 2	-2.48	0.014365
1421895_at	Eif2s3x /// LOC100039419 /// LOC100048746: eukaryotic translation initiation factor 2, subunit 3, structural gene X-linked ///	-1.9	0.003105
1421991_a_at	Igfbp4: insulin-like growth factor binding protein 4	-1.55	0.003013
1422018_at	Hivep2: human immunodeficiency virus type I enhancer binding protein 2	-2.02	0.011775
1422102_a_at	Stat5b: signal transducer and activator of transcription 5B	-1.94	0.00265
1422512_a_at	Ogfr: opioid growth factor receptor	-2.01	0.002948
1422627_a_at	Mkks: McKusick-Kaufman syndrome protein	-2.22	0.0245
1422755_at	Btk: Bruton agammaglobulinemia tyrosine kinase	-1.75	0.008119
1422797_at	Mapbpip: mitogen activated protein binding protein interacting protein	-1.76	0.007724
1422862_at	Pdlim5: PDZ and LIM domain 5	-1.85	0.03874
1422966_a_at	Tfrc: transferrin receptor	-2.17	0.028869
1422967_a_at	Tfrc: transferrin receptor	-4.25	0.031933
1423048_a_at	Tollip: toll interacting protein	-1.69	0.005349
1423062_at	Igfbp3: insulin-like growth factor binding protein 3	2.21	0.038342
1423064_at	Dnmt3a: DNA methyltransferase 3A	-1.76	0.010362
1423184_at	Itsn2: intersectin 2	1.75	0.012928
1423266_at	2810405K02Rik: RIKEN cDNA 2810405K02 gene	-1.92	0.010217
1423521_at	Lmnb1: lamin B1	1.79	0.02712
1423556_at	Akr1b7: aldo-keto reductase family 1, member B7	3.12	0.00072
1423601_s_at	Tcof1: Treacher Collins Franceschetti syndrome 1, homolog	2.1	0.020039
1423652_at	Isca1: iron-sulfur cluster assembly 1 homolog (S. cerevisiae)	-1.79	0.000272
1423862_at	Plekhf2: pleckstrin homology domain containing, family F (with FYVE domain) member 2	-1.74	0.011081

1423895_a_at	Cugbp2: CUG triplet repeat, RNA binding protein 2	1.73	0.011248
1424084_at	Rod1: ROD1 regulator of differentiation 1 (S. pombe)	-1.7	0.012213
1424140_at	Gale: galactose-4-epimerase, UDP	1.9	0.012023
1424474_a_at	Camkk2: calcium/calmodulin-dependent protein kinase kinase 2, beta	1.7	0.029482
1424475_at	Camkk2: calcium/calmodulin-dependent protein kinase kinase 2, beta	1.8	0.011321
1424684_at	Rab5c: RAB5C, member RAS oncogene family	1.91	0.00641
1424724_a_at	D16Ertd472e: DNA segment, Chr 16, ERATO Doi 472, expressed	-1.75	0.047215
1424812_at	BC017158: cDNA sequence BC017158	1.65	0.002773
1424937_at	2310076L09Rik: RIKEN cDNA 2310076L09 gene	-1.82	0.01433
1424981_at	Nln: neurolysin (metallopeptidase M3 family)	-1.82	0.00436
1425330_a_at	LOC100048520 /// LOC666025 /// Ppm1b: protein phosphatase 1B, magnesium dependent, beta isoform ///	-1.59	0.002492
1425457_a_at	Grb10: growth factor receptor bound protein 10	-3.48	0.004811
1425461_at	Fbxw11: F-box and WD-40 domain protein 11	-1.86	0.00425
1425515_at	Pik3r1: phosphatidylinositol 3-kinase, regulatory subunit, polypeptide 1 (p85 alpha)	-2.45	0.032447
1425576_at	Ahcyl1: S-adenosylhomocysteine hydrolase-like 1	-1.89	0.001966
1425617_at	Dhx9: DEAH (Asp-Glu-Ala-His) box polypeptide 9	-2.84	0.002422
1425644_at	Lepr: leptin receptor	-3.33	0.00165
1425713_a_at	Rnf146: ring finger protein 146	-2.12	0.007326
1425732_a_at	Mxi1: Max interacting protein 1	-2.3	0.00104
1425803_a_at	Mbd2: methyl-CpG binding domain protein 2	-1.9	0.000775
1425932_a_at	Cugbp1: CUG triplet repeat, RNA binding protein 1	-1.88	0.003809
1426037_a_at	Rgs16: regulator of G-protein signaling 16	-1.98	0.045117
1426117_a_at	Slc19a2: solute carrier family 19 (thiamine transporter), member 2	-1.73	0.003079
1426229_s_at	Kras: v-Ki-ras2 Kirsten rat sarcoma viral oncogene homolog	-1.94	0.014918
1426519_at	P4ha1: procollagen-proline, 2-oxoglutarate 4-dioxygenase (proline 4-hydroxylase), alpha 1 polypeptide	-3.18	0.001533
1426575_at	Sgms1: sphingomyelin synthase 1	-1.77	0.014299
1426576_at	Sgms1: sphingomyelin synthase 1	-1.86	0.002219
1426743_at	Appl2: adaptor protein, phosphotyrosine interaction, PH domain and leucine zipper containing 2	-1.6	0.014025
1426805_at	Smarca4: SWI/SNF related, matrix associated, actin dependent regulator of chromatin, subfamily a, member 4	2.5	0.006415

1426837_at	Metap1: methionyl aminopeptidase 1	-1.74	0.010894
1427070_at	Snx21: sorting nexin family member 21	-2.55	0.033775
1427359_at	Jhdm1d: jumonji C domain-containing histone demethylase 1 homolog D (S. cerevisiae)	-2.23	0.004561
1427471_at	Fbxl3 /// LOC100044862: F-box and leucine-rich repeat protein 3 /// similar to Fbxl3 protein	-2.56	0.001351
1427483_at	Slc25a24: solute carrier family 25 (mitochondrial carrier, phosphate carrier), member 24	-1.84	0.009051
1427658_at	Ctbs: chitobiase, di-N-acetyl-	-1.72	0.002569
1428492_at	Glipr2: GLI pathogenesis-related 2	-1.67	0.0065
1428662_a_at	Hopx: HOP homeobox	-1.68	0.002337
1428838_a_at	Dck: deoxycytidine kinase	-1.63	0.005373
1429239_a_at	Stard4: StAR-related lipid transfer (START) domain containing 4	-1.92	0.007077
1429474_at	Zadh1: zinc binding alcohol dehydrogenase, domain containing 1	-1.82	0.001921
1429492_x_at	Ptdss2: phosphatidylserine synthase 2	-2.81	0.025099
1429533_at	Immt: inner membrane protein, mitochondrial	-1.92	0.010713
1429775_a_at	Gpr137b /// Gpr137b-ps /// LOC100044979: G protein-coupled receptor 137B /// G protein-coupled receptor 137B, pseudogene ///	-2.18	0.02574
1430019_a_at	EG434858 /// EG665646 /// Hnrnpa1 /// LOC100043855 /// LOC100044632 /// LOC654467: heterogeneous nuclear ribonucleoprotein A1 ///	-1.68	0.00805
1430533_a_at	Ctnnb1: catenin (cadherin associated protein), beta 1	-1.77	0.012823
1430692_a_at	Sel1l: sel-1 suppressor of lin-12-like (C. elegans)	-1.99	0.001872
1431030_a_at	Rnf14: ring finger protein 14	-2.34	0.01264
1431032_at	Agl: amylo-1,6-glucosidase, 4-alpha-glucanotransferase	-1.61	0.032597
1431170_at	Efna3 /// LOC100046031: ephrin A3 /// similar to Ephrin A3	-4.17	0.03907
1431332_a_at	Terf1: telomeric repeat binding factor 1	-1.87	0.016314
1431606_a_at	Angel2: angel homolog 2 (Drosophila)	-1.76	0.028326
1431645_a_at	Gdi2: guanosine diphosphate (GDP) dissociation inhibitor 2	-1.91	0.001702
1431734_a_at	Dnajb4: DnaJ (Hsp40) homolog, subfamily B, member 4	-1.58	0.001498
1431827_a_at	Tlk2: tousled-like kinase 2 (Arabidopsis)	-1.59	0.005797
1432344_a_at	Aplp2: amyloid beta (A4) precursor-like protein 2	-2.31	0.00582
1433479_at	5730410I19Rik: RIKEN cDNA 5730410I19 gene	-1.77	0.006193
1433480_at	2900010J23Rik: RIKEN cDNA 2900010J23 gene	-1.7	0.002073
1433491_at	Epb4.1l2: erythrocyte protein band 4.1-like 2	-1.92	0.001775

1434020_at	Pdap1: PDGFA associated protein 1	2.31	0.011171
1434062_at	Rabgap1l: RAB GTPase activating protein 1-like	-1.71	0.009344
1434181_at	Fermt2: fermitin family homolog 2 (Drosophila)	-1.79	0.003962
1434357_a_at	Kpnb1: karyopherin (importin) beta 1	-2.23	0.007152
1434370_s_at	Faf1: Fas-associated factor 1	-1.84	0.003088
1434419_s_at	Tardbp: TAR DNA binding protein	-1.77	0.000683
1434465_x_at	Vldlr: very low density lipoprotein receptor	-1.91	0.000398
1435872_at	Transcribed locus	-2.88	0.046918
1436746_at	Wnk1: WNK lysine deficient protein kinase 1	2.38	0.03966
1436909_at	Slc25a44: solute carrier family 25, member 44	1.6	0.00352
1437133_x_at	Akr1b3: aldo-keto reductase family 1, member B3 (aldose reductase)	2.17	0.004414
1437289_at	Impad1: inositol monophosphatase domain containing 1	1.68	0.005258
1437324_x_at	Fmod: fibromodulin	-2.48	0.0499
1437513_a_at	Serinc1: serine incorporator 1	-1.64	0.00444
1438167_x_at	Flcn: Folliculin	-1.72	0.01018
1438397_a_at	Rbm39: RNA binding motif protein 39	-2.02	0.030328
1438743_at	Cyp7a1: cytochrome P450, family 7, subfamily a, polypeptide 1	2.61	0.028814
1439036_a_at	Atp1b1: ATPase, Na+/K+ transporting, beta 1 polypeptide	-1.79	0.026428
1439120_at	BC010304: cDNA sequence BC010304	-1.93	0.001818
1439256_x_at	Gpr137b-ps: G protein-coupled receptor 137B, pseudogene	-1.74	0.008774
1440221_at	AA408650: expressed sequence AA408650	1.59	0.004013
1448009_at	LOC100044322: similar to UDP-glucose ceramide glucosyltransferase-like 1	1.89	0.000855
1448127_at	Rrm1: ribonucleotide reductase M1	-1.81	0.000918
1448231_at	Fkbp5: FK506 binding protein 5	-1.83	0.010303
1448239_at	Hmox1: heme oxygenase (decycling) 1	-6.01	0.000075
1448348_at	Caprin1: cell cycle associated protein 1	-1.85	0.006648
1448364_at	Ccng2: cyclin G2	-1.99	0.004915
1448482_at	Slc39a8: solute carrier family 39 (metal ion transporter), member 8	-2.07	0.027961
1448534_at	Sirpa: signal-regulatory protein alpha	-1.73	0.00374
1448607_at	Pbef1: pre-B-cell colony-enhancing factor 1	-2.31	0.045081
1448688_at	Podxl: podocalyxin-like	1.59	0.003046
1448847_at	Serinc3: serine incorporator 3	-1.94	0.013767
1448852_at	Rgn: regucalcin	1.51	0.001215

1449051_at	Ppara: peroxisome proliferator activated receptor alpha	-2.03	0.004285
1449262_s_at	Lin7c: lin-7 homolog C (C. elegans)	-2.49	0.002731
1449335_at	Timp3: tissue inhibitor of metalloproteinase 3	-1.77	0.028633
1449341_a_at	Stom: stomatin	-1.92	0.00229
1449347_a_at	LOC100044048 /// LOC100044049 /// LOC100046087 /// Xlr4a /// Xlr4b /// Xlr4c /// Xlr4e: X-linked lymphocyte-regulated 4B /// 4C /// 4A /// 4E ///	1.94	0.023384
1449348_at	Mpp6: membrane protein, palmitoylated 6 (MAGUK p55 subfamily member 6)	-1.83	0.046581
1449457_at	Acot12: acyl-CoA thioesterase 12	-1.86	0.003299
1449670_x_at	Gpr137b /// LOC100044979: G protein-coupled receptor 137B /// similar to Gpr137b protein	-1.79	0.038478
1449862_a_at	Pi4k2b: phosphatidylinositol 4-kinase type 2 beta	-1.62	0.00329
1449875_s_at	H2-T10 /// H2-T22 /// H2-T9 /// LOC100044190 /// LOC100044191: histocompatibility 2, T region locus 10 /// locus 22 /// locus 9 ///	1.65	0.004279
1449931_at	Cpeb4: cytoplasmic polyadenylation element binding protein 4	-2.51	0.022915
1450006_at	EG627557 /// Ncoa4: nuclear receptor coactivator 4 /// predicted gene, EG627557	-1.86	0.003071
1450007_at	1500003O03Rik /// LOC100048622: RIKEN cDNA 1500003O03 gene /// similar to EF-hand Ca2+ binding protein p22	-2.15	0.005709
1450104_at	Adam10: a disintegrin and metallopeptidase domain 10	-1.96	0.001934
1450109_s_at	Abcc2: ATP-binding cassette, sub-family C (CFTR/MRP), member 2	1.9	0.025603
1450113_at	Mpp5: membrane protein, palmitoylated 5 (MAGUK p55 subfamily member 5)	-1.98	0.002464
1450136_at	Cd38: CD38 antigen	-1.85	0.003523
1450157_a_at	Hmmr: hyaluronan mediated motility receptor (RHAMM)	-1.62	0.001296
1450161_at	Ikbkg: inhibitor of kappaB kinase gamma	-1.7	0.003181
1450368_a_at	Ppp3r1: protein phosphatase 3, regulatory subunit B, alpha isoform (calcineurin B, type I)	-2.24	0.023175
1450387_s_at	Ak3l1 /// LOC100047616: adenylate kinase 3 alpha-like 1 /// similar to adenylate kinase 4	-1.78	0.044632
1450392_at	Abca1: ATP-binding cassette, sub-family A (ABC1), member 1	-2.93	0.001511
1450396_at	Stag2: stromal antigen 2	-1.65	0.00987
1450407_a_at	Anp32a: acidic (leucine-rich) nuclear phosphoprotein 32 family, member A	-1.61	0.01398
1450522_a_at	H1f0: H1 histone family, member 0	-1.64	0.009476
1450703_at	Slc7a2: solute carrier family 7 (cationic amino acid transporter, y+ system), member 2	-2.75	0.014162
1450846_at	Bzw1: basic leucine zipper and W2 domains 1	-1.64	0.004796

1450970_at	Got1: glutamate oxaloacetate transaminase 1, soluble	-1.79	0.019086
1451072_a_at	Rnf4: ring finger protein 4	-1.73	0.004409
1451109_a_at	Nedd4: neural precursor cell expressed, developmentally down-regulted gene 4	-1.67	0.00331
1451263_a_at	Fabp4: fatty acid binding protein 4, adipocyte	-1.74	0.008121
1451355_at	Asah3l: N-acylsphingosine amidohydrolase 3-like	-1.94	0.012644
1451456_at	6430706D22Rik: RIKEN cDNA 6430706D22 gene	2.09	0.004218
1451622_at	Lmbrd1: LMBR1 domain containing 1	-1.69	0.010409
1451658_a_at	Polr3c: polymerase (RNA) III (DNA directed) polypeptide C	-2.47	0.003352
1451743_at	D19Wsu162e: DNA segment, Chr 19, Wayne State University 162, expressed	-1.84	0.014519
1451794_at	Tmcc3: transmembrane and coiled coil domains 3	-1.69	0.003473
1451807_at	Nr1i2: nuclear receptor subfamily 1, group I, member 2	-1.88	0.031888
1451914_a_at	Add2: adducin 2 (beta)	-2.15	0.012339
1451943_a_at	Ppm1a: protein phosphatase 1A, magnesium dependent, alpha isoform	-1.65	0.007818
1452026_a_at	Pla2g12a: phospholipase A2, group XIIA	-1.57	0.001774
1452080_a_at	Dcun1d1: DCUN1D1 DCN1, defective in cullin neddylation 1, domain containing 1 (S. cerevisiae)	-1.58	0.005927
1452162_at	Wdr48: WD repeat domain 48	-1.66	0.019634
1452228_at	Tbc1d23: TBC1 domain family, member 23	-1.8	0.010231
1452315_at	Kif11: kinesin family member 11	-2.13	0.001605
1452427_s_at	Ptplad1: protein tyrosine phosphatase-like A domain containing 1	-2.24	0.000256
1452457_a_at	Prkab1: protein kinase, AMP-activated, beta 1 non-catalytic subunit	-1.84	0.003264
1452504_s_at	Ctbs: chitobiase, di-N-acetyl-	-1.57	0.002394
1452527_a_at	P2rx4: purinergic receptor P2X, ligand-gated ion channel 4	-2.15	0.008256
1452830_s_at	Cad: carbamoyl-phosphate synthetase 2, aspartate transcarbamylase, and dihydroorotase	1.65	0.012043
1452986_at	Hgd: homogentisate 1, 2-dioxygenase	1.75	0.002075
1453604_a_at	Hbs1l: Hbs1-like (S. cerevisiae)	-2.15	0.001737
1453623_a_at	Rad23a: RAD23a homolog (S. cerevisiae)	-1.62	0.005637
1453724_a_at	Serpinf1: serine (or cysteine) peptidase inhibitor, clade F, member 1	-1.54	0.001019
1453748_a_at	Kif23: kinesin family member 23	-2.02	0.022062
1454107_a_at	Kif2a: kinesin family member 2A	-1.67	0.014793
1454120_a_at	Pcgf6: polycomb group ring finger 6	-2.28	0.048782
1454168_a_at	Clpb: ClpB caseinolytic peptidase B homolog (E. coli)	-1.88	0.047516
1454174_a_at	C330007P06Rik: RIKEN cDNA C330007P06 gene	-2.14	0.003745

1455061_a_at	Acaa2: acetyl-Coenzyme A acyltransferase 2 (mitochondrial 3-oxoacyl-Coenzyme A thiolase)	-1.66	0.004763
1455315_at	Trp53i13: transformation related protein 53 inducible protein 13	2.08	0.014328
1455801_x_at	Tbcd: tubulin-specific chaperone d	1.66	0.004664
1455904_at	Gas5: growth arrest specific 5	1.67	0.006306
1456080_a_at	Serinc3: serine incorporator 3	-1.81	0.007701
1456107_x_at	Eftud2: elongation factor Tu GTP binding domain containing 2	1.75	0.002327
1456262_at	Rbm5: RNA binding motif protein 5	1.86	0.038059
1456494_a_at	AI451617 /// Trim30: tripartite motif protein 30 /// expressed sequence AI451617	2.97	0.011689
1456590_x_at	Akr1b3: aldo-keto reductase family 1, member B3 (aldose reductase)	1.94	0.015481
1460279_a_at	Gtf2i: general transcription factor II I	-1.59	0.001799
1460295_s_at	Il6st: interleukin 6 signal transducer	-1.8	0.014423
1460521_a_at	Obfc2a: oligonucleotide/oligosaccharide-binding fold containing 2A	-2.5	0.008642
1428412_at	Tm9sf3: transmembrane 9 superfamily member 3	1.56	0.000915
1429009_at	Snrp70: U1 small nuclear ribonucleoprotein polypeptide A	2.09	0.037677
1429337_at	Tmem87b: transmembrane protein 87B	-1.83	0.016159
1429413_at	Cpm: carboxypeptidase M	-2.89	0.001247
1429501_s_at	Ppm1a: protein phosphatase 1A, magnesium dependent, alpha isoform	-1.79	0.010635
1429545_at	EG546265 /// F830028O17Rik /// LOC100044900 /// Ube2i: ubiquitin-conjugating enzyme E2I /// RIKEN cDNA F830028O17 gene ///	2.75	0.00401
1429778_at	Optn: optineurin	-1.97	0.012328
1429809_at	Tmtc2: transmembrane and tetratricopeptide repeat containing 2	-1.92	0.002831
1430566_at	4733401A01Rik: RIKEN cDNA 4733401A01 gene	2.56	0.001863
1430697_at	Ammecr1: Alport syndrome, mental retardation, midface hypoplasia and elliptocytosis chromosomal region gene 1 homolog (human)	2.72	0.004264
1430981_s_at	Gpbp1: GC-rich promoter binding protein 1	-2.19	0.012382
1430984_at	Azin1: antizyme inhibitor 1	-3.02	0.006748
1431018_at	1810013L24Rik: RIKEN cDNA 1810013L24 gene	-1.62	0.009814
1431061_s_at	Peli1: pellino 1	-2.32	0.00346
1431183_at	1700066M21Rik: RIKEN cDNA 1700066M21 gene	-1.82	0.011274
1431197_at	Arl6ip2: ADP-ribosylation factor-like 6 interacting protein 2	-2.26	0.000657
1431206_at	5730601F06Rik: RIKEN cDNA 5730601F06 gene	-2.05	0.027247
1431430_s_at	LOC630539 /// Trim59: tripartite motif-containing 59 /// similar to mouse RING finger 1	-2.42	0.000373

1432304_a_at	9030624J02Rik: RIKEN cDNA 9030624J02 gene	-2.46	0.005099
1433633_at	Irf2bp2: interferon regulatory factor 2 binding protein 2	-2.3	0.01103
1434905_at	Ndufa4l2: NADH dehydrogenase (ubiquinone) 1 alpha subcomplex, 4-like 2	-1.89	0.011617
1435396_at	Stxbp6: syntaxin binding protein 6 (amisyn)	1.81	0.008299
1435867_at	Jhdm1d: jumonji C domain-containing histone demethylase 1 homolog D (S. cerevisiae)	-1.62	0.001522
1436035_at	3830431G21Rik: RIKEN cDNA 3830431G21 gene	2.46	0.045584
1436070_at	Glo1: glyoxalase 1	2.18	0.005461
1436169_at	C730029A08Rik: RIKEN cDNA C730029A08 gene	1.61	0.001579
1436194_at	Prelid2: PRELI domain containing 2	-1.81	0.008396
1436456_at	9130023D20Rik: RIKEN cDNA 9130023D20 gene	-1.61	0.006166
1437638_at	Srrm2: serine/arginine repetitive matrix 2	2.12	0.036937
1437862_at	Rbm25: RNA binding motif protein 25	1.87	0.009844
1438265_at	NOD-derived CD11c +ve dendritic cells cDNA, RIKEN full-length enriched library, clone:F630001G16 product:	1.89	0.013669
1438268_at	Rc3h2: ring finger and CCCH-type zinc finger domains 2	1.78	0.012543
1438410_at	Prtg: protogenin homolog (Gallus gallus)	-2.33	0.006175
1438433_at	Whdc1: WAS protein homology region 2 domain containing 1	2.78	0.008947
1439158_at	Tlk1: tousled-like kinase 1	-1.79	0.013609
1439173_at	Hook1: hook homolog 1 (Drosophila)	1.73	0.004961
1441272_at	Matr3: Matrin 3	2.06	0.028419
1441860_x_at	Ide: Insulin degrading enzyme	1.77	0.00174
1442041_at	LOC552876: hypothetical LOC552876	1.91	0.019388
1442100_at	Inpp5f: inositol polyphosphate-5-phosphatase F	2.3	0.037039
1442109_at	Activated spleen cDNA, RIKEN full-length enriched library, clone:F830222N19 product:	2.82	0.002018
1442418_at	B930096F20Rik: RIKEN cDNA B930096F20 gene	1.86	0.022219
1442549_at	Mbnl3: muscleblind-like 3 (Drosophila)	1.82	0.004367
1443522_s_at	Phip: pleckstrin homology domain interacting protein	-2.25	0.003737
1443792_at	Tsga14: testis specific gene A14	2.1	0.039553
1444271_at	Anapc1: anaphase promoting complex subunit 1	2.36	0.019917
1444330_at	D2Ertd173e: DNA segment, Chr 2, ERATO Doi 173, expressed	3.45	0.001175
1444333_at	Mm.216315.1	-1.9	0.041505
1444436_at	9630030I15Rik /// Hsf2: heat shock factor 2 /// RIKEN cDNA 9630030I15 gene	2.83	0.001263

1444612_at	3222402P14Rik: RIKEN cDNA 3222402P14 gene	-2.3	0.019401
1444677_at	C77673: expressed sequence C77673	1.8	0.005173
1444827_at	Mm.182613.1	2.24	0.038149
1446284_at	Mtss1: metastasis suppressor 1	2.17	0.03126
1446844_at	Chchd7: coiled-coil-helix-coiled-coil-helix domain containing 7	-1.8	0.017099
1447063_at	Sept14: septin 14	3.15	0.011794
1447258_at	Mm.210555.1	1.8	0.006526
1452906_at	Meg3: maternally expressed 3	2.18	0.002968
1453009_at	Cpm: carboxypeptidase M	-2.54	0.002255
1453041_at	Tmem16j: transmembrane protein 16J	-2.39	0.001034
1453140_at	9030612M13Rik: RIKEN cDNA 9030612M13 gene	2.15	0.000222
1453189_at	Ube2i: ubiquitin-conjugating enzyme E2I	2.31	0.008989
1453227_at	Rhobtb3: Rho-related BTB domain containing 3	-1.88	0.002914
1453290_at	Hmgb2l1: high mobility group box 2-like 1	3.11	0.006481
1453760_at	Mier1: mesoderm induction early response 1 homolog (Xenopus laevis	-2.66	0.016102
1453776_at	Snx21: sorting nexin family member 21	-2.09	0.046079
1454003_at	Afg3l2: AFG3(ATPase family gene 3)-like 2 (yeast)	-3.77	0.000099
1454649_at	Srd5a1: steroid 5 alpha-reductase 1	1.79	0.022663
1455876_at	Slc4a7: solute carrier family 4, sodium bicarbonate cotransporter, member 7	2.58	0.006464
1455933_at	Tra2a: transformer 2 alpha homolog (Drosophila)	2.34	0.013907
1455998_at	LOC667118: similar to Zinc finger BED domain containing protein 4	2.29	0.006551
1456156_at	Lepr: leptin receptor	-1.71	0.008329
1456329_at	Prtg: protogenin homolog (Gallus gallus)	-1.87	0.007925
1456596_at	6430550H21Rik: RIKEN cDNA 6430550H21 gene	-3.53	0.001931
1457122_at	Mm.208214.1	1.71	0.009358
1457542_at	Nup133: nucleoporin 133	1.99	0.036872
1457554_at	Apob: apolipoprotein B	1.84	0.016115
1457782_at	Tln1: talin 1	1.92	0.014177
1457987_at	6030458C11Rik: RIKEN cDNA 6030458C11 gene	5.02	0.000052
1458150_at	D030051N19Rik: RIKEN cDNA D030051N19 gene	2.19	0.035363
1458297_s_at	Marco: macrophage receptor with collagenous structure	-2.13	0.023327
1458403_at	Tnik: TRAF2 and NCK interacting kinase	2.19	0.049389
1458609_at	14 days embryo liver cDNA, RIKEN full-length enriched library, clone:I530025F13 product:	-5.29	0.000046

1458685_at	Garnl1: GTPase activating RANGAP domain-like 1	3.52	0.00907
1458719_at	Transcribed locus, moderately similar to XP_001117064.1 BTB (POZ) domain containing 9 [Macaca mulatta]	1.87	0.009768
1459734_at	Mm.212401.1	1.93	0.002868
1459984_at	Mia3: melanoma inhibitory activity 3	2.19	0.016172

Table AI.15: Candidate probe sets with apparent differential expression for switch versus 9% casein (baseline) class

comparison using low stringency criteria and excluding one sample outlier from each class. Median FDR was 4.9%

Affx Probe set	Gene information	Fold change	p-value
1416193_at	Car1: carbonic anhydrase 1	-1.82	0.015721
1423556_at	Akr1b7: aldo-keto reductase family 1, member B7	2.6	0.006555
1424350_s_at	Lpgat1: lysophosphatidylglycerol acyltransferase 1	1.52	0.005077
1425065_at	Oas2: 2'-5' oligoadenylate synthetase 2	2.01	0.033493
1436462_at	OTTMUSG00000016327: predicted gene, OTTMUSG00000016327	-2	0.010695
1438644_x_at	Commd9: COMM domain containing 9	2.69	0.011373
1452677_at	LOC100044383 /// Pnpt1: polyribonucleotide nucleotidyltransferase 1 ///	3.03	0.032029
1432651_at	2510019K15Rik: RIKEN cDNA 2510019K15 gene	2.02	0.042047
1435770_at	Txndc13: thioredoxin domain containing 13	2.42	0.044705
1440443_at	E030016H06Rik: RIKEN cDNA E030016H06 gene	3.68	0.004556
1442069_at	D5Wsu178e: DNA segment, Chr 5, Wayne State University 178, expressed	2.39	0.02548
1442100_at	Inpp5f: inositol polyphosphate-5-phosphatase F	1.69	0.00733
1443512_at	Mm.103030.1	1.65	0.005017
1445695_at	0 day neonate lung cDNA, RIKEN full-length enriched library, clone:E030049G11 product:	1.84	0.04605
1445826_at	Ankrd17: ankyrin repeat domain 17	1.94	0.048757
1446284_at	Mtss1: metastasis suppressor 1	2.25	0.02209
1457458_at	Zc3h4: zinc finger CCCH-type containing 4	3.03	0.031387
1457554_at	Apob: apolipoprotein B	1.95	0.017958

Table AI.16: Candidate probe sets with apparent differential expression for switch versus 18% casein (baseline) class comparison using low stringency criteria and excluding one sample outlier from each class. Median FDR was 83.3%

Affx probe set	Gene information	Fold change	p-value
1415771_at	Ncl: nucleolin	1.49	0.003631
1415773_at	Ncl: nucleolin	1.96	0.002835
1415784_at	Vps35: vacuolar protein sorting 35	1.94	0.002317
1415988_at	Hdlbp: high density lipoprotein (HDL) binding protein	2.05	0.021049

1416656_at	Clic1: chloride intracellular channel 1	2.05	0.001959
1417576_a_at	Otub2: OTU domain, ubiquitin aldehyde binding 2	1.75	0.020222
1418129_at	Dhcr24: 24-dehydrocholesterol reductase	-3.45	0.013174
1419030_at	Ero1l: ERO1-like (S. cerevisiae)	1.8	0.00129
1419098_at	Stom: stomatin	2.16	0.005589
1419099_x_at	Stom: stomatin	2.21	0.003188
1419382_a_at	Dhrs4: dehydrogenase/reductase (SDR family) member 4	1.63	0.003468
1420904_at	Il17ra: interleukin 17 receptor A	2.16	0.005609
1421008_at	Rsad2: radical S-adenosyl methionine domain containing 2	1.95	0.047598
1421011_at	Hsd17b11: hydroxysteroid (17-beta) dehydrogenase 11	1.74	0.00284
1421076_at	Sertad3: SERTA domain containing 3	1.8	0.004447
1421077_at	Sertad3: SERTA domain containing 3	2.1	0.002635
1421600_a_at	Trim26: tripartite motif protein 26	3.43	0.015389
1421866_at	Nr3c1: nuclear receptor subfamily 3, group C, member 1	2.2	0.012703
1422512_a_at	Ogfr: opioid growth factor receptor	1.78	0.007322
1422797_at	Mapbpip: mitogen activated protein binding protein interacting protein	1.93	0.002532
1422966_a_at	Tfrc: transferrin receptor	1.84	0.034195
1422967_a_at	Tfrc: transferrin receptor	2.48	0.040924
1423601_s_at	Tcof1: Treacher Collins Franceschetti syndrome 1, homolog	-1.76	0.009364
1424684_at	Rab5c: RAB5C, member RAS oncogene family	-1.73	0.014339
1424937_at	2310076L09Rik: RIKEN cDNA 2310076L09 gene	1.72	0.026302
1425451_s_at	Chi3l3 /// Chi3l4: chitinase 3-like 3 /// chitinase 3-like 4	1.99	0.009219
1425457_a_at	Grb10: growth factor receptor bound protein 10	2.47	0.01139
1425617_at	Dhx9: DEAH (Asp-Glu-Ala-His) box polypeptide 9	2.04	0.010173
1425732_a_at	Mxi1: Max interacting protein 1	1.7	0.003673
1426519_at	P4ha1: procollagen-proline, 2-oxoglutarate 4-dioxygenase (proline 4-hydroxylase), alpha 1 polypeptide	1.98	0.004679
1426805_at	Smarca4: SWI/SNF related, matrix associated, actin dependent regulator of chromatin, subfamily a, member 4	-2.13	0.012558
1426975_at	Os9: amplified in osteosarcoma	1.87	0.031046
1427359_at	Jhdm1d: jumonji C domain-containing histone demethylase 1 homolog D (S. cerevisiae)	1.76	0.008571
1431030_a_at	Rnf14: ring finger protein 14	2.02	0.018955
1431213_a_at	LOC100041156 /// LOC100041932: hypothetical protein LOC100041156 /// hypothetical protein LOC100041932	-12.4	0.020197
1431743_a_at	Slc4a1: solute carrier family 4 (anion exchanger), member 1	1.66	0.018424

1432344_a_at	Aplp2: amyloid beta (A4) precursor-like protein 2	1.87	0.016731
1433480_at	2900010J23Rik: RIKEN cDNA 2900010J23 gene	1.78	0.00123
1448231_at	Fkbp5: FK506 binding protein 5	1.73	0.013801
1448239_at	Hmox1: heme oxygenase (decycling) 1	4.7	0.00011
1448332_at	Pex19: peroxisome biogenesis factor 19	1.58	0.00444
1448566_at	Slc40a1: solute carrier family 40 (iron-regulated transporter), member 1	1.57	0.014528
1449051_at	Ppara: peroxisome proliferator activated receptor alpha	1.71	0.008169
1449262_s_at	Lin7c: lin-7 homolog C (C. elegans)	1.76	0.01137
1449341_a_at	Stom: stomatin	1.74	0.00379
1450007_at	1500003O03Rik /// LOC100048622: RIKEN cDNA 1500003O03 gene /// similar to EF-hand Ca2+ binding protein p22	1.82	0.011059
1450392_at	Abca1: ATP-binding cassette, sub-family A (ABC1), member 1	1.92	0.004622
1450703_at	Slc7a2: solute carrier family 7 (cationic amino acid transporter, y+ system), member 2	2.21	0.020347
1450970_at	Got1: glutamate oxaloacetate transaminase 1, soluble	1.72	0.002514
1451658_a_at	Polr3c: polymerase (RNA) III (DNA directed) polypeptide C	1.67	0.008802
1451920_a_at	Rfc1: replication factor C (activator 1) 1	-1.96	0.022646
1452030_a_at	Hnrnpr: heterogeneous nuclear ribonucleoprotein R	1.95	0.037933
1452830_s_at	Cad: carbamoyl-phosphate synthetase 2, aspartate transcarbamylase, and dihydroorotase	-1.65	0.00045
1454174_a_at	C330007P06Rik: RIKEN cDNA C330007P06 gene	1.68	0.009491
1430984_at	Azin1: antizyme inhibitor 1	2.05	0.009384
1431061_s_at	Peli1: pellino 1	1.81	0.009172
1431197_at	Arl6ip2: ADP-ribosylation factor-like 6 interacting protein 2	1.72	0.013244
1431220_at	LOC100040353 /// LOC100046169: similar to splicing coactivator subunit SRm300 /// hypothetical protein LOC100046169	2.09	0.019093
1432304_a_at	9030624J02Rik: RIKEN cDNA 9030624J02 gene	2.02	0.008879
1438763_at	Dnahc2: dynein, axonemal, heavy chain 2	2.8	0.013799
1439882_at	Sec23ip: Sec23 interacting protein	1.58	0.01375
1441915_s_at	2310076L09Rik: RIKEN cDNA 2310076L09 gene	1.68	0.006802
1442760_x_at	Mm.209585.1	-1.84	0.023385
1444330_at	D2Ertd173e: DNA segment, Chr 2, ERATO Doi 173, expressed	-2.36	0.030702
1444436_at	9630030I15Rik /// Hsf2: heat shock factor 2 /// RIKEN cDNA 9630030I15 gene	-2.35	0.006199
1447258_at	Mm.210555.1	-1.87	0.003539
1447757_x_at	Inpp5f: inositol polyphosphate-5-phosphatase F	-2.36	0.013168
1452906_at	Meg3: maternally expressed 3	-2.25	0.038167

1453189_at	Ube2i: ubiquitin-conjugating enzyme E2I	-1.93	0.024951
1453290_at	Hmgb2l1: high mobility group box 2-like 1	-2.55	0.013424
1454003_at	Afg3l2: AFG3(ATPase family gene 3)-like 2 (yeast)	2.37	0.015738
1455773_at	0 day neonate kidney cDNA, RIKEN full-length enriched library, clone:D630004N14 product:unclassifiable, full insert sequence	-2.9	0.00904
1455933_at	Tra2a: transformer 2 alpha homolog (Drosophila)	-2.16	0.017576
1458505_at	LOC552901: hypothetical LOC552901	1.98	0.019674
1458609_at	14 days embryo liver cDNA, RIKEN full-length enriched library, clone:I530025F13 product:unclassifiable, full insert sequence	3.49	0.006039
1459734_at	Mm.212401.1	-1.69	0.008013

Table AI.17: Candidate probe sets with apparent differential expression for 9% casein versus 18% casein (baseline) class

comparison using low stringency criteria and excluding one sample outlier from each class. Median FDR was 23.7%

Appendix II

Electro-blotting transfer buffer, pH 8.3

Tris base 6.06 g
Glycine 22.5 g
SDS 1 g
Methanol 500 ml
Deionised H_2O 1500 ml

Appendix III

Anaesthetic – K.A.T. mix maximum dose per 50 g mouse

Saline	355 µl
100 mg/ml Ketamine	100 µl
10 mg/ml Acepromazine	25 µl
300 µg/ml Buprenorphine (Temgesic)	20 µl
Total	500 µl

Culture Media

Stock	T6 PVP	H6 PVP
H_2O	7.8 ml	7.8 ml
F	1.0 ml	1.00 ml
B	1.0 ml	0.16 ml
G	0.10 ml	0.10 ml
H	0.10 ml	0.10 ml
E	N/A	0.84 ml
BSA	N/A	N/A
PVP	60 mg	60 mg
20% NaCl	40 µl	60 µl
NaCl 15 mg/ml	N/A	N/A
Phenol red	25 µl	N/A

Media Osmolarity 280-290mOsm

Stock solutions

Stock F:

Sodium Chloride	4.720 g
Potassium Chloride	0.110 g
Sodium Dihydrogen Orthophosphate	0.060 g
Magnesium Chloride	0.100 g
D – Glucose	1.000 g
DL – Lactic Acid (60%)	3.4 ml

Make up to 100 ml with H$_2$O
mOsm 2555 +/- 200

Stock G:

Pyruvic Acid	0.030 g
Penicillin	0.060 g
Streptomycin	0.050 g

Add 10 ml of H$_2$O
mOsm 60 +/- 10

Stock B:

Sodium Hydrogen Carbonate	0.210 g

Add 10 ml of H$_2$O
mOsm 444 +/- 20

Stock H:

Calcium Chloride 2 – Hydrate	0.260 g

Add 10 ml of H$_2$O
mOsm 415 +/- 20

Stock E:

Hepes	2.9785 g

Add 50 ml of H$_2$O
mOsm 354 +/- 20
pH to 7.4 with 5M NaOH before checking the mOsm.

Other solutions:

20% sodium Chloride
(2 g in 10 ml H$_2$O)

5 ml Sodium Chloride 15 mg/ml (made up fresh).
Phenol Red is brought in as a solution.

Reference List

Alberts,B., Bray,D., Lewis,J., Raff,M., Roberts,K., and Watson,J. (1994). Molecular Biology of The Cell. (New York: Garland).

Alikhani-Koopaei,R., Fouladkou,F., Frey,F.J., and Frey,B.M. (2004). Epigenetic regulation of 11 beta-hydroxysteroid dehydrogenase type 2 expression. Journal of Clinical Investigation *114*, 1146-1157.

Arishima,K., Nakama,S., Morikawa,Y., Hashimoto,Y., and Eguchi,Y. (1977). Maternal-foetal interrelations of plasma corticosterone concentrations at the end of gestation in the rat. J. Endocrinol. *72*, 239-240.

Arriza,J.L., Weinberger,C., Cerelli,G., Glaser,T.M., Handelin,B.L., Housman,D.E., and Evans,R.M. (1987). Cloning of Human Mineralocorticoid Receptor Complementary-Dna - Structural and Functional Kinship with the Glucocorticoid Receptor. Science *237*, 268-275.

Baba,M., Furihata,M., Hong,S.B., Tessarollo,L., Haines,D.C., Southon,E., Patel,V., Igarashi,P., Alvord,W.G., Leighty,R., Yao,M., Bernardo,M., Ileva,L., Choyke,P., Warren,M.B., Zbar,B., Linehan,W.M., and Schmidt,L.S. (2008). Kidney-targeted Birt-Hogg-Dube gene inactivation in a mouse model: Erk1/2 and Akt-mTOR activation, cell hyperproliferation, and polycystic kidneys. Journal of the National Cancer Institute *100*, 140-154.

Baba,M., Hong,S.B., Sharma,N., Warren,M.B., Nickerson,M.L., Iwamatsu,A., Esposito,D., Gillette,W.K., Hopkins,R.F.3., Hartley,J.L., Furihata,M., Oishi,S., Zhen,W., Burke,T.R., Linehan,W.M., Schmidt,L.S., and Zbar,B. (2006). Folliculin encoded by the BHD gene interacts with a binding protein, FNIP1, and AMPK, and is involved in AMPK and mTOR signaling. Proceedings of the National Academy of Science USA *103*, 15552-15557.

Bagis,H., Mercan,H.O., and Dinnyes,A. (2004). Exposure to warmer postoperative temperatures reduces hypothermia caused by anaesthesia and significantly increases the implantation rate of transferred embryos in the mouse. Laboratory Animals *38*, 50-54.

Bamberger,C.M., Bamberger,A.M., Decastro,M., and Chrousos,G.P. (1995). Glucocorticoid Receptor-Beta, A Potential Endogenous Inhibitor of Glucocorticoid Action in Humans. Journal of Clinical Investigation *95*, 2435-2441.

Bamberger,C.M., Schulte,H.M., and Chrousos,G.P. (1996). Molecular determinants of glucocorticoid receptor function and tissue sensitivity to glucocorticoids. Endocrine Reviews *17*, 245-261.

Barker (1999). Mothers, babies and health in later life, 2nd edition.

Barker,D.J., Hales,C.N., Fall,C.H., Osmond,C., Phipps,K., and Clark,P.M. (1993). Type 2 (non-insulin-dependent) diabetes mellitus, hypertension and hyperlipidaemia (syndrome X): relation to reduced fetal growth. Diabetologia *36*, 62-67.

Barnes,P.J. and Adcock,I.M. (1998). Transcription factors and asthma. European Respiratory Journal *12*, 221-234.

Beck,F., Erler,T., Russell,A., and James,R. (1995). Expression of Cdx-2 in the mouse embryo and placenta: possible role in patterning of the extra-embryonic membranes. Dev. Dyn. *204*, 219-227.

Beckman,D.A., Lloyd,J.B., and Brent,R.L. (1998). Quantitative studies on the mechanisms of amino acid supply to rat embryos during organogenesis. Reproductive Toxicology *12*, 197-200.

Benediktsson,R., Lindsay,R.S., Noble,J., Seckl,J.R., and Edwards,C.R. (1993). Glucocorticoid exposure in utero: new model for adult hypertension. Lancet *341*, 339-341.

Bertram,C., Trowern,A.R., Copin,N., Jackson,A.A., and Whorwood,C.B. (2001). The maternal diet during pregnancy programs altered expression of the glucocorticoid receptor and type 2 11 beta-hydroxysteroid dehydrogenase: Potential molecular mechanisms underlying the programming of hypertension in utero. Endocrinology *142*, 2841-2853.

Bertram,C.E. and Hanson,M.A. (2001). Animal models and programming of the metabolic syndrome. British Medical Bulletin *60*, 103-121.

Bertram,C.E. and Hanson,M.A. (2002). Prenatal programming of postnatal endocrine responses by glucocorticoids. Reproduction *124*, 459-467.

Bronson,F., Dagg,C., and Snell,G. (1966). Reproduction. In Biology of the laboratory mouse, Green E, ed. McGraw-Hill).

Burdge,G.C., Slater-Jefferies,J., Torrens,C., Phillips,E.S., Hanson,M.A., and Lillycrop,K.A. (2007). Dietary protein restriction of pregnant rats in the F0 generation induces altered methylation of hepatic gene promoters in the adult male offspring in the F1 and F2 generations. British Journal of Nutrition *97*, 435-439.

Burns,S.P., Desai,M., Cohen,R.D., Hales,C.N., Iles,R.A., Germain,J.P., Going,T.C., and Bailey,R.A. (1997). Gluconeogenesis, glucose handling, and structural changes in livers of the adult offspring of rats partially deprived of protein during pregnancy and lactation. Journal of Clinical Investigation *100*, 1768-1774.

Campbell,N., Reece,J., and Mitchell,L. (1999). Biology. Addison Wesley Longman).

Campion,J., Lahera,V., Cachofeiro,V., Maestro, B., Dávila,N., Carranza, M.C., Calle, C. (1998). In vivo tissue specific modulation of rat insulin receptor gene expression in an experimental model of mineralocorticoid excess. Molecular and Cellular Biochemistry *185*, (1-2) 177-82.

Caro,J.F., Triester,S., Patel,V.K., Tapscott,E.B., Frazier,N.L., and Dohm,G.L. (1995). Liver glucokinase: decreased activity in patients with type II diabetes. Hormone and Metabolic Research *27*, 19-22.

Cetin,I., Marconi,A.M., Bozzetti,P., Sereni,L.P., Corbetta,C., Pardi,G., and Battaglia,F.C. (1988). Umbilical amino acid concentrations in appropriate and small for gestational age infants: a biochemical difference present in utero. Am. J. Obstet. Gynecol. *158*, 120-126.

Chatelain,A., Dupouy,J.P., and Allaume,P. (1980). Fetal-Maternal Adrenocorticotropin and Corticosterone Relationships in the Rat - Effects of Maternal Adrenalectomy. Endocrinology *106*, 1297-1303.

Chawengsaksophak,K., James,R., Hammond,V.E., Kontgen,F., and Beck,F. (1997). Homeosis and intestinal tumours in Cdx2 mutant mice. Nature *386*, 84-87.

Cole,T.J., Blendy,J.A., Monaghan,A.P., Krieglstein,K., Schmid,W., Aguzzi,A., Fantuzzi,G., Hummler,E., Unsicker,K., and Schutz,G. (1995). Targeted Disruption of the Glucocorticoid Receptor Gene Blocks Adrenergic Chromaffin Cell-Development and Severely Retards Lung Maturation. Genes & Development *9*, 1608-1621.

Conaghan,J., Handyside,A.H., Winston,R.M., and Leese,H.J. (1993). Effects of pyruvate and glucose on the development of human preimplantation embryos in vitro. J. Reprod Fertil *99*, 87-95.

Cross,J.C. and Rossant,J. (2001). Development of the Embryo. R.Harding and A.D.Bocking, eds. (Cambridge: Cambridge University Press).

Dahlman-Wright,K., Wright,A.P., and Gustafsson,J.A. (1992). Determinants of high-affinity DNA binding by the glucocorticoid receptor: evaluation of receptor domains outside the DNA-binding domain. Biochemistry *31*, 9040-9044.

Dalman,F.C., Scherrer,L.C., Taylor,L.P., Akil,H., and Pratt,W.B. (1991). Localization of the 90-Kda Heat-Shock Protein-Binding Site Within the Hormone-Binding Domain of the Glucocorticoid Receptor by Peptide Competition. Journal of Biological Chemistry *266*, 3482-3490.

de Gasparo,M., Milner,G.R., Norris,P.D., and Milner,R.D. (1978). Effect of glucose and amino acids on foetal rat pancreatic growth and insulin secretion in vitro. J. Endocrinol. *77*, 241-248.

Danesh,F.R., Wada,J., Wallner,E.I., Sahai,A., Srivastava,S.K., and Kanwar,Y.S. (2003). Gene regulation of aldose-, aldehyde- and a renal specific oxido reductase (RSOR) in the pathobiology of diabetes mellitus. Curr Med Chem *15*, 1399-1406.

Danielsen,M., Northrop,J.P., and Ringold,G.M. (1986). The Mouse Glucocorticoid Receptor - Mapping of Functional Domains by Cloning, Sequencing and Expression of Wild-Type and Mutant Receptor Proteins. Embo Journal *5*, 2513-2522.

Davies,T.J. and Gardner,R.L. (2002). The plane of first cleavage is not related to the distribution of sperm components in the mouse. Hum. Reprod *17*, 2368-2379.

Delhanty,P.J.D. and Han,V.K.M. (1993). The expression of insulin-like growth factor (IGF)-binding 2 and IGF-II genes in the tissues of the developing ovine fetus. Endocrinology *132,* 41-52.

Desai,M., Byrne,C.D., Meeran,K., Martenz,N.D., Bloom,S.R., and Hales,C.N. (1997a). Regulation of hepatic enzymes and insulin levels in offspring of rat dams fed a reduced-protein diet. American Journal of Physiology, Gastrointestinal Liver Physiology *273*, G899-G904.

Desai,M., Byrne,C.D., Zhang,J., Petry,C.J., Lucas,A., and Hales,C.N. (1997b). Programming of hepatic insulin-sensitive enzymes in offspring of rat dams fed a protein-restricted diet. American Jounal of Physiology, Gastrointestinal Liver Physiology *272*, G1083-G1090.

Devreker,F., Winston,R.M., and Hardy,K. (1998). Glutamine improves human preimplantation development in vitro. Fertil Steril. *69*, 293-299.

Draper,N. and Stewart,P.M. (2005). 11beta-hydroxysteroid dehydrogenase and the pre-receptor regulation of corticosteroid hormone action. J. Endocrinol. *186*, 251-271.

Ecker,D.J., Stein,P., and Xu,Z. (2004). Long-term effects of culture of preimplantation mouse embryos on behaviour. Proc. Natl. Acad. Sci. U. S. A *101*, 1595-1600.

Edwards,C.R., Benediktsson,R., Lindsay,R.S., and Seckl,J.R. (1993). Dysfunction of placental glucocorticoid barrier: link between fetal environment and adult hypertension? Lancet *341*, 355-357.

Edwards,C.R., Benediktsson,R., Lindsay,R.S., and Seckl,J.R. (1996). 11 beta-Hydroxysteroid dehydrogenases: key enzymes in determining tissue-specific glucocorticoid effects. Steroids *61*, 263-269.

Edwards,C.R., Stewart,P.M., Burt,D., Brett,L., McIntyre,M.A., Sutanto,W.S., de Kloet,E.R., and Monder,C. (1988). Localisation of 11 beta-hydroxysteroid dehydrogenase--tissue specific protector of the mineralocorticoid receptor. Lancet *2*, 986-989.

Efstratiadis,A. (1998). Genetics of mouse growth. Int. J. Dev. Biol. *42*, 955-976.

Eggenschwiler,J., Ludwig,T., Fisher,P., Leighton,P.A., Tilghmen,S.M., and Efstratiadis,A. (1997). Mouse mutant embryos over expressing IGF-II exhibit phenotypic

features of Beckman-Wiedemann and Simpson-Golobi-Behmel syndromes. Genes and Development *11*, 3128-3142.

Eisen,M.B., Spellman,P.T., Brown,P.O., and Botstein,D. (1998). Cluster Analysis and Display of Genome-Wide Expression Patterns. Proceedings of the National Academy of Science USA *95*, 14863-14868.

El Khattabi,I., Gregoire,F., Remacle,C., and Reusens,B. (2003). Isocaloric maternal low-protein diet alters IGF-I, IGFBPs, and hepatocyte proliferation in the fetal rat. American Journal of Physiology, Endocrinology and Metabolism *285*, E991-E1000.

Encio,I.J. and Detera-Wadleigh,S.D. (1991). The genomic structure of the human glucocorticoid receptor. J. Biol. Chem. *266*, 7182-7188.

Farese Jr,R., Ruland,S.L., Flynn,L.M., Stokowski,R.P., and Young,S.G. (1995). Knockout of the mouse apolipoprotein B gene results in embryonic lethality in homozygotes and protection against diet-induced hypercholestrolemia in heterozygotes. Proceedings of the National Acadmey of Science USA *92*, 1774-1778.

Fernandez-Gonzalez,R., Moreira,P., and Bilbao,A. (2004). Long-term effect of in vitro culturre of mouse embryos with serum on mRNA expression of imprinting genes, development and behaviour. Proc. Natl. Acad. Sci. U. S. A *101*, 5880-5885.

Fleming,T.P. and Johnson,M.H. (1988). From egg to epithelium. Annu. Rev Cell Biol. *4*, 459-485.

Forhead,A.J., Broughton,P.F., and Fowden,A.L. (2000). Effect of cortisol on blood pressure and the renin-angiotensin system in fetal sheep during late gestation. J. Physiol *526 Pt 1*, 167-176.

Fowden,A.L. (2001). Growth and Metabolism. In Fetal Growth and Development, R.Harding and A.D.Bocking, eds. (Cambridge: Cambridge University Press).

Fowden,A.L., Li,J., and Forhead,A.J. (1998). Glucocorticoids and the preparation for life after birth: are there long term concsequenses of the life insurance? The Proceedings of the Nutrition Society *57*, 113-122.

Fowden,A.L., Giussani,D.A., Forhead,A.J. (2005). Endocrine and metabolic programming during intrauterine development. Early Human Development *81,* 723-734.

Fowden,A.L. (2003). The insulin-like growth factors and feto-placental growth. Placenta *24*, 803-812.

Fowden,A.L. and Forhead,A.J. (2004). Endocrine mechanisms of intrauterine programming. Reproduction *127*, 515-526.

Funder,J. (1996). Corticosteroids- mechansims of action. Austrailian Prescriber *19*, 41-43.

Funder,J.W., Pearce,P.T., Smith,R., and Smith,A.I. (1988). Mineralocorticoid action: target tissue specificity is enzyme, not receptor, mediated. Science *242*, 583-585.

Gardner,D.K., Lane,M., Calderon,I., and Leeton,J. (1996). Environment of the preimplantation human embryo in vivo: metabolite analysis of oviduct and uterine fluids and metabolism of cumulus cells. Fertil Steril. *65*, 349-353.

Gardner,D.K., Lane,M., Stevens,J., and Schoolcraft,W.B. (2001). Noninvasive assessment of human embryo nutrient consumption as a measure of developmental potential. Fertil Steril. *76*, 1175-1180.

Gardner,D.K. and Leese,H.J. (1987). Assessment of embryo viability prior to transfer by the noninvasive measurement of glucose uptake. J. Exp. Zool. *242*, 103-105.

Gardner,D.K. and Leese,H.J. (1990). Concentrations of nutrients in mouse oviduct fluid and their effects on embryo development and metabolism in vitro. J. Reprod Fertil *88*, 361-368.

Gardner,R.L. (1997). The early blastocyst is bilaterally symmetrical and its axis of symmetry is aligned with the animal-vegetal axis of the zygote in the mouse. Development *124*, 289-301.

Gilbert,S. (2000). Developmental Biology. (Massachusetts, USA: Sinauer Associates).

Gluckman,P.D. (1995). Insulin-like growth factors and their binding proteins. In Fetus and Neonate Volume 3 (Growth), M.A.Hanson, J.A.D.Spencer, and C.H.Rodeck, eds. (Cambridge, UK: Cambridge University Press), pp. 97-116.

Gluckman,P.D. and Hanson,M.A. (2004a). Developmental origins of disease paradigm: A mechanistic and evolutionary perspective. Pediatric Research *56*, 311-317.

Gluckman,P.D. and Hanson,M.A. (2004b). Living with the past: Evolution, development, and patterns of disease. Science *305*, 1733-1736.

Gluckman,P.D. and Hanson,M.A. (2004c). The developmental origins of the metabolic syndrome. Trends in Endocrinology and Metabolism *15*, 183-187.

Gomez-Sanchez,E.P., Ganjam,V., Chen,Y.J., Liu,Y., Clark,S.A., and Gomez-Sanchez,C.E. (2001). The 11beta hydroxysteroid dehydrogenase 2 exists as an inactive dimer. Steroids *66*, 845-848.

Gott,A.L., Hardy,K., Winston,R.M., and Leese,H.J. (1990). Non-invasive measurement of pyruvate and glucose uptake and lactate production by single human preimplantation embryos. Hum. Reprod *5*, 104-108.

Hales,C.N. and Barker,D.J.P. (1992). Type 2 (non-insulin dependent) diabetes mellitus: the thrifty phenotype hypothesis. Diabetologia *35*, 595-601.

Hamatani,T., Carter,M.G., Sharov,A.A., and Ko,M.S. (2004). Dynamics of global gene expression changes during mouse preimplantation development. Developmental Cell *6*, 117-131.

Hardy,K., Hooper,M.A., Handyside,A.H., Rutherford,A.J., Winston,R.M., and Leese,H.J. (1989). Non-invasive measurement of glucose and pyruvate uptake by individual human oocytes and preimplantation embryos. Hum. Reprod *4*, 188-191.

Hardy,K. and Spanos,S. (2002). Growth factor expression and function in the human and mouse preimplantation embryo. J. Endocrinol. *172*, 221-236.

Hellerstrom,C., Swenne,I., and Andersson,A. (1988). Islet cell replication and diabetes. In The pathology of the endocrine pancreas in diabetes, P.J.Lefebvre and D.G.Pipeleers, eds. Springer, Heidelberg), pp. 141-170.

Hill,D.J. (1990). Relative abundance and molecular size of immuno-reactive insulin-like growth factors I and II in human fetal tissues. Early Human Development *21*, 49-58.

Hogan,B., Beddington,R., Costantini,F., and Lacy,E. (1994). Manipulating the Mouse Embryo: A Laboratory Manual. Cold Spring Harbor Laboratory Press, New York).

Hollenberg,S.M. and Evans,R.M. (1988). Multiple and cooperative trans-activation domains of the human glucocorticoid receptor. Cell *55*, 899-906.

Hollenberg,S.M., Weinberger,C., Ong,E.S., Cerelli,G., Oro,A., Lebo,R., Thompson,E.B., Rosenfeld,M.G., and Evans,R.M. (1985). Primary Structure and Expression of A Functional Human Glucocorticoid Receptor Cdna. Nature *318*, 635-641.

Holm,P., Walker,S.K., and Seamark,R.F. (1996). Embryo viability, duration of gestation and birth weight in sheep after transfer of in vitro matured and in vitro fertilised zygotes cultured in vitro or in vivo. Journal of Reproduction and Fertility *107*, 175-181.

Hummel,K., Richardson,F., and Fekete,E. (1966). Anatomy. In Biology of the laboratory mouse, Green E, ed. McGraw-Hill).

Huxley,R., Neil,A., and Collins,R. (2002). Unravelling the fetal origins hypothesis: is there really an inverse association between birthweight and subsequent blood pressure? Lancet *360*, 659-665.

Ikegami,M., Jobe,A.H., Newnham,J., Polk,D.H., Willet,K.E., and Sly,P. (1997). Repetitive prenatal glucocorticoids improve lung function and decrease growth in preterm lambs. American Journal of Respiratory and Critical Care Medicine *156*, 178-184.

Jones,J.I. and Clemmons,D.R. (1995). Insulin-like growth factors and their binding proteins: biological actions. Endocrine Reviews *16*, 3-35.

Kaufman,M.H. (1992). The Atlas of Mouse Development. (London: Academic Press).

Kotelevtsev,Y., Holmes,M.C., Burchell,A., Houston,P.M., Schmoll,D., Jamieson,P., Best,R., Brown,R., Edwards,C.R.W., Seckl,J.R., and Mullins,J.J. (1997). 11 beta-hydroxysteroid dehydrogenase type 1 knockout mice show attenuated glucocorticoid-inducible responses and resist hyperglycemia on obesity or stress. Proceedings of the National Academy of Sciences of the United States of America *94*, 14924-14929.

Krozowski,Z.S. and Funder,J.W. (1983). Renal Mineralocorticoid Receptors and Hippocampal Corticosterone-Binding Species Have Identical Intrinsic Steroid Specificity. Proceedings of the National Academy of Sciences of the United States of America-Biological Sciences *80*, 6056-6060.

Kunieda,T., Xian,M.W., Kobayashi,E., Imamichi,T., Moriwaki,K., and Toyoda,Y. (1992). Sexing of Mouse Preimplantation Embryos by Detection of Y-Chromosome-Specific Sequences Using Polymerase Chain-Reaction. Biology of Reproduction *46*, 692-697.

Kwong,W.Y., Miller,D.J., Ursell,E., Wild,A.E., Wilkins,A.P., Osmond,C., Anthony,F.W., and Fleming,T.P. (2006). Imprinted gene expression in the rat embryo-fetal axis is altered in response to periconceptual maternal low protein diet. Reproduction *132*, 265-277.

Kwong,W.Y., Miller,D.J., Wilkins,A.P., Dear,M.S., Wright,J.N., Osmond,C., Zhang,J., and Fleming,T.P. (2007). Maternal Low Protein Diet Restricted to the Preimplantation Period Induces a Gender-Specific Change on Hepatic Gene Expression in Rat Fetuses. Molecular Reproduction and Development *74*, 48-56.

Kwong,W.Y., Osmond,C., and Fleming,T.P. (2004). Support for Barker hypothesis upheld in rat model of maternal undernutrition during the preimplantation period: application of integrated 'random effects' statistical model. Reproductive Biomedicine Online *8*, 574-576.

Kwong,W.Y., Wild,A.E., Roberts,P., Willis,A.C., and Fleming,T.P. (2000). Maternal undernutrition during the preimplantation period of rat development causes blastocyst abnormalities and programming of postnatal hypertension. Development *127*, 4195-4202.

Lakshmi,V. and Monder,C. (1985a). Evidence for independent 11-oxidase and 11-reductase activities of 11 beta-hydroxysteroid dehydrogenase: enzyme latency, phase transitions, and lipid requirements. Endocrinology *116*, 552-560.

Lakshmi,V. and Monder,C. (1985b). Extraction of 11 beta-hydroxysteroid dehydrogenase from rat liver microsomes by detergents. J. Steroid Biochem. *22*, 331-340.

Langley,S.C. and Jackson,A.A. (1994). Increased Systolic Blood-Pressure in Adult-Rats Induced by Fetal Exposure to Maternal Low-Protein Diets. Clinical Science *86*, 217-222.

Langley-Evans,S.C. (1997a). Hypertension induced by foetal exposure to a maternal low-protein diet, in the rat, is prevented by pharmacological blockade of maternal glucocorticoid synthesis. J. Hypertens. *15*, 537-544.

Langley-Evans,S.C. (1997b). Maternal carbenoxolone treatment lowers birthweight and induces hypertension in the offspring of rats fed a protein-replete diet. Clinical Science *93*, 423-429.

Langley-Evans,S.C. (1997c). Intrauterine programming of hypertension by glucocorticoids. Life Sciences *60*, 1213-1221.

Langley-Evans,S.C. (2000). Critical differences between two low protein diet protocols in the programming of hypertension in the rat. Int. J. Food Sci. Nutr. *51*, 11-17.

Langley-Evans,S.C. (2001). Fetal programming of cardiovascular function through exposure to maternal undernutrition. Proceedings of the Nutrition Society *60*, 505-513.

Langley-Evans,S.C. and Jackson,A.A. (1995). Captopril normalises systolic blood pressure in rats with hypertension induced by fetal exposure to maternal low protein diets. Comp Biochem. Physiol A Physiol *110*, 223-228.

Langley-Evans,S.C., Phillips,G.J., Benediktsson,R., Gardner,D.S., Edwards,C.R.W., Jackson,A.A., and Seckl,J.R. (1996a). Protein intake in pregnancy, placental glucocorticoid metabolism and the programming of hypertension in the rat. Placenta *17*, 169-172.

Langley-Evans,S.C., Phillips,G.J., Gardner,D.S., and Jackson,A.A. (1996b). Role of glucocorticoids in programming of maternal diet-induced hypertension in the rat. Journal of Nutritional Biochemistry *7*, 173-178.

Langley-Evans,S.C., Welham,S.J.M., Sherman,R.C., and Jackson,A.A. (1996c). Weanling rats exposed to maternal low-protein diets during discrete periods of gestation exhibit differing severity of hypertension. Clinical Science *91*, 607-615.

Lee,J.E., Lintar,J., and Efstratiadis,A. (1990). Pattern of the insulin-like growth factor II gene expression during early mouse embryogenesis. Development *110*, 151-159.

Lee,T.M. and Zucker,I. (1988). Vole Infant Development Is Influenced Perinatally by Maternal Photoperiodic History. American Journal of Physiology *255*, R831-R838.

Li,C. and Wong,W.H. (2001). Model-based analysis of oligonucleotide arrays: Expression index computation and outlier detection. Proceedings of the National Academy of Sciences of the United States of America *98*, 31-36.

Liggins,G.C. (1994). The Role of Cortisol in Preparing the Fetus for Birth. Reproduction Fertility and Development *6*, 141-150.

Liggins,G.C. and Howie,R.N. (1972). Controlled Trial of Antepartum Glucocorticoid Treatment for Prevention of Respiratory Distress Syndrome in Premature Infants. Pediatrics *50*, 515-517.

Lillycrop,K.A., Phillips,E.S., Jackson,A.A., Hanson,M.A., and Burdge,G.C. (2005). Dietary Protein Restriction of Pregnant Rats Induces and Folic Acid Supplementation Prevents Epigenetic Modification of Hepatic Gene Expression in the Offspring. The Journal of Nutrition 1382-1386.

Lillycrop,K.A., Slater-Jefferies,J.L., Hanson,M.A., Godfrey,K.M., Jackson,A.A., and Burdge,G.C. (2007). Induction of altered epigenetic regulation of the hepatic glucocorticoid receptor in the offspring of rats fed a protein-restricted diet during pregnancy suggests that reduced DNA methyltransferase-1 expression is involved in impaired DNA methylation and changes in histone modifications. British Journal of Nutrition *97*, 1064-1073.

Lindsay,R.S., Lindsay,R.M., Edwards,C.R., and Seckl,J.R. (1996). Inhibition of 11-beta-hydroxysteroid dehydrogenase in pregnant rats and the programming of blood pressure in the offspring. Hypertension *27*, 1200-1204.

Mahesh,V.B. and Ulrich,F. (1960). Metabolism of cortisol and cortisone by various tissues and subcellular particles. J. Biol. Chem. *235*, 356-360.

Manejwala,F.M., Cragoe,E.J., Jr., and Schultz,R.M. (1989). Blastocoel expansion in the preimplantation mouse embryo: role of extracellular sodium and chloride and possible apical routes of their entry. Dev. Biol. *133*, 210-220.

Mangelsdorf,D.J., Thummel,C., Beato,M., Herrlich,P., Schutz,G., Umesono,K., Blumberg,B., Kastner,P., Mark,M., Chambon,P., and Evans,R.M. (1995). The nuclear receptor superfamily: the second decade. Cell *83*, 835-839.

McCormick,S.P., Ng,J.K., Veniant,M., Boren,J., Pierotti,V., Flynn,L.M., Grass,D.S., Connolly,A., and Young,S.G. (1996). Transgenic Mice That Overexpress Mouse Apolipoprotein B: Evidence that the DNA sequences controlling intestinal expression of the apolipoprotein B gene are distant from the structural gene. The Journal of Biological Chemistry *271*, 11963-11970.

McLaren,A. and Michie,D. (1960). Control of prenatal growth in mammals. Nature *187*, 363-365.

McQueen,M.J., Hawken,S., Wang,X., Ounpuu,S., Sniderman,A., Probstfield,J., Steyn,K., Sanderson,J.E., Hasani,M., Volkova,E., Kazmi,K., Yusuf,S., and INTERHEART study investigators (2008). Lipids, lipoproteins and apolipoproteins as risk markers of myocardial infarction in 52 countries (the INTERHEART study): a case-control study. Lancet *9634*, 224-233.

Monder,C. and Lakshmi,V. (1990). Corticosteroid 11 beta-dehydrogenase of rat tissues: immunological studies. Endocrinology *126*, 2435-2443.

Nelson,M. and Evans,H.M. (1953). Relation of dietary protein levels to reproduction in the rat. J. Nutr. *51*, 71-84.

Niiyama,Y., Kishi,K., Endo,S., and Inoue,G. (1973). Effect of diets devoid of one essential amino acid on pregnancy in rats maintained by ovarian steroids. J. Nutr. *103*, 207-212.

Novy,M.J. and Walsh,S.W. (1983). Dexamethasone and Estradiol Treatment in Pregnant Rhesus Macaques - Effects on Gestational Length, Maternal Plasma Hormones, and Fetal Growth. American Journal of Obstetrics and Gynecology *145*, 920-931.

Oakley,R.H., Sar,M., and Cidlowski,J.A. (1996). The human glucocorticoid receptor beta isoform - Expression, biochemical properties, and putative function. Journal of Biological Chemistry *271*, 9550-9559.

Palmieri,S.L., Peter,W., Hess,H., and Scholer,H.R. (1994). Oct-4 transcription factor is differentially expressed in the mouse embryo during establishment of the first two extraembryonic cell lineages involved in implantation. Dev. Biol. *166*, 259-267.

Picard,D. and Yamamoto,K.R. (1987). Two signals mediate hormone-dependent nuclear localization of the glucocorticoid receptor. EMBO J. *6*, 3333-3340.

Piotrowska,K. and Zernicka-Goetz,M. (2001). Role for sperm in spatial patterning of the early mouse embryo. Nature *409*, 517-521.

Plusa,B., Piotrowska,K., and Zernicka-Goetz,M. (2002). Sperm entry position provides a surface marker for the first cleavage plane of the mouse zygote. Genesis. *32*, 193-198.

Pratt,W.B. (1993). The Role of Heat-Shock Proteins in Regulating the Function, Folding, and Trafficking of the Glucocorticoid Receptor. Journal of Biological Chemistry *268*, 21455-21458.

Randall,D., Burggren,W., and French,K. (2002). Animal Physiology: Mechanisms and Adaptations. (New York: W.H Freeman and co.).

Rees,W.D., Hay,S.M., Brown,D.S., Antipatis,C., and Palmer,R.M. (2000). Maternal protein deficiency causes hypermethylation of DNA in the livers of rat fetuses. Journal of Nutrition *130*, 1821-1826.

Reeves,P.G., Nielsen,F.H., and Fahey,G.C., Jr. (1993). AIN-93 purified diets for laboratory rodents: final report of the American Institute of Nutrition ad hoc writing committee on the reformulation of the AIN-76A rodent diet. J. Nutr. *123*, 1939-1951.

Reinisch,J.M., Simon,N.G., Karow,W.G., and Gandelman,R. (1978). Prenatal exposure to prednisone in humans and animals retards intrauterine growth. Science *202*, 436-438.

Renard,J.P., Philippon,A., and Menezo,Y. (1980). In-vitro uptake of glucose by bovine blastocysts. J. Reprod Fertil *58*, 161-164.

Ricketts,M.L., Verhaeg,J.M., Bujalska,I., Howie,A.J., Rainey,W.E., and Stewart,P.M. (1998). Immunohistochemical Localisation of Type 1 11B-Hydroxysteroid

Dehydrogenase in Human Tissues. Journal of Clinical Endocrinology and Metabolism *83*, 1325-1335.

Rinaudo,P. and Schultz,R.M. (2004). Effects of embryo culture on global pattern of gene expression in preimplantation mouse embryos. Reproduction *128*, 301-311.

Roseboom,T.J., van der Meulen,J.H.P., Ravelli,A.C.J., Osmond,C., Barker,D.J.P., and Bleker,O.P. (2001). Effects of prenatal exposure to the Dutch famine on adult disease in later life: an overview. Molecular and Cellular Endocrinology *185*, 93-98.

Rosen,M.B., Thibodeaux,J.R., Wood,C.R., Zerhr,R.D., Schmid,J.E., and Lau,C. (2007). Gene expression profiling in the lung and liver of PFOA-exposed mouse fetuses. Toxicology *239*, 15-33.

Rugh,R. (1990). The Mouse: It's Reproduction and Development. Oxford University Press).

Rulicke,T., Haenggli,A., Rappold,K., Moehrlen,U.,Stallmach,T. (2006). No transuterine migration of fertilised ova after unilateral embryo transfer in mice. Reproduction, Fertility and Development *18*, 885-891.

Rusvai,E. and Naray-Fejes-Toth,A. (1993). A new isoform of 11 beta-hydroxysteroid dehydrogenase in aldosterone target cells. J. Biol. Chem. *268*, 10717-10720.

Seckl,J.R. (2004). 11beta-hydroxysteroid dehydrogenases: changing glucocorticoid action. Curr. Opin. Pharmacol. *4*, 597-602.

Seckl,J.R. and Brown,R.W. (1994). 11-beta-hydroxysteroid dehydrogenase: on several roads to hypertension. J. Hypertens. *12*, 105-112.

Seckl,J.R. and Meaney,M.J. (2004). Glucocorticoid programming. Ann. N. Y. Acad. Sci. *1032*, 63-84.

Sheppard,K. and Funder,J.W. (1987). Mineralocorticoid specificity of renal type I receptors: in vivo binding studies. Am. J. Physiol *252*, E224-E229.

Sinclair,K.D., McEvoy,T.G., Maxfield,E.K., Maltin,C.A.Y.L.E., Wilmut,I., Broadbent,P.J., and Robinson,J.J. (1999). Aberrant fetal growth and development after in vitro culture of sheep zygotes. Journal of Reproduction and Fertility *116*, 177-186.

Singh,J.S., Rall,L.B., and Styne,D.E. (1991). Insulin-like growth factors I and II gene expression in Balb/C mouse line during postnatal development. Biology of the Neonate *60*, 7-18.

Slack,J.M. (2006). Essential Developmental Biology. Blackwell Publishing).

Snoeck,A., Remacle,C., Reusens,B., and Hoet,J.J. (1990). Effect of a low protein diet during pregnancy on the fetal rat endocrine pancreas. Biol. Neonate *57*, 107-118.

Stewart,P.M., Corrie,J.E., Shackleton,C.H., and Edwards,C.R. (1988). Syndrome of apparent mineralocorticoid excess. A defect in the cortisol-cortisone shuttle. J. Clin. Invest *82*, 340-349.

Tangalakis,K., Lumbers,E.R., Moritz,K.M., Towstoless,M.K., and Wintour,E.M. (1992). Effect of cortisol on blood pressure and vascular reactivity in the ovine fetus. Exp. Physiol *77*, 709-717.

Thompson,A., Han,V.K., and Yang,K. (2004). Differential expression of 11beta-hydroxysteroid dehydrogenase types 1 and 2 mRNA and glucocorticoid receptor protein during mouse embryonic development. J. Steroid Biochem. Mol. Biol. *88*, 367-375.

Thompson,J.G., Gardner,D.K., Pugh,P.A., McMillan,W.H., and Tervit,H.R. (1995). Lamb birth weight is affected by culture stsyem utilised during in vitro pre-elongation development of ovine embryos. Biology of Repreoduction *53*, 1385-1391.

Ulick,S., Levine,L.S., Gunczler,P., Zanconato,G., Ramirez,L.C., Rauh,W., Rosler,A., Bradlow,H.L., and New,M.I. (1979). A syndrome of apparent mineralocorticoid excess associated with defects in the peripheral metabolism of cortisol. J. Clin. Endocrinol. Metab *49*, 757-764.

vom Saal,F.S. (1981). Variation in Phenotype Due to Random Intrauterine Positioning of Male and Female Fetuses in Rodents. Journal of Reproduction and Fertility *62*, 633-650.

vom Saal,F.S. (1983). Variation in infanticide and parental behavior in male mice due to prior intrauterine proximity to female fetuses: elimination by prenatal stress. Physiol Behav. *30*, 675-681.

vom Saal,F.S. and Bronson,F.H. (1978). In utero proximity of female mouse fetuses to males: effect on reproductive performance during later life. Biol. Reprod *19*, 842-853.

vom Saal,F.S. and Bronson,F.H. (1980a). Sexual characteristics of adult female mice are correlated with their blood testosterone levels during prenatal development. Science *208*, 597-599.

vom Saal,F.S. and Bronson,F.H. (1980b). Variation in length of the estrous cycle in mice due to former intrauterine proximity to male fetuses. Biol. Reprod *22*, 777-780.

Wang,Q.T., Piotrowska,K., Ciemerych,M.A., Milenkovic,L., Scott,M.P., Davis,R.W., and Zernicka-Goetz,M. (2004). A genome-wide study of gene activity reveals developmental signaling pathways in the preimplantation mouse embryo. Developmental Cell *6*, 133-144.

Waterston,R.H., *et al.* (2002). Initial sequencing and comparative analysis of the mouse genome. Nature *420*, 520-562.

Watkins,A.J., Platt,D., Papenbrock,T., Wilkins,A., Eckert,J., Kwong,W.Y., Osmond,C., Hanson,M., and Fleming,T.P. (2007). Mouse embryo culture induces changes in postnatal

phenotype including raised systolic blood pressure. Proc. Natl. Acad. Sci. U. S. A *104*, 5449-5454.

Watkins,A.J., Ursell,E., Panton,R., Papenbrock,T., Hollis,L., Cunningham,C., Wilkins,A., Perry,V.H., Sheth,B., Kwong,W.Y., Eckert,J.E., Wild,A.E., Hanson,M.A., Osmond,C., and Fleming,T.P. (2008). Adaptive Responses by Mouse Early Embryos to Maternal Diet Protect Fetal Growth but Predispose to Adult Onset Disease. Biology of Reproduction *78*, 299-306.

Watson,A.J., Watson,P.H., Arcellia-Paulilo,M., Warnes,D., Walker,S.K., Schultz,G.A., Armstrong,D.T., and Seamark,R.F. (1994). A growth factor phenotype map for ovine pre-implantation development. Biology of Repreoduction *50*, 725-733.

Whorwood,C.B., Firth,K.M., Budge,H., and Symonds,M.E. (2001). Maternal undernutrition during early to midgestation programs tissue-specific alterations in the expression of the glucocorticoid receptor, 11beta-hydroxysteroid dehydrogenase isoforms, and type 1 angiotensin ii receptor in neonatal sheep. Endocrinology *142*, 2854-2864.

Young,L.E., Sinclair,K.D., and Wilmut,I. (1998). Large offspring syndrome in cattle and sheep. Reviews of Reproduction *3*, 155-163.

Zeng,F., Baldwin,D., and Schultz,R. (2004). Transcript profiling during preimplantation mouse development. Developmental Biology *272*, 496.